**POLYTECHNIQUE MONTRÉAL**
affiliée à l'Université de Montréal

# Peel and Bound: Solving Discrete Optimization Problems with Decision Diagrams and Separation

**ISAAC RUDICH**
Département de mathématiques et de génie industriel

Thèse présentée en vue de l'obtention du diplôme de *Philosophiæ Doctor*
Génie informatique

May 2024

**POLYTECHNIQUE MONTRÉAL**
affiliée à l'Université de Montréal

Cette thèse intitulée :

**Peel and Bound: Solving Discrete Optimization Problems with Decision Diagrams and Separation**

présentée par **Isaac RUDICH**
en vue de l'obtention du diplôme de *Philosophiæ Doctor*
a été dûment acceptée par le jury d'examen constitué de :

**Michel GENDREAU**, président
**Louis-Martin ROUSSEAU**, membre et directeur de recherche
**Quentin CAPPART**, membre et codirecteur de recherche
**Andrea LODI**, membre
**Laurent MICHEL**, membre externe

## DEDICATION

*"It is exhausting, having to reason all the time*
*in a universe which wasn't meant to be reasonable."*
*- Breakfast of Champions by Kurt Vonnegut*

# ACKNOWLEDGEMENTS

Many small interactions got me here, and I wish to express my gratitude to those who impacted my path, whether through brief encounters or prolonged engagements. In 2018, I was trying to figure out what to do next on my very unconventional career trajectory. I had no formal math background, but I found myself drawn to solving scheduling problems and seeking advice on my next steps. This search led me to the offices of Michael Trick and Willem-Jan van Hoeve, both of whom generously recommended graduate programs and helped clarify my goals. I had never even heard the term *Operations Research* before those conversations, and I doubt I would have discovered this lovely field without them.

My advisors, Louis-Martin Rousseau and Quentin Cappart, significantly shaped my research and provided invaluable guidance throughout my journey. Before even arriving in Canada, Louis-Martin suggested I read *Decision Diagrams for Optimization* to determine if it aligned with my research interests. It did. This book not only captivated my attention but also led me to the 2018 Decision Diagrams Symposium. Although I was merely an observer with little to contribute at the time, I could not have anticipated how instrumental some of the attendees would be in influencing the direction of my thesis.

Reflecting on these crucial interactions, I am grateful to a broader community of peers, colleagues, and mentors who have supported, enlightened, and encouraged me. It is with deep appreciation that I extend my thanks to each of them for enriching my academic and personal growth. In particular, notable conversations with Willem-Jan van Hoeve, Michael Römer, Andre Cire, Laurent Michel, Xavier Gillard, Manuel López-Ibáñez, Moira MacNeil, and Vianney Coppé sparked significant insights that greatly enriched my research.

I also cherish the deep friendships formed along the way. Augustin Parjadis, thank you for easing my transition to a French school, and for countless hours spent playing board games. Anthony Karahalios, you've been a dear friend, as well as an excellent sounding board for my myriad ideas. Dani Ripsman, though our collaboration and friendship are relatively new, they feel longstanding.

Special thanks to my family members Avi Rudich and Rachel Rue for the weekly Decision Diagram journal club, which evolved into a *Trying to Solve Stochastic Games* club, that has met nearly every week for four years.

Also thanks to Robin for being supportive. None of this would've been possible without my cats: Sir Sqwonk and Countess Pizazz. And finally to Zenith, for being part of the journey.

# RÉSUMÉ

Cette thèse présente des avancées significatives dans la théorie et l'implémentation des méthodes d'optimisation basées sur les diagrammes de décision : tout d'abord le développement et l'amélioration de l'algorithme Peel-and-Bound (PnB) comme une étude sur la construction d'un solveur utilisant des diagrammes de décision (DD), et l'introduction de DD relaxés implicites qui généralise une idée cruciale pour l'implémentation efficace de PnB.

Les DD relaxés sont un outil graphique pour construire des bornes de relaxation combinatoires pour des problèmes d'optimisation. L'algorithme PnB démontre le potentiel puissant des solveurs basés sur les DD exploitant la séparation, une méthode de construction de DD relaxés partant d'un petit DD représentant une relaxation initiale faible qui est ensuite améliorée par division de nœuds. PnB est un algorithme hautement parallélisable, construit autour de la production de DD relaxés par séparation, qui peut échanger toute la mémoire disponible contre de l'efficacité de calcul.

L'implémentation de PnB a été testée sur les 467 instances de référence du problème du voyageur de commerce avec fenêtre de temps (TSP-TW) utilisées pour tester le solveur branch-and-bound (BnB) ddo basé sur les DD. Même lorsque ddo utilise le calcul parallèle, PnB surpasse ddo. De plus, PnB a résolu 15 instances qui, à notre connaissance, étaient ouvertes dans la littérature. Dans notre test final de PnB, nous avons exécuté la nouvelle implémentation de PnB sur la variante du makespan des 467 instances du TSP-TW. PnB a résolu 94 % des instances de makespan, et 3 % supplémentaires lorsqu'il était initialisé avec la meilleure solution connue. L'implémentation de l'algorithme PnB a montré des performances de pointe sur les instances de référence du TSP-TW, surpassant le solveur branch-and-bound basé sur les DD existant.

Cette thèse fait progresser davantage les méthodes d'optimisation basées sur les DD en généralisant le concept de DD relaxés implicites, une méthode générique de génération de DD qui ne nécessite pas que les arcs soient étiquetés. Au lieu de cela, cette information est déplacée vers les nœuds. Les DD relaxés implicites sont une méthode facile à implémenter pour obtenir des accélérations massives dans les solveurs basés sur les DD. Ce concept a été crucial pour atteindre des résultats de pointe avec notre implémentation de PnB.

L'utilité de PnB et des DD relaxés implicites a été démontrée par une application au problème de routage d'astéroïdes (ARP). Ce problème peut être considéré comme une variante du célèbre problème du voyageur de commerce où toutes les villes (astéroïdes) sont dans l'espace, et donc en mouvement constant. L'algorithme trouve des solutions réalisables de

haute qualité pour plusieurs instances de l'ARP, dont beaucoup sont optimales sous une légère hypothèse sur la qualité de l'optimiseur interne. C'est la première méthode dans la littérature plus efficace que la force brute pour trouver des solutions exactes aux problèmes d'optimisation de trajectoire globale comme l'ARP. Le cadre définissant l'algorithme est polyvalent, hautement évolutif et applicable à une large gamme de problèmes de séquençage exigeants en complexité.

Cette thèse non seulement fait progresser la compréhension et l'application des DD à travers l'introduction de méthodes innovantes comme le peel-and-bound et les DD relaxés implicites, mais elle ouvre également la voie à de futures percées dans des défis d'optimisation complexes qui nécessitent de résoudre un problème d'optimisation combinatoire externe comportant un problème d'optimisation interne coûteux en calcul.

# ABSTRACT

This thesis presents significant advancements in the theory and implementation of Decision-Diagram-based optimization methods: primarily the development and enhancement of the Peel-and-Bound (PnB) algorithm as a study in how to construct a solver using Decision Diagrams (DDs), and the introduction of implicit relaxed DDs which generalizes an idea critical to efficient implemention of PnB.

Relaxed DDs are a graphical tool for constructing combinatorial relaxed bounds for optimization problems. The PnB algorithm demonstrates the powerful potential of DD-based solvers that leverage separation, a method of constructing relaxed DDs by starting from a small DD representing a weak initial relaxation and improving that relaxation by splitting nodes. PnB is a highly parallelizable algorithm, built around constructing relaxed DDs by separation, which can trade memory for computational efficiency.

The PnB implementation was tested on the 467 benchmark instances of Traveling Salesman Problem with Time Windows (TSP-TW) used to test the DD-based branch-and-bound (BnB) solver (ddo). Even when ddo is using parallel processing, PnB outperforms ddo. Furthermore, PnB closed 15 instances that, to the best of our knowledge, were open in the literature. In our final test of PnB, we ran the new implementation of PnB on the makespan variant of the 467 TSP-TW instances. PnB closed 94% of the makespan instances, and an additional 3% when seeded with the best known solution. The implementation of the PnB algorithm had a cutting-edge performance on the benchmark instances of the TSP-TW, outperforming the existing DD-based branch-and-bound (BnB) solver.

This thesis further advances DD-based optimization methods by generalizing the concept of implicit relaxed DDs, a generic method of generating DDs that does not require the arcs to be labeled. Instead, information that would have been stored in arc labels is moved to the nodes. Implicit relaxed DDs are an easy-to-implement method for achieving massive speed-ups in DD-based solvers. This concept was critical to achieving cutting edge results with our PnB implementation.

The utility of both PnB and implicit relaxed DDs was demonstrated with an application to the Asteroid Routing Problem (ARP). This problem can be thought of as a variant of the well-known Travelling Salesman Problem where all of the cities (asteroids) are in Space, and thus in constant motion. The ARP has an outer combinatorial problem that requires finding the optimal permutation to visit the asteroids, and an inner non-linear non-convex optimization problem that requires computing the optimal trajectory between two asteroids

at specific points in time. The algorithm finds high-quality feasible solutions for several instances of the ARP, many of which are optimal under a mild assumption about the quality of the inner optimizer. This is the first method in the literature more efficient than brute force for finding exact solutions to global trajectory optimization problems like the ARP. The framework defining the algorithm is versatile, highly scalable, and applicable to a diverse range of computationally demanding sequencing problems.

This thesis not only advances the understanding and application of DDs through the introduction of innovative methods like peel-and-bound and implicit relaxed DDs, but also sets the stage for future breakthroughs in complex optimization challenges that require solving an outer combinatorial optimization problem that has a computationally expensive inner optimization problem.

# TABLE OF CONTENTS

# LIST OF TABLES

# LIST OF FIGURES

# LIST OF SYMBOLS AND ACRONYMS

Acronyms:

| | |
|---|---|
| ARP | Asteroid Routing Problem |
| BDD | Binary Decision Diagram |
| BnB | Branch-and-Bound |
| CP | Constraint Program(ming) |
| DD | Decision Diagram |
| DP | Dynamic Program(ming) |
| LP | Linear Program(ming) |
| MDD | Multivalued Decision Diagram |
| MIP | Mixed Integer Progam(ming) |
| OR | Operations Research |
| PnB | Peel-and-Bound |
| SAT | Boolean Satisfiability |
| SOP | Sequence Ordering Problem |
| TSP | Travelling Salesman Problem |
| TSP-TW | Travelling Salesman Problem with Time Windows |
| TSP-TD | Travelling Salesman Problem with Time Dependent Travel Times |

General Symbols:

| | |
|---|---|
| $\mathcal{P}$ | a discrete optimization problem |
| $Sol(\mathcal{P})$ | the set of feasible solutions to $\mathcal{P}$ |
| $\pi$ | a solution to an optimization problem |
| $\pi^*$ | the optimal solution to an optimization problem |
| $z^*$ | the value of an optimal solution to an optimization problem |
| $z^*(\mathcal{P})$ | the value of an optimal solution to $\mathcal{P}$ |
| $d(x)$ | the domain of variable $x$ |

Decision Diagram Symbols:

| | |
|---|---|
| $r$ | a root node |
| $t$ | a terminal node |
| $\oplus$ | a merge operator for nodes |
| $\ominus$ | a split operator for nodes |
| $a_{uv}$ | an arc that goes from node $u$ to node $v$ |
| $l$ | an arc label |
| $l(a)$ | the label on arc $a$ |
| $w(a)$ | the weight of arc $a$ |
| $\ell$ | a layer index of a Decision Diagram |
| $\ell(u)$ | the layer index of node $u$ |
| $L$ | a layer of a Decision Diagram (a set of nodes) |
| $d(u)$ | the domain of a node (a set of arc labels) |
| $f(u)$ | the value of the objective function at $u$ |
| $\omega$ | the maximum width of a Decision Diagram |
| $\mathcal{M}$ | a Decision Diagram |
| $\mathcal{M}(u)$ | a partial Decision Diagram rooted at $u$ |
| $\mathcal{M}(u, v)$ | a partial Decision Diagram rooted at $u$ with terminal $v$ |
| $\mathcal{M}_\omega$ | a Decision Diagram with width $\omega$ |
| $\mathcal{M}^-$ | a restricted Decision Diagram |
| $\mathcal{M}^+$ | a relaxed Decision Diagram |
| $d(\mathcal{M})$ | the set of solutions encoded by Decision Diagram $\mathcal{M}$ |
| $All_u^\downarrow$ | the set of labels that appear on every path from $r$ to $u$ |
| $Some_u^\downarrow$ | the set of labels that appear on at least one path from $r$ to $u$ |
| $All_u^\uparrow$ | the set of labels that appear on every path from $u$ to $t$ |
| $Some_u^\uparrow$ | the set of labels that appear on at least one path from $u$ to $t$ |
| $z(\mathcal{M})$ | the value of the best path through $\mathcal{M}$ |
| $z_u^\downarrow$ | the value of the best path from $r$ to $u$ |
| $z_u^\uparrow$ | the value of the best path from $u$ to $t$ |

# LIST OF APPENDICES

# CHAPTER 1 INTRODUCTION

Operations Research (OR) is the science of applying mathematical tools to provide a quantitative foundation for decision-making. The use of these tools is widespread: logistics companies utilize them to schedule deliveries and route vehicles, hospitals employ them to optimize patient flow, schools apply them to organize course schedules, investment firms leverage them for risk management, and manufacturers rely on them to minimize resource waste. OR tools are essential for the functioning of modern society. However, the need for new and improved tools consistently surpasses their supply. With increasing data availability, access to computing power, and the desire to optimize new domains, there is a growing demand for OR that exceeds its capabilities.

Traditional techniques often struggle with computational efficiency when faced with intricate constraints or large data sets. Additionally, evolving challenges have created a need for tools that can represent and solve problems more flexibly. This environment set the stage for Multivalued Decision Diagrams (MDDs) to emerge as a new tool capable of addressing gaps in existing methodologies and offering novel ways to represent optimization problems.

OR provides a range of tools, such as Linear Programming (LP), Mixed Integer Programming (MIP), Dynamic Programming (DP), Constraint Programming (CP), Boolean Satisfiability (SAT), and an extensive range of heuristics. Each tool has a dedicated and active research community working to improve it. This diversity persists because no single tool can outperform the others across all problems. Each tool excels in certain areas, but falls short in others. In 2016, the book *Decision Diagrams for Optimization* organized and compiled several papers, supplemented them with examples and data, and made the case that MDDs could serve as a novel OR tool to bridge gaps left by existing techniques [1]. Decision Diagrams (DDs) have long been used in Computer Science, but the framework presented in this book demonstrated their potential as a tool for optimization as well.

Since 2016, research into leveraging DD-based techniques in other OR tools has surged, alongside the development of dedicated DD-based solvers. These two approaches are symbiotic: methods and insights from one often benefit the other, and both have evolved in parallel. A 2022 survey of DD research, which reviewed over 100 papers, offers just a glimpse of the ongoing work, and the community of DD researchers continues to expand each year [2]. While most DD research has focused on integrating DD techniques with other tools, a few groups are making significant efforts to develop state-of-the-art DD-based solvers. This thesis details one of these initiatives.

## 1.1 Research Goal

The goal of this thesis is to offer insight into how DD-based techniques can be applied to advanced optimization challenges, emphasizing the crucial decisions involved in implementing Decision Diagrams. In addition, I aim to provide practical advice for developing a DD-based solver, offering context for the rationale behind the decisions made during its implementation.

This work delves into the specific challenges faced when adapting DD-based methods to various applications and highlights best practices for ensuring the efficiency and effectiveness of a DD-based solver. By exploring the nuances of decision-making and design choices, I hope to guide researchers and practitioners in leveraging these techniques for cutting-edge optimization, ultimately expanding the scope and impact of Decision Diagram methodologies.

## 1.2 Contributions

The main contributions of this work are:

- **Peel-and-Bound Framework**: Development of a generic framework for a DD-based solver, known as *peel-and-bound* (PnB), and its open-source implementation in Julia [3]. This implementation demonstrates cutting-edge results on the Traveling Salesman Problem with Time Windows, closing 15 open benchmark instances, and making the framework a valuable resource for researchers and practitioners.
- **Embedded Restricted Decision Diagrams**: Introduction of a novel DD-based search technique for finding feasible solutions to optimization problems called *Embedded Restricted Decision Diagrams*, which is also referred to as *Embedded Search*. This work generalizes the concept of *rough bounding* [4,5] by demonstrating that Embedded Search can leverage rough bounding in a problem-agnostic manner.
- **Implicit Relaxed Decision Diagrams**: A generic algorithm for constructing relaxed DDs without needing to label the arcs. This construction is easier to implement than standard relaxed DDs, and substantially more efficient at run-time.
- **Framework for Finding Exact Solutions to Outer/Inner Optimization**: Establishment of a framework for using peel-and-bound to identify optimal solutions to optimization problems with an outer combinatorial problem and a complex or computationally expensive inner problem, under a mild assumption about the quality of the inner optimizer. The framework is demonstrated through its application to the Asteroid Routing Problem (ARP), marking the first instance where a global trajectory

optimization problem is solved exactly through a method more efficient than brute force.

## 1.3 Publications

A large portion of this thesis is based on work that has been previously published in the following papers. This is noted at the beginning of each relevant chapter.

- *Peel-and-Bound: Generating Stronger Relaxed Bounds with Multivalued Decision Diagrams* by Isaac Rudich, Quentin Cappart, and Louis-Martin Rousseau, was published at the 28th International Conference on Principles and Practice of Constraint Programming (CP 2022) where it won the Best Paper award [6]. In this paper, we introduced the peel-and-bound framework for making a DD-based solver, and we implemented a simple test showing that a naive implementation of PnB outperforms a naive implementation of the branch-and-bound (BnB) framework for a DD-based solver [7, 8].
- *Improved Peel-and-Bound: Methods for Generating Dual Bounds with Multivalued Decision Diagrams* by Isaac Rudich, Quentin Cappart, and Louis-Martin Rousseau, was published in the Journal of Artificial Intelligence Research in 2023 [9]. In this paper, significant effort was devoted to implementing PnB as efficiently as possible, and to detailing the steps required to achieve cutting-edge results. This paper closed several open instances of the Traveling Salesman Problem with Time Windows (TSP-TW).
- *An Exact Framework for Solving the Space-Time Dependent TSP* by Isaac Rudich, Quentin Cappart, Manuel López-Ibáñez, Michael Römer, and Louis-Martin Rousseau is currently only available as a preprint. In this paper, PnB was used to close several open instances of the Asteroid Routing Problem, demonstrating a framework for solving optimization problems with an outer combinatorial problem, and a computationally expensive inner optimization problem. This marks the first time a technique more efficient than brute force was applied to a global trajectory optimization problem.

## 1.4 Outline

Chapter 2 begins the thesis proper with a decision diagram tutorial. The tutorial includes figures new for this thesis demonstrating every concept with two different examples. Chapter 3 introduces peel-and-bound, which is the foundation for everything else in this thesis. Chapter 4 builds on the initial concept of peel-and-bound, improving the theory and demonstrating

that our PnB solver can achieve cutting edge results. Chapter 5 presents the novel concept of Implicit Relaxed DDs, which has not been published elsewhere. Chapter 6 explains how we used PnB to find exact solutions to the ARP under a mild assumption about the quality of the inner optimizer. Chapter 7 closes the thesis with my parting thoughts.

# CHAPTER 2 DECISION DIAGRAMS FOR OPTIMIZATION

The standard approach for explaining the use of Decision Diagrams (DDs) serves two main purposes: (1) to justify their use, and (2) to explain the methodology. A foundational tutorial is presented in the book *Decision Diagrams for Optimization* [1], while a more recent example is available in *Discrete optimization with decision diagrams : design of a generic solver, improved bounding techniques, and discovery of good feasible solutions with large neighborhood search* [5]. There are earlier works as well [10–14], but *Decision Diagrams for Optimization* unified and expanded on these earlier works. This standard approach justifies the use of DDs by illustrating how a DD representing a problem can be built from the Dynamic Programming (DP) model for that problem. This establishes an intuitive understanding of why DDs are valuable and provides insight into the origins of DD-based methods. However, this approach is widely available, and other intuitive methods for explaining DD-based techniques can provide equally valuable insight. Every DP model can be turned into a DD, but not every DD can be turned into a DP model [15].

This chapter provides model-agnostic motivation for using DDs for optimization. In other words, for the purposes of this explanation, a DD will be the problem model, constructed directly from the problem description. This will be of particular practical use in Chapter 6 where we solve the Asteroid Routing Problem (ARP). Writing out the objective function for even a small instance of the ARP is intractable. Thus, constructing a DD for the ARP from a DP model in the traditional way is impossible, and we instead construct the DD directly from the problem description.

The explanation detailed in this chapter is based almost entirely on ideas compiled in *Decision Diagrams for Optimization*, but differs in that it starts from decision trees instead of a Dynamic Program [1, 7, 8]. For further references to key literature, see Section 2.7.

## 2.1 Optimization Problems: Notation and Examples

Let $\mathcal{P}$ be an instance of a discrete minimization problem with $n$ variables $\{x_1, ..., x_n\}$, let $Sol(\mathcal{P})$ be the set of feasible solutions to $\mathcal{P}$, let $\pi^*(\mathcal{P})$ be an optimal solution to $\mathcal{P}$, let $z^*(\mathcal{P})$ be the value of an optimal solution to $\mathcal{P}$, and let $d(x_i)$ be the domain of variable $x_i, i \in \{1, ..., n\}$.

### 2.1.1 Knapsack Example

In this chapter, two examples will be used. The first example is an instance of the knapsack problem, $\mathcal{P}_{sack}$ [16]. In the knapsack problem, there is a bag with a limited weight capacity, and several items that can be placed into the bag. Each item has a utility and a weight. The objective is to maximize the utility of items placed in the bag without exceeding the weight capacity. The instance we will be using is shown below in Table 2.1.

**Knapsack Capacity:** 10

| **Item** | **Weight** | **Utility** |
|---|---|---|
| A | 3 | 6 |
| B | 4 | 8 |
| C | 5 | 7 |
| D | 8 | 9 |

Table 2.1 Knapsack instance values ($\mathcal{P}_{sack}$)

Let the variables for $\mathcal{P}_{sack}$ be $\{x_A, x_B, x_C, x_D\}$ where $x_i \in \{0, 1\}$ and $i \in \{A, B, C, D\}$; a value of 0 means the item is not included in the sack, and a value of 1 means the item is included in the sack. For reference, the optimal solution to this instance is $[x_A = 0, x_B = 1, x_C = 1, x_D = 0]$ with a value of 15.

### 2.1.2 Sequence Ordering Example

The second example is an instance of the Sequence Ordering Problem (SOP) ($\mathcal{P}_{SOP}$) [17]. In the SOP, there is a list of tasks (or elements), and the goal is to find the least expensive ordering of those tasks in which each task is performed exactly once. Additionally, certain precedence constraints must be respected, meaning that some tasks must appear earlier than others for a sequence to be feasible. In other words, the SOP is an asymmetric TSP with precedence constraints.

Defining a SOP instance requires providing the cost $c_{ij}$ of following item $x_i$ with $x_j$, for each valid ordered pair $\{i, j\}$. The cost matrix in Table 2.2 defines $\mathcal{P}_{SOP}$. The precedence constraints are that A must come before everything else, and B must come before D; these are indicated by X in the cost matrix.

Let the variables for $\mathcal{P}_{SOP}$ be $\{x_1, x_2, x_3, x_4\}$. The domain of each variable is in $\{A, B, C, D\}$, and $x_i = A$ indicates that $A$ is the $i^{th}$ element in the sequence. For reference, the optimal solution to this instance is $[x_1 = A, x_2 = B, x_3 = D, x_4 = C]$ with a cost of 17.

| From \ To | A | B | C | D |
|---|---|---|---|---|
| A | - | 8 | 5 | 0 |
| B | X | - | 5 | 8 |
| C | X | 5 | - | 5 |
| D | X | X | 1 | - |

Table 2.2 SOP instance ($\mathcal{P}_{SOP}$)

Transition cost of $c_{row,col}$ to go from $row$ to $col$.

## 2.2 Exact Decision Diagrams

An exact DD for an optimization problem $\mathcal{P}$, is a directed layered acyclic graph with a root $r$ and terminal $t$, such that every path from $r$ to $t$ encodes a feasible solution to $\mathcal{P}$, and every feasible solution to $\mathcal{P}$ is encoded as a path from $r$ to $t$. So a DD is an exact representation of $\mathcal{P}$ if the set of solutions it encodes is equal to $Sol(\mathcal{P})$.

To build an intuition for what this looks like, we will construct an exact DD for $\mathcal{P}_{sack}$ (see Section 2.1.1). The following method is inefficient, but educational. Begin by drawing the decision tree that represents every feasible solution to $\mathcal{P}_{sack}$ as its own branch. The result is shown below in Figure 2.1. At each node in the tree K is the remaining capacity, and U is the utility. Nodes that exceed the total capacity are removed from the tree, because those solutions are infeasible.

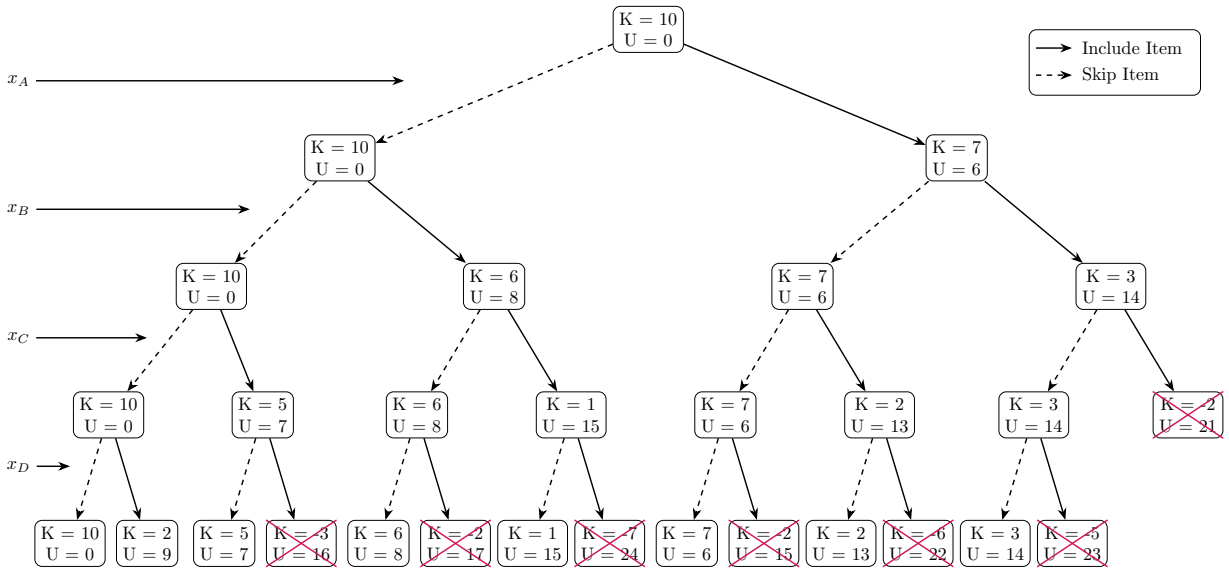


Figure 2.1 Decision Tree for $\mathcal{P}_{sack}$

K:= remaining capacity, U:= utility.

### 2.2.1 Merging Equivalent Nodes

Making a decision tree to store every feasible solution is possible for small problems, but quickly becomes intractable. An exact DD can often accomplish the task with substantially fewer nodes. We will now turn the decision tree into a decision diagram by merging nodes [18, 19]. For the diagram to remain exact, merges must not add or remove any paths. This is done using a recursive procedure.

Let $a$ be an arc, and let $l(a)$ be the label on an arc, i.e. the value assigned to a decision variable by $a$. Let $a_{uv}$ be an arc from $u$ to $v$. In $\mathcal{P}_{sack}$, every arc has a label $l \in \{0, 1\}$, indicated by a dashed line or solid line, respectively. Let two nodes $u$ and $v$ be *equivalent* if, for every out-arc of $u$ there is an out-arc of $v$ with the same label and destination node, and similarly for every out-arc of $v$ there is an out-arc of $u$ with the same label and destination node. So, if $u$ and $v$ are equivalent, then for each out-arc $a_{uz}$ of $u$ there is an out-arc $a_{vz}$ of $v$ such that $l(a_{uz}) = l(a_{vz})$, and *vice versa*. In addition, $u$ and $v$ must be on the same layer.

Merging two equivalent nodes requires defining a merge operator. Let $u$ and $v$ be two equivalent nodes to be merged. In general, when equivalent nodes are merged, the following happens: (1) a new node $m_{uv}$ is created on the same layer as the merging nodes, (2) the destination of the in-arcs of $u$ and the in-arcs of $v$ is changed to be $m_{uv}$, and (3) chosen arbitrarily, the out-arcs of either $u$ or $v$ are changed so that their origin is $m_{uv}$. This is formalized in Algorithm 1.

**Algorithm 1:** Generic Merge Operation for Equivalent Nodes

**Input:** equivalent nodes $u$ and $v$
Create a new node $m$
**foreach** *in-arc* $a_{zu}$ *of* $u$ **do**
    Adjust the arc so that its destination is $m$ instead of $u$, becoming $a_{zm}$
**end**
**foreach** *in-arc* $a_{zv}$ *of* $v$ **do**
    Adjust the arc so that its destination is $m$ instead of $v$, becoming $a_{zm}$
**end**
**foreach** *out-arc* $a_{uz}$ *of* $u$ **do**
    Adjust the arc so that its origin is $m$ instead of $u$, becoming $a_{mz}$
**end**
Delete $u$ and $v$
**return** $m$

When two equivalent nodes are merged, a procedure for merging the information stored on the nodes must be defined. This definition will be specific to the optimization problem being solved and the information being stored. In $\mathcal{P}_{sack}$, each node is tracking the remaining

capacity of the knapsack $K$, and the utility $U$ achieved so far. Let $K_1$ and $K_2$ be the merging $K$ values, $U_1$ and $U_2$ be the merging $U$ values, $K'$ be the merged $K$ value, and $U'$ be the merged $U$ value. If a new value for the remaining capacity stored on the merged node is defined as the smallest of the old values for remaining capacity $K' = min(K_1, K_2)$, then $K'$ represents the remaining capacity if the heaviest path to the merged node is taken. Note that it is equally valid to define the new value as the largest of the old values $K' = max(K_1, K_2)$, but $K'$ will instead represent the remaining capacity if the lightest path to that node is taken. In this example, we will choose the former definition ($min(K_1, K_2)$), because tracking the heaviest path to each node may provide insight about the domain of the node. When merging the utility values, we will always keep the largest value $U' = max(U_1, U_2)$, so that $U'$ represents the value of the highest-utility path to that node.

### 2.2.2 Finding a Compact Decision Diagram

With the merge operator and equivalency defined, we have all of the tools necessary to turn a decision tree into a much more compact exact DD. All of the nodes in the bottom layer of a decision tree are trivially equivalent because the set of out-arcs for each such node is $\emptyset$. Thus, they can all be merged together without adding or removing any paths from the diagram. After merging all of the nodes on the bottom layer into a single node, denoted $t$, all of the nodes on the previous layer have only one destination. Thus, many of the nodes on the layer above $t$ may be equivalent, and can be merged together. This process can be repeated for each layer, from the bottom to the top, until all equivalent nodes have been merged. This is formalized in Algorithm 2, and demonstrated for $\mathcal{P}_{sack}$ in Figure 2.2.

**Algorithm 2:** Shrink Decision Tree into Decision Diagram

```
Input: A decision tree T with n + 1 layers, where n is the number of decision variables
Let Q be the set of nodes on layer n + 1
Let ⊕ be the merge operator defined in Algorithm 1
foreach index i, from n + 1 to 1 do
    foreach node u in layer i do
        foreach node v ≠ u in layer i do
            if u and v are equivalent then
                u ← u ⊕ v
            end
        end
    end
end
return T
```

Note that the process of shrinking a DD in Algorithm 2 is focused on clarity, not efficiency. An actual implementation would take care not to repeat checks for pairs of nodes and may pre-sort the nodes to make identifying equivalency candidates faster. Also note that there is no need to start from a decision tree; the process can start from any exact DD and will try to generate a more compact exact DD. All three of the diagrams with a single terminal node shown in Figure 2.2 are valid exact DDs for $\mathcal{P}_{sack}$.

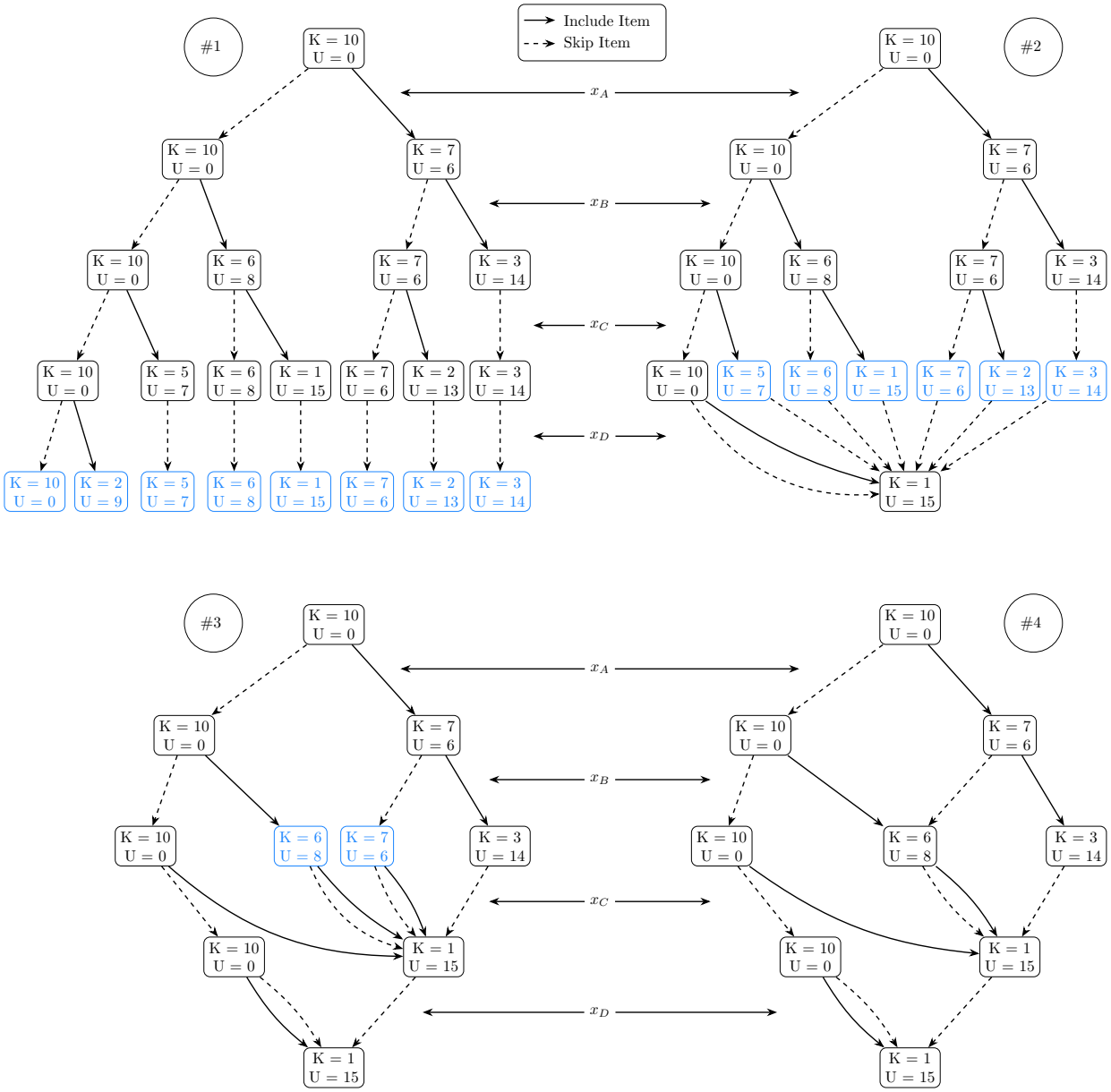


Figure 2.2 Shrinking the Decision Diagram for $\mathcal{P}_{sack}$

K:= remaining capacity, U:= utility. Nodes in blue are merged.

### 2.2.3 Reading a Solution

Once you have a valid exact DD for an optimization problem $\mathcal{P}$, finding the optimal solution to $\mathcal{P}$ is trivial. It can be done by recursively finding the best node at each layer starting from the bottom. *Best* means smallest for minimization problems, and largest for maximization problems.

Let $l(a)$ be the label of arc $a$, and let $\ell(u)$ be the index of the layer of node $u$. Let $f(a_{uv})$ be the objective value stored at node $u$, plus the impact on the objective function of traversing arc $a_{uv}$. In other words, $f(a_{uv})$ is the impact of setting $x_{\ell(u)} = l(a_{uv})$. Start from the terminal node $t$, and find the best $f(a_{ut})$ value, $f^* = f(a^*_{u^*t})$, where $u^* \in \{\text{nodes with an arc to } t\}$. The label $l(a^*)$ is the value of the decision variable represented by that layer; as we are starting from the bottom, $x_n = l(a^*)$. Then the process is repeated, replacing $t$ with $u^*$. This repeats layer by layer until the best path from the root to the terminal is identified. This path encodes the optimal solution. This process is formalized in Algorithm 3, and demonstrated in Figure 2.3 using $\mathcal{P}_{sack}$.

**Algorithm 3:** Read Solution from Decision Diagram

1 **NOTE:** This is normalized for minimization problems. For maximization problems change $\infty$ to $-\infty$ on Line 6, and change $f^* > f(a_{uq})$ to $f^* < f(a_{uq})$ on Line 9.
2 **Input:** A decision diagram with terminal node $t$ and root node $r$
3 Initialize $\pi^* \leftarrow \emptyset$
4 $q \leftarrow t$
5 **while** $q \neq r$ **do**
6 $\quad f^* \leftarrow \infty$
7 $\quad$ **foreach** *node $u$ with an arc to $q$* **do**
8 $\quad\quad$ **foreach** *arc $a_{uq}$ from $u$ to $q$* **do**
9 $\quad\quad\quad$ **if** $f^* > f(a_{uq})$ **then**
10 $\quad\quad\quad\quad f^* \leftarrow f(a_{uq})$
11 $\quad\quad\quad\quad u^* \leftarrow u$
12 $\quad\quad\quad\quad a^* \leftarrow a_{uq}$
13 $\quad\quad\quad$ **end**
14 $\quad\quad$ **end**
15 $\quad$ **end**
16 $\quad \pi^* \leftarrow \pi^* \cup \{l(a^*)\}$
17 $\quad q \leftarrow u^*$
18 **end**
19 Reverse the order of $\pi^*$
20 **return** $\pi^*$

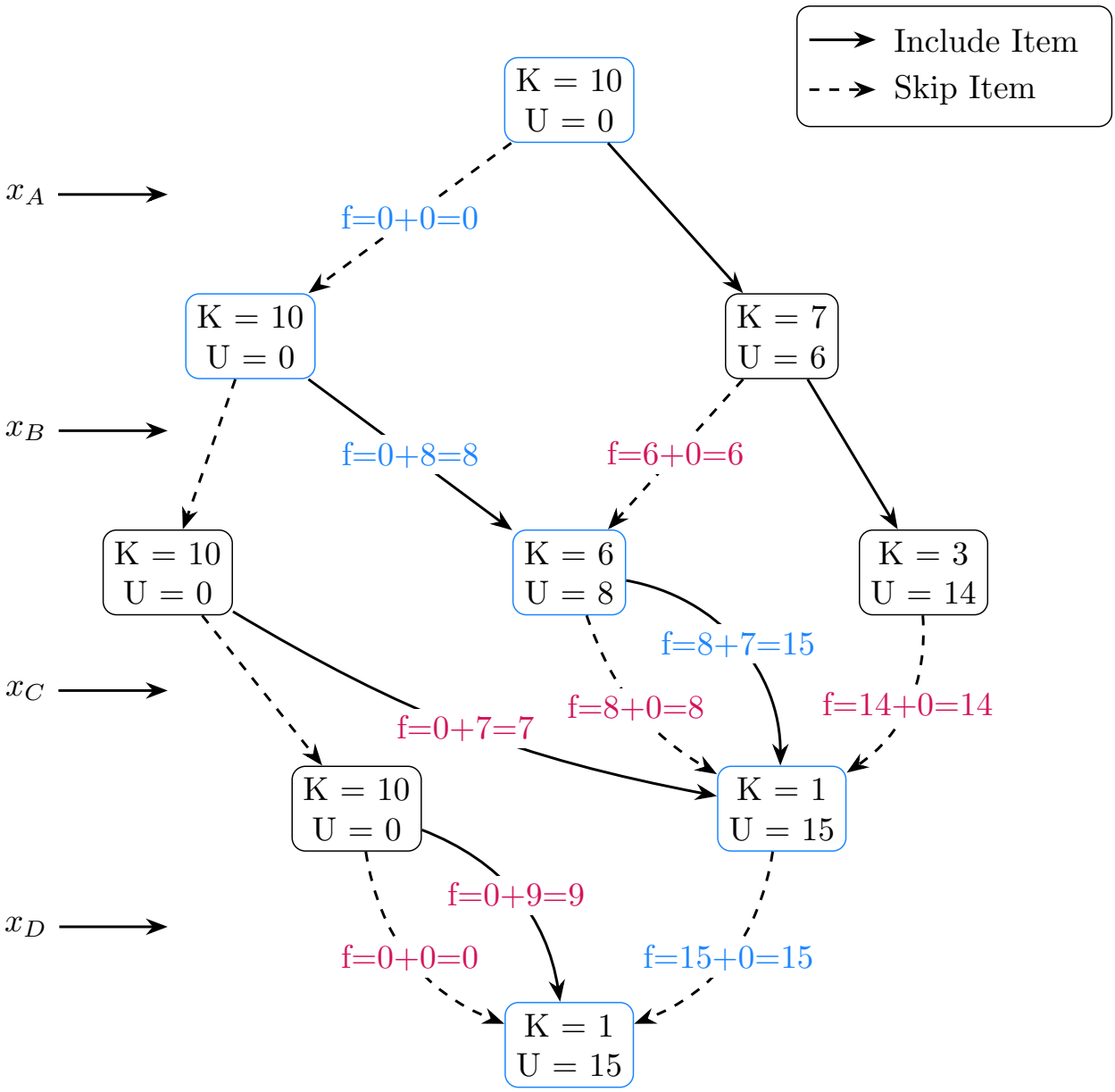


Figure 2.3 Reading the optimal solution for $\mathcal{P}_{sack}$

K:= remaining capacity, U:= utility.
Nodes and arcs in blue are part of the optimal solution.
Arcs in red are read but not explored.

### 2.2.4 Weighted & Multivalued Decision Diagrams

Up to this point, we have only considered an example with binary decision variables. Each item in $\mathcal{P}_{sack}$ is either included (1) or excluded (0). A DD that has binary arcs only is called a *Binary Decision Diagram* (BDD). So the DDs for $\mathcal{P}_{sack}$ in Figure 2.2 are all BDDs.

However, the methods described thus far also work when the domains of the decision variables are larger, as long as they are discrete. The only difference is that each node can have an out-arc for each element in its domain. Decision Diagrams with non-binary arcs are called *Multivalued Decision Diagrams* (MDDs). We are introducing this terminology because it is common in the literature. In this thesis, we often use DDs to refer to both BDDs and MDDs.

An example of an MDD is shown in Figure 2.4 using the $\mathcal{P}_{SOP}$ example from Section 2.1.2. In the $\mathcal{P}_{SOP}$ example, the only difference between the decision tree and the exact DD is that the nodes on the bottom layer have been merged into a single terminal node. This happens because the solution space is highly constrained by the precedence constraints. Note that each arc is storing two pieces of information. The first is the label of the arc, the second is the impact on the objective function of assigning the label of that arc to the decision variable on its layer. In this thesis, we will refer to this impact sometimes as the *weight* of the arc, and sometimes as the *cost* of the arc depending on the situation. When the arcs have weights, the DD is called *weighted* [20, 21].

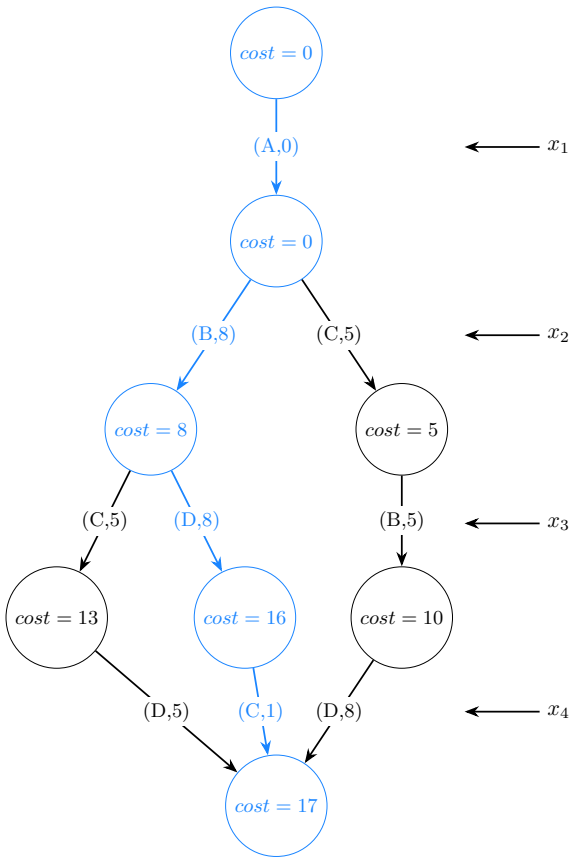


Figure 2.4 Exact Weighted MDD for $\mathcal{P}_{SOP}$

Optimal solution indicated in blue.

### 2.2.5 Top-Down Compilation

So far, this section has shown how a DD can exactly represent the solution space for an optimization problem $\mathcal{P}$, but the method described for generating an exact DD is useless because it requires a brute force exploration of the entire solution space. However, an exact DD can be constructed top-down without exploring the entire solution space using a technique inspired by Dynamic Programming [20–22].

This process begins as before; for each feasible initial decision, add a new node $u$, and add an arc $a_{ru}$ from the root $r$ to $u$. Let $d(u)$ be the *domain* of node $u$. The domain of a node $u$ is the set of assignments of values to the decision variable $x_{\ell(u)}$ that can be made on paths that pass through $u$. Equivalently, the domain of a node $u$ is the set of labels on out-arcs of $u$. Let the *aggregate domain* of a node $u$ be the set of every feasible partial solution that starts at $u$ and ends at $t$, i.e., the set of paths from $u$ to $t$ in a complete version of the DD.

If two nodes have the same aggregate domain, they are equivalent and can be merged. In this way, equivalent nodes can be merged top-down as the DD is created, instead of bottom-up after the fact. Thus, if $\mathcal{P}$ is a problem where the aggregate domain of a node pair can be proved equivalent without a brute force exploration of the solution space, then $\mathcal{P}$ may be a good candidate for generating an exact DD top-down. Algorithm 4 formalizes this process.

The $\mathcal{P}_{sack}$ example is a good example of a problem where an exact DD can be compiled top-down. The aggregate domain of a node in a knapsack problem is dependent only on its remaining capacity. Thus, if two nodes have the same remaining capacity, they have the same aggregate domains, and they are equivalent. Furthermore, there may be ranges of remaining capacity at each layer with matching aggregate domains that are easy to calculate. For example, at layer 3, the weights of the remaining items are 5 and 8 for items $C$ and $D$, respectively. In order to put both items in the knapsack, the knapsack would have to have a remaining capacity $K$ of 13, which exceeds the total weight limit of 10. Thus, having the maximum remaining capacity of 10 will only allow one of those items to be placed into the knapsack. Also, having a remaining capacity of 4 or less prevents item $C$ from being added to the knapsack, and having a remaining capacity of 7 or less prevents item $D$ from being added to the knapsack. Therefore, on layer 3, nodes with $K \in [0, 4]$ are equivalent, as are nodes with $K \in [5, 7]$ and nodes with $K \in [8, 10]$. Thus, if you generated an exact DD for $\mathcal{P}_{sack}$ top-down, the two highlighted nodes in DD #3 in Figure 2.2 could be proven equivalent without a brute force exploration of the solution space, because $K = 6$ and $K = 7$ are equivalent on layer 3.

In general, for the SOP, two nodes have the same aggregate domain if their in-arcs all have

**Algorithm 4:** Top-Down Compilation of Exact Decision Diagrams

**Input:** An unfinished Decision Diagram $\mathcal{M}$ with exactly one node, the root node $r$
Let $\oplus$ be the merge operator defined in Algorithm 1
Initialize $Q \leftarrow \{r\}$
Initialize $Q_{next} \leftarrow \emptyset$
**while** $Q \neq \emptyset$ **do**
    $Q_{next} \leftarrow \emptyset$
    **foreach** *node* $u \in Q$ **do**
        **foreach** *label* $l \in d(u)$ **do**
            Create a new node $v$
            $Q_{next} \leftarrow Q_{next} \cup \{v\}$
            Add arc $a_{uv}$ from $u$ to $v$
        **end**
    **end**
    **foreach** *pair of nodes* $\{u, v\} \in Q_{next}$ **do**
        **if** *$u$ and $v$ have the same aggregate domain* **then**
            $Q_{next} \leftarrow Q_{next} \backslash \{u, v\}$
            $Q_{next} \leftarrow Q_{next} \cup \{u \oplus v\}$
        **end**
    **end**
    $Q \leftarrow Q_{next}$
**end**
**return** $\mathcal{M}$

the same label and all incoming paths have visited the same set of elements. For example, a node with exactly one incoming path $[A, B, C]$ could be merged with a node in the same layer with exactly one incoming path $[B, A, C]$.

### 2.3 Restricted Decision Diagrams

In the previous section (2.2), we discussed what an exact DD is, and how one might be constructed. However, for most meaningful problems, constructing an exact DD is intractable. Exact DDs have their uses and remain an active area of research, but they are not a panacea. Restricted DDs are an alternative method of leveraging DDs [1].

A restricted DD for an optimization problem $\mathcal{P}$ encodes only feasible solutions to $\mathcal{P}$, but it may not encode every feasible solution to $\mathcal{P}$. Let $\mathcal{M}^-$ be a restricted DD for $\mathcal{P}$, and let $d(\mathcal{M})$ be the set of solutions encoded by Decision Diagram $\mathcal{M}$. A restricted DD for an optimization problem $\mathcal{P}$, is one where $d(\mathcal{M}^-) \subseteq Sol(\mathcal{P})$. Thus, the best path through $\mathcal{M}^-$, shortest for minimization and longest for maximization, is easy to find, feasible, and the best solution

encoded in the DD. Methods of generating restricted DDs are methods of generating a primal bound on $\mathcal{P}$ by searching for feasible solutions.

**Algorithm 5:** Top-Down Compilation of Restricted Decision Diagrams

**Input:** A unfinished Decision Diagram $\mathcal{M}^-$ with exactly one node, the root node $r$
Recall: $\ell(u)$ is the layer of node $u$
Let $\oplus$ be the merge operator defined in Algorithm 1
Initialize $Q \leftarrow \{r\}$
Initialize $Q_{next} \leftarrow \emptyset$
**while** $Q \neq \emptyset$ **do**
  $Q_{next} \leftarrow \emptyset$
  **foreach** *node* $u \in Q$ **do**
    **foreach** *label* $l \in d(u)$ **do**
      Create a new node $v$
      $Q_{next} \leftarrow Q_{next} \cup \{v\}$
      Add arc $a_{uv}$ from $u$ to $v$
    **end**
  **end**
  **foreach** *pair of nodes* $\{u, v\} \in Q_{next}$ **do**
    **if** *$u$ and $v$ have the same aggregate domain* **then**
      $Q_{next} \leftarrow Q_{next} \backslash \{u, v\}$
      $Q_{next} \leftarrow Q_{next} \cup \{u \oplus v\}$
    **end**
  **end**
  **if** $|Q_{next}| > \omega$ **then**
    Sort $u \in Q_{next}$ from best to worst by $f(u)$
    Trim $Q_{next}$ to length $\omega$ by removing the last elements
  **end**
  $Q \leftarrow Q_{next}$
**end**
**return** $\mathcal{M}^-$

Constructing restricted DDs is a straightforward process. Let $f(u)$ be the value of the objective function at node $u$. In other words, $f(u)$ is the sum of the arc weights on the best path from $r$ to $u$. First, a maximum width $\omega$ is selected. Then, you proceed as if generating a decision tree, but every time the width of the DD exceeds $\omega$, you remove the least promising nodes. The definition of *least promising* is heuristic, but for the sake of simplicity, we will assume in this section that the nodes with the least optimal objective function values are the least promising. Essentially, a restricted DD is just a generalized greedy heuristic [4, 23–25]. Note that we can still merge nodes with the same aggregate domains, because doing so will never remove or add any paths from the DD, just store them more efficiently. This process

is formalized in Algorithm 5.

The process of building a restricted DD with $\omega = 2$ is demonstrated for $\mathcal{P}_{sack}$ in Figure 2.5 and for $\mathcal{P}_{SOP}$ in Figure 2.6. In Section 2.2.5, we defined a method of determining if two nodes were equivalent for the SOP. However, in our experiments, we observed that the work of finding equivalent nodes in a restricted DD for a SOP often outweighed the benefit of being able to merge nodes. Thus, our implementation in Chapter 3 does not leverage equivalent node merging for the SOP.

In Figure 2.5, observe that the restricted DD contains the optimal solution, but unlike an exact DD, does not constitute proof that the solution is optimal. By contrast, in Figure 2.6, the optimal solution is excluded from the DD as it is constructed.

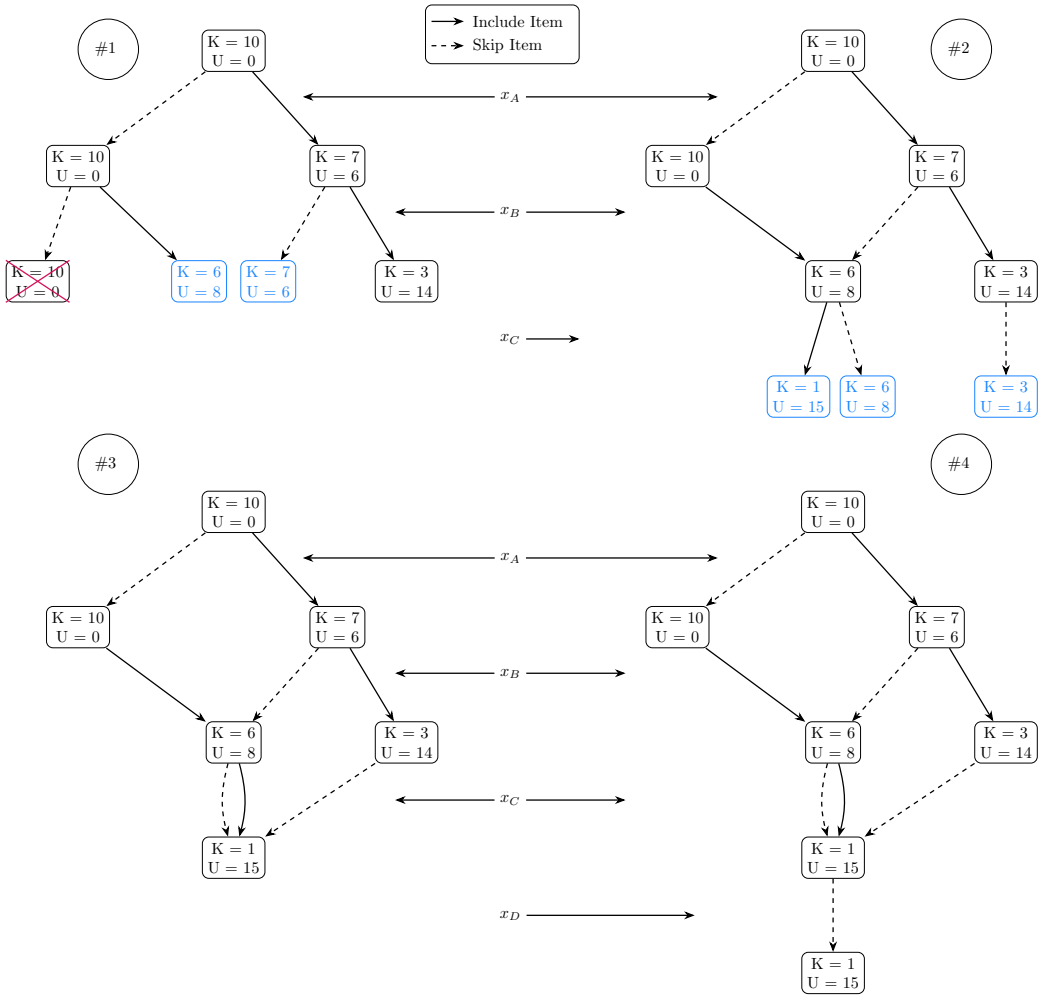


Figure 2.5 Restricted Decision Diagram for $\mathcal{P}_{sack}$

K:= remaining capacity, U:= utility. Nodes in blue are merged.

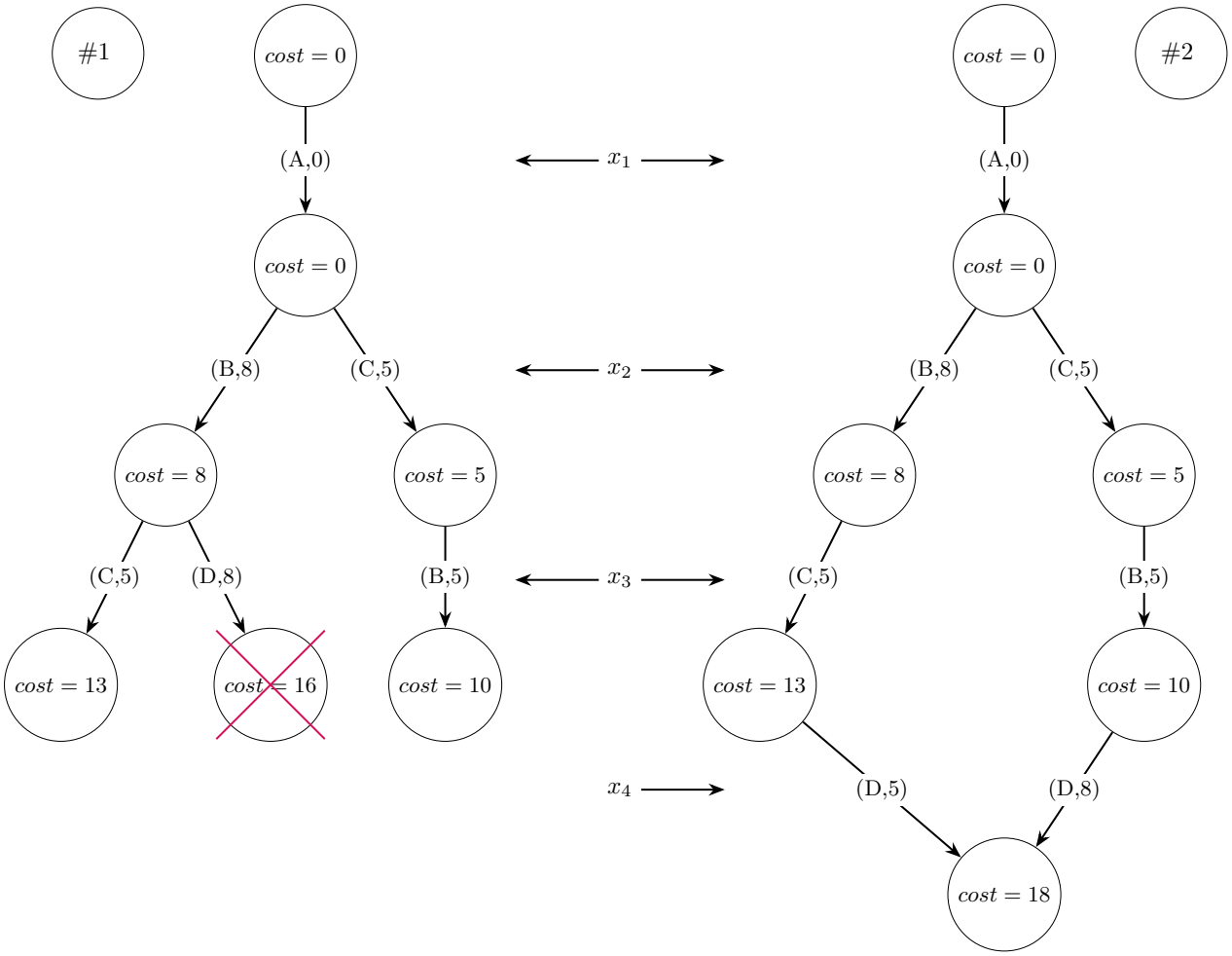


Figure 2.6 Restricted Decision Diagram for $\mathcal{P}_{SOP}$

## 2.4 Relaxed Decision Diagrams

As discussed in Section 2.3, restricted DDs provide a structure for searching for feasible solutions by encoding a subset of the feasible solutions. Relaxed DDs instead provide a relaxed (dual) bound on an optimization problem $\mathcal{P}$ [10–12, 26].

A relaxed DD for $\mathcal{P}$ encodes every feasible solution to $\mathcal{P}$, but it might also encode infeasible solutions to $\mathcal{P}$. Let $\mathcal{M}^+$ be a relaxed DD for $\mathcal{P}$. A relaxed DD for $\mathcal{P}$ is one where $Sol(\mathcal{P}) \subseteq d(\mathcal{M}^+)$. Thus, the best path through $\mathcal{M}^+$ is easy to find, potentially infeasible, and provides a dual bound on the best possible solution $\mathcal{P}$.

### 2.4.1 Top-Down Relaxed Decision Diagrams

Constructing a relaxed DD top-down requires more effort than constructing a restricted DD, but is conceptually similar. The algorithm is almost entirely the same, except that when the maximum width $\omega$ is exceeded, two nodes are merged together, as opposed to a node being removed. When nodes that are not equivalent are merged, potentially infeasible solutions are added to the DD, but no feasible solutions are removed. This is how adding infeasible solutions to the DD allows the DD to store all of the feasible solutions compactly [1, 10, 12, 26, 27].

Before we construct a relaxed DD, it is necessary to redefine the merge operator. In Algorithm 1, we detail a method of merging equivalent nodes, but now we will be merging non-equivalent nodes. The new procedure is almost the same as before, but instead of copying the out-arc from one of the nodes arbitrarily, we must now copy every out-arc of both nodes onto the new merged node. DDs are deterministic, so an arc is defined by its label and any repeat arc labels will be merged into a single arc. The new procedure is detailed in Algorithm 6. Note that this procedure also works on equivalent nodes, but the *if* statement on Line 13 will never trigger because $d(u) = d(v)$ by definition for equivalent nodes.

**Algorithm 6:** Generic Merge Operation for Non-Equivalent Nodes

```
1  Input: nodes u and v
2  Create a new node m
3  foreach in-arc a_zu of u do
4  |  Adjust the arc so that its destination is m instead of u, becoming a_zm
5  end
6  foreach in-arc a_zv of v do
7  |  Adjust the arc so that its destination is m instead of v, becoming a_zm
8  end
9  foreach out-arc a_uz of u do
10 |  Adjust the arc so that its origin is m instead of u, becoming a_mz
11 end
12 foreach out-arc a_vz of v do
13 |  if l(a_vz) ∉ d(m) then
14 |  |  Adjust the arc so that its origin is m instead of v, becoming a_mz
15 |  end
16 end
17 Delete u and v
18 return m
```

Now, we have the tools to build a relaxed DD. Recall that $f(u)$ is the sum of the arc weights on the best path from $r$ to $u$. First, a maximum width $\omega$ is selected. Then, the algorithm

proceeds as if generating a decision tree, but every time the width of the DD exceeds $\omega$, two nodes are selected and merged. The selection of those nodes is heuristic. Selecting the nodes strategically may result in a stronger relaxed bound, but the result will still be valid if you select randomly. In this section, for simplicity, we will use a heuristic that always merges the least promising nodes. Note that we can still merge nodes with the same aggregate domains, because doing so will never remove or add any paths from the DD, just store them more efficiently. The process of constructing a relaxed DD top-down is formalized in Algorithm 7.

**Algorithm 7:** Top-Down Compilation of Relaxed Decision Diagrams

**Input:** A unfinished Decision Diagram $\mathcal{M}^+$ with exactly one node, the root node $r$
Recall: $\ell(u)$ is the layer of node $u$
Let $\oplus$ be the merge operator defined in Algorithm 6
Initialize $Q \leftarrow \{r\}$
Initialize $Q_{next} \leftarrow \emptyset$
**while** $Q \neq \emptyset$ **do**
    $Q_{next} \leftarrow \emptyset$
    **foreach** *node* $u \in Q$ **do**
        **foreach** *label* $l \in d(u)$ **do**
            Create a new node $v$
            $Q_{next} \leftarrow Q_{next} \cup \{v\}$
            Add arc $a_{uv}$ from $u$ to $v$
        **end**
    **end**
    **foreach** *pair of nodes* $\{u, v\} \in Q_{next}$ **do**
        **if** $u$ *and* $v$ *have the same aggregate domain* **then**
            $Q_{next} \leftarrow Q_{next} \backslash \{u, v\}$
            $Q_{next} \leftarrow Q_{next} \cup \{u \oplus v\}$
        **end**
    **end**
    **while** $|Q_{next}| > \omega$ **do**
        Sort $u \in Q_{next}$ from best to worst by $f(u)$ `// heuristic`
        Let $u$ and $v$ be the last two elements $\in Q_{next}$
        $Q_{next} \leftarrow Q_{next} \backslash \{u, v\}$
        $Q_{next} \leftarrow Q_{next} \cup \{u \oplus v\}$
    **end**
    $Q \leftarrow Q_{next}$
**end**
**return** $\mathcal{M}^+$

In the $\mathcal{P}_{sack}$ example, two pieces of information stored on the nodes need to be merged: remaining capacity and utility. In order for the relaxed DD to yield a valid dual bound on

$\mathcal{P}_{sack}$, the information has to be merged in a way that does not remove any feasible paths from the aggregate domain of either node. This requires modifying one of the two rules defined in Section 2.2.1 for restricted DDs. Keeping the larger utility value $U$ when merging still tracks the best path, thus providing a bound on the longest feasible path to that node. However, for the $K$ values, we now must keep the larger of the $K$ values being merged. If we keep the smaller value, we may prevent items from being added to the knapsack even when there exists a feasible path through the node that includes it. Top-down compilation of a relaxed DD for $\mathcal{P}_{sack}$ is shown in Figure 2.7. The relaxed DD yields an upper (dual) bound of $U = 24$ on $\mathcal{P}_{sack}$. However, the solution that encodes that bound is $[x_A = 1, x_B = 1, x_C = 0, x_D = 1]$, which would have a remaining capacity of $-5$ and is infeasible. Thus, this is a dual bound but not an optimal solution.

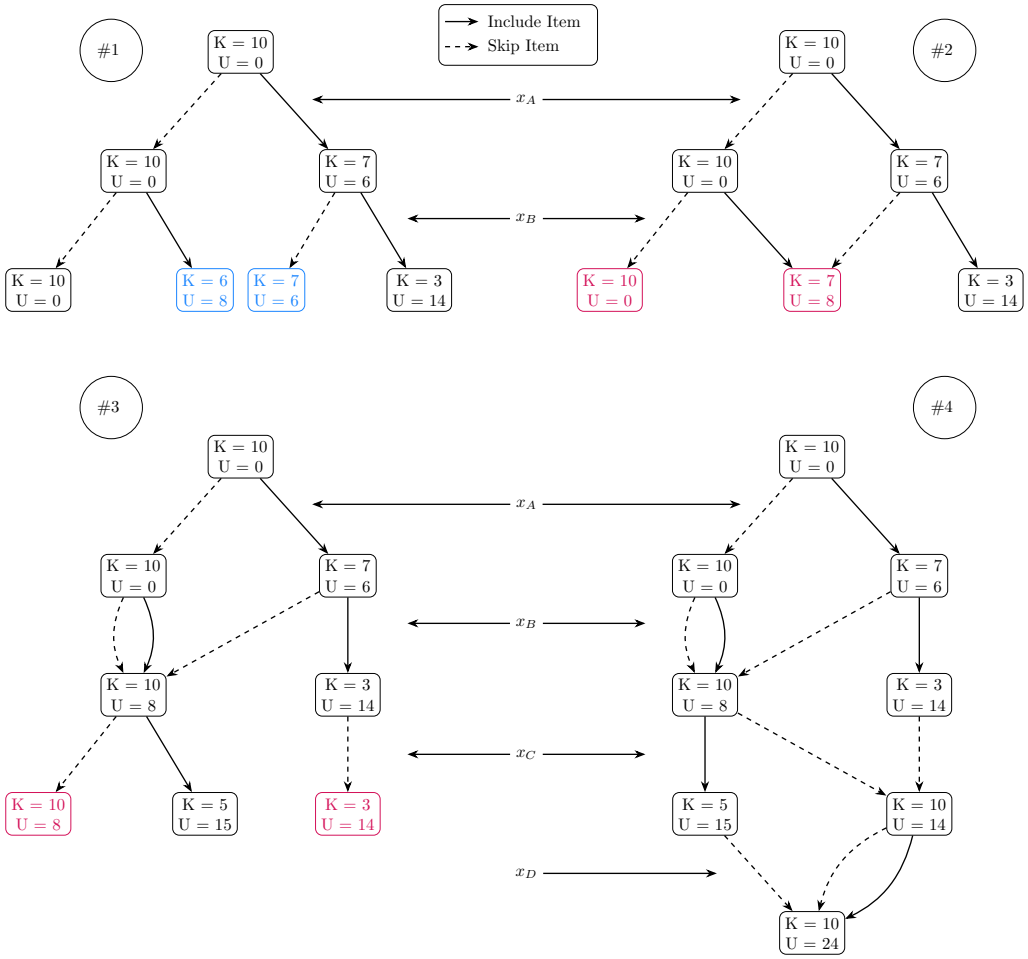


Figure 2.7 Top-Down Compilation of Relaxed Decision Diagram for $\mathcal{P}_{sack}$

K:= remaining capacity, U:= utility.
Equivalent node merges shown in blue.
Non-equivalent node merges shown in red.

$\mathcal{P}_{SOP}$ is a minimization problem instead of a maximization problem. Here, cost takes the place of utility, and the lower cost is kept when two nodes are merged. This way, the shortest path to each node is tracked. Another piece of information was being implicitly tracked that we will now explicitly track. When generating the arcs for a node $u$, the available arc labels $d(u)$ are the subset of labels that have not appeared on the path to $u$, and are not ruled out by precedence constraints. Therefore, going forward, we will track this information explicitly on the nodes. When we merge nodes $u$ and $v$ in a relaxed DD for $\mathcal{P}_{SOP}$, the domain of the new node is $d(u) \cup d(v)$. As a final step, observe that it is possible for the weight of an arc to be unclear. If one path to a node ends in $A$ and the other in $B$, then an out-arc with a $C$ label could take on either transition cost $c_{AC}$ or $c_{BC}$. To maintain the property that the DD is a valid relaxation, we will always use the smaller transition cost. Top-down compilation of a relaxed DD for $\mathcal{P}_{sack}$ is shown in Figure 2.8. The dual bound on $\mathcal{P}_{SOP}$ from the relaxed DD, with $cost = 14$, is valid but not feasible. It uses the solution $[x_1 = A, x_2 = B, x_3 = C, x_4 = C]$ which repeats $C$ twice.

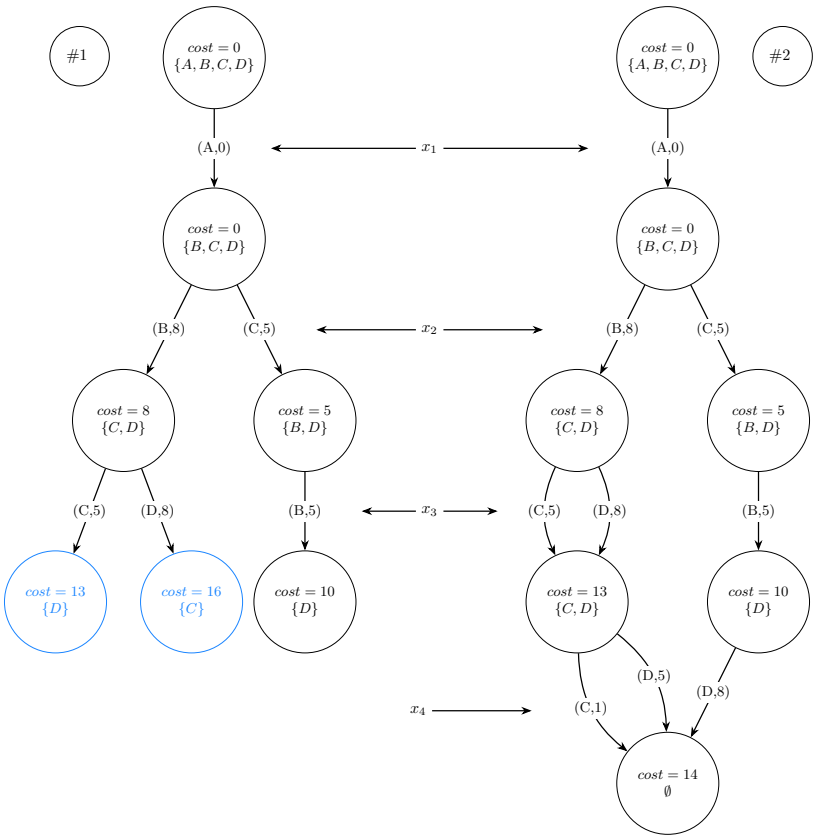


Figure 2.8 Top-Down Compilation of Relaxed Decision Diagram for $\mathcal{P}_{SOP}$

Node merges shown in blue.

### 2.4.2 Relaxed Decision Diagrams by Separation

Top-down generation of relaxed DDs is appealing because it is conceptually simple and quite powerful. However, there is another approach that allows for substantially more structural manipulation of the DD. A relaxed DD can instead be constructed by separation [12, 26]. The fundamental insight in making the shift from top-down to separation is recognizing that it is trivial to construct a relaxed DD with $\omega = 1$. If you were to make a $\omega = 1$ DD top-down, you would merge every layer into a single node. If $u$ is a node in that diagram on layer $\ell$, then $d(u) = d(x_\ell)$. Thus, $u$ will have one out-arc for each element $\in d(x_\ell)$. Figures 2.9 and 2.10 show $\omega = 1$ relaxed DDs for $\mathcal{P}_{sack}$ and $\mathcal{P}_{SOP}$ respectively.

To construct a relaxed DD top-down, you merge nodes on each layer until they do not exceed $\omega$. To construct a relaxed DD by separation, you instead split nodes on each layer until you have reached $\omega$, or there are no valid splits left to make. A split is a merge in reverse. A merge combines two nodes into a single node, reducing the size of the DD, and introducing potentially infeasible solutions. A split turns a single node into two nodes, increasing the size of the DD and removing infeasible solutions in the process. To perform a split, first, a node $u$ is selected to be split into $u$ and a new node $u'$. Then, a Boolean function is used to determine which in-arcs go to $u$ and which go to $u'$. All of the out-arcs of $u$ are copied onto $u'$. Finally, a filtering function is used to remove out-arcs of $u$ and $u'$ that are now infeasible.

The choice of Boolean function is heuristic, but we use the same one for all of the work in this thesis [28]. Normally, when a node $u$ is selected to be split, it is because a path being removed passes through $u$. Let $\phi$ be the label of the in-arc of $u$ on that path. In order to choose a subset of the arcs pointing at the old node $u$ during a split, we need a Boolean function for the in-arcs of $u$. Let $All_v^{\downarrow}$ be the set of labels visited by every path from the root node $r$ to node $v$. We use the function $h(a_{vu}, \phi)$, defined as follows:

$$h(a_{vu}, \phi) = \begin{cases} \textbf{true} & \text{if } \phi \in \left(All_v^{\downarrow} \cup label(a_{vu})\right) \\ \textbf{false} & \text{otherwise} \end{cases} \tag{2.1}$$

The result of using this function when splitting is that we now know that $\phi$ is on every path to $u'$. Using this function, node splitting is formalized in Algorithm 8.

Let an *exact node* be a node $u$ such that every path from $r$ to $u$ would result in a node with the same aggregate domain in a decision tree for the problem being solved. In other words, an exact node is a node that has only ever merged with equivalent nodes, and has only exact nodes as parents and ancestors. An exact node never needs to be split because the information encoded by the node is exact and not relaxed. With that in mind, to construct

**Algorithm 8:** Node Splitting [28]

**Input:** a node $u$ on layer $L$ in relaxed DD $\mathcal{M}^+$

Let $in(u)$ be the the set of arcs that end at $u$
Let $out(u)$ be the set of arcs that originate from $u$
Let $a_{vu}$ be an arc going from node $v$ to node $u$
Let $h(a_{vu}, \dots)$ be a function that takes in an arc (as well as any other relevant information) and returns *true* or *false* (see Eq. 2.1)

Create a new node $u'$
$L \leftarrow L \cup \{u'\}$
**foreach** $a_{vu} \in in(u)$ **do**
    **if** $h(a_{vu}, ...)$ **then**
        Redirect $a$ such that $a_{vu'}$
    **end**
**end**
**foreach** $a_{uv} \in out(u)$ **do**
    Create and add arc $a_{u'v}$ such that $l(a_{uv}) = l(a_{u'v})$
    filter($a_{uv}$), filter($a_{u'v}$) `// filter(a) removes arcs that violate constraints`
**end**
**return** $\mathcal{M}^+$

a relaxed DD by separation, you split nodes on each layer until you have reached $\omega$, or until all remaining nodes in the layer are exact nodes. In both the original work [28] and in this work, we split the nodes in each layer going from the top down. There is no reason that it must be done in this order, but our efforts to find an alternative order that performs better, or even as well, have been unsuccessful.

There are two more heuristic choices to be made before finalizing a procedure for constructing a relaxed DD by separation. Each time a node is split, that node must have been chosen from its layer. The heuristic we use for node selection is to pick the node containing the best path through the DD. For the sake of this explanation, let $\mathcal{P}_{\min}$ be a minimization problem. In a relaxed DD $\mathcal{M}^+$ for $\mathcal{P}_{\min}$, the length $z$ of the shortest path $\pi$ is a dual bound on the value of the optimal solution $z^*$. If $\pi$ is feasible, then $\pi$ is the optimal solution, and $\mathcal{P}_{\min}$ has been solved. If $\pi$ is infeasible, then removing it from $\mathcal{M}^+$ will cause a new path $\pi'$ with length $z'$ to become the new shortest path through $\mathcal{M}^+$. This new path has the property that $z \leq z' \leq z^*$. Thus, by selecting the node to split that contains the best path, we are making an attempt to improve the dual bound generated by $\mathcal{M}^+$.

The second heuristic decision follows directly from node selection. Once a node $u$ is selected to be split, a decision must be made about which arc label to split on. The heuristic we just described for selecting a node to split was premised on a desire to remove the best path from $\mathcal{M}^+$. In order to follow through on that premise, we will simply select the arc label on an in-arc of $u$ that contains that path. Now all of the heuristic decisions have been addressed, and Algorithm 9 formalizes this procedure for constructing relaxed DDs by separation.

**Algorithm 9:** Compilation of Relaxed Decision Diagrams by Separation [28]

**Input:** A $\omega = 1$ relaxed Decision Diagram $\mathcal{M}^+$
Recall: $\ell(u)$ is the layer of node $u$
Recall: $f(a_{vu}) = f(v)$ plus the impact on the objective function of setting $x_{\ell(u)} = l(a_{vu})$
Let $\ominus(u, a)$ be the split operation defined by Algorithm 8 that splits on node $u$ and passes arc $a$ to a Boolean function to sort the arcs
Let $in(u)$ be the set of arcs that end at $u$
**foreach** *layer* $L$ *of* $\mathcal{M}^+$ **do**
  **while** $U = \{u : u \in L, u \text{ is not exact}\} \neq \emptyset$ *AND* $|L| < \omega$ **do**
    Select a node $u \in U$ with the best $f(u)$
    Select the arc $a_{vu} \in in(u)$ with the best $f(a_{vu})$
    $u' \leftarrow \ominus(u, a_{vu})$
    $L \leftarrow L \cup \{u'\}$
  **end**
**end**
**return** $\mathcal{M}^+$

Figure 2.9 demonstrates the construction of a relaxed DD by separation for $\mathcal{P}_{sack}$. Note that this DD is different from the one constructed top-down (Figure 2.7). Despite being different, both DDs yield a valid dual bound on $\mathcal{P}_{sack}$. The DD constructed by separation provides a stronger bound in this instance. There is no theoretical guarantee of this, but in practice, there is often more information available about the impact a split might have during separation, than about the impact a merge might have during top-down construction. This is because when constructing a DD top-down, you only have information about the layers you have already constructed, but when constructing a DD by separation, you have information about every layer.

Figure 2.10 demonstrates the construction of a relaxed DD by separation for $\mathcal{P}_{SOP}$. This DD is the same as the one generated top-down (Figure 2.8), but this is merely a coincidence. As shown by $\mathcal{P}_{sack}$, there is no theoretical guarantee that this will happen.

Note that if you did not pick a maximum width $\omega$ when constructing a relaxed DD by separation, and instead continued to split nodes until every layer contained only exact nodes,

then the resulting DD would be exact. This method works well on some problems, but it is not typically powerful enough on its own to solve problems of a useful size.

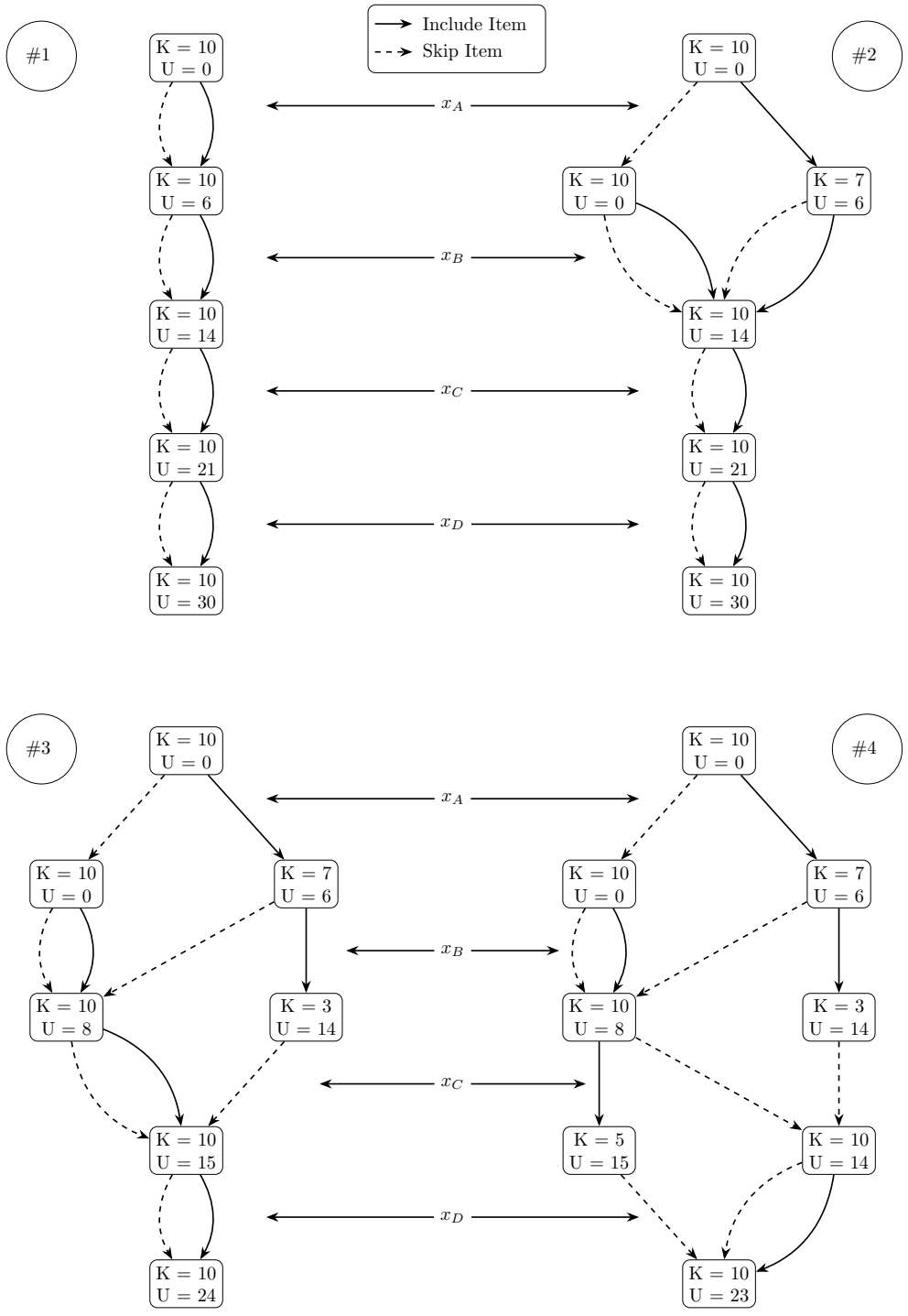


Figure 2.9 Compilation of Relaxed Decision Diagram by Separation for $\mathcal{P}_{sack}$

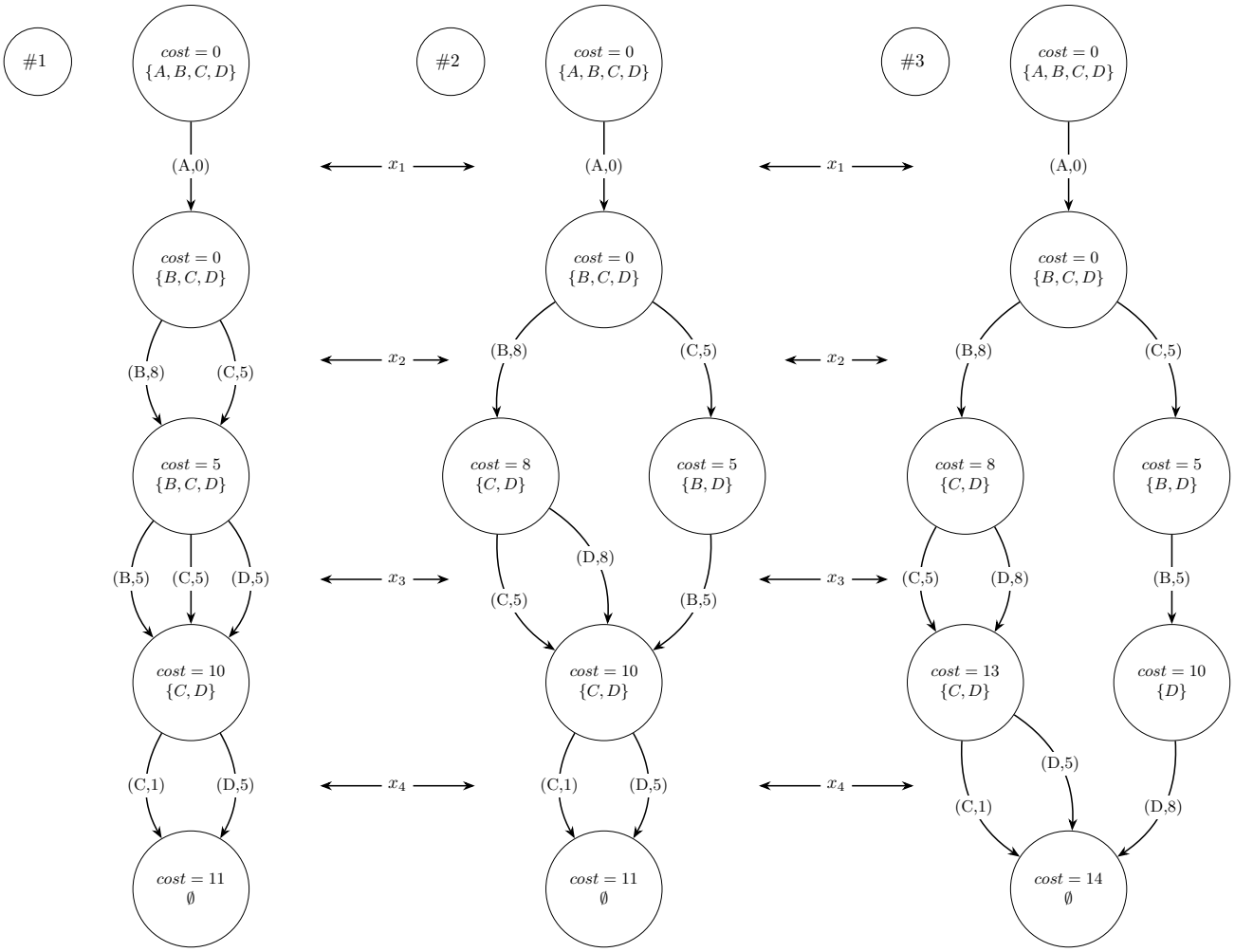


Figure 2.10 Compilation of Relaxed Decision Diagram by Separation for $\mathcal{P}_{SOP}$

## 2.5 Decision Diagrams for Sequencing Problems

In this section, we will dive into specific methods for using relaxed DDs to solve sequencing problems. While the content of this section is included in *Decision Diagrams for Optimization* [1, 10, 28], it is not typically included in a general explanation of Decision Diagrams. It is included here because the work in this thesis makes extensive use of these techniques. Furthermore, understanding these techniques is worthwhile, because they clearly demonstrate the utility of constructing relaxed DDs by separation.

Sequencing problems have the constraint that each variable must take a different value. For example, in the well-known Traveling Salesman Problem (TSP), the salesman must visit each city in a list of $n$ cities exactly once. Let $i, j \in \{1, ..., n\}$ and $i \neq j$, and let $x_i$ be the $i^{th}$ city

visited. In any solution where $x_i = x_j$, then there is a city being visited more than once, and so the solution is infeasible. More concretely, every variable in the TSP must take a different value. This is often referred to as the *AllDifferent* constraint by the Constraint Programming (CP) community [29].

### 2.5.1 Encoding the AllDifferent Constraint

The presence of an AllDifferent constraint, which includes all of the decision variables, allows for substantial trimming of nodes and arcs; this is the form constraint propagation takes when generating relaxed DDs by separation. In Section 2.4.2, we introduced the notation $All_u^{\downarrow}$ as the set of labels visited by every path from the root node $r$ to node $u$. We now also define the symmetric notation $All_u^{\uparrow}$ as the set of labels visited by every path from $u$ to $t$. Similarly, we define $Some_u^{\downarrow}$ as the set of labels visited by at least one path from the root node $r$ to node $u$, and $Some_u^{\uparrow}$ as the set of labels visited by at least one path from $u$ to $t$.

When constructing a relaxed DD top-down, you can track $All_u^{\downarrow}$ and $Some_u^{\downarrow}$, but the symmetric information, $All_u^{\uparrow}$ and $Some_u^{\uparrow}$, about paths to $t$, is not available. By contrast, when constructing a relaxed DD by separation, you start from a valid relaxed DD with $\omega = 1$. All four pieces of information can be recursively stored on each node in this initial DD. $All_u^{\downarrow}$ and $Some_u^{\downarrow}$ are recursively calculated for each node going top-down, and then $All_u^{\uparrow}$ and $Some_u^{\uparrow}$ are recursively calculated for each node going bottom-up. When a node is split, the values of these pieces of information for the new nodes can be recalculated easily from the values stored in their parents and children. Algorithm 10 explains how to calculate the initial values for $Some_u^{\downarrow}$, and can be trivially modified to handle $Some_u^{\uparrow}$, $All_u^{\downarrow}$, and $All_u^{\uparrow}$ as well.

**Algorithm 10:** Calculating Initial $Some_u^{\downarrow}$ Values [28]

**Input:** A relaxed Decision Diagram $\mathcal{M}^+$ with root node $r$
**foreach** *layer* $L \in \mathcal{M}^+$ **do**
  **foreach** $u \in L$ **do**
    $Some_u^{\downarrow} \leftarrow \emptyset$
    **foreach** *parent* $v$ *of* $u$ **do**
      $Some_u^{\downarrow} \leftarrow Some_u^{\downarrow} \cup Some_v^{\downarrow}$
      **foreach** *arc* $a_{vu}$ *from* $v$ *to* $u$ **do**
        $Some_u^{\downarrow} \leftarrow Some_u^{\downarrow} \cup \{l(a_{vu})\}$
      **end**
    **end**
  **end**
**end**
**return** $\mathcal{M}^+$

Once the four path-based pieces of information are known, they can be used to trim nodes and arcs. We will not enumerate every method of doing so here, but we will provide two examples. In a DD with the AllDifferent constraint, a feasible path must contain every label exactly once. Given a node $u$, if $|Some_u^{\downarrow} \cup Some_u^{\uparrow}| \neq n$, then there is at least one label that does not appear on any path passing through $u$. Thus, there are no feasible paths that pass through $u$, and $u$ can be removed from the DD. Alternatively, if $|All_u^{\downarrow} \cap All_u^{\uparrow}| \geq 1$, then there is at least one label on every path from $r$ to $u$ that is also on every path from $u$ to $t$. Again, there are no feasible paths that pass through $u$, and $u$ can be removed from the DD.

As a final note, recall that in Section 2.4.2, we defined an exact node as a node $u$ such that every path from $r$ to $u$ results in a node with the same aggregate domain. For sequencing problems with the AllDifferent constraint, a node is exact if, and only if, $Some_u^{\downarrow} = All_u^{\downarrow}$, and all in-arcs of $u$ originate from exact nodes. In other words, every label that is on any path to $u$ must be on every path to $u$.

### 2.5.2 Encoding a Generalizable Optimality Constraint

Path-based information is not the only information that can be leveraged. Specific problems may have other specific information worth storing, but some information is relevant to any optimization problem $\mathcal{P}$ being solved with a relaxed DD constructed by separation. For example, using the same recursive method that was used to calculate the path-based pieces of information, you can also calculate values that track the objective function. Let $z_u^{\downarrow}$ be the length of the best path from $r$ to $u$, and let $z_u^{\uparrow}$ be the length of the best path from $u$ to $t$. Let $z$ be the value of the best known solution to a minimization problem $\mathcal{P}_{\min}$. If there is a node $u$ such that $z_u^{\downarrow} + z_u^{\uparrow} \geq z$, then there is no path through $u$ with a value lower than the value of the best known solution. Thus, $u$ can be removed from the DD, because every path through $u$ is worse than, or equivalent to, the best known solution. The *filter* function, referred to in Algorithm 8, leverages all of the constraints encoded using methods like the ones described in this section.

In general, any constraint that can be encoded using methods like those described in the preceding paragraphs can be used to trim nodes from the DD. The *filter* function, referred to in Algorithm 8, is adapted to each specific optimization problem for the purpose of removing nodes that violate constraints, both general constraints that apply to any optimization problem and constraints specific to the individual problem.

## 2.6 Branch-and-Bound with Decision Diagrams

Branch-and-bound (BnB) is a well-known method for solving optimization problems, particularly Mixed Integer Programs (MIPs). This algorithm divides the problem into smaller sub-problems (branching) and explores the sub-problems by estimating their bounds. If the bound of a particular sub-problem proves it cannot possibly contain the optimal solution, that sub-problem is not further explored (bounding). This approach helps significantly reduce the number of calculations by eliminating large parts of the search space.

Traditionally, BnB solvers use a linear relaxation in the form of an LP to generate dual bounds on sub-problems. A DD-based BnB solver, instead, uses a combinatorial relaxation in the form of a relaxed DD. This idea inspired a new field of research studying the potential and limitations of such a solver. This thesis is part of that effort, focused on making a cutting-edge DD-based solver that leverages DDs constructed by separation.

In a typical BnB algorithm, the branching takes place by splitting on the domain of the variables. With decision diagrams, the branching takes place on the nodes themselves by selecting a set of exact nodes that represents the problem [1,7,8]. The solver outline from [1] defines an exact node as a node $u$ for which every path from $r$ to $u$ ends in an equivalent state. This is the language of Dynamic Programming and is equivalent to the definition given in Section 2.4.2 that every such path results in an equivalent aggregate domain.

An *exact cutset* is defined as a set of exact nodes that contain every path from $r$ to $t$. Let $\mathcal{M}^+(u)$ be a relaxed decision diagram with root $u$, and let $\mathcal{M}^-(u)$ be a restricted decision diagram with root $u$. The branch-and-bound algorithm for DDs proceeds by selecting an exact cutset of $\mathcal{M}^+$, and using each node $u$ in the cutset as the root for a new restricted decision diagram $\mathcal{M}^-(u)$, and relaxed decision diagram $\mathcal{M}^+(u)$. A node can be removed from the queue if the relaxation of that node is not better than the best known solution to $\mathcal{P}$, otherwise the exact cutset of the new node is added to the queue, and the process repeats until the queue is empty. This is detailed by Algorithm 11.

Figure 2.11 demonstrates DD-based BnB with $\omega = 2$ for $\mathcal{P}_{sack}$. The initial restricted DD is the one from Figure 2.5, and the initial relaxed DD is the one from figure 2.7. In step #1, the initial restricted DD $\mathcal{M}^-$ is constructed, but it is not exact, so the best solution in $\mathcal{M}^-$ is stored: $z_{opt} = z(\mathcal{M}^-)$. In step #2, the initial relaxed DD $\mathcal{M}^+$ is constructed. The upper bound on utility provided by $\mathcal{M}^+$ of $U = 24 > z_{opt}$, so there may still be a better solution. An exact cutset of $\mathcal{M}^+$ is identified, and then in steps #3 and #4, restricted DDs are generated for each node in the cutset. In this case, they are both exact, and no better solution was found, so $z_{opt} = z^*(\mathcal{P}_{sack}) = 15$. If one of the restricted DDs had not been

**Algorithm 11:** Decision Diagram based Branch-and-Bound (BnB) [8]

**Note:** This is normalized for minimization
Let $\mathcal{M}(uu')$ be a partial DD with root $u$ and terminal $u'$
Let $z(\mathcal{M})$ be the length of the best (shortest) path through $\mathcal{M}$
Let $z_{opt}$ be the value of the best known solution
$Q = \{r\}$
$v(r) \leftarrow 0$
$z_{opt} \leftarrow \infty$
**while** $Q \neq \emptyset$ **do**
  $u \leftarrow$selectNode($Q$), $Q \leftarrow Q \backslash \{u\}$ ;  `// selects a node to process arbitrarily`
  $\mathcal{M}^- \leftarrow \mathcal{M}^-(u)$
  **if** $z(\mathcal{M}^-) + v(u) < z_{opt}$ **then**
    $z_{opt} \leftarrow z(\mathcal{M}^-) + v(u)$
  **end**
  **if** $\mathcal{M}^-$ *is not an exact DD* **then**
    $\mathcal{M}^+ \leftarrow \mathcal{M}^+(u)$
    **if** $z(\mathcal{M}^+) + v(u) < z_{opt}$ **then**
      $S \leftarrow$ exactCutset($\mathcal{M}^+$)
      **foreach** $u' \in S$ **do**
        $v(u') \leftarrow v(u) + z(\mathcal{M}^+(uu'))$
        $Q \leftarrow Q \cup u'$
      **end**
    **end**
  **end**
**end**
**return** $z_{opt}$

exact, a relaxed DD would have been generated for that branch, and the process would have continued for another iteration.

Figure 2.12 demonstrates DD-based BnB with $\omega = 2$ for $\mathcal{P}_{SOP}$. The initial restricted DD is the one from Figure 2.6, and the initial relaxed DD is the one from Figure 2.10. The process unfolds almost exactly as it does with BnB for $\mathcal{P}_{sack}$.

A notable advantage of this procedure is that memory use is kept minimal. At each step, the previous DD is removed from memory, and the next one takes its place. The only thing that needs to be stored is the processing queue of exact nodes. Thus, even on large problems, memory use can be managed by changing $\omega$. However, memory use cannot be strictly defined, because the size of the processing queue is unpredictable.

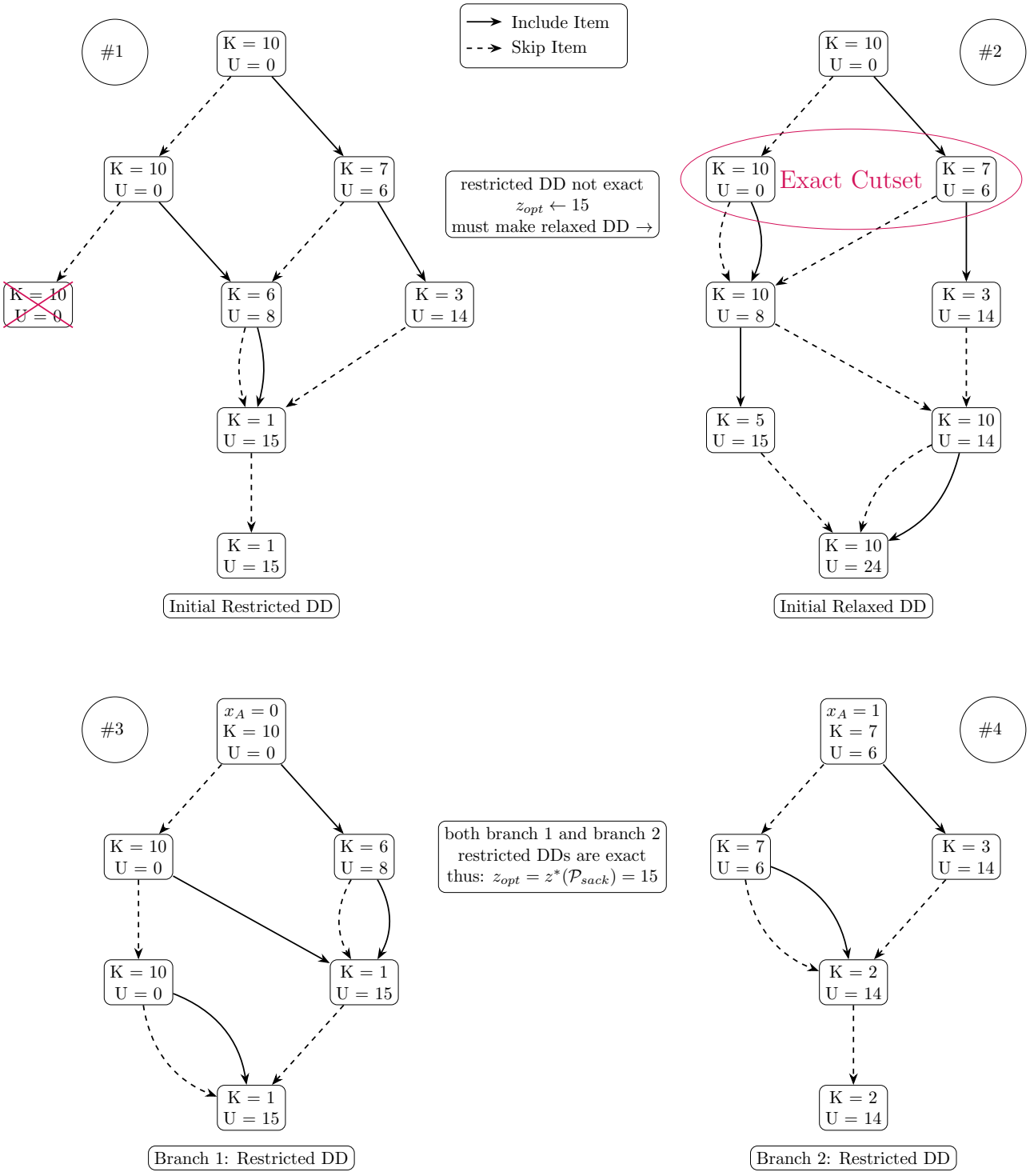


Figure 2.11 DD-Based Branch-and-Bound on $\mathcal{P}_{sack}$

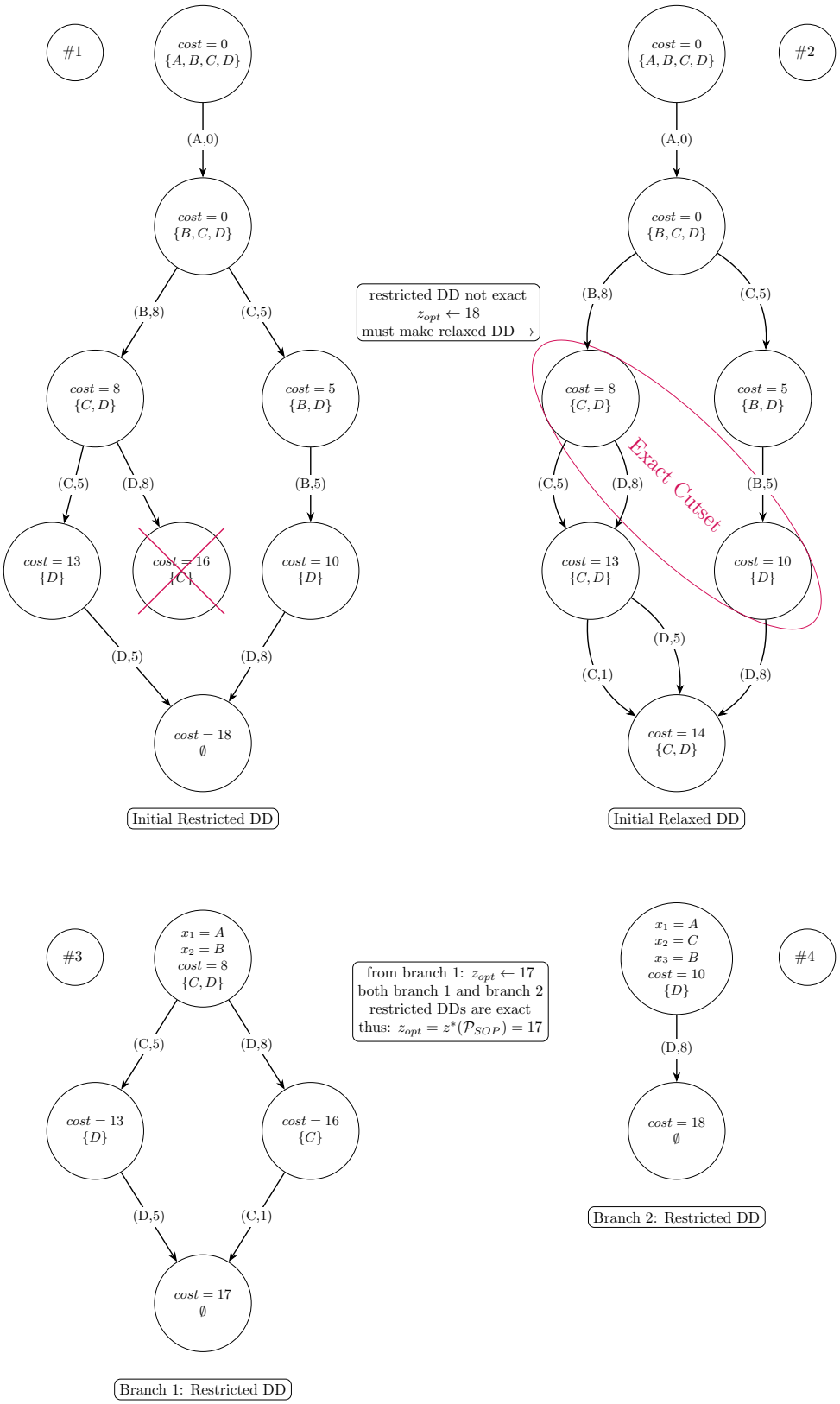


Figure 2.12 DD-Based Branch-and-Bound on $\mathcal{P}_{SOP}$

## 2.7 Other Innovations in DD-Based Solvers

In recent years, there have been significant advancements in DD-based solvers and related techniques. This research has proven the utility of DDs, applying them effectively to a variety of complex problems. This exploration has been symbiotic with other fields, with researchers continually discovering innovative ways to integrate DDs with other types of solvers. These novel methods often enhance DD-based solvers as well. As the field is still relatively new, it holds tremendous opportunity for substantial improvements in solver capabilities. This section explores some of the major efforts to leverage and enhance DD-based techniques.

### 2.7.1 ddo

An effort closely aligned with the work in this thesis is the development of the *decision-diagram-based optimization* solver (ddo) [5, 30]. To the best of our knowledge, ddo currently represents the only other initiative exploring techniques for implementing the original DD-based branch-and-bound algorithm (Algorithm 11) in a generic way. The principal difference between the ddo approach and the one detailed in this thesis is that the work on the ddo focuses on what can be achieved with relaxed DDs that are constructed top-down, compared to our emphasis on DDs constructed by separation. Although our implementations have diverged significantly, some of their ideas have directly inspired aspects of our work. These influences are discussed in the relevant chapters, but we will briefly touch on the pertinent techniques here.

In an early paper on this topic, Algorithm 11 is improved by incorporating a local search [4]. The modified algorithm uses a heuristic to quickly compute a *rough relaxed bound* at each node. If the sum of the shortest path length to a node with the rough relaxed bound for that node exceeds the best known solution, the node can be removed. More formally, let $\mathcal{P}_{\min}$ be a minimization problem, let $rrb(u)$ be a rough relaxed bound on the distance between $u$ and $t$, let $v(u)$ be the shortest distance from $r$ to $u$, and let $z_{opt}$ be the value of best known solution to $\mathcal{P}_{\min}$. If $v(u) + rrb(u) > z_{opt}$, the node can be removed. The authors demonstrate that if $rrb(u)$ is inexpensive to compute, it can be useful for filtering nodes in $\mathcal{M}^+$ and $\mathcal{M}^-$. However, their approach necessitates the creation of problem-specific heuristics. In Section 4.2.2, we introduce a generalized version of this concept, termed *embedded restricted decision diagrams*. This concept was developed independently from, but concurrently with, their work on dominance-based pruning [25, 31], which also uses rough relaxed bounding techniques. Thus, embedded restricted decision diagrams share some similarities with this work.

### 2.7.2 Arc-Flow Formulation

The arc-flow formulation presents a different approach to utilizing DDs. In these algorithms, each path through the DD encodes a partial solution, and achieving a complete solution involves iteratively solving a linear programming problem (LP) [32, 33]. For instance, in graph coloring [34], a DD is constructed where each path represents a single color. Then an LP is solved, treating the DD as a maximum flow graph where each unit of flow corresponds to a color. If the resulting flow is non-integer, the DD is refined, and the LP is rerun until the coloring is feasible.

This technique is quite powerful and also offers an easy way to integrate continuous variables into a DD-based solver. In a collaboration with Danielle Ripsman that has not been published yet, we applied the arc-flow formulation to design radiation therapy treatments with limited apertures. In radiation therapy, a beam is directed through a custom aperture with the objective of targeting all harmful cells while minimizing damage to healthy ones. First, we construct a DD, then we solve a MIP flow model where each positive flow on an arc signifies its use in an aperture, and finally, we refine the DD until a feasible aperture design is achieved using the MIP.

### 2.7.3 HADDOCK

The HADDOCK project, short for Handling Automatically Decision Diagrams Over Constraint Kernels, introduces a language and framework designed to integrate Decision Diagrams (DDs) with Constraint Programming (CP) techniques. This integration aims to guide and enhance the CP search process [35]. A significant focus of this work has been to fully embed a DD-based solver within a CP solver [36], leading to the development of numerous encodings, similar to those detailed in Section 2.5.

These efforts underscore the vast potential of research into blending DD-based methods with concepts from other disciplines, showcasing the innovative ways these integrations can advance work in multiple fields. The HADDOCK project also has particularly well-thought out implementations of DDs for use with other solvers. It provides a strong starting point for considering how DDs are handled in memory, and how to make DD-based operations efficient.

### 2.7.4 DIDP

Domain Independent Dynamic Programming (DIDP) is a new area of research parallel to work on DD-based solvers [37]. The ideas for DD-based solvers were directly inspired by

Dynamic Programming (DP), and DIDP is similarly inspired by DP. There are multiple implementations of the DIDP solver, all using the Dynamic Programming Description Language (DyPDL), a formalism introduced to define DP models based on a state transition system inspired by AI planning.

Since DIDP and DDs are both inspired by DP, DIDP solver techniques incorporate ideas from the DD literature for guiding searches. DIDP also integrates methods from AI planning with those DD-based techniques. This exploration will undoubtedly yield new methods of incorporating ideas from other fields alongside DDs.

### 2.7.5 Variable Ordering

It is also worth mentioning some of the relevant literature on variable ordering. The success of a DD-based algorithm can vary greatly based on the variable order used to construct the underlying DDs [21]. The study of how to generate good orderings is an active area of research.

There is an enormous amount of work on variable ordering for DDs that predates their use for optimization [38–41]. However, there has also been some research dedicated to variable ordering techniques for DD-based optimization. Two notable works include using reinforcement learning to find better orderings for a given problem [42] and using a portfolio approach to run multiple orderings in parallel and select the most successful one [43]. Further research on general improvements to variable ordering may lead to substantially more efficient DD-based solvers.

# CHAPTER 3 PEEL-AND-BOUND

**Contributions and Publication Information**

This chapter is largely based on *Peel-and-Bound: Generating Stronger Relaxed Bounds with Multivalued Decision Diagrams*, by Isaac Rudich, Quentin Cappart, and Louis-Martin Rousseau. It was published at the 28th International Conference on Principles and Practice of Constraint Programming (CP 2022) [6], where it won the Best Paper award. The paper introduces a novel paradigm for DD-based solvers and includes a performance test demonstrating its competitive edge against DD-based branch-and-bound.

This chapter also includes content from *Improved Peel-and-Bound: Methods for Generating Dual Bounds with Multivalued Decision Diagrams* by Isaac Rudich, Quentin Cappart, and Louis-Martin Rousseau, which was published in the Journal of Artificial Intelligence Research in 2023 [9]. The content included from this paper is solely explanatory, and does not contain the paper's contributions.

**Differences:** While the content of this chapter is based on the aforementioned papers, much of it has been rewritten, and the figures demonstrating peel-and-bound have been changed.

## 3.1 Motivation

The motivation for peel-and-bound (PnB) stems from an observation about how DD-based branch-and-bound (BnB) (Algorithm 11) interacts with the generation of relaxed DDs by separation (Algorithm 9). When a relaxed DD $\mathcal{M}^+$ is constructed by separation in a BnB structure, a large portion of the work done while generating each $\mathcal{M}^+$ is repeated at every iteration. To create the relaxed DD $\mathcal{M}^+_\omega(u)$ rooted at exact node $u$ with width $\omega$, the relaxed DD $\mathcal{M}^+_1(u)$ is constructed and then refined. To refine $\mathcal{M}^+_1(u)$, you iterate over each layer from the top down, splitting nodes until each layer either reaches the maximum width $\omega$, or has no valid splits remaining.

Consider the usual scenario where the nodes are split in a predetermined order. The static order of node splits means that for each node $v \in \mathcal{M}^+_1(u)$, the first split performed on $v$ is the same in both $\mathcal{M}^+_1(r)$ and $\mathcal{M}^+_1(u)$. The existing in-arcs of $v$ will be sorted in the same

way in both $\mathcal{M}_1^+(r)$ and $\mathcal{M}_1^+(u)$. The only difference between the two DDs is the possibility of filtering arcs in $\mathcal{M}_1^+(u)$ that could not be filtered in $\mathcal{M}_1^+(r)$ due to the added constraint that all paths, in every valid construction of $\mathcal{M}^+(u)$, pass through $u$. The extra filtered arcs are the reason that $\mathcal{M}^+(u)$ may produce a stronger bound than $\mathcal{M}^+(r)$. However, because splits are performed in the same order and manner each time, many arcs that were filtered while constructing $\mathcal{M}^+(r)$ will be filtered again while constructing $\mathcal{M}^+(u)$.

There is a sub-graph of $\mathcal{M}^+(r)$, induced by node $u$, that contains all of the paths that will be encoded in $\mathcal{M}^+(u)$, but does not contain the arcs that are filtered from both DDs during construction. Thus, less work needs to be performed at each iteration of BnB by starting from that sub-graph instead of $\mathcal{M}_1^+(u)$.

If the split order is static, the same DD is generated starting from either $\mathcal{M}_1^+(u)$, or the sub-graph induced by $u$. If the split order changes between BnB iterations, the sub-graph induced by $u$ is still a valid construction of $\mathcal{M}^+(u)$, but the generated DD will differ from the one that was refined from $\mathcal{M}_1^+(u)$.

Later in Section 3.3, a repeated sub-graph during BnB is visualized in Figure 3.1.

## 3.2 Algorithm

The mechanism for starting each relaxed DD after $\mathcal{M}^+(r)$ from a sub-graph of a previously generated DD, can be embedded into a slightly modified version of DD-based BnB (Algorithm 11). In PnB, the queue stores DDs instead of nodes. After the initial relaxation $\mathcal{M}^+(r)$ is generated, the entire DD is placed into the queue $Q$ such that $Q = \{\mathcal{M}^+(r)\}$. Then, a DD $\mathcal{M}^+(u)$ is selected from $Q$ (for the first iteration $\mathcal{M}^+(u) = \mathcal{M}^+(r)$). However, instead of selecting an exact cutset of $\mathcal{M}^+(u)$, only a single exact node $e$ from $\mathcal{M}^+(u)$ is selected. Then, $e$ will be *peeled* from $\mathcal{M}^+(u)$. The process of selecting a DD and exact node are heuristic decisions that are discussed in Section 3.4.

The process of peeling $e$ to construct $\mathcal{M}^+(e)$ is as follows. Remove $e$ from $\mathcal{M}^+(u)$, and then let $e$ be the root node of a new DD $\mathcal{M}^+(e)$. Note that $e$ still has out-arcs that end in $\mathcal{M}^+(u)$. For each node $v$ in $\mathcal{M}^+(u)$ with an in-arc that originates in $\mathcal{M}^+(e)$, a new node $v'$ is made and added to $\mathcal{M}^+(e)$. Each in-arc $a_{ov}$ of $v$ that originates in $\mathcal{M}^+(e)$ is removed, and then arc $a_{ov'}$ is added to $\mathcal{M}^+(e)$. Then, a copy of each out-arc of $v$ is made with origin $v'$ instead of $v$, and the out-arcs of $v$ and $v'$ are filtered using filter functions like the ones described in Section 2.5. The process of removing and adding arcs is repeated until there are no arcs ending in $\mathcal{M}^+(u)$ that originate in $\mathcal{M}^+(e)$. Notably, this procedure not only accomplishes a top-down reading of the sub-graph induced by $e$, it also potentially strengthens $\mathcal{M}^+(u)$ by

removing nodes and arcs in the process. The peel operation is formalized in Algorithm 12.

**Algorithm 12:** Peeling Procedure

**Input:** A relaxed DD $\mathcal{M}^+$ with root $r$ and terminal $t$, and a node $u$ in $\mathcal{M}^+$
**Output:** a relaxed DD $\mathcal{M}^+(u)$ peeled from $\mathcal{M}^+$, and what remains of $\mathcal{M}^+$
**Notation Reference:**
$in(u)$ is the set of arcs that end at node $u$
$out(u)$ is the set of arcs that originate from node $u$
$in(\mathcal{M}^+)$ is the set of arcs that end in DD $\mathcal{M}^+$
$out(\mathcal{M}^+)$ is the set of arcs that originate in DD $\mathcal{M}^+$
Let $\mathcal{M}^+(u)$ be an empty DD
$in(u) \leftarrow \emptyset$ `// remove the in-arcs of` $u$
$\mathcal{M}^+ \leftarrow \mathcal{M}^+ \backslash u$
$\mathcal{M}^+(u) \leftarrow u$ `// initialize` $\mathcal{M}^+(u)$ `to be just` $u$
**while** $in(\mathcal{M}^+) \cap out\Big(\mathcal{M}^+(u)\Big) \neq \emptyset$ **do**
  **foreach** *node* $m \in \mathcal{M}^+$ *with an in arc that originates in* $\mathcal{M}^+(u)$ **do**
    Create a new node $m'$, and add it to $\mathcal{M}^+(u)$
    **foreach** *arc* $a_{md} \in out(m)$ **do**
      Add arc $a_{m'd}$
    **end**
    **foreach** *arc* $a \in in(m)$ *that originates in* $\mathcal{M}^+(u)$ **do**
      Change the destination of $a$ to $m'$
      filter($a$)
    **end**
    **foreach** *arc* $a \in out(m)$ **do**
      filter($a$)
    **end**
  **end**
**end**
**while** $\exists m \in \mathcal{M}^+$ *with* $in(m) = \emptyset \vee out(m) = \emptyset$ *(excluding* $r$ *and* $t$*)* **do**
  $in(m) \leftarrow \emptyset$
  $out(m) \leftarrow \emptyset$
  $\mathcal{M}^+ \leftarrow \mathcal{M}^+ \backslash \{m\}$
**end**
**return** $(\mathcal{M}^+(u), \mathcal{M}^+)$

PnB simply performs peels and refinements until optimality can be proven. If the shortest path through the modified $\mathcal{M}^+(u)$ is more optimal than the best known solution, $\mathcal{M}^+(u)$ is put back into $Q$. Then $\mathcal{M}^+(m)$ is refined using Algorithm 9, and, if the shortest path through the refined $\mathcal{M}^+(m)$ is more optimal than the best known solution, $\mathcal{M}^+(m)$ is added to $Q$. The whole procedure is repeated until there are no nodes left in the queue ($Q = \emptyset$). PnB is formalized in Algorithm 13.

**Algorithm 13:** Peel-and-Bound (PnB) Algorithm

**Input:** The initial relaxed DD $\mathcal{M}^+(r)$
**Notation Reference:**
$z(\mathcal{M})$ is the length of the best (shortest) path through $\mathcal{M}$
$Q \leftarrow \{\mathcal{M}^+(r)\}$
$z_{opt} \leftarrow \infty$ `// Value of the best known solution.`
**while** $Q \neq \emptyset$ **do**
  $\mathcal{D} \leftarrow$selectDiagram($Q$), $Q \leftarrow Q \backslash \{\mathcal{D}\}$
  $u \leftarrow$selectExactNode($\mathcal{D}$)
  $\mathcal{M}^+(u), \mathcal{D}^* \leftarrow$ peel($\mathcal{D}$, $u$) `// See Algorithm 12`
  **if** $z(\mathcal{D}^*) < z_{opt}$ **then**
    $Q \leftarrow Q \cup \{\mathcal{D}^*\}$
  **end**
  $\mathcal{M}^- \leftarrow \mathcal{M}^-(u)$. `// See Algorithm 5`
  **if** $z(\mathcal{M}^-) < z_{opt}$ **then**
    $z_{opt} \leftarrow z(\mathcal{M}^-)$
  **end**
  **if** $\mathcal{M}^-$ *is not exact* **then**
    $\mathcal{M}^+ \leftarrow \mathcal{M}^+(u)$ `// See Algorithm 9`
    **if** $z(\mathcal{M}^+) < z_{opt}$ **then**
      $Q \leftarrow Q \cup \{\mathcal{M}^+\}$
    **end**
  **end**
**end**
**return** $z_{opt}$

### 3.2.1 Complexity Analysis

Separating each node $u$ during a peel requires creating a new node $u'$, moving the in-arcs of $u$ that originate in the peeled DD $u$ to $u'$, copying the out-arcs of $u$ to $u'$, and then filtering the out-arcs of $u$ and $u'$. Creating a new node in our implementation has a time in $\mathcal{O}(n)$, where $n$ is the number of possible decisions, due to storing state information that has a size in $\mathcal{O}(n)$ (such as $All^{\downarrow}_u$). However, it is possible that, in other applications, the size of a node is in $\mathcal{O}(1)$. The number of in-arcs of $u$ is at most $\omega$, although this worst case is unlikely in practice because it requires $\mathcal{M}^+$ to have width $\omega$, and for each node in $\mathcal{M}^+$ on layer $\ell(u)-1$ to have an arc ending at $u$. Thus, moving the in-arcs of $u$ has a time in $\mathcal{O}(\omega)$. The number of out-arcs of $u$ is at most $n$, and each arc has a size in $\mathcal{O}(1)$, so copying the out-arcs has a time in $\mathcal{O}(n)$. Each individual filtering process has a time in $\mathcal{O}(1)$ as it uses only existing state information from $u$ and $u'$, and it is performed on the (at most $2n$) out-arcs of $u$ and $u'$. Thus, filtering the out-arcs has a time in $\mathcal{O}(n)$. Therefore, separating one node during

the peel process has a time in $\mathcal{O}(n+\omega)$. Separations during a standard relaxation procedure require selecting a node ($\mathcal{O}(\omega)$), making a new node ($\mathcal{O}(n)$), partitioning the in-arcs ($\mathcal{O}(n\omega)$), copying the out-arcs ($\mathcal{O}(n)$), and filtering the out-arcs ($\mathcal{O}(n)$). The reason that there can be more in-arcs during a standard relaxation procedure is because the nodes in a $\omega = 1$ DD can have in-arcs with different labels coming from the same node, whereas the structure of the DD during a peel guarantees that each node $u$ can have only one in-arc from each node on the layer $\ell(u) - 1$. Thus, the total time for a separation in a standard relaxation is in $\mathcal{O}(n\omega)$.

The maximum number of separations during a peel is the maximum number of nodes in the peeled DD. A peeled DD can have at most $(n-3)\times\omega+2$ nodes, and thus the number of nodes is in $\mathcal{O}(n\omega)$. Therefore, the entire peel process has a time in $\mathcal{O}(n^2w + n\omega^2)$. The maximum number of separations during a standard relaxation is the exact same as during a peel, since the resulting DD will be the same size. Thus, the standard relaxation has a total time in $\mathcal{O}(n^2\omega^2)$. However, PnB uses a peel to generate some fraction of the nodes, then a standard relaxation to generate the rest. Let $\alpha$ be the percent of nodes that are peeled during the peel. It follows that the total time for an iteration of PnB is in $\mathcal{O}(\alpha(n^2\omega + n\omega^2) + (1-\alpha)(n^2\omega^2))$. Therefore, the larger that $\alpha$ grows, the more time PnB saves over BnB.

### 3.3 Example and Visualization

To visualize a peel operation, we use a SOP instance, but not the one described in Section 2.1.2, because it has too few arcs to yield an informative visualization. Consider a new SOP instance where the goal is to order the elements $[A, B, C, D]$, subject to the precedence constraint that $A$ must precede $D$, an alphabetical ordering heuristic, and $\omega = 3$. For the sake of simplicity, we ignore arc costs.

First, we motivate PnB by identifying where BnB is repeating computations. Figure 3.1 shows $\mathcal{M}^+(r)$, and identifies an exact node $e$. Then, it shows $\mathcal{M}^+(e)$ in three stages. The first stage is the initial $\omega = 1$ DD. The second stage is after one split on each layer, and the third stage is the complete DD. The sub-graph shared by $\mathcal{M}^+(r)$ and $\mathcal{M}^+(e)$ is highlighted in blue, indicating that, in this case, the first two splits could have been read from $\mathcal{M}^+(r)$ instead of being re-created from scratch.

Figure 3.2 demonstrates a peel operation. Observe that the subgraph from Figure 3.1 is identified and peeled from the graph, without the need to redo work. Additionally, note that the DD the peel was initiated from was refined during the peel process. There is now less remaining work needed for PnB to process the DD than there was before the peel.

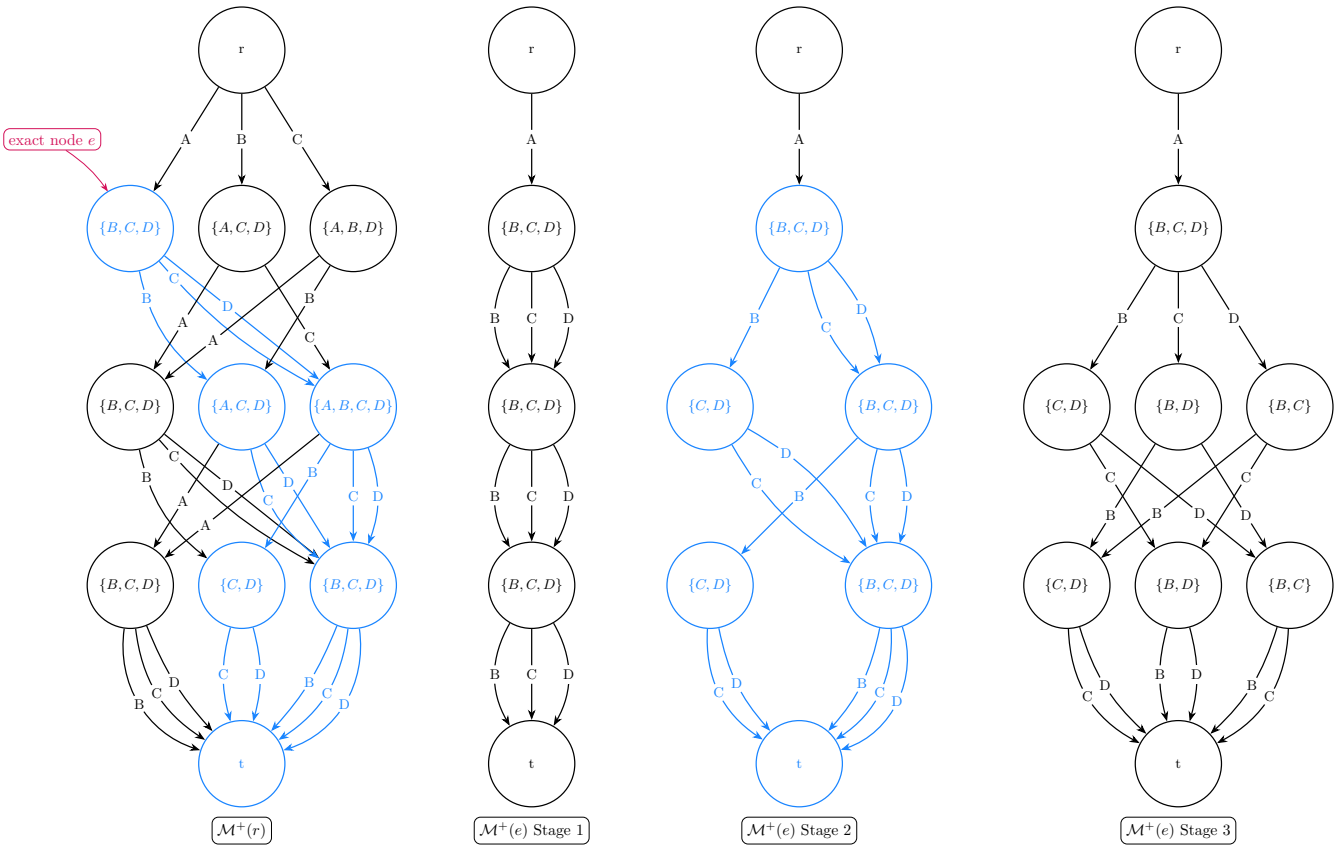


Figure 3.1 Example of a Repeated Sub-Graph During Branch-and-Bound

A sub-graph (shown in blue), and the associated relaxed DD with the same root, for a SOP instance. The objective is to order the elements $[A, B, C, D]$, subject to the precedence constraint that $A$ must precede $D$, an alphabetical ordering heuristic, and $\omega = 3$.

## 3.4 Advantages and Implementation Decisions

### 3.4.1 Node Selection

The original DD-based BnB algorithm [8] requires selecting an exact cutset of $\mathcal{M}^+$. PnB requires selecting a DD from the queue and an exact node to start the peel process. The choice of node has a substantial impact on how quickly the process converges to an optimal solution, because it serves two purposes simultaneously. As discussed earlier, the first purpose of peeling is to avoid recreating a portion of the DD at each iteration. The second purpose is to strengthen the overall relaxation.

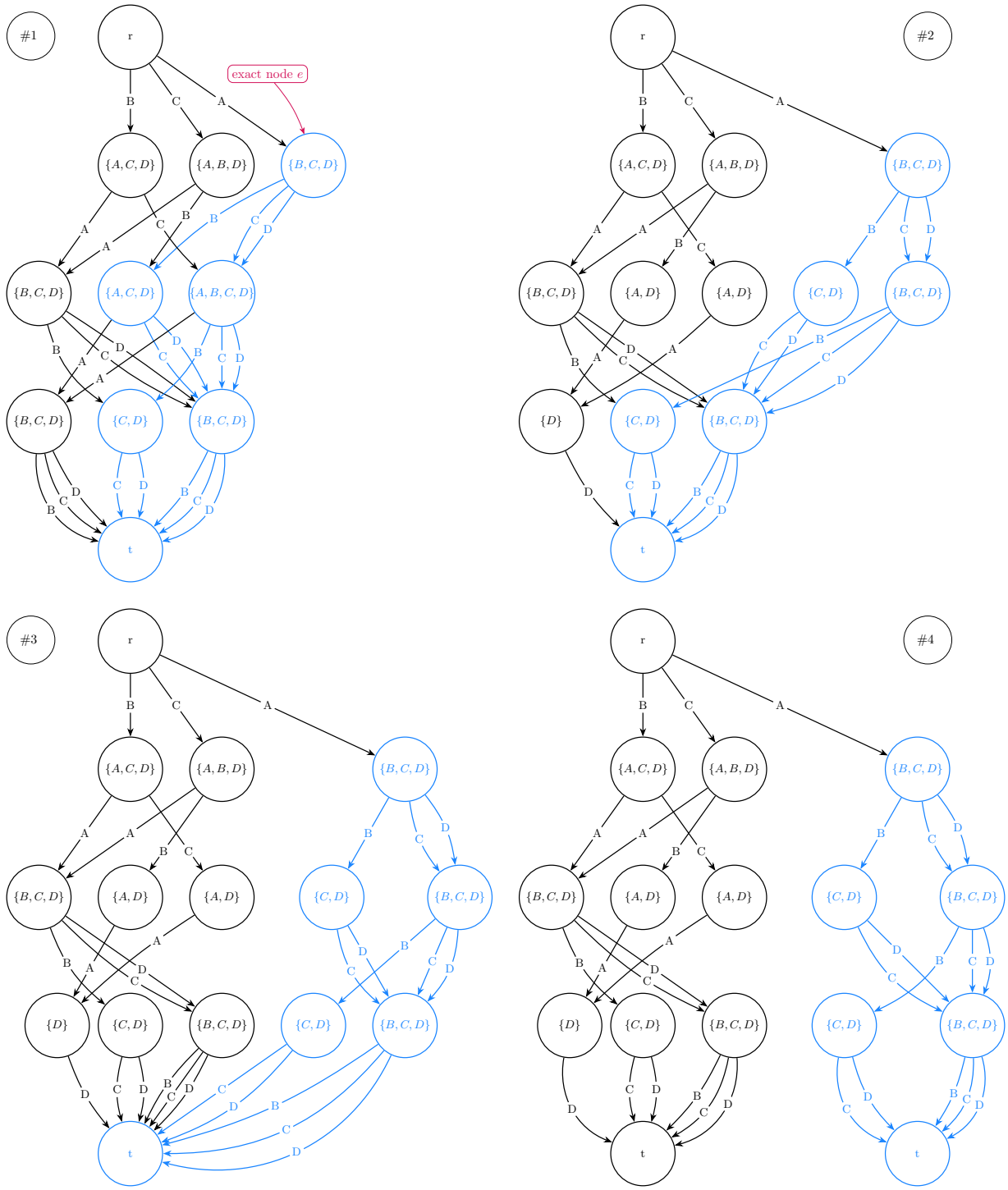


Figure 3.2 Example of a Peel Operation

In (1), $e$ is selected to induce the peel process and removed from the the original DD ($\mathcal{M}^+(r)$ from Figure 3.1). In (2) the arcs that connect $e$ to the original DD are moved to copies of the nodes they originally ended at, and infeasible arcs are filtered. In (3) and (4) the process is repeated until the DDs are disconnected.

Let $\mathcal{M}^+(u)$ be a DD peeled from $\mathcal{M}^+$, and let $\mathcal{M}^+_*$ be $\mathcal{M}^+$ after the peel operation. If $Sol(\mathcal{P}) \subseteq Sol(\mathcal{M}^+)$ then $Sol(\mathcal{P}) \subseteq Sol(\mathcal{M}^+_*) \cup Sol(\mathcal{M}^+(u))$. The only step of PnB that removes paths is the *filter* step, which only removes an arc if no feasible solutions can pass through that arc. If the node the peel is induced from contains the shortest path through $\mathcal{M}^+$, then there will be a new shortest path through $\mathcal{M}^+_*$ with $z(\mathcal{M}^+_*) \geq z(\mathcal{M}^+)$. Similarly after peeling, the peeled DD is going to be strengthened and $z(\mathcal{M}^+_\omega(u)) \geq z(\mathcal{M}^+(u))$. Therefore, when implementing the *selectDiagram* and *selectExactNode* functions from Algorithm 13, we propose selecting the DD $\mathcal{D}$ with the weakest bound, and an exact node from $\mathcal{D}$ that contains $z^*(\mathcal{D})$ at each iteration. Using these parameters, the peel step of PnB strengthens the relaxed bound of $\mathcal{P}$, in addition to providing a stronger initial DD to use when generating $\mathcal{M}^+(u)$.

We originally proposed two heuristics for selecting a node from $\mathcal{D}$ that contains $z(\mathcal{D})$. The first heuristic picks the first node in the shortest path through the DD with at least one child that is not exact, we call this the *last exact node*. The second heuristic picks the *frontier* node, the highest-index exact node that contains $z(\mathcal{D})$. Taking the last exact node is more of a breadth-first search that peels a large set of nodes where all of the paths to the nodes in the set share a beginning with $z^*(\mathcal{D})$. In contrast, taking the frontier node is more of a depth-first search, taking fewer nodes and exploring those nodes at greater depth.

### 3.4.2 Limitations and Handling Memory

The experiments we performed are on sequencing problems, but PnB can be easily applied to other optimization problems. However, some existing DD-based methods conflict with PnB. For example, some DD algorithms use a dynamic variable order [43], such that the variables the layers on $\mathcal{M}^-$ are mapped to in one iteration of BnB, are different in the next. PnB as it is presented in this work cannot be paired with a dynamic variable order. Furthermore, the method in this work is specific to DDs generated using separation. We explain how to extend the framework to DDs that use a merge operator in Section 4.2.3.

Memory limitations present a problem for PnB in theory, but not in practice. Each open DD remains in the queue, and thus must be stored in memory. However, this problem can be handled in many ways; two are given here. A dynamic method of handling the problem is to start targeting large DDs with bounds close to $z_{opt}$ as memory limitations start to become a problem. Such DDs can usually be closed quickly, and subsequently removed from memory, freeing up space for the algorithm to continue. Alternatively, the DDs with bounds closest to $z_{opt}$ can be deleted in favor of storing just the root node, then when they need to be processed, initial DDs are generated for those once again. This method essentially falls back to BnB until memory limitations cease to be a problem. Additional approaches for working

with memory limitations, and evidence that the problem can be handled efficiently have also explored [44].

### 3.4.3 Integrating Rough Relaxed Bounds

This implementation incorporates the rough relaxed bounding method (Section 2.7.1) [4]. Rough relaxed bounding was used to trim the domain of each node during construction of the restricted DDs, and was also added as a check to the *filter* function in Algorithm 9. When the initial model is created, a map is also created from each node $u$, to a list of the other nodes sorted by their distance from $u$. For the SOP (Section 2.1.2), the rough relaxed bound $rrb(a)$ of an arc $a_{fg}$ was calculated as follows. For each node $u$ that has not necessarily been visited ($u \notin All_g^{\downarrow}$), look up the shortest distance from that node to a different node that has also not been visited. Then, sort the resulting list, and repeatedly remove the largest value until the list has a length equal to the number of remaining decisions. The sum of the values in the list, plus the value of the shortest path from $r$ to the end of $a$, is the rough relaxed bound of $a$. If $rrb(a)$ is worse than the best known solution, the arc is removed.

### 3.4.4 Parallelization

The DD-based BnB shown in Algorithm 11 is particularly amenable to parallelization [5, 7]. Algorithms seeking to parallelize must overcome the data-race problem. In other words, if multiple processors are working on a problem simultaneously, then there must be a process in place to stop them from trying to write to the same place in memory at the same time. For many algorithms, this poses a substantial challenge or creates substantial overhead. However, for both DD-based BnB, and PnB, the solution is simple. As a problem is being solved, nodes (or DDs in the case of PnB) are placed into a processing queue. Each node/DD represents a discrete problem that needs to be solved, and can be processed separately. Given access to a sufficiently large number of processors, each node/DD added to the queue could be immediately dispatched to an available processor for processing. The only communication required between the processors is the current value of the best known solution.

In theory, this method of parallel processing could result in a linear improvement in time spent solving a problem when increasing the number of processors available, because $k$ processors may be able to process $k$ nodes, in the time it takes 1 processor to process 1 node. This process could also result in a superlinear speedup due to the non-deterministic processing order of elements in the queue. In the parallel implementation, one processor may find an improved bound which can then be utilized by the other processors. Therefore, elements from the queue could be processed using bounds that are better than the bounds used by

the single-thread deterministic implementation. The ability to identify better bounds earlier while parallel processing could yield less elements that need to be processed overall. In practice, however, there are heuristic decisions that must be made that can have a large impact on solve time.

The dilemma one encounters in implementation is the existence of a critical path in the solution finding process. To demonstrate this with an extreme example, consider a problem that does the following when solved using PnB on a single processor. Each time a node is peeled, one of the two resulting DDs is solved and closed without requiring any additional peel operations. Then, the single remaining DD is processed again, a node is peeled, and the whole process repeats itself $m$ times. In this example, there are roughly $2m$ DDs that need to be processed, but only 2 are ever available at the same time. So in this case, $k$ processors would take exactly as long as 2 processors to solve the problem. We propose two methods of handling this dilemma. The first is simple; reduce the maximum width of the DDs. When solving a problem that is encountering this critical path problem, the work can be divided more equitably among the available processors by reducing the amount of work done at each iteration. When using a single processor, a higher maximum width is almost always more desirable as long as the DDs can still be generated quickly, because the extra space makes it more likely that the DD will be solved instead of producing more DDs to add to the queue. Reducing the maximum width will increase the number of DDs that need to be processed to solve the problem, but also produces those DDs more quickly. A width too low can generate an enormous number of DDs without closing any of them. The optimal width to use is one that generates enough DDs for all available processors to have consistent work, but does not generate a large backlog of work.

The second method of handling the critical path issue is to use the peel process to redistribute work as needed. Each time a processor is available and not being used, the peel procedure can peel off a sub-graph for that processor to work on. The downside of this is that often, a lot of the work that only needed to be performed once will occur on both DDs. The first method of simply lowering the maximum width accomplishes the same goal, but each DD reaches its assigned maximum width before it is further processed, so arcs that can be processed out only need to be processed out of one DD. Any implementation of this second method would likely require more heuristic decisions to ensure the task scheduler distributes the work in a useful way.

## 3.5 Experiments on the Sequence Ordering Problem

The goal of this section is to assess the performances of PnB (Algorithm 13) as it compares to the standard DD-based BnB algorithm (BnB, Algorithm 11). Both algorithms were implemented in Julia and are open-source[1].

To ensure a fair comparison, both algorithms resort to the same function for generating relaxed DDs (Algorithm 9), and the same function for generating restricted DDs (Algorithm 5). While the functions being called are the same, there are two differences at run-time. At the end of line 11 in Algorithm 9, an additional operation runs during BnB where the values of the arcs leaving layer $j$ are updated. The second difference is that BnB starts each relaxation from a $\omega = 1$ DD, while PnB passes a partially completed DD to the relaxation function as a starting point.

The testing environment was built from scratch to ensure a fair comparison, so it lacks the many propagators used by cutting-edge solvers like CPO to remove nodes from the PnB/BnB queue [28, 45]. However, it provides a clean comparison of the two algorithms by requiring that every function used by both BnB and PnB is exactly the same between the two, with the only differences arising due to PnB's ability to ensure that all arcs are exact from the beginning. All of the heuristic decisions that were made are identical for both algorithms.

### 3.5.1 Description of the Heuristics Considered

The SOP can be considered an asymmetric TSP with precedence constraints (Section 2.1.2). The objective is to find a minimum cost path that visits each of the $n$ elements exactly once, and respects the precedence constraints. The method used for generating relaxed DDs requires creating a heuristic ordering of all possible arc assignments by importance. The arc values in this case are representative of the $n$ elements in the path. The ordering used was generated by sorting the $n$ elements, first by their average distance from the other elements, and then by the number of elements each element must precede. The resulting order places a higher importance on elements that are far away from other elements and must precede many other elements.

The BnB algorithm processes nodes in an order designed to try and improve the existing relaxed bound at each iteration. When a node $u$ is added to the BnB queue, it is assigned a value equal to the value of the shortest path from the root $r$ to the terminal $t$, that passes through $u$. The best known relaxed bound on the problem is the smallest value of a node in the queue, and that node is always chosen to be processed. PnB is implemented with the

[1] https://github.com/IsaacRudich/ImprovedPnB

same goal of improving bounds at each iteration. However, PnB stores DDs, not nodes. Let the value of a DD be the value of the shortest path to the terminal. At each iteration of PnB, the DD with the lowest value is selected, and then a node is chosen from that DD to induce the peel process. All of the experiments in this chapter used a process where the selected node is the first node in the shortest path from $r$ to $t$ with a child node that is not exact (the last exact node). Testing was done to determine whether using the last exact node or the frontier node would perform better for the problem being considered, but there was not a significant difference between the two during any of the tests. Several of the benchmark problems were run using various DD widths, and the last exact node was chosen because it sometimes showed a very slight improvement over the frontier node. While it is likely that this choice makes a difference on some problems, it does not matter for the SOP.

### 3.5.2 Experimental Results

The experiments were performed on a computer equipped with an AMD Rome 7532 at 2.40 GHz with 64Gb RAM. The solver was tested using DD widths of $64, 128$, and 256 on the 41 SOP problems available in TSPLIB [46]. For comparisons between PnB and BnB, a timestamp, new bounds, and the length of the remaining queue were recorded each time the bounds on a problem were improved. Another experiment was performed to test the scalability of PnB at width 2048, for which only the final bounds were recorded. Execution time was limited to $3,600$ seconds.

The smallest DD width tested for both methods was 64, and the largest DD width tested was 256. Table 3.1 has summary statistics for those widths as the percentage improvement demonstrated by PnB. A positive percentage always indicates that PnB performed better than BnB in that category, while a negative percentage indicates that BnB performed better. Figure 3.3 shows performance profiles for all of the experiments. Table 3.2 contains summary statistics comparing PnB at width 256 to PnB at width 2048, where a positive percentage always indicates that the width of 2048 performed better.

| | Width: 64 | | | | Width: 256 | | | |
|---|---|---|---|---|---|---|---|---|
| | RB | BS | OG | QL | RB | BS | OG | QL |
| Average % Improvement | 114% | 0.5% | 22.8% | 1,647% | 545% | 3.3% | 181% | 308% |
| Median % Improvement | 26% | 0.05% | 17.4% | 734% | 80% | 1.7% | 35% | 141% |

Table 3.1 Summary Statistics: Percentage Improvement of Peel-and-Bound Over Branch-and-Bound

RB = Relaxed Bound, BS = Best Solution, OG = Optimality Gap, QL = Queue Length. Tables A.1 and A.2 in Appendix A show the comprehensive results.

| | PnB: 2048 vs PnB: 256 | | |
|---|---|---|---|
| | Relaxed Bound | Best Solution | Optimality Gap |
| Average % Improvement | 19.5% | 0.8% | 18.6% |
| Median % Improvement | 16.3% | 0.5% | 13.7% |

Table 3.2 Summary Statistics: Percentage Improvement of Peel-and-Bound at $\omega = 2048$ over Peel-and-Bound at $\omega = 256$

Table A.3 in Appendix A shows the comprehensive results.

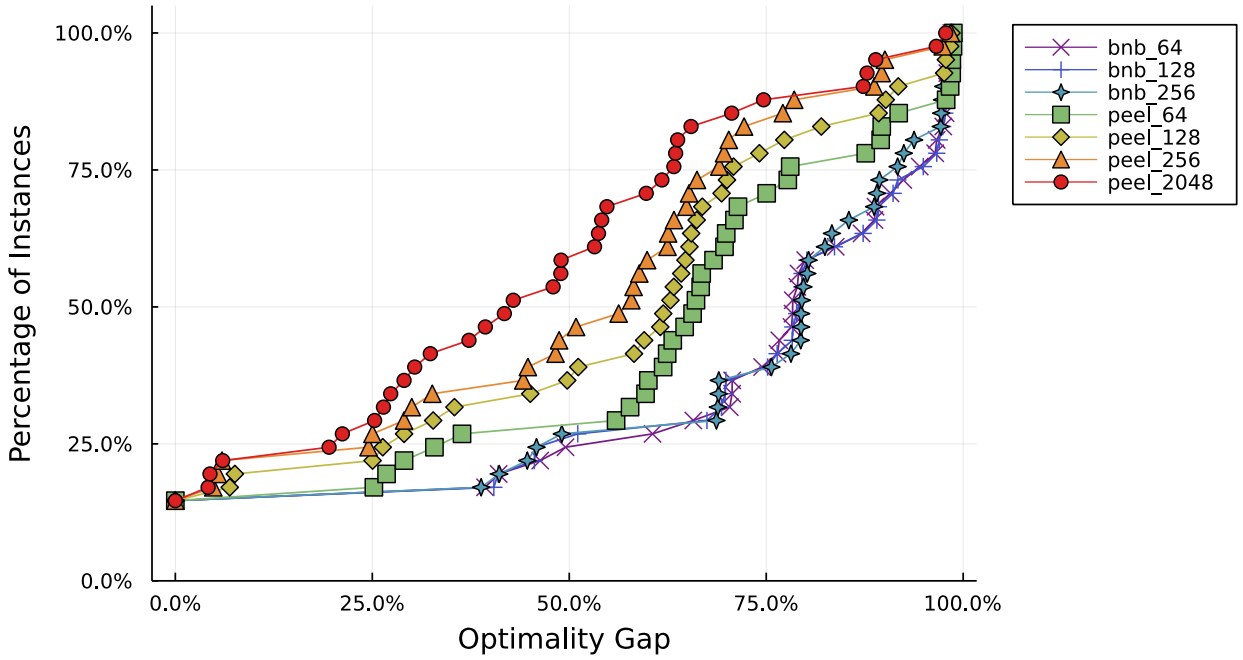


Figure 3.3 Performance Profiles: Peel-and-Bound and Branch-and-Bound

$$\text{optimality gap} = \frac{upper\_bound - lower\_bound}{upper\_bound}$$

As shown in Table 3.1, PnB vastly outperforms BnB in these experiments. The average and median improvements from using PnB at both widths are significant in terms of the relaxed bound, the remaining optimality gap, and the number of nodes that still need to be processed. The best solution found by the end of the runtime also tends to be slightly better with PnB, but the found solutions are often so close to the real optimal solutions that there is little room for improvement. At both widths, six of the problems were solved to optimality. BnB was faster in only one of those cases, and, in that case, the difference was .04 seconds. The median time for PnB to close in these cases was 191% faster at a width of 64, and 580% faster at a width of 256. The relaxed bound produced by PnB at a width of 64 was better for 28 of the remaining 35 problems, and at a width of 256 was better for 34 of the remaining 35 problems. The optimality gap was similarly better for PnB on every problem except the ones where BnB found a better relaxed bound. However, of the problems where BnB had a better optimality gap, the improvement was less than 1% for all but one problem.

Figure 3.3 reinforces that even though there are some instances where a specific BnB setting slightly outperforms a specific PnB setting, the gap in those cases is small relative to the general gap between all PnB settings and all BnB settings. As shown in Table 3.2, increasing the width to 2048 from 256 led to an 19.5% average improvement (16.3% median improvement) in the relaxed bound. Figure 3.3 also shows that the performance of PnB nearly uniformly increases with the maximum allowable width. Similar to the difference between BnB and PnB, some specific instances see a small out-performance of the PnB running at a smaller width, but the gap is small relative to the usual gap between the 2048-width experiment and the rest of the experiments. Finally, Figure 3.3 shows that peel_2048 solved 50% of instances to within a 42% optimality gap, peel_64 solved 50% of instances to within a 67% optimality gap, and the best performing branch and bound (bnb_64) solved 50% of instances to within only a 79% optimality gap. The overall performance of PnB improves as more problems are considered, especially as the maximum allowable width for the DDs is increased.

The selected graphs shown in Figure 3.4 are representative of the two main types of behavior observed over the problem set. On problems where the underlying relaxation method works well, the relaxed bound moves quickly towards convergence with the best found solution. On problems where the underlying relaxation does not work well, both algorithms slowly improve the relaxed bound, but PnB starts stronger as it can use exact arc values, and it maintains the advantage throughout. It is clear from the time-series data that to be competitive with cutting-edge solvers, PnB must be combined with other constraint programming propagators. However, it is also clear that PnB can have a significant edge over a propagator that generates the required DDs from scratch at each iteration.

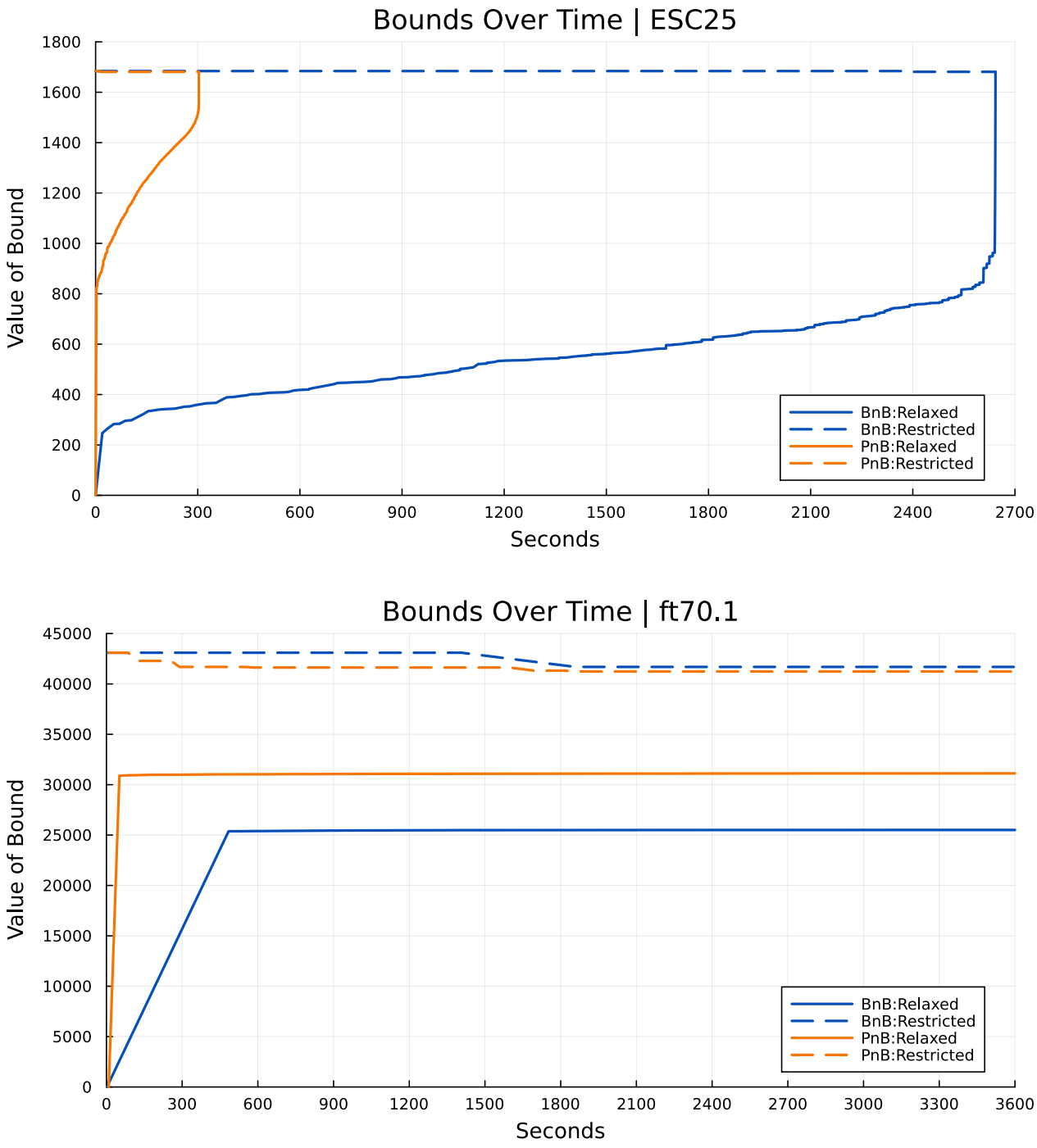


Figure 3.4 Dual bounds for ESC25 and ft70.1

ESC25 was solved within the time limit, and ft70.1 was not solved within the time limit. Both use $\omega = 256$.

## 3.6 Summary

In this chapter, we introduced the PnB algorithm as a novel alternative to DD-based BnB. In PnB, constructed DDs are repeatedly reused to avoid unnecessary computation. We discussed various heuristic strategies that can optimize PnB, and explored its potential applications to other problems.

We compared the performance of a PnB scheme to a BnB scheme using the same DD-based propagator. We tested both algorithms on the 41 instances of the SOP from TSPLIB. The results demonstrated that PnB significantly outperforms BnB on the SOP by generating substantially stronger relaxed bounds on instances that were not closed during the experiment, and reaching optimality faster when the instances were closed. This research underscores the advantages of re-using work in DD-based solvers. Additionally, PnB benefits from scaling the maximum allowable width. Thus, relaxed DDs that yield strong bounds at scale, but are too costly to generate iteratively, only need to be constructed once.

In the following chapter, we will delve into the transition from this initial implementation of PnB, to an implementation that has achieved cutting-edge results. We will outline the enhancements and optimizations that were integral to evolving the algorithm from a theoretical model into an efficient tool.

# CHAPTER 4 IMPROVED PEEL-AND-BOUND

**Contributions and Publication Information**

This chapter is largely based on *Improved Peel-and-Bound: Methods for Generating Dual Bounds with Multivalued Decision Diagrams* by Isaac Rudich, Quentin Cappart, and Louis-Martin Rousseau, which was published in the Journal of Artificial Intelligence Research in 2023 [9]. It discusses methods of implementing DD-based solvers efficiently, and includes experiments where PnB achieved cutting-edge performance on TSP-TW and Makespan problems, closing 15 open benchmark instances of TSP-TW.

This chapter also includes a very small amount of text from *An Exact Framework for Solving the Space-Time Dependent TSP*. The only content that is included is from the section explaining embedded restricted DDs.

**Differences:** While the content of this chapter is based on the aforementioned paper, parts of it have been rewritten.

## 4.1 Motivation

The initial inspiration for implementing PnB was that DD-based BnB repeats numerous computations while constructing DDs. PnB aims to avoid re-computations. However, the goal of the initial implementation was to simply make a clean comparison between a naive PnB implementation and a naive DD-based BnB implementation. That test (Section 3.5.2) showed that PnB was worth pursuing. We then built a new implementation from scratch, carefully considering how to make the algorithm efficient and scalable, so we could test it against other solvers.

Our primary target for improvement involved identifying and addressing bottlenecks in the algorithm. The slowest part of the first implementation is handling arcs. Benchmarking the code made it clear that having the computer perform read and write operations for every arc in the DD was consuming most of the runtime. In Section 4.2.1, we discuss a method of making all of the arc values implicit for sequencing problems. This change represents the most significant component of the speed-up we achieved. The second major improvement arose from our new search procedure detailed in Section 4.2.2, which reads a restricted DD from an existing relaxed DD, instead of generating it from scratch.

## 4.2 Improvements to the Theory

### 4.2.1 Handling Non-Separable Objective Functions

When a problem is represented with an Integer Program, the value or cost of making a decision is separate for each variable; in other words the objective function is separable. However, when using DDs to represent a problem, the objective function can be non-separable. In the example SOP used in Section 2.1.2, the cost of an arc leaving a node $u$ is dependent on the labels of the arcs that end at $u$. If the arcs have conflicting labels, then arcs leaving $u$ may not have an exact cost. The algorithm for using DDs to solve sequencing problems [28] proposed that each iteration of Algorithm 9 starts from a $\omega = 1$ DD. However, for PnB with a non-separable objective function, starting from a $\omega = 1$ DD poses a problem. The arcs in such a DD do not have exact values, because they are dependent on the state of the node they originate from. As nodes are peeled, the values of those arcs must be updated, and the operation becomes computationally expensive at scale.

When solving sequencing problems where the non-separability of transition costs arises from their dependency on the previous element in the sequence, this problem can be avoided by creating the initial DD using a structure where all of the arcs ending at a given node have the same label. The resulting initial DD has a width of $n$, and each node on the layer is assigned to one state $s \in \{1, ..., n\}$. Then every possible feasible arc between consecutive layers is added. Thus, the nodes of $\mathcal{M}^+$ do not have relaxed states, and each arc can only take one possible value. Starting from such a DD not only removes the need to update arc values, it ensures that every arc generated during PnB is an exact copy of an arc that exists in the initial DD, since arcs are only copied or removed, never updated or added. Using this structure makes implementation easier by removing the need to store any information on the arcs at all. As each node will only have one state, the label and weight of an arc is implied by the state of the node it originates from, and the node it points to. This allows all information in a DD to be stored on the nodes, and thus only the information on the nodes ever needs to be read or updated.

When transition costs are dependent on factors other than the previous element in a sequence, such as the Time-Dependent TSP (TSP-TD), modifications to the described method become necessary. In general an exact cost may not be computable, but a relaxed bound on cost can be made computable by storing the relevant values as a range at each node. Consider a DD for the TSP-TD where nodes $u$ and $v$ are connected by an arc. Let $[a_u, b_u]$ be the range of possible times one can arrive at $u$. While an exact cost for the arc from $u$ to $v$ is not available, a relaxed bound can be found by varying the time from $a_u$ to $b_u$, and then using

the best value found as the cost. As the DD is peeled, the gap between $a_u$ and $b_u$ may grow smaller, but it will never grow larger. When the gap decreases, the previously calculated cost is still a valid relaxed bound. Thus, the cost can be updated to retrieve an improved bound, but it is not necessary to do so with every peel operation. Many problems will require modifying this concept to fit their particular constraints, but this method is easy to adapt in most cases. An alternative method of handling non-separable objective functions has also been explored [15, 47, 48].

### 4.2.2 Embedded Restricted Decision Diagrams

In both DD-based BnB (Algorithm 11), and PnB (Algorithm 13), at each branch a restricted DD is created before the relaxed DD. This is useful not just for solution finding, but also because the process of creating a restricted DD is often several orders of magnitude faster than the process of refining a relaxed DD. When the restricted DD is exact, the relaxed DD can be closed without any additional processing. PnB provides an opportunity to leverage relaxed DDs to improve the associated restricted DDs. As dicussed in Section 2.7.1, this concept was developed independently from, but concurrently with, work on dominance-based pruning, which was also inspired by rough relaxed bounding techniques [25, 31]. Thus, embedded restricted DDs share some similarities with this work.

A path in both a restricted DD and a relaxed DD represents a sequence of decisions. In a restricted DD, each path from the root to a node in the DD represents a feasible partial solution to the problem being solved. A relaxed DD contains every feasible solution, partial or otherwise. Thus, each path in a restricted DD will also exist in the associated relaxed DD. Furthermore, DDs are deterministic, so each path in a DD maps to exactly one node. This means that any possible path (sequence of decisions) in a restricted DD, will map to exactly one node in the associated relaxed DD. In other words, every possible restricted DD for an optimization problem will be embedded in a relaxed DD for that problem.

Formally, each path to a node $u^-$ in a restricted DD $\mathcal{M}^-$ can be mapped to exactly one node $u^+$ in a relaxed DD $\mathcal{M}^+$. Recall that the domain of a node $u$ is the set of feasible arc labels on out-arcs of $u$. When generating $\mathcal{M}^-$, each node in $\mathcal{M}^-$ creates a child node on the next layer for every element in its domain, and then the new layer is trimmed down to a pre-chosen maximum width $\omega$.

The mapping from restricted DDs to relaxed DDs can be leveraged to improve the restricted DD as it is being generated. Let $d(u^-)$ be the domain of $u^-$. Set $d(u^-) \leftarrow d(u^-) \cap d(u^+)$ before generating the child nodes of $u^-$. This way, if an arc has been proven to be sub-optimal in $\mathcal{M}^+$, it will not be created when generating $\mathcal{M}^-$.

This also allows for easy intensification of the search when combined with peel operations. If a node $u$ has been peeled from $\mathcal{M}^+$ into $\mathcal{M}^+(u)$, then $\mathcal{M}^-$ will not include any solutions that pass through $u$. Similarly, if a restricted DD $\mathcal{M}^-(u)$ is generated that is embedded in $\mathcal{M}^+(u)$, it will only explore solutions that pass through $u$.

Without using this intersection operation as a way to trim the domain, $\mathcal{M}^-$ will search the entire solution space that starts from the same root as $\mathcal{M}^+$, even if the peeled DDs have already been fully explored and are known to be sub-optimal. Using this method, each restricted DD will only search the solutions encoded within the matching relaxed DD. This means that each restricted DD has a significantly improved chance of finding the best solution embedded in the relaxed DD it maps to, because the solution space it must explore becomes smaller with each peeled node.

### 4.2.3 Peel-and-Bound with Top-Down Compilation

The structure of PnB is designed to take advantage of relaxed DDs that are compiled by separation. Here we propose a method for applying PnB to relaxed DDs that are compiled top-down. However, we have not tested this method, and it remains a topic of future research to determine if it would be useful in practice. The goal of PnB is to re-use work already done by reusing DDs. When performing top-down compilation, nodes are merged instead of separated. The peel procedure can be used exactly as before, but after a node is peeled, the remaining DDs must be altered so that new nodes can be added top-down using a merge procedure. However, there are no nodes to add, the DDs already represent feasible bounds on the problem, and so some nodes must be removed. Begin by selecting a relaxed node $u$ (in other words some node $u$ that is not exact), and removing it from the DD. Then remove any arcs in the DD that are sub-optimal or no longer feasible due to the removed node. For each arc $a_{vu}$ that used to point to $u$, create a new arc $a_{vu\prime}$ that points to a new node $u\prime$ created by following the top-down compilation rules being used. Finally, proceed to perform top-down compilation using the set of new nodes as root nodes for the procedure.

## 4.3 Improvements to the Heuristics

### 4.3.1 Node Selection Heuristic

Recall from Section 3.4.1 that we initially only discussed, and experimented with, two heuristics for selecting which node to peel from a DD. After our initial experiments we have added a third node selection heuristic. We pick what we call the *maximal* node. The maximal node is simply the node on the second layer that contains $z(\mathcal{D})$. This peels as many nodes as

possible while still picking a node that contains $z(\mathcal{D})$.

### 4.3.2 Search Diversification

The structure of PnB yields another method of searching for solutions that forces increased diversification. The embedded restricted DDs described in Section 4.2.2 take advantage of the reduced search space embedded in the relaxed DD, but make no effort to explore substantially different regions, and thus are at risk of getting stuck in a local optimum. Here we propose a simple method of diversifying the solutions explored. Starting from the root, and moving down layer by layer, map each node $u$ in the relaxed DD to the best feasible path that ends at $u$, and is a continuation of a path a parent of $u$ maps to. The obvious drawback is that many paths will becomes infeasible or sub-optimal, and many of the relaxed nodes might not map to a feasible path using this method, simply because the paths that were being explored in their parents were bad paths. To fix this, the number of paths stored can be expanded. Let $k$ be any positive integer; if each node maps to the $k$ best paths to that node, then as the value of $k$ increases there is a much higher likelihood of new, and better, solutions being found. However, as the number of nodes in the DD can be quite large, even small values of $k$ can be computationally expensive. So this method can be a powerful tool for diversification, but it comes with a significant drawback in terms of compute time. It has the potential to be valuable if used just once at the beginning of the PnB process to search for initial solutions, but is unlikely to be useful if repeated often. This idea may also benefit from being combined with the large neighborhood search using restricted DDs [23].

## 4.4 Experiments with our Improved Implementation

The first implementation of PnB, which was used to generate the results in Section 3.5.2, was designed to create a fair comparison of PnB and BnB; it was also limited to the SOP. The re-implementation of PnB is generic, and the new version is similarly open-source[1]. All of the raw data from the following experiments can be found with the code. In this section, we further explore the performance of the algorithm. The experiments were performed on a computer equipped with an AMD Rome 7532 at 2.40 GHz with 186Gb RAM.

### 4.4.1 Node Selection Heuristic

In Sections 3.4.1 & 4.3.1, we propose three heuristics for selecting a node to be peeled: frontier, last exact node, and maximal. Here we compare the performance of those three

[1] https://github.com/IsaacRudich/ImprovedPnB

different settings on the same set of SOP instances we tested in Section 3.5.2; we similarly limit the runtime of the solver to 3600 seconds. We include the results from the most successful run performed by the original implementation of PnB to show how much the new implementation has improved in general. The results are shown in Figure 4.1. The first graph is a scatter-plot displaying the solve time of each problem that was solved to optimality, for each of the three node selection settings. The second graph shows performance profiles for the same tests, and includes data from the best run of the first implementation of PnB to show the overall improvement of the solver. All of the new tests were performed using $\omega = 2048$, and included a diversified search with $k = 5$ using the procedure described in Section 4.3.2.

Figure 4.1 makes it clear that choosing between the node selection heuristics has little effect on solving the SOP. The number of instances solved to optimality is identical, with maximal having a slight lag on the final two problems, and the performance profiles are nearly identical. The performance profiles also serve to demonstrate the progress of the solver, with the percentage of instances closed to any given optimality gap being about 10% higher.

### 4.4.2 Traveling Salesman Problem with Time Windows

The Traveling Salesman Problem with Time Windows (TSP-TW) is a variation of the TSP where a salesman must find the shortest cycle that visits each customer once, but each customer may have an added constraint requiring they be visited within a specific time window. It provides a useful metric for benchmarking the performance of the implementation of PnB, as DD focused algorithms are more likely to outperform traditional methods on highly constrained problems than highly unconstrained problems, and the TSP-TW instances are highly constrained. For the following tests we include both a standard and seeded run of the solver, where seeded means that the solver started out knowing the value of the best known solution, and skipped the initial diversified search. The seeded version is of interest because the solver can leverage heuristically generated solutions to reach proof of optimally faster. The difference between the standard and seeded run may help to determine if taking that step is worthwhile when solving a specific problem. We test our solver on the same set of 467 benchmark instances used by ddo [4] to test their implementation of DD-based BnB. These instances are available online [49], and include the following sets: AFG [50], Dumas [51], GendreauDumas [52], Langevin [53], Ohlmann-Thomas [54], Solomon-Pesant [55], and Solomon-Potvin-Bengio [56]. Figure 4.2 shows a time to solve graph for the closed instances, once with PnB on a single thread, once with seeded PnB on a single thread, once with ddo on a single thread, and once with ddo using 24 threads. The experiments were limited to 3600 seconds. Figure 4.2 also shows the performance profiles of PnB using the

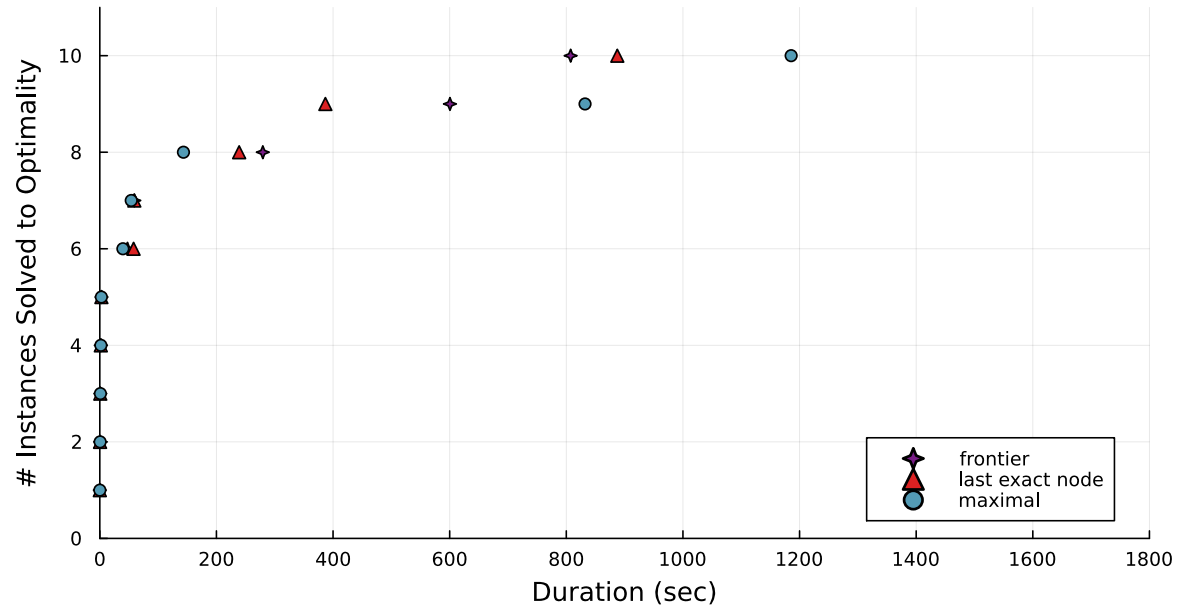


SOP Instances Solved over Time: $\omega = 2048$

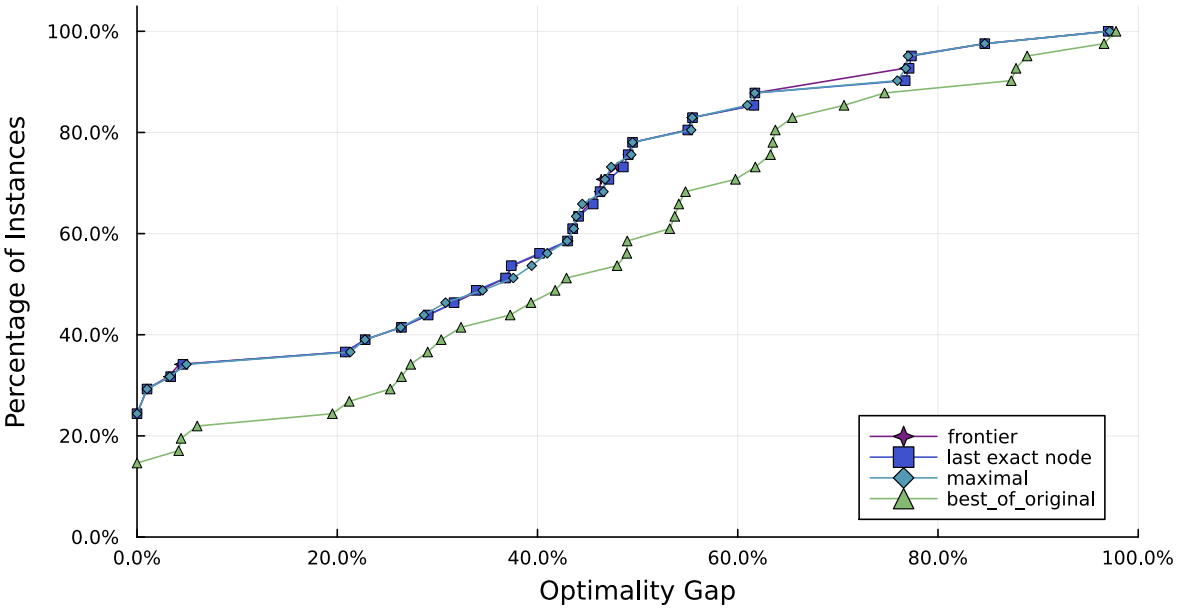


Performance Profiles on the SOP: $\omega = 2048$

Figure 4.1 Performance of Improved Peel-and-Bound on SOP

same data. Since the solution space of TSP-TW tends to be drastically more constrained than SOP, at least for the benchmark instances, it is more difficult to find feasible solutions, and we use a width of 100 for the initial diversified search.

It is clear from Figure 4.2, that PnB outperforms ddo on the TSP-TW benchmark set. Al-

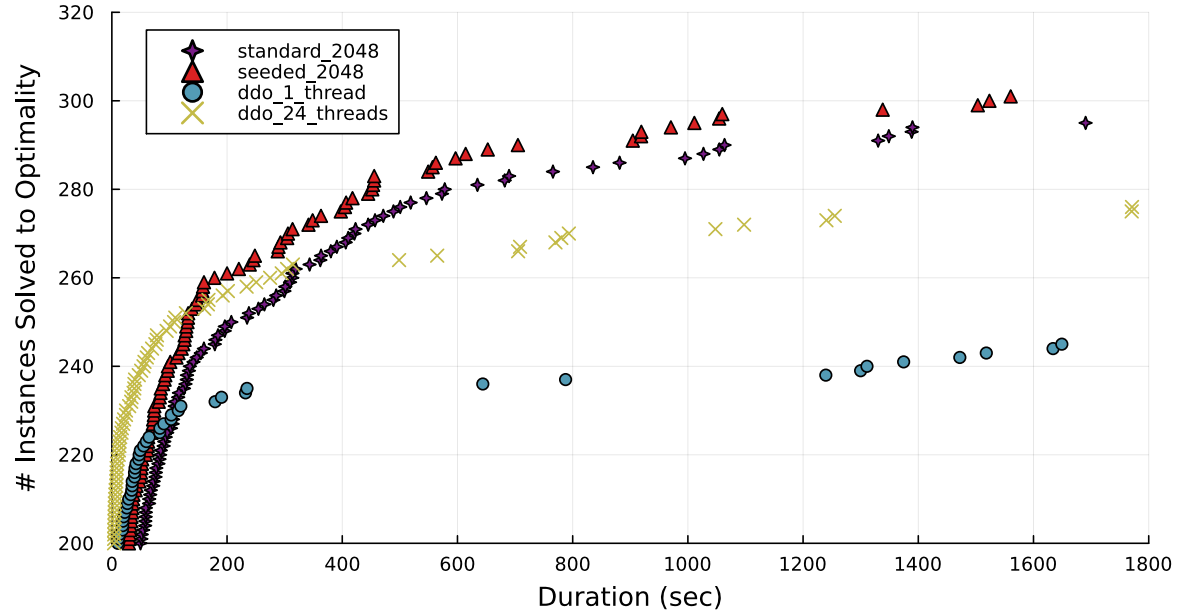


TSP-TW Instances Solved over Time: DDO vs. Peel-and-Bound

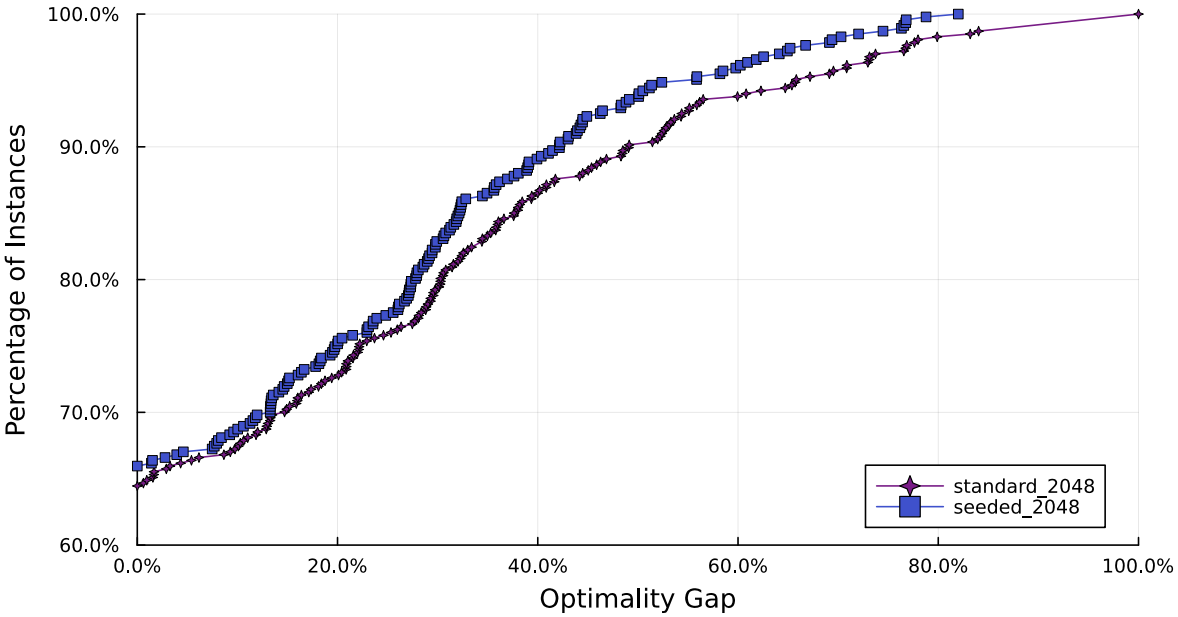


TSP-TW Performance Profiles

Figure 4.2 Performance of Improved Peel-and-Bound on TSP-TW

though ddo is faster to start, PnB on a single thread solves about 60 more instances than ddo on a single thread, and about 20 more instances than ddo using 24 threads. This experiment plainly demonstrates the advantages of trading memory for speed when using DDs. The performance profiles show that PnB solved about 65% of the instances to optimality. The

seeded version of the solver performed only slightly better. Looking at the raw data (available in the repository), it is also clear that performance degrades when PnB has trouble finding good solutions, and when the size of the time windows is large (causing the problem to be more unconstrained than others in the benchmark set).

To the best of our knowledge, the last paper to report relaxed bounds on the instances in these benchmark sets is from 2012 [57]. We use those results as a reference for comparison. The standard run closes 14 open instances, and the seeded run closes 1 additional instance. The results for these instances, and the previously known relaxed bounds, are reported in Table 4.1. A table with every problem from the benchmark set that remains open to the best of our knowledge (in other words, those unsolved by both the reference paper and PnB), is available in Appendix A: Table A.4. The full data is available in Appendix A: Tables A.6-A.11. The raw data is also available in the repository with the solver.

| Problem Information | | | Baldacci et al. (2012) | Single Thread: 2048 | | | | Seeded Single Thread: 2048 | | | |
|---|---|---|---|---|---|---|---|---|---|---|---|
| Set | Name | Best Known Solution | LB | LB | UB | Time | OG | LB | UB | Time | OG |
| AFG | rbg086a.tw | 8400 | 8399 | 8400 | 8400 | 254.47 | - | 8400 | 8400 | 132.49 | - |
| | rbg092a.tw | 7158 | 7156.6 | 7158 | 7158 | 1917.74 | - | 7158 | 7158 | 288.02 | - |
| GendreauDumas | n20w200.004.txt | 293 | 289.484 | 293 | 293 | 27.97 | - | 293 | 293 | 15.47 | - |
| | n40w200.002.txt | 303 | 302.091 | 303 | 303 | 1388.47 | - | 303 | 303 | 417.75 | - |
| | n80w100.004.txt | 649 | 645.408 | 649 | 649 | 2372.02 | - | 649 | 649 | 904.33 | - |
| SolomonPesant | rc203.1 | 726.99 | 726.66 | 726.99 | 726.99 | 299.58 | - | 726.99 | 726.99 | 200.01 | - |
| SolomonPotvinBengio | rc_202.3.txt | 837.72 | 835.87 | 837.72 | 837.72 | 9.66 | - | 837.72 | 837.72 | 8.67 | - |
| | rc_202.4.txt | 793.03 | 791.54 | 793.03 | 793.03 | 108.08 | - | 793.03 | 793.03 | 73.79 | - |
| | rc_205.4.txt | 760.47 | 756.95 | 760.47 | 760.47 | 13.65 | - | 760.47 | 760.47 | 9.74 | - |
| | rc_206.2.txt | 828.06 | 826.66 | 828.06 | 828.06 | 102.63 | - | 828.06 | 828.06 | 68.91 | - |
| | rc_206.4.txt | 831.67 | 827.54 | 831.67 | 831.67 | 107.39 | - | 831.67 | 831.67 | 84.51 | - |
| | rc_207.1.txt | 732.68 | 731.57 | 732.68 | 732.68 | 195.9 | - | 732.68 | 732.68 | 157.17 | - |
| | rc_207.2.txt | 701.25 | 694.22 | 701.25 | 701.25 | 1690.43 | - | 701.25 | 701.25 | 92.84 | - |
| | rc_207.3.txt | 682.40 | 677.23 | 682.40 | 682.40 | 1054.62 | - | 682.40 | 682.40 | 596.7 | - |
| | rc_208.1.txt | 789.25 | 785.69 | 751.20 | 794.17 | - | 5.41 | 789.25 | 789.25 | 2511.58 | - |

Table 4.1 TSP-TW Results for Newly Closed Problems

LB = Lower Bound, UB = Upper Bound, OG = Optimality Gap. In all cases the existing best known solution was proven optimal by Peel and Bound.

### 4.4.3 Traveling Salesman Problem with Time Windows - Makespan

Makespan adjusts the objective function of TSP-TW so the total time includes any idle time spent waiting for a customer to be available when the salesman arrives early, as opposed to just the distance traveled. To test this problem, we use the same benchmark instances that we did in Section 4.4.2, and simply adjust the objective function. The tests all use the same settings as the test for TSP-TW, and the results are presented in the same way in Figure 4.3.

While we were unable to find a a benchmark comparison in the literature with relaxed bounds for the makespan variant of these benchmark sets, the results from testing PnB on makespan speak for themselves. Just over 94% of the instances were closed to optimality by

the unseeded run of the solver, and just over 97% were closed by the seeded run. For the unseeded run, just over 97.5% were closed to 1% optimality gap, and 99% for the seeded run. In total, 26 instances were not closed by the unseeded run, and 12 of those were not closed by the seeded run. The results and bounds for those 26 instances are shown in Table 4.2. We are unsure if any of the makespan problems are considered to be open, but we can say that the only ones that aren't definitively closed are the 12 not in bold that were not solved during the seeded run of the solver. Of those, only 2 have an optimality gap larger than 2%. For the 455 closed instances, the best existing solution was reported [49]. A table with full results for the benchmark sets, and time to solve for all of the closed problems, is shown in Appendix A: Tables A.12-A.18. The raw data is also available in the repository with the solver.

| Problem Information | | | Single Thread: 2048 | | | Seeded Single Thread: 2048 | | |
|---|---|---|---|---|---|---|---|---|
| Set | Name | Best Known Solution | LB | UB | OG | LB | UB | OG |
| AFG | rbg050b.tw | 11957 | 11748 | 11957 | 1.75 | 11748 | 11957 | 1.75 |
| | rbg172a.tw | 17783 | 17766 | 17784 | 0.10 | 17766 | 17783 | 0.10 |
| Dumas | **n150w60.002.txt** | **940** | **940** | **941** | **0.11** | **940** | **940** | **-** |
| | **n200w40.002.txt** | **1137** | **1137** | **-** | **100** | **1137** | **1137** | **-** |
| GendreauDumas | n100w100.003.txt | 819 | 818 | 819 | 0.12 | 818 | 819 | 0.12 |
| | **n100w80.003.txt** | **829** | **829** | **839** | **1.19** | **829** | **829** | **-** |
| | **n60w200.003.txt** | **560** | **560** | **561** | **0.18** | **560** | **560** | **-** |
| | n80w140.005.txt | 739 | 725 | 739 | 1.89 | 725 | 739 | 1.89 |
| | **n80w160.002.txt** | **654** | **652** | **665** | **1.95** | **654** | **654** | **-** |
| | n80w180.002.txt | 633 | 631 | 639 | 1.25 | 631 | 633 | 0.32 |
| | n80w180.005.txt | 632 | 444 | 632 | 29.75 | 444 | 632 | 29.75 |
| | n80w200.004.txt | 667 | 660 | 671 | 1.64 | 660 | 667 | 1.05 |
| OhlmannThomas | **n150w120.004.txt** | **925** | **925** | **929** | **0.43** | **925** | **925** | **-** |
| | **n150w140.002.txt** | **1020** | **1020** | **1021** | **0.10** | **1020** | **1020** | **-** |
| | **n150w140.004.txt** | **898** | **898** | **919** | **2.29** | **898** | **898** | **-** |
| | **n150w140.005.txt** | **926** | **826** | **926** | **10.8** | **926** | **926** | **-** |
| | **n150w160.002.txt** | **890** | **861** | **912** | **5.59** | **890** | **890** | **-** |
| | **n150w160.004.txt** | **912** | **912** | **943** | **3.29** | **912** | **912** | **-** |
| | n200w120.001.txt | 1089 | 1086 | 1089 | 0.28 | 1086 | 1089 | 0.28 |
| | n200w120.002.txt | 1072 | 1065 | 1072 | 0.65 | 1065 | 1072 | 0.65 |
| | **n200w140.001.txt** | **1138** | **929** | **1146** | **18.94** | **1138** | **1138** | **-** |
| | n200w140.003.txt | 1083 | 979 | 1083 | 9.60 | 1082 | 1083 | 0.09 |
| | **n200w140.005.txt** | **1121** | **961** | **1121** | **14.27** | **1121** | **1121** | **-** |
| SolomonPesant | **rc204.2** | **870.52** | **728.94** | **914.89** | **20.33** | **870.52** | **870.52** | **-** |
| SolomonPotvinBengio | rc_204.1.txt | 917.83 | 915.22 | 918.01 | 0.30 | 915.22 | 917.83 | 0.28 |
| | rc_208.3.txt | 686.80 | 606.15 | 686.80 | 11.74 | 610.58 | 686.80 | 11.10 |

Table 4.2 Makespan Results for Problems Not Closed by the Unseeded Run

LB = Lower Bound, UB = Upper Bound, OG = Optimality Gap. The bolded instances were closed by the seeded run.

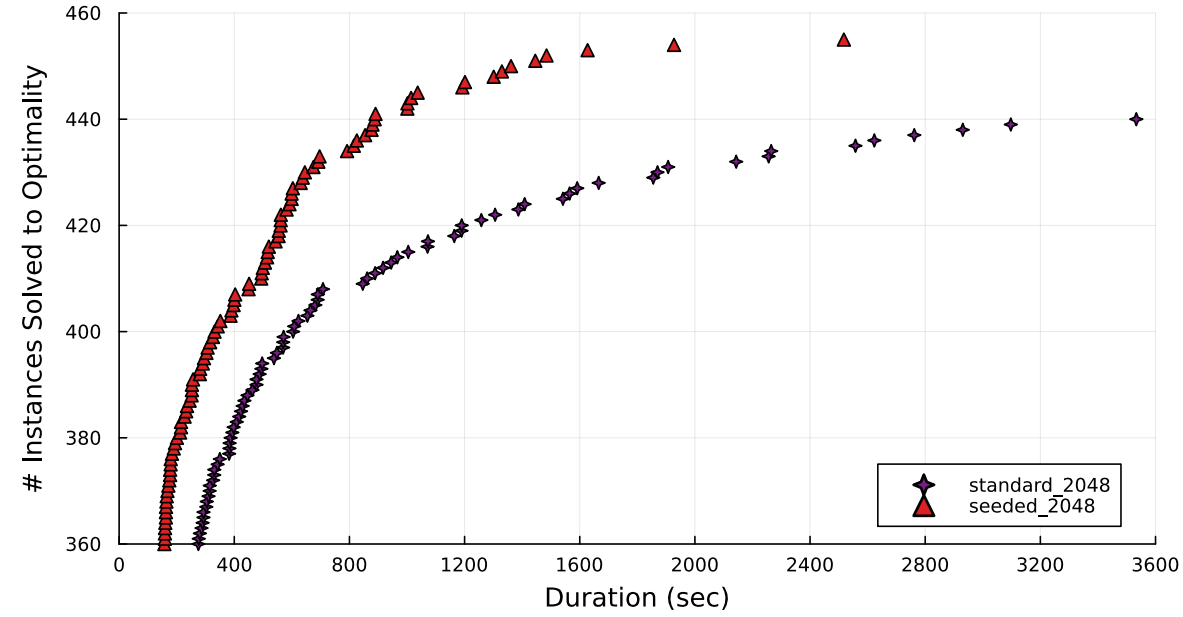


Makespan Instances Solved over Time

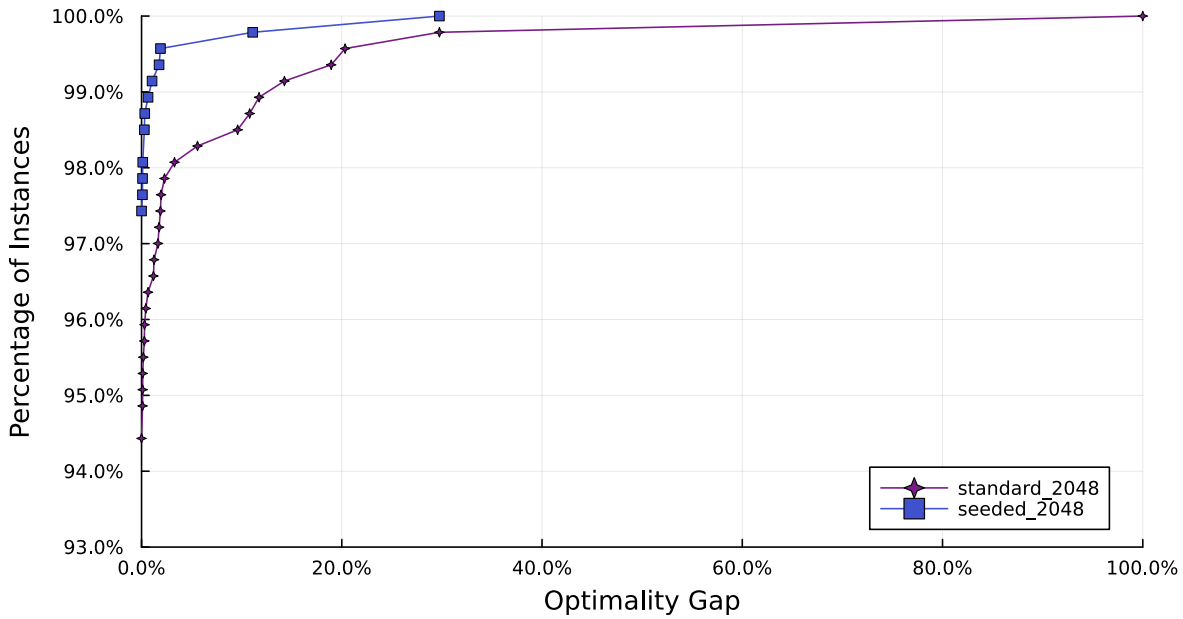


Makespan Performance Profiles

Figure 4.3 Performance of Improved Peel-and-Bound on Makespan

## 4.5 Summary

This work improved on the previous implementation of peel-and-bound, but it also improved the theory behind the algorithm. We introduced a method of generating the initial DD where nodes are labeled instead of arcs. This not only allows for efficient handling of problems with

non-separable objective functions, it also provides a method for implementing DDs without needing to store or update arcs. We will expand on this in Chapter 5. We also introduced embedded restricted DDs, a method of reading restricted DDs from existing relaxed DDs instead of generating them separately.

This chapter also presented PnB as an algorithm capable of achieving cutting edge results. We re-implemented the algorithm to be both more efficient and generic. We tested the new implementation on the 467 benchmark instances of TSP-TW used to test the DD-based BnB solver (ddo) [4]. The results show that PnB outperforms ddo on TSP-TW, even when ddo is using parallel processing. Furthermore, PnB closed 15 instances that, to the best of our knowledge, are open in the literature. In our final test, we ran the new implementation of PnB on the makespan variant of the 467 TSP-TW instances. PnB closed 94% of the makespan instances, and an additional 3% when seeded with the best known solution. We provide best known bounds for all TSP-TW and makespan instances that we believe to be open.

The next chapter generalizes the idea for creating a relaxed DD with exact arcs to any discrete optimization problem. It also discusses how this impacts our implementation of a PnB solver, and what the next steps are in a path to making the implementation capable of taking in a generic model without requiring specific knowledge of the solver.

# CHAPTER 5 IMPLICIT RELAXED DECISION DIAGRAMS

**Contributions and Publication Information**

This chapter only contains content that has not been published elsewhere.

This chapter explores how one of the techniques presented in this thesis offer insights applicable to other implementations of DDs, not just PnB. It aims to equip researchers pursuing other DD-based solving methods with an essential insight from my experience that can be readily integrated into their own implementations.

## 5.1 Algorithm

In Section 4.2.1, we discussed a method of handling non-separable objective functions for sequencing problems by constructing an initial relaxed DD with a width equal to the number of variables. However, the method described works for any discrete optimization problem, is remarkably efficient, and has a straightforward implementation. This section will formalize the generalized procedure, then discuss its theoretical and practical benefits.

Let $\mathcal{P}$ be a discrete optimization problem with variables $X = \{x_1, ..., x_n\}$, and let $d(x_i)$ be the domain of variable $x_i$. Create a root node $r$, and then for each value $l$ in the domain of $x_1$, add a node $u$ with label $l$. Then, repeat this in a new layer for each subsequent variable, adding a terminal node $t$ at the end. Let a pointer be a reference to the memory location of another object. Let the phrase *add an implicit arc from $u$ to $v$* mean: add a pointer at $u$ to $v$ indicating $v$ is a child of $u$, and add a pointer at $v$ to $u$ indicating $u$ is a parent. Then, add an implicit arc from every node on a layer $i$ to every node on layer $i + 1$. Note that $t$ is a dummy node, and all of the implicit arcs to $t$ will have a weight of 0, because there is no associated decision variable. This construction is a valid relaxed DD for any $\mathcal{P}$. Once it is constructed, the arcs can be filtered using problem specific constraint propagation (See Section 2.5 for examples). Algorithm 14 formalizes this procedure.

The result of using this data structure is a DD where the arc labels are stored on the nodes instead of the arcs. In optimization problems with separable objective functions, the weight of an arc is usually dependent on the state information of the parent node and the label of the arc. Now the weight of an arc is dependent on the state information of the parent node and the label of the child node. In optimization problems with non-separable objective functions, the weight of an arc is now dependent on the state information of the parent node,

the label of the parent node, and the label of the child node. In either case, the weight of an arc can be retrieved using only information stored at its origin and destination. The arc itself does not need to be stored, it just needs to be known that it exists. Hence, these decision diagrams are implicit, because they are arc-less.

**Algorithm 14:** Generating Implicit Relaxed Decision Diagrams

**Input:** An optimization problem $\mathcal{P}$ with variables $X = \{x_1, ..., x_n\}$
**Notation Reference:**
$d(x_i)$ is the domain of variable $x_i$
Let a pointer be a reference to the memory location of another object
Let $ptr(u)$ be a pointer to node $u$
Redefine $in(u)$ to be a set of pointers containing the implicit parents of $u$
Redefine $out(u)$ to be a set of pointers containing the implicit children of $u$
Create a root node $r$
$out(r) \leftarrow \emptyset$
$\mathcal{M}^+ \leftarrow \{r\}$ `// Initialize the DD to be just` $r$
**foreach** $x_i \in X$ *from* 1 *to* $n$ **do**
    $\alpha \leftarrow$ the set of nodes on layer $i - 1$
    **foreach** $l \in d(x_i)$ **do**
        Create a node $u$ with layer index $i$ and label $l$
        $\mathcal{M}^+ \leftarrow \mathcal{M}^+ \cup \{u\}$
        $in(u) \leftarrow \emptyset$
        $out(u) \leftarrow \emptyset$
        **foreach** $v \in \alpha$ **do**
            $in(u) \leftarrow ptr(v)$
            $out(v) \leftarrow ptr(u)$
        **end**
    **end**
**end**
Create a terminal node $t$
$\mathcal{M}^+ \leftarrow \mathcal{M}^+ \cup \{t\}$
$in(t) \leftarrow \emptyset$
**foreach** *node* $u$ *on layer* $n$ **do**
    $in(t) \leftarrow ptr(u)$
    $out(u) \leftarrow ptr(t)$
**end**
**foreach** *implicit arc* $a \in \mathcal{M}^+$ **do**
    $filter(a)$ `// problem-specific constraint propagation`
**end**
**return** $\mathcal{M}^+$

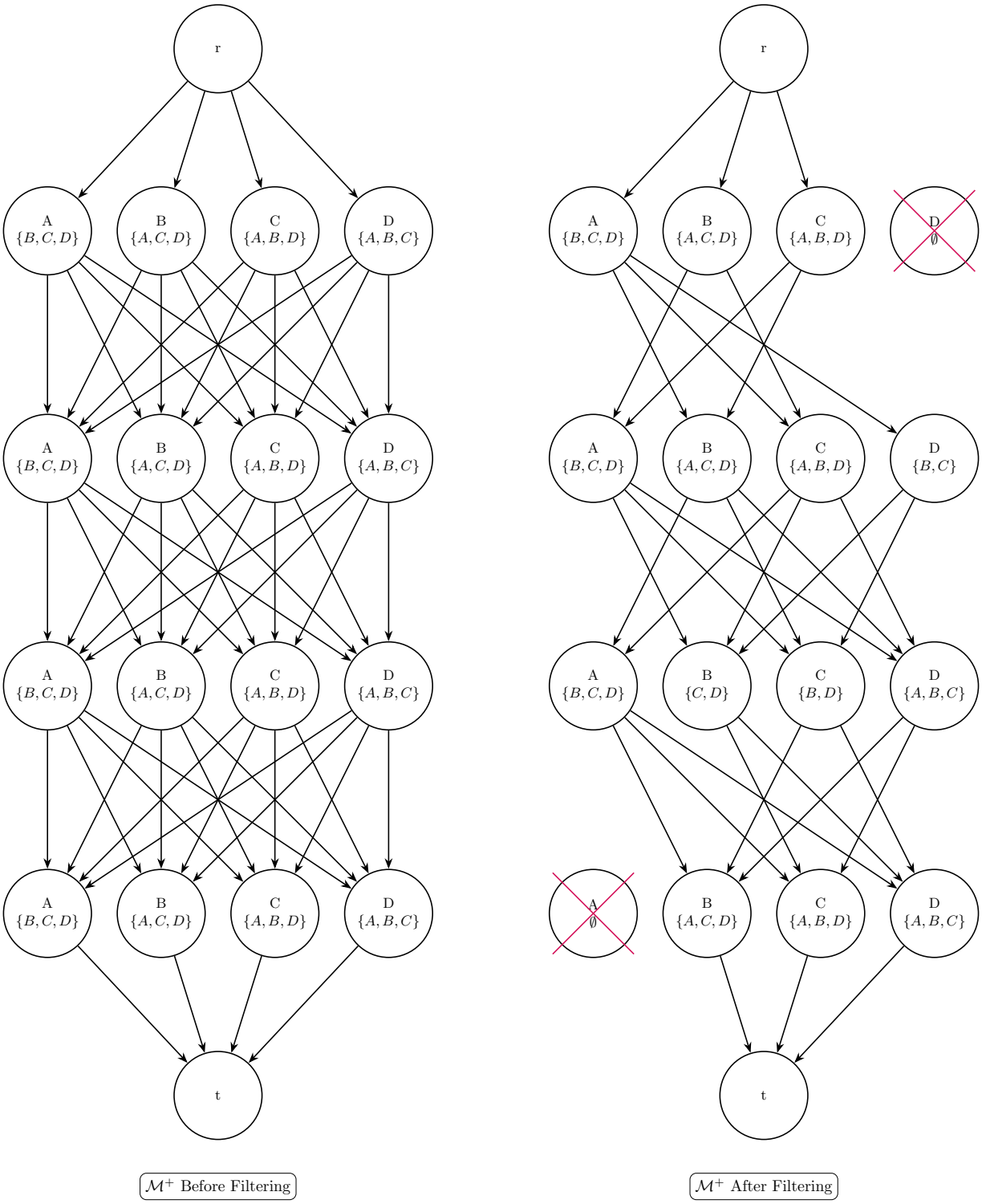


Figure 5.1 Implicit Relaxed DD, Before and After Filtering

SOP example with elements $[A, B, C, D]$, and the constraint that $A$ must precede $D$. Implicit arcs are drawn, but not labeled or weighted.

In the SOP example from Section 3.3, the goal is to order the elements $[A, B, C, D]$, subject to the precedence constraint that $A$ must precede $D$. For the sake of simplicity, we ignore arc costs. Figure 3.1 showed a $\omega = 3$ construction of $\mathcal{M}^+(r)$ for this example. Figure 5.1 shows the implicit initial relaxed DD for this example, both before and after filtering the arcs.

### 5.1.1 Complexity Analysis

Assume you are generating a relaxed DD by separation starting from a $\omega = 1$ diagram. Let $\omega^*$ be the maximum allotted width. Every time a node $u$ is split, its out-arcs are copied onto the new node $u'$. Recall that the layer index of $u$ is $\ell(u)$. The maximum number of possible out-arcs to be copied during a split of $u$ is $|d(x_{\ell(u)}|$. Let $|d(X)|$ be $\sum_{i=1}^{n} |d(x_i)|$. The maximum number of splits is $n(\omega^* - 1)$. So the maximum number of arcs copied is at most $n(\omega^* - 1) \cdot \frac{|d(X)|}{|X|}$.

Now, assume you are generating a relaxed DD by separation starting from the initial implicit DD. The number of arcs copied during each split is the same, but the number of splits is slightly smaller at $n(\omega^* - \frac{|d(X)|}{|X|})$. However, this difference is clearly negligible. The maximum number of arcs copied in either case is at most $\mathcal{O}(n \cdot \omega^* \cdot \frac{|d(X)|}{|X|})$. In the case of problems like the SOP, where the average domain size is $n - 1$, this simplifies to $\mathcal{O}(n^2 \cdot \omega^*)$.

In general, reading and writing to memory are among the most expensive operations when implementing anything with a standard CPU. Whether or not an implicit DD is being used, pointers connecting the parents and children are required. However, when using an implicit DD, arc labels do not need to be read or written, saving $\mathcal{O}(n \cdot \omega^* \cdot \frac{|d(X)|}{|X|})$ reads and writes.

## 5.2 Ease of Implementation

A hidden benefit of structuring relaxed DDs this way is that they are much easier to implement. When a node $u$ is split into $u$ and a new node $u'$, the state information of both $u$ and $u'$ needs to be updated. If the arcs are explicit and weighted, this can require iterating over the in-arcs of both nodes and updating their weights. If the arcs are implicit, all of the information is available on the nodes. You do not need to write code to handle updating arc information, you do not need to write code defining a data structure for your arcs, and you do not need to consider the trade-offs and implications of where you store your arcs in memory. Implicit relaxed DDs are not just more efficient, they require less work to implement and maintain in a solver.

### 5.3 The Future of Peel-and-Bound

At the time I am writing this thesis, the PnB solver is not capable of taking inputs that are restricted to a transition function and a split function. Using the solver requires writing several custom functions. Almost all of those functions fall into the category of being tedious to automate, but conceptually straightforward. The challenges involved with those functions are software engineering challenges, not mathematical challenges. However, a challenge I had viewed as a more significant hurdle was automating the generation of the initial relaxed DD. Now with Algorithm 14 worked out, that challenge has been solved. The next time I have a project that the PnB solver is a good tool for, I intend to generalize the initial relaxed DD generation using Algorithm 14. This will take the solver one enormous step closer to being as easy to use as any other general purpose DD-based solver.

# CHAPTER 6 APPLICATION TO FINDING EXACT SOLUTIONS TO THE SPACE-TIME DEPENDENT TSP

**Contributions and Publication Information**

This chapter is largely based on *An Exact Framework for Solving the Space-Time Dependent TSP* by Isaac Rudich, Manuel López-Ibáñez, Michael Römer, Quentin Cappart, and Louis-Martin Rousseau, which is available as a preprint on arXiv.

**Differences:** The original paper intertwines an explanation of DDs with how each component applies to the Asteroid Routing Problem. That explanation contains a lot of content that is redundant with Chapter 2, and the redundant content is not included here.

## 6.1 Motivation

In various real-world scenarios, we must determine the optimal sequence for visiting a number of locations, or scheduling jobs, where the travel cost between two locations is defined by an expensive black-box function without a closed form. These scenarios include a class of bi-level optimization problems. The *outer* problem involves finding an optimal permutation, while evaluating the cost of a given, possibly partial, permutation requires solving a different *inner* optimization problem that depends on the permutation. When the inner problem is computationally expensive and/or black-box, finding exact solutions to the bi-level optimization problem is difficult in practice.

Examples of this problem are time-dependent routing problems [58], especially variants where the travel costs must be computed on-demand [59] or are given by solving an inner optimization problem that, for example, determines vehicle speed [60]. This problem class also arises when planning missions in Space [61], such as finding a tour of the Jupiter Galilean moons [62], global optimization for multiple gravity assist trajectories [63–66], active space debris removal [58] and spacecraft formation control [67]. These problems are often solved by means of bi-level heuristics that combine numerical optimization methods with tree search methods such as Beam-Search [68], Lazy Race Tree Search [62], Monte-Carlo Tree Search [69] and Beam-ACO [70]. Other approaches treat the inner problem as a black-box function whose evaluation is expensive [71–74]. To the best of our knowledge, no exact method has ever been proposed to find optimal solutions for such problems. In the context of Space exploration,

solutions to global trajectory optimization problems represent huge economic costs, hundreds of millions of dollars, and long mission horizons, from years to decades. Thus, optimality is highly desirable.

We propose a framework for finding exact solutions by representing the outer problem using decision diagrams (DDs) [1, 28] and then solving that model using PnB (Algorithm 13) with DD-based search techniques [5]. Our proposed approach treats the inner problem as an expensive black-box function evaluated on-demand, but it uses problem-specific knowledge about this black-box function to speed-up the search, and reduce the number of black-box evaluations needed to solve the problem.

As a case study, we consider the Asteroid Routing Problem (ARP) [75], which is a benchmark problem inspired by the $11^{\text{th}}$ Global Trajectory Optimization Competition (`https://gtoc11.nudt.edu.cn`). The ARP can be thought of as a Space-time dependent variant of the TSP. In the ARP, a spacecraft launched from Earth is tasked with visiting a specific set of asteroids. The goal is to find the permutation of asteroids that minimizes both fuel consumption and total travel time, which are aggregated into a single objective function. Travelling from one asteroid to another requires identifying optimal departure and travel times, which constitutes the inner problem. The ARP treats this inner problem as a black-box function that is solved by a pre-defined deterministic optimizer. Thus, in the ARP, the evaluation of a given permutation of the asteroids always yields the same objective function value. These characteristics make the ARP a simplified benchmark for the class of problems described above, and allow researchers to focus on the *outer* problem of optimizing the permutation of asteroids. As in the problems mentioned above, a brute force search is the only known method for identifying an optimal solution to the ARP, which is only computationally tractable for a very small number of asteroids. All approaches proposed so far are heuristic and time-consuming [74, 75].

In this chapter, we propose the first exact approach for solving the ARP. Our framework proves optimality of the outer problem under the assumption that the inner problem is optimized with sufficient quality. We address the quality of the inner optimizer in our experimental results (Section 6.7). We also discuss how this technique can be made scalable, and how it can be used to quickly generate strong heuristic solutions to the ARP. We provide exact solutions, and new best known solutions for several ARP instances.

## 6.2 Background

In this section we detail the ARP and how DDs can be applied to the ARP.

### 6.2.1 The Asteroid Routing Problem

In the ARP [75], we are given a set of $n$ asteroids $A = \{a_1, \ldots, a_n\}$ orbiting around the Sun that a spacecraft launched from Earth ($a_0$) must visit. The spacecraft does not need to return to Earth. For simplicity, the ARP treats the transfer of the spacecraft from Earth to the first-visited asteroid as any other transfer between asteroids, i.e., there is no escape velocity of Earth.

A transfer of the spacecraft between two asteroids $a$ and $a'$ that starts no earlier than time (epoch) $\eta$ is computed with the following black-box function:

$$\mathcal{B}(a, a', \eta)\colon A \times A \times \mathbb{R}^+ \to [0, \tau_{\max}] \times [1, t_{\max}] \times \mathbb{R}^+ \tag{6.1}$$

which returns three values $(\tau, t, z)$, where $\tau$ is how long the spacecraft waits at $a$ before departing, $t$ is how long the spacecraft travels until it arrives at $a'$, such that arrival time is $\eta + \tau + t$, and $z$ is the cost of this transfer. A transfer is depicted in Figure 6.1.

As shown above, the wait time $\tau$ and travel time $t$ are bounded by $[0, \tau_{\max}]$ and $[1, t_{\max}]$, respectively. The wait time $\tau$ has a lower bound of 0 because it is possible to depart immediately without waiting. The travel time $t$ has a lower bound of 1 because a transfer will always require a nonzero time (at least 1 day in the ARP). The upper bounds $\tau_{\max}$ and $t_{\max}$ are set to 730 days in the original definition of the ARP [75].

Given a solution $\pi = (\pi_0 = a_0, \pi_1, \ldots, \pi_n)$, where the subsequence $(\pi_1, \ldots, \pi_n)$ is a permutation of the asteroids in $A$ that indicates the order in which they will be visited, the objective function of the ARP is:

$$\text{Minimize} \quad f(\pi) = \sum_{i=1}^{n} z_i \qquad \text{where} \quad (\tau_i, t_i, z_i) = \mathcal{B}(\pi_{i-1}, \pi_i, \eta_i) \tag{6.2}$$

Besides, $\eta_i = \eta_{i-1} + \tau_{i-1} + t_{i-1}$ is the arrival time at $\pi_{i-1}$ and $\eta_1$ is a given mission start time, which can be simplified to be zero. A solution is visualized in Figure 6.2.

The black-box function $\mathcal{B}$ depends not only on the two asteroids being visited, but also on the arrival time $\eta_i$. Thus the ARP is an example of the class of time-dependent problems discussed in the introduction.

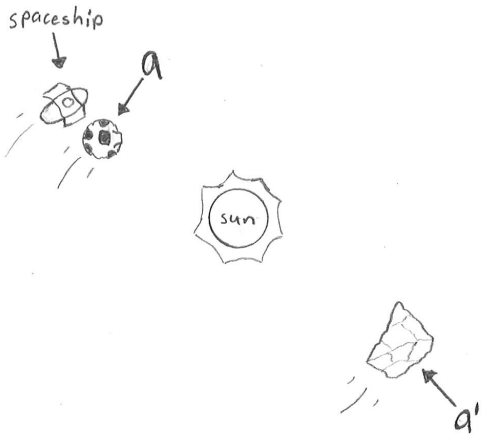


(a) At time $\eta$, the spaceship in in $a$'s orbit.

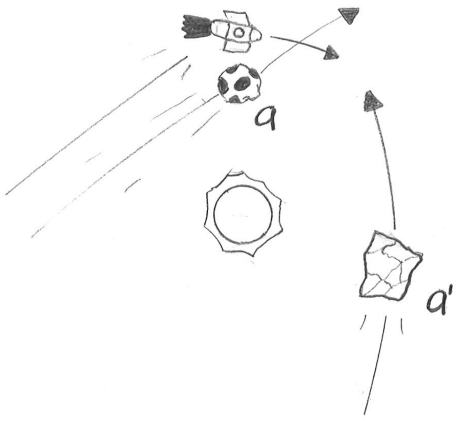


(b) After $\tau$ days, at time $\eta + \tau$, the spaceship initiates a transfer to $a'$.

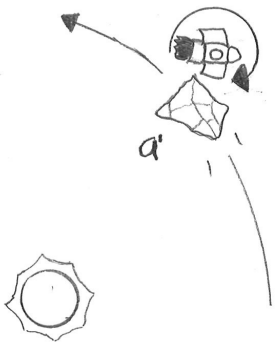


(c) After $t$ days, at time $\eta + \tau + t$, the spaceship intersects $a'$ and performs a maneuver to align itself with $a'$ 's orbit.

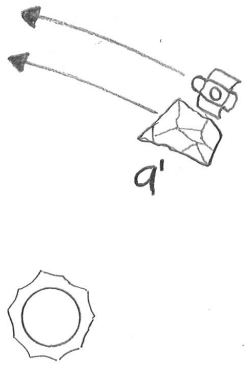


(d) Still at time $\eta + \tau + t$, the spaceship is now in the same orbit as $a'$.

Figure 6.1 Depiction of a transfer from $a$ to $a'$

### 6.2.2 Trajectory Optimization

In the ARP, and in many trajectory optimization problems, the spacecraft only uses *impulsive* maneuvers. An impulsive maneuver changes the spacecraft velocity in a negligible amount of time, thereby simplifying the calculation of the maneuver's effect on the spacecraft's orbit. As a result, the effect of the maneuver can be modeled as an instant change in the spacecraft's velocity vector $\Delta\vec{v}$, without accounting for the dynamics of the propulsion system, or the influence of external forces during the thrust application.

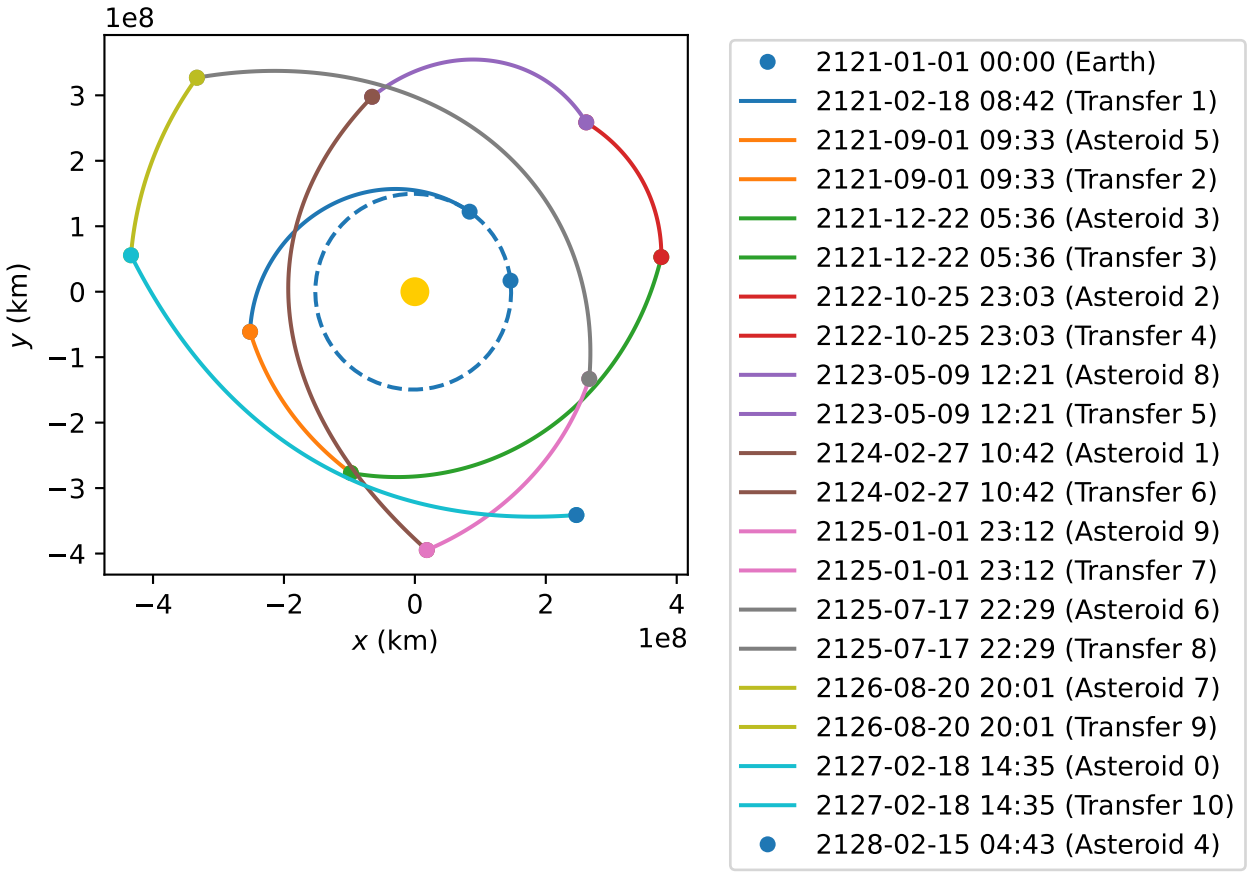


Figure 6.2 Visualization of best known solution to instance with $n = 10$ and *seed*$= 8$.

Lambert's Problem [76] calculates an orbit that connects two points in space-time departing at time $\eta + \tau$ and arriving at time $\eta + \tau + t$. Using the solution to Lambert's Problem, a transfer between the orbits of two asteroids $a$ and $a'$ can be achieved with just two impulsive maneuvers. Initially, at time (epoch) $\eta$, the spacecraft follows the same orbit around the Sun as asteroid $a$. *Waiting* in this orbit does not consume any fuel, but does change its relative distance to other asteroids. The first impulse $\Delta\vec{v}_1$ happens $\tau$ days after the current time $\eta$ (epoch), and moves the spacecraft from its current orbit to an orbit that will intercept the target asteroid $a'$ after traveling for $t$ days. When the spacecraft intercepts $a'$, the second impulse $\Delta\vec{v}_2$ modifies its orbit to match the orbit of $a'$, so that the spacecraft follows the same orbit as $a'$ without consuming any additional fuel. Usually the total magnitude of velocity change (the Euclidean L2 norm) is used as a surrogate for fuel consumption/energy costs:

$$\Delta V = \|\Delta\vec{v}_1\|_2 + \|\Delta\vec{v}_2\|_2 \qquad \text{where} \quad (\Delta\vec{v}_1, \Delta\vec{v}_2) = \text{Lambert}(a, a', \eta + \tau, t) \tag{6.3}$$

We still need to decide $\tau$, how long should the spacecraft wait at $a$, and $t$, how long the transfer should take until arriving at $a'$. Waiting changes the relative distance to other asteroids, which may reduce the fuel or total time needed to reach the next asteroid. The optimal values of $\tau$ and $t$ depend on which objectives are being optimized.

In trajectory optimization there are many possible objectives. Two typical objectives are the minimization of fuel (energy) consumption and of the total mission time $(\tau + t)$. These two objectives are often in conflict. The ARP aggregates the two objectives as shown below:

$$\begin{aligned} z = f_{\text{inner}}(a, a', \eta, \tau, t) &= \Delta V + \frac{2\,\text{km/s}}{30\,\text{days}} \cdot (\tau + t) \\ \text{s.t.} \quad & \tau \in [0, \tau_{\max}],\ t \in [1, \tau_{\max}] \\ \text{where} \quad & \Delta V = \|\Delta\vec{v}_1\|_2 + \|\Delta\vec{v}_2\|_2 \quad \text{and} \quad (\Delta\vec{v}_1, \Delta\vec{v}_2) = \text{Lambert}(a, a', \eta + \tau, t) \end{aligned} \tag{6.4}$$

where the trade-off constant $\frac{2\,\text{km/s}}{30\,\text{days}}$ was chosen by [75].

The above becomes an *inner* optimization problem whose solution gives the values $\tau$, $t$ and $z$ returned by $\mathcal{B}$ (Eq. 6.2).

In the ARP, this inner problem is solved by using Sequential Least Squares Programming (SLSQP) [77], which is a deterministic optimizer. In this way, each permutation of the asteroids corresponds to a unique solution. SLSQP iteratively calculates the position and velocity of the asteroids, and then solves Lambert's Problem in order to evaluate the above objective. Even if time is discretized into days, this inner optimization would be too slow to allow us to calculate the cost of every optimal trajectory for every pair of asteroids at every point in time.

A mission with $n$ asteroids may have up to $n(\tau_{\max} + t_{\max})$ possible values of $\eta$. In a mission where $n = 10$, calculating every possible trajectory from just one asteroid to one other asteroid for every possible departure time when time is discretized into days would take about 10 minutes using the inner optimizer in our implementation. Thus, calculating the full cost matrix for every ordered pair of asteroids ($n(n-1)$ pairs) at every possible departure day would take about 15 hours. Furthermore, departure time is continuous, not discrete, so this cost matrix would not even fully represent the problem, although it would certainly provide information that is useful for solving it.

### 6.2.3 Relaxed Decision Diagrams for the ARP

To initialize a relaxed DD for the ARP we are going to denote the root as *Earth* and the terminal as *done*. We use the implicit DD construction explained in Chapter 5. This means that in our implementation, we do no store arcs. However, in our figures here we include the implied arc labels for the sake of clarity. Note that we temporarily assume we have valid arc weights; we explain how to compute these in Section 6.3.3.

Figure 6.3a displays a valid relaxed DD for an ARP with asteroids $\{A, B, C\}$. Each arc is labeled with the decision about which asteroid is the next destination, and each node is labeled with the current asteroid. Every feasible permutation of asteroids is trivially encoded as a path from the root to the terminal, but so are several infeasible solutions, such as $A \rightarrow B \rightarrow A$. Figure 6.3b displays a weighted version of Figure 6.3a. Each arc still assigns the same decision, but the arc weights now display the lower bounds on the cost of transferring between those two asteroids at that point in the sequence. Each node is now also labeled with the length of the shortest path to that node. Thus, the length of the shortest path ($A \rightarrow B \rightarrow C$, which is highlighted), is a bound on this ARP. In other words, no matter what permutation of asteroids you use, and no matter how well you optimize the trajectories between them, there is no route for the spacecraft that admits a cost less than 10 for this example.

In the well-known Travelling Salesman Problem (TSP), the weights on the arcs would be the transition costs of going from one city to the next. However, in the TSP the arc weights are not dependent on all of the preceding cities, and the transition costs are easy to calculate. In this paper, we are handling a problem where calculating arc weights requires calling a black-box function $\mathcal{B}$ with non-negligible computation time. Furthermore, the exact arc weight for arc $a$ is dependent on the path taken to reach $a$. In principle, this dependency requires the evaluation of all possible paths from $r$ to $a$, in order to find the optimal one. However, if we can find, via relaxation of the $\mathcal{B}$ function, a globally valid bound on the arc weights, that bound can be used to prune sub-optimal paths.

In the case of the ARP, this relaxation is given by a no-wait variant of $\mathcal{B}$ where the cost of waiting is removed from the objective function; this is defined in Section 6.3.2. This no-wait variant can be used to find a globally valid bound on the cost of any transition between two asteroids. Thus for the ARP, the arcs will be weighted with valid lower bounds on their transition costs instead of exact values. This idea is explored and formalized in Section 6.3. To refine the diagram we will be using the methods for solving sequencing problems with DDs discussed in Section 2.5 [28] together with PnB (Algorithm 11).

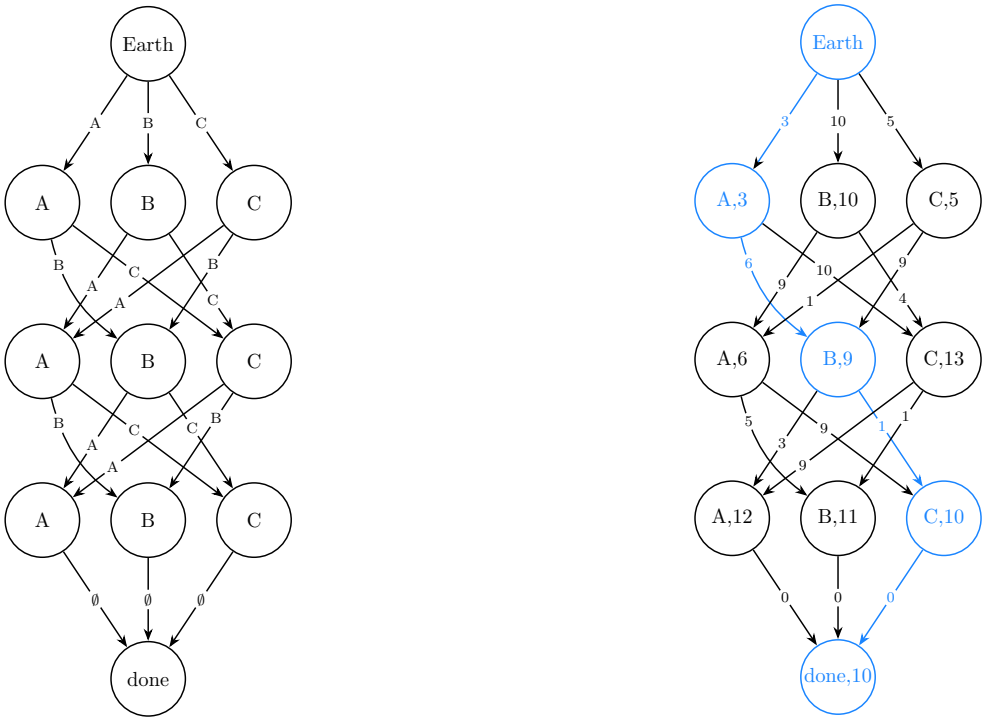


(a) Unweighted (b) Weighted

Figure 6.3 Relaxed decision diagrams for an ARP with asteroids $\{A, B, C\}$.

## 6.3 The Initial Decision Diagram

This section details a technique for constructing a relaxed DD for the ARP that yields a valid relaxed bound.

### 6.3.1 Initial Setup

We begin by constructing a relaxed DD $\mathcal{M}$ exactly as shown in Figure 6.3a. We start with a root node at layer 0, a terminal node at layer $n+1$, and $n$ nodes on each layer with index $i$, where $1 \leq i \leq n$. Each node $u$ in a layer $i$ is given a label $l$ unique to that layer. Remember that node labels are conceptually the same as arc labels. Each node and each arc has exactly one label, always representing either *Earth* or an asteroid.

An arc represents the transition from one node to another, and so in the ARP, an arc represents a transfer of the spacecraft. The arc label is the asteroid being transferred to. A node represents a state, and in the ARP, part of that state is the location of the spacecraft (either *Earth* or an asteroid). Thus, the node label is either *Earth* for the root, or an asteroid

for the other non-terminal nodes. The terminal node is a dummy node. Then, each node $v$ in layer $i-1$ is the origin for an arc ending at $u$, as long as $v$ has a different label. An arc with a null label is added from each node in layer $n$ to the terminal. The result is a relaxed DD that encodes every feasible sequence of asteroids as a path from the root to the terminal.

### 6.3.2 Relaxing the Black-Box

In real-world problems that depend on a black-box function or an inner problem, it is often possible to define relaxed versions of such functions that provide useful bounds or heuristic values [59, 60].

In the ARP, we can define a relaxed version of Eq. 6.4 that removes the cost of waiting as follows:

$$\begin{aligned} f'_{\text{inner}}(a, a', \eta, \tau, t) &= \Delta V + \frac{2\,\text{km/s}}{30\,\text{days}} \cdot t \\ \text{s.t.} \quad & \tau \in [0, \tau_{\text{f}}],\ t \in [1, \tau_{\max}] \\ \text{where} \quad & \Delta V = \|\Delta\vec{v}_1\|_2 + \|\Delta\vec{v}_2\|_2 \quad \text{and} \quad (\Delta\vec{v}_1, \Delta\vec{v}_2) = \text{Lambert}(a, a', \eta + \tau, t) \end{aligned} \tag{6.5}$$

Since $f'_{\text{inner}}$ removes the cost of waiting, we also relax the upper bound of $\tau$ to a parameter $\tau_{\text{f}}$. We can now define the following relaxed variant of $\mathcal{B}$:

$$\mathcal{B}'(a, a', \eta, \tau_{\text{f}})\colon A \times A \times \mathbb{R}^+ \to [0, \tau_{\text{f}}] \times [1, t_{\max}] \times \mathbb{R}^+ \tag{6.6}$$

which returns three values $(\tau, t, z)$, where $\tau$ and $t$ are the values that minimize $f'_{\text{inner}}$ given $a$, $a'$, $\eta$ and $\tau_{\text{f}}$, and $z$ is its minimal value. Note that this is only a relaxation in the sense that it removes part of the cost from the objective function, it does not change the method used to solve it. The procedure for solving $\mathcal{B}'$ is exactly the same as the procedure for solving $\mathcal{B}$.

Note that we will only ever use $\mathcal{B}'$ to compute bounds on costs, we will never use it to evaluate the cost of a permutation of asteroids. We always use $\mathcal{B}$ to evaluate the cost of solutions and partial solutions, so that the values we report can be compared with the values reported by [75].

### 6.3.3 Calculating Valid Arc Bounds

The examples in Section 6.2 assumed the availability of bounds on the arc weights. In this section, we will explain how they can be calculated. We also mentioned that calculating arc

bounds is expensive because it requires calculating the black-box function $\mathcal{B}$. In the ARP, this means that the inner problem must be solved using SLSQP. The algorithm we propose is designed to minimize the number of times we need to calculate the value of $\mathcal{B}$.

When using constraint propagation, arcs are filtered and removed, but never added. When splits and peels are performed, the number of arcs in the DD may grow, but only when the out-arcs of a node are copied. When this occurs, the asteroid that an arc is traveling from, and the asteroid that the arc is traveling to, remain unchanged. Therefore, when splitting or peeling, a valid bound on the cost of an arc is also a valid bound on its copy. While it may be desirable to recalculate the bound on an arc after a split to get a tighter bound, peels and splits can be carried out as many times as memory limitations allow, without the need to re-evaluate $\mathcal{B}$. We propose a two-phase algorithm for creating an initial relaxed DD. This initial construction is intentionally computationally expensive, because we will make enough evaluations of $\mathcal{B}$, that $\mathcal{B}$ does not need to be evaluated again after the initial relaxed DD is constructed, except when evaluating feasible solutions.

**Phase One**

Now we weight the DD. The arcs going from layer 0 to layer 1 are straightforward. A valid weight for an arc must be a valid lower bound on the cost of making the transfer represented by that arc. So a valid weight on arc $a_{uv}$ going from node $u$ to $v$ with labels $l(u) = Earth$ and $l(v)$ is given by the $z$ value returned by $\mathcal{B}(Earth, l(v), \eta = 0)$. There is no possibility for $\eta$ other than 0, so that $z$ value will be the smallest possible cost of going from Earth to $l(v)$.

In the ARP, these costs from layer 0 to layer 1 are exact, because the inner problem is only solved for one pair of asteroids at a time for simplicity [75]. In other words, $\mathcal{B}$ does not depend on the path from node $v$ to the terminal. Thus, we can assume that the value of $\mathcal{B}$ for an arc only depends on the earliest start time at the starting node, which only depends on the path from the root node to that starting node. In the general trajectory optimization problem, it is possible to globally optimize the inner problem for a whole sequence of asteroids by optimizing all waiting and transfer times simultaneously. This simultaneous optimization may further reduce the cost of the sequence; for example, it may be that increasing the waiting time between early transfers leads to a reduction in the transfer cost of later transfers. In that case, the value of $\mathcal{B}$ at a given arc may also depend on the path from the destination node to the terminal.

Our proposed method works for either type of problem because the sum of the arc weights on a path is still a globally valid bound on the cost of the sequence represented by that path. A dependence on the path from a node to the terminal simply makes the evaluation

of feasible solutions more expensive because we need to re-optimize all waiting and transfer times simultaneously every time we weight an arc. In the ARP, if there is only one path from the root to a node $u$, and we know both the cost of the path from the root to $u$ and the earliest start time at the previous node, then the exact cost of that path can be calculated with a single evaluation of $\mathcal{B}$ that only optimizes the wait and transfer times of the arc that ends at $u$. In our implementation, we leverage this property by updating the weights of arcs on such a path with their exact cost, and track the earliest start time for each node. This is not necessary to find an optimal solution, but it is a useful heuristic.

The arcs going from layers $i$ to $i+1$ for $i \in \{1, n-1\}$ remain to be weighted. We begin by finding a valid bound on the transfer between each ordered pair of asteroids $a, a' \in A$, with $a \neq a'$. We can use the no-wait $\mathcal{B}'$ (Eq. 6.6) for that purpose by noticing that the maximum time that any solution requires is trivially bounded by the sum of the upper bounds on the waiting times and travel times of the trajectories, i.e., $n(\tau_{\max} + t_{\max})$. Therefore, the latest start time for the final transfer is bounded by $n(\tau_{\max} + t_{\max}) - t_{\max}$. That means that the transfer from an asteroid $a$ to an asteroid $a'$ can wait $\tau \in [est(a), n(\tau_{\max}+t_{\max})-t_{\max}]$, where $est(a)$ is the earliest start time at $a$. Initially, $est(a) = \tau^* + t^*$, where $\tau^*$ and $t^*$ are the values returned by $\mathcal{B}(Earth, a, \eta = 0)$ as described above. We can now define:

$$z_{\min}(a, a') := z \quad \text{where} \quad (\tau, t, z) = \mathcal{B}'(a, a', \eta = est(a), \tau_{\mathrm{f}} = n(\tau_{\max} + t_{\max}) - t_{\max}) \tag{6.7}$$

Because $\mathcal{B}'$ does not penalize waiting time, the waiting time $\tau$ returned by $\mathcal{B}'$ above gives an optimal $\eta$ for minimizing the actual cost of the transfer using $\mathcal{B}$ (Eq. 6.1). In other words, the cost $z_{\min}(a, a')$ is the smallest possible cost of the transfer from $a$ to $a'$, and thus a lower bound of the $z$ value returned by $\mathcal{B}(a, a', \eta = est(a) + \tau)$. Computing $z_{\min}(a_i, a_j)$ for all pairs $a_i, a_j$, where $i, j \in \{1, ..., n\}$ and $i \neq j$ requires $n^2 - n$ calls to $\mathcal{B}'$.

We add the pre-calculated $z_{\min}(a, a')$ values as arc weights. A valid weight for an arc $a_{uv}$ going from node $u$ with label $l(u)$ to $v$ with label $l(v)$, is simply $z_{\min}(l(u), l(v))$, which is the best possible transfer between $l(u)$ and $l(v)$ when ignoring waiting time at $l(u)$. The resulting relaxed DD contains valid weights such that the sum of the costs of the arcs on any path from the root to the terminal provide a lower bound on the true cost of the permutation represented by the labels of the nodes on that path. However, this lower bound is quite weak, so we perform a second phase to strengthen the arc weights.

**Phase Two**

In this phase, we will use a heuristic solution $z^-$ to strengthen the arc weights. There are many methods available in the literature for finding a strong heuristic solution in trajectory optimization problems such as the ARP [78, 79]. In the ARP, any valid permutation of the asteroids is a feasible solution. For simplicity, our implementation uses a Euclidean distance heuristic to find the initial $z^-$. It picks asteroids one by one, always moving to the closest unvisited asteroid as measured by Euclidean distance at the time of arrival to the last visited asteroid. This simple heuristic is exceptionally effective and our proposed algorithm has no trouble rapidly finding strong feasible solutions. In Section 6.4, we will describe the method we use for finding feasible solutions in more detail.

Before we can make use of $z^-$, we need to store some information on the nodes. We begin by recursively updating each node $u$ with the length of the shortest path from the root to $u$, denoted by $z_\downarrow(u)$, as well as the length of the shortest path from $u$ to the terminal, denoted by $z_\uparrow(u)$ [28]. Recall that the length of a path from the root to the terminal is a valid lower bound on the cost of the associated permutation. It follows that $z_\downarrow(u) + z_\uparrow(u)$ is a valid lower bound on the cost of any path that passes through $u$, because the shortest path that passes through $u$ is trivially the shortest path from the root to $u$ merged with the shortest path from $u$ to the terminal. Note that this implies that if $z_\downarrow(u) + z_\uparrow(u) > z^-$, then the optimal solution cannot pass through $u$, and we can remove $u$ from the DD because the shortest path that passes through $u$ has a higher cost than a known feasible solution.

Now consider an arc $a_{uv}$ connecting nodes $u$ to node $v$ with weight $w(a_{uv})$. Similarly, $z_\downarrow(u) + w(a_{uv}) + z_\uparrow(v)$ is a valid lower bound on the cost of any path that can pass through $a_{uv}$. This is because the shortest path passing through an arc is the shortest path to the origin of that arc, then the arc itself, then the shortest path from the destination of the arc to the terminal. As before, we know that if $z_\downarrow(u) + w(a_{uv}) + z_\uparrow(v) > z^-$, then the optimal solution cannot pass through $a_{uv}$, and thus $a_{uv}$ can be removed from the graph. We will leverage this constraint to calculate new stronger arc weights.

Let us consider arc $a_{uv}$, and let the layer of $u$ be $1 \leq i \leq n-1$. The latest possible start time $\eta$ for arcs going from layer $i$ to $i+1$ is $i \cdot (\tau_{\max} + t_{\max})$. Thus, a naive approach to improving the quality of the weight of $a_{uv}$ is $\mathcal{B}'(l(u), l(v), \eta = est(u), \tau_f = i \cdot (\tau_{\max} + t_{\max}) + \tau_{\max})$, which returns the optimal transfer $(\tau, t, z)$ between two asteroids when waiting is free.

This $z$ value is a valid weight for each such arc $a_{uv}$, and greatly improves the weights on arcs on higher indexed layers over the weights calculated in phase one. However, this will do very little to improve the weights of arcs at lower indexed layers. This method is valid, but as

we will see next, it is extremely inefficient. Consequently, we will now use the concepts we covered in this section so far to motivate a method that scales better with the layer index.

Recall the constraint that for arc $a_{uv}$, it must be that $z_{\downarrow}(u) + w(a_{uv}) + z_{\uparrow}(v) \leq z^{-}$, or we can remove the arc. In the previous method, we used $i \cdot (\tau_{\max} + t_{\max})$ as a bound on the free waiting time an arc can leverage. A better bound can be retrieved by recognizing that the true cost of $w(a_{uv})$ includes the cost of wait time as a component. Let $\tau_a$ be the wait time used by $a_{uv}$, and recall that the cost of time in the *inner* objective function (Eq. 6.4) is $\frac{2}{30}$. It must also be the case that $z_{\downarrow}(u) + \frac{2}{30}\tau_a + z_{\uparrow}(v) \leq z^{-}$. This is because if $\tau_a$ is large enough to cause that constraint to be violated, then $w(a_{uv})$ will also be large enough to cause its constraint to be violated, because $w(a_{uv})$ is a sum of components that include $\frac{2}{30}\tau_a$. This yields the constraint that:

$$\tau_a \leq \frac{30}{2}(z^{-} - z_{\downarrow}(u) - z_{\uparrow}(v)) \tag{6.8}$$

where the right-hand-side of Eq. (6.8) is a constant because $z_{\downarrow}(u)$ and $z_{\uparrow}(v)$ are known. This means that we can use this bound for $\tau_a$ to define a stronger bound per layer:

$$z_{\min}(u, v, i) := z \text{ where } (\tau, t, z) = \mathcal{B}'(l(u), l(v), \eta = est(u), \tau_{\mathrm{f}}) \text{ and } \tau_{\mathrm{f}} = \tfrac{30}{2}(z^{-} - z_{\downarrow}(u) - z_{\uparrow}(v)) \tag{6.9}$$

Starting with $i = 1$, we calculate a new bound for every arc on a layer ($z_{\min}(u, v, i)$), then we update the values of $z_{\downarrow}(v)$ for each $v$ (in other words, each node on layer $i + 1$), then we set $i \leftarrow i + 1$, and repeat until $i = n + 1$. Therefore, we do not update the arcs with a weight of 0 that go to the terminal. After this process is done, the $z_{\uparrow}$ values of the nodes need to be updated as they are dependent on the weights of the arcs.

Phase two requires performing a total of $n^3 - 2n^2 + n$ evaluations of $\mathcal{B}'$, but results in strong enough initial bounds that, after this initial setup, our algorithm for the ARP only needs to call the black-box function $\mathcal{B}$ to evaluate the true cost of partial feasible solutions; it does not need to evaluate $\mathcal{B}$ or $\mathcal{B}'$ for the purposes of bounding.

The weights are improved based on the $z_{\downarrow}$ and $z_{\uparrow}$ values, but the values of $z_{\downarrow}$ and $z_{\uparrow}$ are updated based on the new arc weight. It is possible to run phase two repeatedly until the values converge. However, each additional update requires a huge amount of computation, and in practice yields minuscule changes. So the decision of how many repetitions to perform while constructing the initial DD is heuristic. In our implementation, we found that this process almost never improves the bound enough to be useful, so we did not include it.

**Earliest Start and Arrival Times**

So far we have assumed that the black-box function, and thus the inner optimization, only depends on the transfer locations and the arrival time at the origin location (Eq. 6.1). In practice, this is often not the case, and it is in fact possible to optimize the all of the inner problem variables for a given permutation at once to find a better solution. More generally, the objective function $f(\pi)$ may be completely black-box and not linearly separable as in Eq. 6.2. Even in such cases, it may still be possible to apply our proposed method.

In the case of the ARP, and many global trajectory optimization problems, given a permutation of the asteroids or celestial bodies to be visited, it is possible in principle to globally optimize all times $\tau_i$ and $t_i$ for all $i = 1, ..., n$ in Eq. 6.2, and further improve the objective function value. The original definition of the ARP [75] does not perform this global inner optimization because it does not guarantee finding a better objective function value, and it makes evaluating each permutation significantly more time-consuming. Nevertheless, in practical global trajectory optimization problems, performing such global inner optimization may be beneficial if enough computation time is available. Thus, we explain here how to adapt our proposed method to handle such cases.

For the ARP as originally defined, calculating earliest start times is an unnecessary but useful heuristic. As explained in Section 6.3.3, $\mathcal{B}(Earth, l(u), \eta = 0)$ returns the $z$ value for an arc going from Earth to a node $u$ in layer 1 as well as the exact $\tau + t$ value that the transfer requires, which is the exact earliest start time at $u$ for any valid sequence. However, if we optimize all of the inner problem decision variables for a valid sequence at the same time, the earliest start time may be different. We describe next a valid alternative.

First, we define a variant of $\mathcal{B}$ that limits the maximum total time $\theta$ for the transfer:

$$\begin{aligned} \tilde{\mathcal{B}}(a, a', \eta, \theta) &= (\tau^*, t^*, z^*) \\ \text{where} \quad & z^* = f_{\text{inner}}(a, a', \tau^*, t^*) \quad \text{and} \quad (\tau^*, t^*) = \arg\min f_{\text{inner}}(a, a', \tau, t) \\ \text{s.t.} \quad & \tau + t \leq \theta,\ \tau \in [0, \tau_{\max}],\ t \in [1, t_{\max}] \end{aligned} \tag{6.10}$$

The above function $\tilde{\mathcal{B}}$ also returns three values $(\tau, t, z)$ with the same meaning as they have for $\mathcal{B}$, but the inner problem has the additional constraint that $\tau + t \leq \theta$.

Given a relaxed DD where the nodes store $z_{\downarrow}(u)$ and $z_{\uparrow}(u)$, we can use the above function to find the earliest start time ($est$) for any node $u$ in layer 1. In other words, we can use $\tilde{\mathcal{B}}$ to find the $est$ for visiting an asteroid $l(u)$ from Earth. This is accomplished by performing

a binary search with a starting range of $[0, \tau_{\max} + t_{\max}]$ to find the value $\theta$ such that:

$$z^- - z_\uparrow(u) = \tilde{z} \quad \text{where} \quad (\tau, t, \tilde{z}) = \tilde{\mathcal{B}}(Earth, a, \eta = 0, \theta) \tag{6.11}$$

However, the $z$ values returned by $\mathcal{B}$, and thus $\tilde{\mathcal{B}}$, are not necessarily smooth, so the equality may not be strictly satisfiable because the target value may not be in the range of $\tilde{\mathcal{B}}$. When this is the case, the goal of the binary search should be modified to find the value of $\theta$ that produces the largest value of $\tilde{z} \leq z^- - z_\uparrow(u)$.

The earliest arrival time (*eat*) to reach the end of an arc $a_{uv}$ can be similarly found by performing a binary search to find the value of $\theta$ such that:

$$\tilde{z} = z^- - z_\downarrow(u) - z_\uparrow(v) \quad \text{where} \quad (\tau, t, \tilde{z}) = \tilde{\mathcal{B}}(l(u), l(v), \eta = est(u), \theta) \tag{6.12}$$

The *est* of a node $v$ is the minimum *eat* of arcs ending at $v$, which allows us to repeat the search for the nodes in the next layer. However, performing this search on a node $v$ requires running a binary search on every single arc ending at $v$, which is significantly time-consuming. If using this method, we recommend only using it on nodes with one parent.

## 6.4 Heuristic Search with Embedded Restricted Decision Diagrams

A benefit of leveraging embedded restricted DDs, and a critical benefit for solving ARPs, is that each node $u$ in a relaxed DD can also be labeled with the length of the shortest path from $u$ to the terminal, which we have already denoted as $z_\uparrow(u)$ in this paper. This provides a simple but powerful heuristic for deciding which nodes to explore. This heuristic is directly inspired by, but substantially different from, the rough bounding proposed in [30].

Let $\omega_s$ be the maximum width allotted to the search. Given a node to be processed $u^-$ in a partially constructed restricted DD $\mathcal{M}^-$, the typical method for figuring out which of $u^-$'s children to explore would be to generate all of them and then repeatedly throw away the node $v^-$ in the layer being constructed with the highest $z_\downarrow(v)$ until the width of the layer is $\omega_s$. However, for the ARP, each creation of a child requires a transfer from the last asteroid visited to an unvisited one, which requires a call to $\mathcal{B}$, causing such a search to become rapidly intractable.

In order for the embedded restricted DDs to be generated quickly, it is critical to limit the number of calls to $\mathcal{B}$. Evaluating a single feasible solution to the ARP requires $n-1$ calls to $\mathcal{B}$. Our goal is to perform a heuristic search that requires at most $\omega_s(n-1)$ calls to $\mathcal{B}$.

Let $V^-$ be the set of potential child nodes that could be created during the procedure. Instead of generating every possible child node $v^- \in V^-$, we calculate a bound on the true cost of a solution passing through each $v^-$. Then, we generate the $\omega_s$ child nodes in $v^-$ with the lowest bounds. For a potential node $v^-$ with parent $u^-$, associated nodes in the relaxed DD $v^+$ and $u^+$ respectively, and arc $a_{u^+v^+}$ with weight $w(a_{u^+v^+})$, the bound $b(v^-)$ is calculated as:

$$b(v^-) = z_{\downarrow}(u^-) + w(a_{u^+v^+}) + z_{\uparrow}(v^+) \tag{6.13}$$

For any node $u^-$ in a restricted DD $\mathcal{M}^-$, let $u^+$ be the associated node in $\mathcal{M}^+$. Let $r^+$ be the root of an existing relaxed DD $\mathcal{M}^+$. The procedure begins by creating $r^-$, without creating it's children. Then it iterates over the nodes in $\mathcal{M}^+$ associated with the potential children of $r^-$, and creates the $\omega_s$ best candidate children of $r^-$, where candidacy is determined by the value returned by Eq. 6.13. Then this is repeated for each layer of the restricted DD. This procedure is formalized in Algorithm 15.

## 6.5 Using Peel-and-Bound for the ARP

In many problems, such as the TSP, the arc weights are exact, thus if the shortest path through the relaxed diagram is feasible, then it is also optimal. However, if the arc weights are just lower bounds, as in the ARP, the length of the shortest path might be a relaxed bound on the true cost, even if the path is feasible.

The only change required to use PnB for the ARP is in the decision of when to add a DD to the queue. In the original presentation of PnB, when the shortest path through a relaxed DD is a feasible solution, that DD is not placed back into the processing queue because the best known feasible solution encoded in that DD is known. However, the shortest path through a relaxed DD for the ARP being a feasible solution does not prove that path to be the optimal path in that DD because the arc weights are not exact. Thus, in order to refrain from adding a DD back into the queue for the ARP, there must be a known feasible solution with a cost that is not larger than the length of the shortest path in that DD.

## 6.6 Implementation Details

This section details the data structures and heuristic decisions that we used to design an efficient implementation of the algorithms in this paper.

**Algorithm 15:** Heuristic Search Procedure

**Input:** maximum width $\omega_s$; relaxed DD $\mathcal{M}^+$ with root $r$ on layer 0
Let $w(a_{xy})$ be the weight of the arc connecting $x$ to $y$.
Let $\mathcal{M}^-$ be a restricted DD with the same number of layers as $\mathcal{M}^+$, where each layer is initialized to $\emptyset$ except layer 0 which is initialized to $\{r\}$.
For any node $u^- \in \mathcal{M}^-$, let $u^+$ be the associated node in $\mathcal{M}^+$.
**foreach** *layer of nodes* $L$ *in* $\mathcal{M}^-$ **do**
    $q \leftarrow \emptyset$ `// q: empty list of nodes.`
    $b \leftarrow \emptyset$ `// b: empty mapping of nodes to values.`
    **foreach** *node* $u^- \in L$ **do**
        Let the domain of $u^-$ be $d(u^-)$, initialized to be the set of node labels on the path from $r$ (Earth) to $u^-$
        Let $d(u^+)$ be the set of node labels used by children of $u^+$
        $d(u^-) \leftarrow d(u^-) \cap d(u^+)$
        **foreach** *label* $l \in d(u^-)$ **do**
            Create a new node $v^-$ as a child of $u^-$ with label $l$, but don't weight arc $a_{u^-v^-}$
            $b(v^-) \leftarrow z_{\downarrow}(u^-) + w_{a_{u^+v^+}} + z_{\uparrow}(v^+)$
            $q \leftarrow q \cup \{v^-\}$
        **end**
    **end**
    Sort the elements $v^- \in q$ from least to greatest by their bounds $b(v^-)$
    **while** $|q| > \omega_s$ **do**
        Remove the last element of $q$ (the largest bound) from both $q$ and $\mathcal{M}^-$
    **end**
    **foreach** *node* $v^- \in q$ **do**
        $\tau^*, t^*, z^* \leftarrow \mathcal{B}(l(u^-), l(v^-), est(u^-))$
        $w(a_{u^-v^-}) \leftarrow z^*$
        $est(v^-) \leftarrow est(u^-) + \tau^* + t^*$
    **end**
**end**
**return** $\mathcal{M}^-$

### 6.6.1 Memoization of $\mathcal{B}$

The number of arcs stored in the processing queue during PnB can grow extremely rapidly. A core optimization when implementing PnB is refraining from performing unneeded writes to memory. As mentioned before, when new arcs are generated during PnB, they are copies of existing arcs, and have the same cost. Therefore, we only want to store the cost once. Instead of storing costs on the arcs, we need a single location in memory where all such costs are stored. Storing feasible solutions can be accomplished in a straightforward way, but storing arc bounds efficiently requires a more complex data structure.

### Storing Feasible Solutions

The arc costs for feasible solutions are stored in a basic decision tree to avoid redundant evaluations of $\mathcal{B}$. The tree is initialized with a root node $r$ having cost $c(r) = 0$ and a label of *Earth*. When evaluating the cost of a partial (or complete) solution, the root node is queried for the first element (asteroid) $a$ in the sequence after *Earth*. If the root node has a child $v$ whose label is also $a$, then the cost of going from Earth to $a$ is $c(v)$, and the next element in the sequence is compared with the labels of the children of $v$. This process is repeated for each element of the given sequence, adding each individual node cost to a sum total, until either the whole sequence is found in the tree and the total cost is returned, or the next element $a$ in the sequence is not among the labels of the children of the corresponding tree node $u$. If $u$ does not have a child with the same label as $a$, then node $v$ is added to the tree and its fields are set as follows:

$$\begin{aligned} \tau^*, t^*, z^* &\leftarrow \mathcal{B}(l(u)), l(v), est(u)) \\ c(v) &\leftarrow z^* \\ est(v) &\leftarrow est(u) + \tau^* + t^* \end{aligned} \tag{6.14}$$

The above process ensures that the cost of any feasible solution, partial or complete, is only computed once. Although a complete tree for an instance of size $n$ has $1 + \sum_{i=1}^{n} \prod_{j=0}^{i-1}(n-j)$ nodes, in practice only a very small part of the tree is generated. Even with a complete tree where the children of each node are kept sorted, it would take at most $\mathcal{O}(k \log n)$ comparisons to retrieve the cost of a sequence of length $k \leq n$, which is much faster than evaluating the sequence.

### Memoizing Arc Bounds

During PnB, we need to calculate arc weights every time we peel a DD (Algorithm 12), and every time we need to compute the shortest path through a DD. However, we would like to reuse the values already computed by the $z_{\min}$ functions of phase one and two (Eqs. 6.7 and 6.9, respectively). Thus, we wish to look-up a pre-computed value of $z_{\min}$ that would be valid for the new arc.

Both definitions of $z_{\min}$ only depend on the evaluation of $\mathcal{B}'(a, a', \eta, \tau_{\mathrm{f}})$. Moreover, by the definition of the inner optimization problem (Eq. 6.5), we also know that $\mathcal{B}'(a, a', \eta', \tau'_{\mathrm{f}})$ cannot return a cost $z$ better than $\mathcal{B}'(a, a', \eta, \tau_{\mathrm{f}})$ if $[\eta', \eta' + \tau'_{\mathrm{f}}] \subseteq [\eta, \eta + \tau_{\mathrm{f}}]$, because the inner optimization problem is the same but with tighter bounds on $\tau$ for the former.

During a run of PnB, the time intervals $[\eta, \eta + \tau_{\mathrm{f}}]$ implied by the arcs can only decrease in

the above manner. Let $u$ be a node that is split into $u'_1$ and $u'_2$, and let $c(u)$ be the cost of node $u$. The bounds on the new nodes must be at least as tight as the bounds on the old nodes so $c(u) \leq c(u'_1), c(u) \leq c(u'_2)$. The earliest starting time of the nodes can increase but not decrease, so $est(u) \leq est(u'_1)$, $est(u) \leq est(u'_2)$. This means that the interval start can get larger but not smaller. Let $\tau_u$ be the wait time associated with $u$, the wait time of the peeled nodes can decrease but not increase, $\tau_u \geq \tau_{u'_1}$, $\tau_u \geq \tau_{u'_2}$, which means that the interval end can get smaller but not larger. Thus, the time interval $[\eta, \eta + \tau_{\mathrm{f}}]$ used to compute the arc weight associated with a node $u$, must contain the time intervals that would be required to compute the arc weights associated with $u'_1$ and $u'_2$.

Let us store in an interval tree the $z_{\min}$ values resulting from any evaluation of $\mathcal{B}'$ with origin $a$ and destination $a'$ together with the time intervals used in the evaluation. Given an arc that has an associated time interval and whose origin and destination correspond to $a$ and $a'$, every stored $z_{\min}$ value with a time interval that contains the time interval of the arc is a valid bound for the arc. The highest value among those stored, provides the strongest bound.

Interval trees are a standard data structure designed for efficiently finding all intervals that overlap with any given interval or point. They have a lookup time for finding overlapping intervals in $\mathcal{O}(n+m)$ where $n$ is the number of intervals in the tree, and $m$ is the number of intervals that satisfy the query. A standard interval tree is optimized for finding overlapping intervals; each tree-node stores the maximum value of its descendants. In our case, we only ever need to find containing intervals, thus we also store the minimum value (interval start) of its descendants in each tree-node. This prevents wasted time from looking for containing intervals on a branch of the tree when the lower bound on that branch is higher than the start time of our interval. We also adjusted the lookup function to only return containing intervals, instead of all overlapping intervals.

### 6.6.2 Heuristic Decisions

In our implementation, we test two different methods for selecting a DD from $Q$ (line 7 in Algorithm 13): worst bound, and largest index. Selecting the DD with the worst bound is similar to performing a breadth-first-search; it is making a decision to try to always improve the current lower bound on the problem, but can lead to a very large $Q$. Selecting the DD with a root node whose index in the initial DD was highest is similar to performing a depth-first search; it prioritizes keeping $Q$ small over improving the lower bound as quickly as possible.

We also test two different methods for selecting a node to peel from DD $Q$ (line 7 in Algorithm 13). The first method is to pick the last exact node, which is the highest indexed exact node

on the shortest path through $Q$. The second method is to pick the maximal node, which is the lowest indexed node on the shortest path through $Q$. These methods are discussed in detail in [9].

### 6.6.3 Limitations of the Inner Optimizer

The inner problem is non-convex and non-linear, making it impossible in general to prove that a local optimum is also a global optimum. In $\mathcal{B}$, the search space is small enough that local optima are likely to be global optima as well. Even if this is not the case, the inner optimizer is deterministic, meaning that the same permutation will yield the same local optima for the inner optimization problems. The goal is to find the globally optimal permutation. When using $\mathcal{B}'$, the inner optimizer searches within a superset of the search space induced by $\mathcal{B}$, potentially finding a local optimum that is worse than the one returned by $\mathcal{B}$. In such cases, the outer optimization might be misled about which permutation is optimal. However, the permutation found is still a solution (possibly suboptimal) to the original ARP, because feasible solutions are always evaluated using $\mathcal{B}$, not $\mathcal{B}'$.

More concretely, the inner optimization that computes $\mathcal{B}$ in [75] consists of a single deterministic run of SLSQP, as explained in Section 6.2.1. A single run of SLSQP almost always returns a global optimum when $\tau_\mathrm{f} \leq \tau_\mathrm{max}$ as set in the original paper. However, SLSQP may return a locally optimal solution when $\tau_\mathrm{f} \gg \tau_\mathrm{max}$, as we set it here when computing $\mathcal{B}'$ (Eq. 6.6). That is, $\mathcal{B}'(a, a', \eta = 0, \tau_\mathrm{f})$ may return $(\tau', t', z')$ as optimal yet $\mathcal{B}'(a, a', \eta = \tau', \tau_\mathrm{f})$ may return a better solution even though the time interval $[\tau', \tau_\mathrm{f}]$ is contained within $[0, \tau_\mathrm{f}]$. This problem can be alleviated by performing multiple restarts of SLSQP for each evaluation of $\mathcal{B}'$. In other words, when optimizing the relaxed inner problem (Eq. 6.5), we can partition the range $[\eta, \eta + \tau_\mathrm{f}]$ into disjoint intervals, run SLSQP for each interval, and keep the best solution. We report experiments with different number of restarts that show their effect on runtime and solution quality.

SLSQP could be replaced with a more effective optimizer, such L-BFGS-B [80] or CMA-ES [81]. For other inner problems, it may be possible to ensure that the inner optimizer returns a global optimum. In this paper, we decided to keep SLSQP as the inner optimizer in order to compare our results on the ARP with those reported by [75]. The following experiments (Section 6.7) show that increasing the quality of the inner optimizer does lead to better solutions, but not always, and not by much, so it is likely that we are already finding the optimal solutions for several of the ARP instances.

## 6.7 Experimental Results

An ARP instance with $n$ asteroids is constructed by randomly selecting $n$ asteroids from a database containing $83,453$ asteroids. The selection process is controlled by a *seed* value, ensuring that specific instances can be consistently replicated. In [75], they test their algorithms with $n \in \{10, 15, 20, 25, 30\}$ and $seed \in \{42, 73\}$. We ran experiments with the same $n$ values, but added three randomly chosen seeds: 8, 22, and 59. The experiments were performed on a computer equipped with an AMD Rome 7532 at 2.40 GHz with 64Gb RAM. Our code and raw experimental data are available at `https://zenodo.org/doi/10.5281/zenodo.12675217`. Several of the results tables in this section have a *queue* column. This value is the number of DDs remaining in the processing queue when the solver ran out of time.

### 6.7.1 Note on Optimality

As discussed in Section 6.6.3, changing the quality of the inner optimizer may impact the quality of solutions returned by our framework. For several of the problems in this section, we report different optimal solutions using different settings. These different solutions are the result of the inner optimizer not being of sufficient quality for some settings, and thus are intentional, and do not represent a mistake in the implementation.

### 6.7.2 Initial Experiment: Determining Best Settings

In our first test, shown in Table 6.1, we sought to determine which peel setting would be the most effective, which DD-widths $\omega$ would be the most effective, and the effect of using depth-first search (dfs, see Section 6.6.2). The value of $\omega$ used can have a large impact on the solve time because relaxed DDs with larger widths generally yield better bounds, but also take longer to compute. The best value for $\omega$ is the one that balances this quality/time trade-off.

We tested $n = 15$ with all 5 seeds, 2 days of runtime, and no SLSQP restarts ($multi = 1$ means one SLSQP run for solving the inner optimization problem). Figure 6.4 summarizes these results; the lines show the mean gap (or mean time) over the ARP instances.

We tested two peel settings: maximal and last exact node. Although there is no clear winner, maximal generally performs better and performs only slightly worse when it does not. Consequently, we will use the maximal setting in all future experiments. The effectiveness of the depth-first-search (dfs) queue ordering appears random based on summary data. The raw data, which is also available in the repository, contains a timestamp and bounds for each improvement to the bounds made during a run of PnB. The raw data suggests the

success of dfs mainly depends on whether the best solution is found in an early branch. It also suggests that dfs is slightly worse for the *maximal* peel setting and both $\omega = 512$ and $\omega = 2048$, as also shown in the left plot of Fig. 6.4. We disabled dfs ordering in the remaining experiments, opting for the default ordering that processes the DD with the weakest bound, likely reducing the optimality gap in unresolved problems. Regarding relaxed DD-width, we tested 512, 1024, and 2048. While 2048 showed the greatest success in closing problems and narrowing the optimality gap, 512 resolved specific settings significantly faster. Moving forward, we will retest 512 and 2048, and introduce a new width of 256. We do not include tests with widths larger than 2048 because in our experience with DDs, the slowdown in construction time from increasing the width starts to become substantial around 2048. This happens because the number of arcs at each layer is at most $\mathcal{O}(\omega^2 n)$, and small increases in the width beyond 2048 can lead to enormous increases in the construction time.

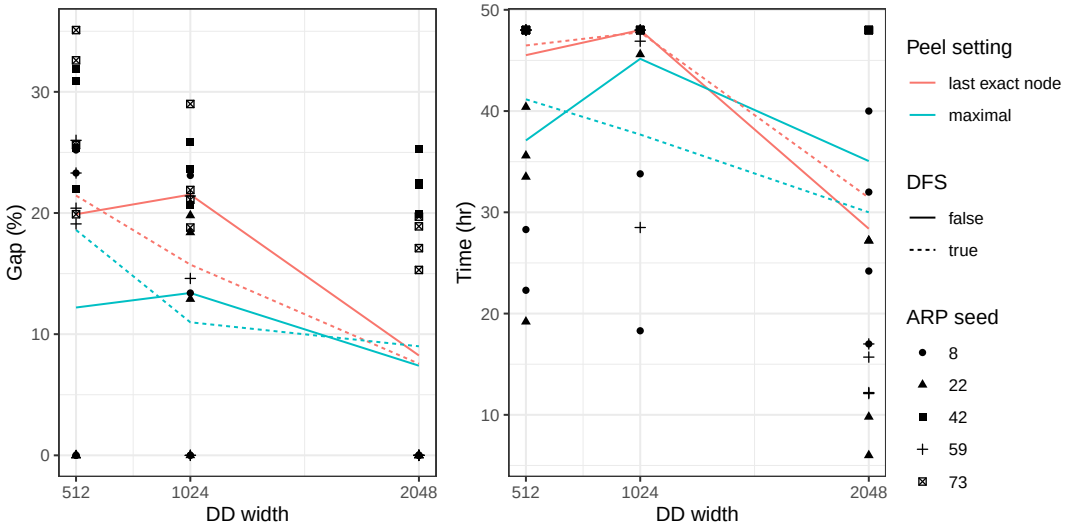


Figure 6.4 ARP instances with $n = 15$, a 2 day runtime, an embedded search width of 100, and $multi = 1$ (Table 6.1)

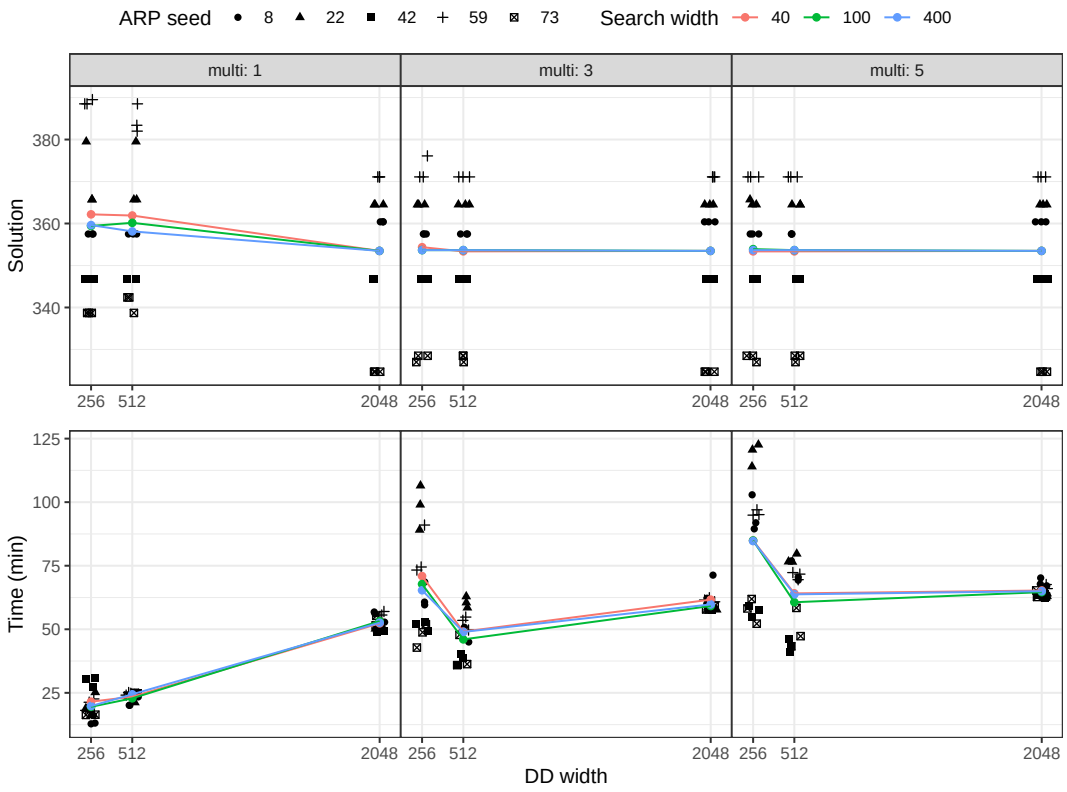


Figure 6.5 ARP instances with $n = 10$. Lines show mean value over ARP instances (Table 6.2)

Table 6.1 ARP instances with $n = 15$, a 2 day runtime, an embedded search width of 100, and $multi = 1$

| seed | peel setting | dfs | DD width | lb | ub | gap (%) | time (hr) |
|---|---|---|---|---|---|---|---|
| 8 | last exact node | true | 512 | 406.0 | 528.9 | 23.3 | - |
| | | | 1024 | 433.3 | 500.4 | 13.4 | - |
| | | | 2048 | 499.5 | 499.5 | 0.0 | 17.0 |
| | maximal | true | 512 | 499.5 | 499.5 | 0.0 | 28.3 |
| | | | 1024 | 500.1 | 500.1 | 0.0 | 18.3 |
| | | | 2048 | 504.5 | 504.5 | 0.0 | 32.0 |
| | last exact node | false | 512 | 411.3 | 550.0 | 25.2 | - |
| | | | 1024 | 412.6 | 536.5 | 23.1 | - |
| | | | 2048 | 500.9 | 500.9 | 0.0 | 24.2 |
| | maximal | false | 512 | 499.5 | 499.5 | 0.0 | 22.3 |
| | | | 1024 | 499.5 | 499.5 | 0.0 | 33.8 |
| | | | 2048 | 503.8 | 503.8 | 0.0 | 40.0 |
| 22 | last exact node | true | 512 | 472.4 | 472.4 | 0.0 | 40.4 |
| | | | 1024 | 400.9 | 500.0 | 19.8 | - |
| | | | 2048 | 501.7 | 501.7 | 0.0 | 27.2 |
| | maximal | true | 512 | 472.4 | 472.4 | 0.0 | 33.5 |
| | | | 1024 | 501.7 | 501.7 | 0.0 | 45.6 |
| | | | 2048 | 481.9 | 481.9 | 0.0 | 9.8 |
| | last exact node | false | 512 | 472.4 | 472.4 | 0.0 | 35.6 |
| | | | 1024 | 406.6 | 498.5 | 18.4 | - |
| | | | 2048 | 482.3 | 482.3 | 0.0 | 6.0 |
| | maximal | false | 512 | 472.4 | 472.4 | 0.0 | 19.2 |
| | | | 1024 | 438.9 | 504.0 | 12.9 | - |
| | | | 2048 | 501.7 | 501.7 | 0.0 | 27.2 |
| 42 | last exact node | true | 512 | 351.2 | 508.2 | 30.9 | - |
| | | | 1024 | 382.3 | 500.1 | 23.6 | - |
| | | | 2048 | 393.4 | 507.5 | 22.5 | - |
| | maximal | true | 512 | 346.0 | 508.2 | 31.9 | - |
| | | | 1024 | 376.7 | 508.2 | 25.9 | - |
| | | | 2048 | 379.6 | 508.2 | 25.3 | - |
| | last exact node | false | 512 | 379.3 | 508.2 | 25.4 | - |
| | | | 1024 | 8.1 | 508.2 | 23.6 | - |
| | | | 2048 | 394.5 | 507.5 | 22.3 | - |
| | maximal | false | 512 | 395.3 | 506.9 | 22.0 | - |
| | | | 1024 | 402.2 | 506.9 | 20.7 | - |
| | | | 2048 | 406.0 | 506.9 | 19.9 | - |
| 59 | last exact node | true | 512 | 416.6 | 523.2 | 20.4 | - |
| | | | 1024 | 523.2 | 523.2 | 0.0 | 46.9 |
| | | | 2048 | 530.4 | 530.4 | 0.0 | 17.0 |
| | maximal | true | 512 | 403.7 | 545.8 | 26.0 | - |
| | | | 1024 | 523.2 | 523.2 | 0.0 | 28.5 |
| | | | 2048 | 530.4 | 530.4 | 0.0 | 12.2 |
| | last exact node | false | 512 | 420.9 | 548.9 | 23.3 | - |
| | | | 1024 | 426.3 | 542.7 | 21.4 | - |
| | | | 2048 | 530.4 | 530.4 | 0.0 | 15.7 |
| | maximal | false | 512 | 440.3 | 543.9 | 19.1 | - |
| | | | 1024 | 446.7 | 523.2 | 14.6 | - |
| | | | 2048 | 530.4 | 530.4 | 0.0 | 12.1 |
| 73 | last exact node | true | 512 | 333.9 | 495.2 | 32.6 | - |
| | | | 1024 | 389.2 | 498.0 | 21.9 | - |
| | | | 2048 | 419.5 | 495.2 | 15.3 | - |
| | maximal | true | 512 | 326.3 | 502.5 | 35.1 | - |
| | | | 1024 | 351.7 | 495.2 | 29.0 | - |
| | | | 2048 | 402.3 | 500.8 | 19.7 | - |
| | last exact node | false | 512 | 373.8 | 502.5 | 25.6 | - |
| | | | 1024 | 396.3 | 502.5 | 21.1 | - |
| | | | 2048 | 407.6 | 502.5 | 18.9 | - |
| | maximal | false | 512 | 398.7 | 498.1 | 19.9 | - |
| | | | 1024 | 408.1 | 502.5 | 18.8 | - |
| | | | 2048 | 416.3 | 502.1 | 17.1 | - |

*dfs* = depth first search (queue processing order), *DD width* = width of relaxed DD, *lb* = lower bound, *ub* = upper bound, *gap* = optimality gap, *time* = time to solve

Table 6.2 ARP instances with $n = 10$

| seed | search | DD width | $multi = 1$ | | $multi = 3$ | | $multi = 5$ | |
|---|---|---|---|---|---|---|---|---|
| | | | solution | time(min) | solution | time(min) | solution | time(min) |
| 8 | 40 | 256 | 357.5 | 13.1 | 357.5 | 60.7 | 357.5 | 89.5 |
| | | 512 | 357.5 | 20.1 | 357.5 | 49.6 | 357.5 | 69.3 |
| | | 2048 | 360.4 | 52.8 | 360.4 | 71.3 | 360.4 | 70.2 |
| | 100 | 256 | 357.5 | 12.8 | 357.5 | 59.6 | 357.5 | 91.9 |
| | | 512 | 357.5 | 20.1 | 357.5 | 45.0 | 357.5 | 70.5 |
| | | 2048 | 360.4 | 56.1 | 360.4 | 60.0 | 360.4 | 67.8 |
| | 400 | 256 | 357.5 | 16.1 | 357.5 | 68.6 | 357.5 | 102.9 |
| | | 512 | 357.5 | 23.4 | 357.5 | 50.8 | 357.5 | 76.9 |
| | | 2048 | 360.4 | 56.8 | 360.4 | 62.2 | 360.4 | 67.1 |
| 22 | 40 | 256 | 379.5 | 25.2 | 364.5 | 99.0 | 364.5 | 120.6 |
| | | 512 | 379.5 | 24.5 | 364.5 | 58.5 | 364.5 | 79.7 |
| | | 2048 | 364.5 | 50.2 | 364.5 | 57.7 | 364.5 | 63.0 |
| | 100 | 256 | 365.7 | 16.2 | 364.5 | 106.5 | 365.7 | 122.6 |
| | | 512 | 365.7 | 21.2 | 364.5 | 60.5 | 364.5 | 76.6 |
| | | 2048 | 364.5 | 51.4 | 364.5 | 58.5 | 364.5 | 64.1 |
| | 400 | 256 | 365.7 | 18.9 | 364.5 | 89.1 | 364.5 | 114.0 |
| | | 512 | 365.7 | 23.8 | 364.5 | 62.9 | 364.5 | 76.5 |
| | | 2048 | 364.5 | 51.2 | 364.5 | 58.8 | 364.5 | 64.0 |
| 42 | 40 | 256 | 346.7 | 30.3 | 346.7 | 51.9 | 346.7 | 57.5 |
| | | 512 | 346.7 | 23.7 | 346.7 | 36.0 | 346.7 | 40.9 |
| | | 2048 | 346.7 | 50.1 | 346.7 | 59.3 | 346.7 | 63.9 |
| | 100 | 256 | 346.7 | 30.9 | 346.7 | 49.5 | 346.7 | 54.9 |
| | | 512 | 346.7 | 24.8 | 346.7 | 38.6 | 346.7 | 43.3 |
| | | 2048 | 346.7 | 49.3 | 346.7 | 58.0 | 346.7 | 62.4 |
| | 400 | 256 | 346.7 | 27.2 | 346.7 | 52.9 | 346.7 | 59.3 |
| | | 512 | 346.7 | 25.1 | 346.7 | 40.4 | 346.7 | 46.3 |
| | | 2048 | 346.7 | 49.1 | 346.7 | 57.7 | 346.7 | 63.3 |
| 59 | 40 | 256 | 388.5 | 22.6 | 376.1 | 91.0 | 371.1 | 94.9 |
| | | 512 | 383.4 | 25.1 | 371.1 | 53.5 | 371.1 | 72.3 |
| | | 2048 | 371.1 | 57.0 | 371.1 | 60.8 | 371.1 | 63.8 |
| | 100 | 256 | 388.5 | 21.3 | 371.1 | 74.5 | 371.1 | 97.0 |
| | | 512 | 388.5 | 24.1 | 371.1 | 49.7 | 371.1 | 69.5 |
| | | 2048 | 371.1 | 53.9 | 371.1 | 61.5 | 371.1 | 66.0 |
| | 400 | 256 | 389.5 | 18.1 | 371.1 | 73.3 | 371.1 | 95.1 |
| | | 512 | 382.0 | 24.8 | 371.1 | 54.8 | 371.1 | 71.7 |
| | | 2048 | 371.1 | 55.6 | 371.1 | 62.4 | 371.1 | 67.6 |
| 73 | 40 | 256 | 338.7 | 16.4 | 327.0 | 52.0 | 327.0 | 61.9 |
| | | 512 | 342.4 | 23.9 | 327.0 | 47.8 | 327.0 | 58.4 |
| | | 2048 | 324.7 | 51.5 | 324.7 | 59.2 | 324.7 | 65.3 |
| | 100 | 256 | 338.7 | 16.3 | 328.5 | 48.8 | 328.5 | 58.2 |
| | | 512 | 342.4 | 24.0 | 328.5 | 36.3 | 328.5 | 43.3 |
| | | 2048 | 324.7 | 55.3 | 324.7 | 57.8 | 324.7 | 62.7 |
| | 400 | 256 | 338.7 | 18.7 | 328.5 | 42.8 | 328.5 | 52.2 |
| | | 512 | 338.7 | 25.0 | 328.5 | 35.9 | 328.5 | 47.3 |
| | | 2048 | 324.7 | 50.2 | 324.7 | 57.8 | 324.7 | 62.9 |

*search* = width of embedded search, *DD width* = width of relaxed dd
*time* = time to solve

### 6.7.3 Second Experiment: Test of Smaller Instances

Our first round of experiments gave us a rough idea of what settings might be successful. Our second round of experiments makes up the bulk of our tests. As discussed in the previous paragraph we test relaxed DD-widths of 256, 512, and 2048. For the embedded search widths ($\omega_s$ from Algorithm 15) we tested 40, 100, and 400, where previously we just used 100. In typical DD literature [1], the size of the search for feasible solutions would be as big or bigger than the size of the relaxed DD, because it is relatively computationally cheap. However, for

the ARP, the search for feasible solutions is computationally expensive because of the inner-optimization that requires evaluating the black-box function $\mathcal{B}$. This suggested to us that larger embedded search widths are unlikely to be worth it. However, the following results indicate that might not be true. We also tested $multi \in \{1, 3, 5\}$. Table 6.2 (Fig. 6.5) show the results of the second round of experiments for $n = 10$, Table 6.4 (Fig. 6.6) for $n = 15$, and Table 6.5 (Fig. 6.7) for $n = 20$. In Table 6.2, every solution is optimal, so it does not include the *gap* columns.

The largest search settings, i.e., an embedded search width of 400 and a relaxed DD-width of 2048, clearly dominate the results, with tighter optimality gaps and more problems solved. For the remainder of the discussion, we will be referring primarily to those results. Recall from Section 6.6.3 that different *multi* values can have different optimal solutions because the inner optimizer may return a local optimum instead of the global optimum. When $n = 10$ (Table 6.2 and Fig. 6.5) and $multi = 1$, all of the problems are solved to optimality in under 1 hour, and when $multi = 5$, they are solved to optimality in under 2 hours. In some cases the largest search settings alleviates some of the negative effects of $multi = 1$ (in Table 6.2, seed 22, DD width 512, compare search width 40 to search width 100). This is likely because a larger search provides more opportunities to stumble on improved solutions that will later be trimmed as a result of using a low *multi*. For the the largest search settings, the effect of *multi* is only to increase the runtime, however settings with smaller DD widths make it clear that *multi* can have a strong impact on the underlying arc calculations. For example, seed 59, with search width 40, and relaxed DD-width 256, has a different exact solution with $multi = 1$ than it does with $multi = 5$; the cost drops from 388.5 to 371.1. Recall that because the inner problem in the ARP is nonlinear and nonconvex, it is not possible to prove optimality in general. In lieu of that, *multi* can be increased arbitrarily to increase confidence in the solutions. If *multi* is increased, and the algorithm returns the same permutation as it did for a lower *multi* value, that provides evidence that the optimal solution is stable. The larger the increase in *multi*, the stronger the evidence.

We now focus on the results obtained with an embedded search width of 400 and a relaxed DD-width of 2048 on instances of size $n \in \{15, 20\}$ (Tables 6.4 and 6.5) with a maximum runtime of 7 days. With $multi = 1$, three of the problems were solved in under a day, with the other two taking around two days. However, many of the solutions are improved with a higher *multi* (see the top row of Figures 6.6 and 6.7). For $n = 15$, the setting $multi = 1$ is unlikely to yield optimal solutions. With $multi = 5$, only seeds 8 and 22 were solved exactly, but they yielded much better solutions. In seed 22 for example, the best solution drops from 501.7 to 466.3. With $n = 20$, none of the problems were solved to optimality within the 7 day limit.

The only available comparison we can make is with [75]. However, because they assume that the inner problem is a total black box, and we take advantage of the structure of the black box, any time/computation comparison is meaningless. So we will merely be comparing our solutions to theirs, to show that our method yields high quality solutions. They only used seeds 42 and 73, so for the other problems we can only report our solutions. These results are shown in Table 6.3. Notably the solution reported by Peel-and-Bound's preferred setting ($\omega_s = 400$, $\omega = 2048$, *multi*$= 5$) is the same as the best previously found for $n = 10$, and better than those previously reported for $n = 15$ and $n = 20$. In some cases, the gap is quite large, for example with $n = 20$, seed$= 42$, our solution is 12.0% better. We also report the best observed solution from any setting, and for 13 of the 15 instances the preferred setting found the same solution as the best solution found by any setting. All of theses results use $\mathcal{B}$ to evaluate the cost of a permutation, and thus they are directly comparable. In other words, the values listed are not dependent on the optimality of the inner problem.

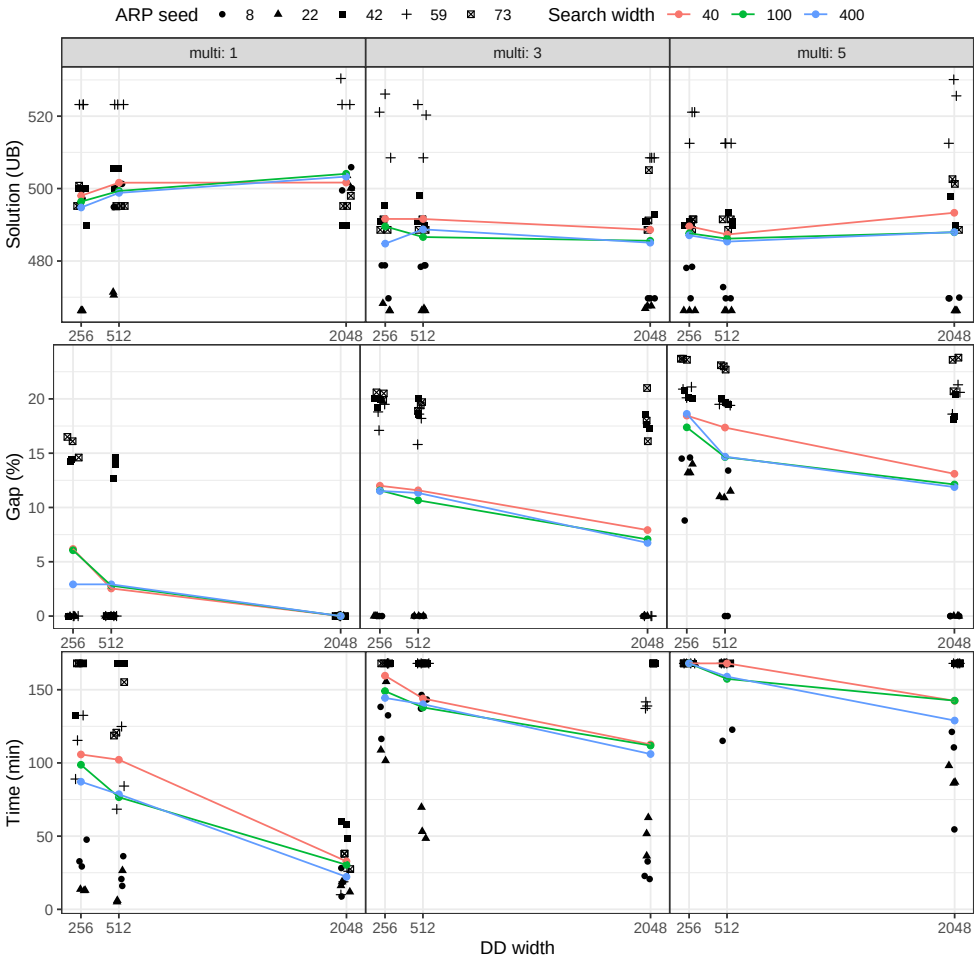


Figure 6.6 ARP instances with $n = 15$ and a 7 day runtime (Table 6.4)

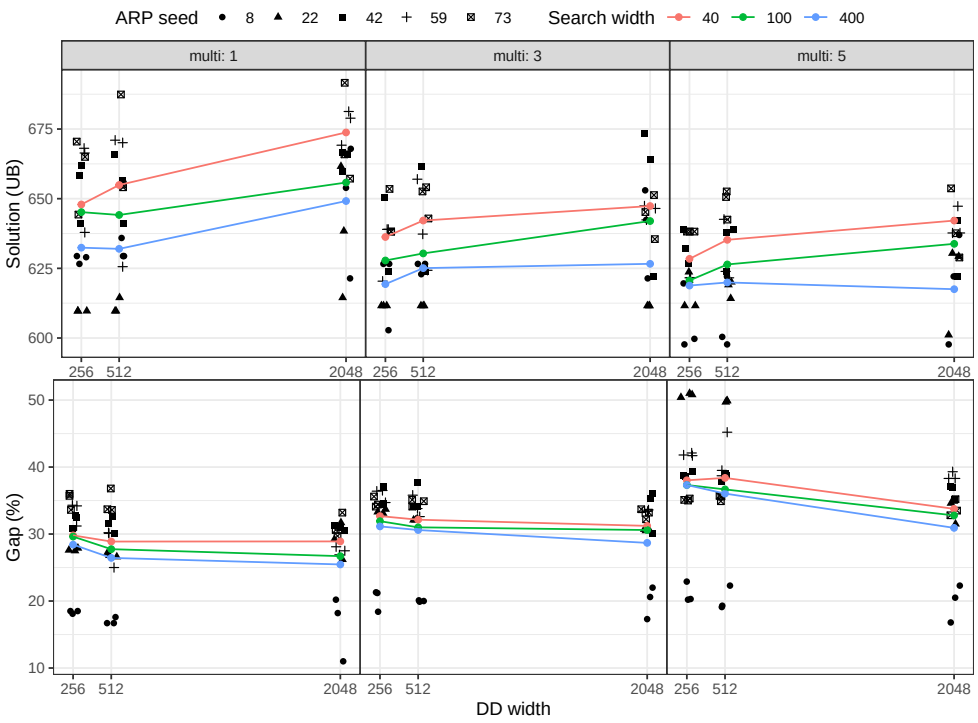


Figure 6.7 ARP instances with $n = 20$ and a 7 day runtime (Table 6.5)

Table 6.3 Best solutions for $n \in \{10, 15, 20\}$

| n | seed | [75]* | | Peel-and-Bound: Preferred Settings** | | Peel-and-Bound: Best Found*** | |
|---|---|---|---|---|---|---|---|
| | | Average Value | Best Value | Value | Optimality Gap (%) | Value | Optimality Gap (%) |
| 10 | 8 | - | - | 360.4 | 0.0 | 357.5 | 0.0 |
| | 22 | - | - | 364.5 | 0.0 | 364.5 | 0.0 |
| | 42 | 374.9 | 346.7 | 346.7 | 0.0 | 346.7 | 0.0 |
| | 59 | - | - | 371.1 | 0.0 | 371.1 | 0.0 |
| | 73 | 355.9 | 324.7 | 324.7 | 0.0 | 324.7 | 0.0 |
| 15 | 8 | - | - | 469.7 | 0.0 | 469.7 | 0.0 |
| | 22 | - | - | 466.3 | 0.0 | 466.3 | 0.0 |
| | 42 | 497.2 | 490.9 | 489.7 | 18.1 | 489.7 | 0.0 |
| | 59 | - | - | 525.6 | 20.6 | **508.5** | 0.0 |
| | 73 | 525.6 | 519.9 | 488.6 | 20.7 | 488.6 | 16.1 |
| 20 | 8 | - | - | 597.7 | 16.8 | 597.7 | 20.3 |
| | 22 | - | - | 601.1 | 31.5 | 601.1 | 31.5 |
| | 42 | 737.0 | 707.2 | 622.2 | 35.2 | 622.2 | 30.1 |
| | 59 | - | - | 637.7 | 38.3 | **619.9** | 41.7 |
| | 73 | 661.8 | 652.5 | 628.9 | 32.8 | 628.9 | 32.8 |

* The results from [75] in the *Average Found* column are the average solution cost over several runs of the same stochastic algorithm. *Best Found* reports the best solution found in any run of the algorithm.

** The preferred settings for Peel-and-Bound are: $\omega_s = 400$, $\omega = 2048$, *multi*$= 5$.

*** The bold values are the only instances where the best found solution by any setting is better than the solution found using the preferred setting.

Table 6.4 ARP instances with $n = 15$ and a 7 day runtime

| seed | search | DD width | *multi* = 1 | | | | | *multi* = 3 | | | | | *multi* = 5 | | | | |
|---|---|---|---|---|---|---|---|---|---|---|---|---|---|---|---|---|---|
| | | | lb | ub | gap (%) | time(hr) | queue | lb | ub | gap (%) | time(hr) | queue | lb | ub | gap (%) | time(hr) | queue |
| 8 | 40 | 256 | 499.8 | 499.8 | 0.0 | 47.6 | 0 | 478.8 | 478.8 | 0.0 | 138.3 | 0 | 408.1 | 478.1 | 14.6 | - | 1172 |
| | | 512 | 494.9 | 494.9 | 0.0 | 36.3 | 0 | 478.4 | 478.4 | 0.0 | 146.4 | 0 | 409.3 | 472.8 | 13.4 | - | 579 |
| | | 2048 | 500.1 | 500.1 | 0.0 | 28.2 | 0 | 469.7 | 469.7 | 0.0 | 22.8 | 0 | 469.7 | 469.7 | 0.0 | 121.2 | 0 |
| | 100 | 256 | 497.2 | 497.2 | 0.0 | 29.3 | 0 | 478.8 | 478.8 | 0.0 | 132.5 | 0 | 428.4 | 469.7 | 8.8 | - | 311 |
| | | 512 | 501.3 | 501.3 | 0.0 | 20.7 | 0 | 478.8 | 478.8 | 0.0 | 137.1 | 0 | 469.7 | 469.7 | 0.0 | 115.1 | 0 |
| | | 2048 | 505.9 | 505.9 | 0.0 | 18.8 | 0 | 469.7 | 469.7 | 0.0 | 32.7 | 0 | 469.9 | 469.9 | 0.0 | 110.6 | 0 |
| | 400 | 256 | 499.5 | 499.5 | 0.0 | 32.8 | 0 | 469.7 | 469.7 | 0.0 | 116.4 | 0 | 409.2 | 478.4 | 14.5 | - | 1011 |
| | | 512 | 499.5 | 499.5 | 0.0 | 16.0 | 0 | 478.8 | 478.8 | 0.0 | 143.3 | 0 | 469.7 | 469.7 | 0.0 | 122.7 | 0 |
| | | 2048 | 499.5 | 499.5 | 0.0 | 8.8 | 0 | 469.7 | 469.7 | 0.0 | 20.7 | 0 | 469.7 | 469.7 | 0.0 | 54.6 | 0 |
| 22 | 40 | 256 | 466.3 | 466.3 | 0.0 | 12.8 | 0 | 466.3 | 466.3 | 0.0 | 155.6 | 0 | 404.6 | 466.3 | 13.2 | - | 1152 |
| | | 512 | 494.7 | 494.7 | 0.0 | 26.5 | 0 | 466.9 | 466.9 | 0.0 | 69.7 | 0 | 415.0 | 466.3 | 11.0 | - | 179 |
| | | 2048 | 500.1 | 500.1 | 0.0 | 11.9 | 0 | 466.9 | 466.9 | 0.0 | 62.7 | 0 | 466.3 | 466.3 | 0.0 | 86.9 | 0 |
| | 100 | 256 | 466.3 | 466.3 | 0.0 | 13.0 | 0 | 468.3 | 468.3 | 0.0 | 108.8 | 0 | 404.7 | 466.3 | 13.2 | - | 1099 |
| | | 512 | 471.4 | 471.4 | 0.0 | 5.1 | 0 | 466.3 | 466.3 | 0.0 | 48.5 | 0 | 415.6 | 466.3 | 10.9 | - | 167 |
| | | 2048 | 503.6 | 503.6 | 0.0 | 18.8 | 0 | 467.6 | 467.6 | 0.0 | 51.7 | 0 | 466.3 | 466.3 | 0.0 | 98.2 | 0 |
| | 400 | 256 | 466.3 | 466.3 | 0.0 | 13.7 | 0 | 466.3 | 466.3 | 0.0 | 101.6 | 0 | 401.2 | 466.3 | 14.0 | - | 1058 |
| | | 512 | 470.6 | 470.6 | 0.0 | 6.1 | 0 | 466.3 | 466.3 | 0.0 | 53.2 | 0 | 412.9 | 466.3 | 11.5 | - | 206 |
| | | 2048 | 501.7 | 501.7 | 0.0 | 16.2 | 0 | 467.6 | 467.6 | 0.0 | 36.5 | 0 | 466.3 | 466.3 | 0.0 | 86.2 | 0 |
| 42 | 40 | 256 | 428.0 | 500.1 | 14.4 | - | 1259 | 396.5 | 495.4 | 20.0 | - | 1672 | 392.6 | 490.9 | 20.0 | - | 1634 |
| | | 512 | 436.7 | 500.1 | 12.7 | - | 316 | 398.2 | 498.0 | 20.0 | - | 747 | 394.6 | 493.5 | 20.0 | - | 712 |
| | | 2048 | 489.7 | 489.7 | 0.0 | 59.7 | 0 | 401.4 | 492.9 | 18.6 | - | 141 | 396.4 | 497.9 | 20.4 | - | 147 |
| | 100 | 256 | 428.9 | 500.1 | 14.2 | - | 1203 | 396.6 | 490.9 | 19.2 | - | 1643 | 391.4 | 489.7 | 20.1 | - | 1537 |
| | | 512 | 434.8 | 505.6 | 14.0 | - | 414 | 399.8 | 490.9 | 18.6 | - | 752 | 395.2 | 490.9 | 19.5 | - | 709 |
| | | 2048 | 489.7 | 489.7 | 0.0 | 57.7 | 0 | 406.0 | 490.9 | 17.3 | - | 105 | 399.6 | 489.7 | 18.4 | - | 127 |
| | 400 | 256 | 489.7 | 489.7 | 0.0 | 132.3 | 0 | 392.9 | 490.9 | 19.9 | - | 1312 | 388.0 | 489.7 | 20.8 | - | 1232 |
| | | 512 | 431.7 | 505.6 | 14.6 | - | 397 | 398.3 | 489.7 | 18.7 | - | 671 | 393.1 | 489.7 | 19.7 | - | 646 |
| | | 2048 | 489.7 | 489.7 | 0.0 | 48.5 | 0 | 404.4 | 490.9 | 17.6 | - | 109 | 400.8 | 489.7 | 18.1 | - | 126 |
| 59 | 40 | 256 | 523.2 | 523.2 | 0.0 | 132.5 | 0 | 423.4 | 526.1 | 19.5 | - | 1617 | 412.0 | 521.1 | 20.9 | - | 1490 |
| | | 512 | 523.2 | 523.2 | 0.0 | 124.9 | 0 | 427.8 | 523.2 | 18.2 | - | 721 | 412.9 | 512.5 | 19.4 | - | 661 |
| | | 2048 | 523.2 | 523.2 | 0.0 | 26.0 | 0 | 508.5 | 508.5 | 0.0 | 141.7 | 0 | 417.1 | 530.1 | 21.3 | - | 156 |
| | 100 | 256 | 523.2 | 523.2 | 0.0 | 115.4 | 0 | 423.1 | 521.1 | 18.8 | - | 1517 | 411.0 | 521.1 | 21.1 | - | 1386 |
| | | 512 | 523.2 | 523.2 | 0.0 | 68.4 | 0 | 428.1 | 508.5 | 15.8 | - | 655 | 411.7 | 512.5 | 19.7 | - | 591 |
| | | 2048 | 523.2 | 523.2 | 0.0 | 18.8 | 0 | 508.5 | 508.5 | 0.0 | 138.9 | 0 | 417.4 | 512.5 | 18.6 | - | 144 |
| | 400 | 256 | 523.2 | 523.2 | 0.0 | 89.0 | 0 | 421.5 | 508.5 | 17.1 | - | 1330 | 409.5 | 512.5 | 20.1 | - | 1208 |
| | | 512 | 523.2 | 523.2 | 0.0 | 84.2 | 0 | 423.6 | 520.3 | 18.6 | - | 543 | 412.6 | 512.5 | 19.5 | - | 613 |
| | | 2048 | 530.4 | 530.4 | 0.0 | 10.0 | 0 | 508.5 | 508.5 | 0.0 | 137.2 | 0 | 417.6 | 525.6 | 20.6 | - | 147 |
| 73 | 40 | 256 | 418.2 | 500.8 | 16.5 | - | 1,253 | 390.9 | 491.5 | 20.5 | - | 1,653 | 375.7 | 491.5 | 23.6 | - | 1,557 |
| | | 512 | 495.2 | 495.2 | 0.0 | 155.2 | 0 | 394.5 | 491.5 | 19.7 | - | 737 | 378.4 | 491.5 | 23.0 | - | 689 |
| | | 2048 | 495.2 | 495.2 | 0.0 | 38.1 | 0 | 399.3 | 505.1 | 21.0 | - | 152 | 382.9 | 502.6 | 23.8 | - | 149 |
| | 100 | 256 | 415.5 | 495.2 | 16.1 | - | 1,010 | 391.2 | 488.6 | 19.9 | - | 1,672 | 375.1 | 491.5 | 23.7 | - | 1,509 |
| | | 512 | 495.2 | 495.2 | 0.0 | 120.7 | 0 | 396.3 | 488.6 | 18.9 | - | 741 | 378.0 | 491.5 | 23.1 | - | 671 |
| | | 2048 | 498.0 | 498.0 | 0.0 | 37.9 | 0 | 403.0 | 491.2 | 18.0 | - | 134 | 383.2 | 501.3 | 23.6 | - | 144 |
| | 400 | 256 | 422.7 | 495.2 | 14.6 | - | 1,098 | 387.7 | 488.6 | 20.6 | - | 1,361 | 372.9 | 488.6 | 23.7 | - | 1,284 |
| | | 512 | 495.2 | 495.2 | 0.0 | 118.7 | 0 | 393.9 | 488.6 | 19.4 | - | 658 | 377.6 | 488.6 | 22.7 | - | 641 |
| | | 2048 | 495.2 | 495.2 | 0.0 | 27.5 | 0 | 410.1 | 488.6 | 16.1 | - | 77 | 387.5 | 488.6 | 20.7 | - | 135 |

*search* = width of embedded search, *DD width* = width of relaxed dd
*lb* = lower bound, *ub* = upper bound, *gap* = optimality gap,
*time* = time to solve if solved, *queue* = nodes in the processing queue

Table 6.5 ARP instances with $n = 20$ and a 7 day runtime

| seed | search | DD width | *multi* = 1 | | | | *multi* = 3 | | | | *multi* = 5 | | | |
|---|---|---|---|---|---|---|---|---|---|---|---|---|---|---|
| | | | lb | ub | gap (%) | queue | lb | ub | gap (%) | queue | lb | ub | gap (%) | queue |
| 8 | 40 | 256 | 512.7 | 629.4 | 18.5 | 1,012 | 493.5 | 626.6 | 21.2 | 708 | 477.4 | 619.6 | 22.9 | 639 |
| | | 512 | 524.0 | 635.9 | 17.6 | 557 | 501.4 | 626.6 | 20.0 | 360 | 483.2 | 622.1 | 22.3 | 332 |
| | | 2048 | 533.2 | 667.9 | 20.2 | 90 | 509.7 | 653.0 | 22.0 | 70 | 495.0 | 637.0 | 22.3 | 70 |
| | 100 | 256 | 513.3 | 626.6 | 18.1 | 1,101 | 492.9 | 626.6 | 21.3 | 679 | 478.2 | 599.7 | 20.3 | 678 |
| | | 512 | 524.2 | 629.4 | 16.7 | 598 | 500.4 | 626.6 | 20.1 | 353 | 484.7 | 600.4 | 19.3 | 369 |
| | | 2048 | 535.2 | 653.9 | 18.2 | 102 | 510.3 | 642.4 | 20.6 | 76 | 494.7 | 622.1 | 20.5 | 75 |
| | 400 | 256 | 512.7 | 629.0 | 18.5 | 948 | 492.1 | 602.8 | 18.4 | 626 | 476.7 | 597.7 | 20.2 | 581 |
| | | 512 | 524.3 | 629.4 | 16.7 | 509 | 499.3 | 622.9 | 19.9 | 328 | 483.4 | 597.7 | 19.1 | 344 |
| | | 2048 | 552.9 | 621.4 | 11.0 | 84 | 514.1 | 621.4 | 17.3 | 94 | 497.5 | 597.7 | 16.8 | 91 |
| 22 | 40 | 256 | 442.3 | 609.7 | 27.5 | 710 | 408.8 | 611.6 | 33.1 | 644 | 305.6 | 623.7 | 51.0 | 629 |
| | | 512 | 447.5 | 614.5 | 27.2 | 380 | 415.6 | 611.6 | 32.1 | 331 | 310.9 | 620.1 | 49.9 | 320 |
| | | 2048 | 451.8 | 661.6 | 31.7 | 69 | 423.9 | 611.6 | 30.7 | 69 | 410.6 | 630.4 | 34.9 | 66 |
| | 100 | 256 | 441.2 | 609.7 | 27.6 | 649 | 407.7 | 611.6 | 33.3 | 590 | 303.5 | 611.6 | 50.4 | 578 |
| | | 512 | 447.5 | 609.7 | 26.6 | 389 | 415.4 | 611.6 | 32.1 | 319 | 310.3 | 619.1 | 49.9 | 314 |
| | | 2048 | 453.8 | 614.5 | 26.2 | 80 | 425.4 | 611.6 | 30.5 | 69 | 411.5 | 629.3 | 34.6 | 66 |
| | 400 | 256 | 439.8 | 609.7 | 27.9 | 582 | 405.6 | 611.6 | 33.7 | 515 | 301.3 | 611.6 | 50.8 | 496 |
| | | 512 | 446.2 | 609.7 | 26.8 | 357 | 414.2 | 611.6 | 32.3 | 297 | 308.8 | 614.2 | 49.7 | 284 |
| | | 2048 | 451.8 | 638.4 | 29.2 | 69 | 425.4 | 611.6 | 30.5 | 68 | 412.1 | 601.1 | 31.5 | 67 |
| 42 | 40 | 256 | 445.6 | 661.9 | 32.7 | 616 | 409.0 | 650.6 | 37.1 | 613 | 387.8 | 638.8 | 39.3 | 598 |
| | | 512 | 448.7 | 665.8 | 32.6 | 321 | 412.3 | 661.5 | 37.7 | 331 | 391.0 | 638.8 | 38.8 | 331 |
| | | 2048 | 457.6 | 666.5 | 31.3 | 66 | 430.6 | 673.5 | 36.1 | 65 | 404.3 | 642.3 | 37.1 | 65 |
| | 100 | 256 | 444.4 | 658.2 | 32.5 | 591 | 409.2 | 623.7 | 34.4 | 597 | 386.9 | 632.2 | 38.8 | 575 |
| | | 512 | 448.8 | 656.5 | 31.6 | 327 | 411.3 | 623.7 | 34.1 | 301 | 389.1 | 638.0 | 39.0 | 297 |
| | | 2048 | 459.3 | 665.8 | 31.0 | 67 | 429.8 | 664.2 | 35.3 | 63 | 404.8 | 642.3 | 37.0 | 63 |
| | 400 | 256 | 443.1 | 641.2 | 30.9 | 548 | 408.6 | 623.7 | 34.5 | 522 | 384.9 | 626.7 | 38.6 | 499 |
| | | 512 | 448.4 | 641.2 | 30.1 | 290 | 411.0 | 623.7 | 34.1 | 276 | 388.1 | 623.7 | 37.8 | 273 |
| | | 2048 | 458.3 | 659.6 | 30.5 | 66 | 435.0 | 622.2 | 30.1 | 65 | 403.2 | 622.2 | 35.2 | 63 |
| 59 | 40 | 256 | 439.0 | 668.1 | 34.3 | 612 | 406.4 | 639.0 | 36.4 | 594 | 361.9 | 621.7 | 41.8 | 589 |
| | | 512 | 468.4 | 671.0 | 30.2 | 331 | 422.1 | 657.0 | 35.8 | 316 | 352.4 | 642.6 | 45.2 | 311 |
| | | 2048 | 489.6 | 681.3 | 28.1 | 68 | 429.9 | 647.4 | 33.6 | 70 | 392.7 | 647.3 | 39.3 | 67 |
| | 100 | 256 | 438.5 | 666.4 | 34.2 | 592 | 405.8 | 639.0 | 36.5 | 568 | 359.7 | 621.6 | 42.1 | 560 |
| | | 512 | 468.2 | 670.1 | 30.1 | 325 | 421.9 | 637.3 | 33.8 | 308 | 377.4 | 623.9 | 39.5 | 301 |
| | | 2048 | 492.6 | 678.9 | 27.5 | 71 | 430.7 | 646.5 | 33.4 | 68 | 393.3 | 637.7 | 38.3 | 69 |
| | 400 | 256 | 438.9 | 637.9 | 31.2 | 595 | 404.8 | 620.4 | 34.7 | 514 | 361.7 | 619.9 | 41.7 | 469 |
| | | 512 | 469.2 | 625.6 | 25.0 | 351 | 420.9 | 624.3 | 32.6 | 293 | 381.1 | 621.6 | 38.7 | 283 |
| | | 2048 | 489.3 | 669.2 | 26.9 | 72 | 428.4 | 642.4 | 33.3 | 67 | 393.4 | 637.7 | 38.3 | 66 |
| 73 | 40 | 256 | 429.0 | 670.5 | 36.0 | 630 | 420.8 | 653.5 | 35.6 | 614 | 414.0 | 638.2 | 35.1 | 559 |
| | | 512 | 434.1 | 687.4 | 36.8 | 312 | 424.6 | 654.1 | 35.1 | 314 | 419.5 | 652.6 | 35.7 | 313 |
| | | 2048 | 462.0 | 691.6 | 33.2 | 74 | 431.6 | 651.3 | 33.7 | 68 | 423.9 | 653.7 | 35.2 | 66 |
| | 100 | 256 | 427.8 | 665.0 | 35.7 | 562 | 420.3 | 638.2 | 34.1 | 571 | 415.0 | 638.2 | 35.0 | 558 |
| | | 512 | 434.6 | 655.1 | 33.7 | 321 | 424.6 | 652.6 | 34.9 | 316 | 419.4 | 650.6 | 35.6 | 309 |
| | | 2048 | 462.2 | 665.9 | 30.6 | 69 | 430.7 | 645.2 | 33.2 | 66 | 423.9 | 637.6 | 33.5 | 68 |
| | 400 | 256 | 427.5 | 644.3 | 33.6 | 543 | 418.9 | 638.2 | 34.4 | 485 | 412.9 | 638.2 | 35.3 | 507 |
| | | 512 | 434.1 | 654.1 | 33.6 | 300 | 423.8 | 642.9 | 34.1 | 291 | 418.2 | 642.5 | 34.9 | 288 |
| | | 2048 | 462.2 | 657.2 | 29.7 | 70 | 431.1 | 635.5 | 32.2 | 63 | 422.7 | 628.9 | 32.8 | 65 |

*search* = width of embedded search, *DD width* = width of relaxed dd
*lb* = lower bound, *ub* = upper bound, *gap* = optimality gap,
*queue* = nodes in the processing queue

### 6.7.4 Final Experiment: Test of Larger Instances

In our final round of experiments we run the larger instances with $n \in \{25, 30\}$. Due to limited resource availability we had to use a slightly less powerful computer equipped with an Intel E5-2650 v4 Broadwell 2.2GHz CPU with 64Gb RAM. We use a relaxed DD-width of 2048, and we test larger embedded search sizes than before: 400, 1024, and 2048. We limit the runtime to 3 days, again due to resource availability, but this has the added benefit of showing that the algorithm works well within a smaller time-frame than the 7 days used in

Section 6.7.3.

The results, shown in Tables 6.6 and 6.7, suggest that increasing the width of the embedded search may be worth the extra computational cost of constructing the additional solutions, but the results are not enough to be conclusive. $\omega_s = 2048$ finds the best solutions more often than the other settings, so as before we will choose the largest search setting to be the preferred setting. More experiments would be needed to make a strong recommendation between the search settings, but it is clear that all of the settings used in this section are effective.

We again compare our results with [75] where possible, and record the best solution found using our preferred setting as well as the best solutions found by any setting. This is shown in Table 6.8. As before, the solutions from our preferred setting are better than the best solutions found by [75] for all of the problems. The preferred solution only matches the best found solution for 5 of the 10 problems. However, the gap between the two solutions is quite small for the other 5 instances. The largest difference, which occurs with $n = 25$ and seed= 42, is only 2.4%.

Table 6.6 ARP instances with $n = 25$, a relaxed DD-width of 2048, and a 3 day runtime

| Seed | Search | *multi* = 1 | | | | *multi* = 3 | | | | *multi* = 5 | | | |
|---|---|---|---|---|---|---|---|---|---|---|---|---|---|
| | | lb | ub | gap (%) | queue | lb | ub | gap (%) | queue | lb | ub | gap (%) | queue |
| 8 | 400 | 538.1 | 781.5 | 31.2 | 4 | 510.3 | 778.7 | 34.5 | 10 | 503.2 | 760.6 | 33.8 | 9 |
| | 1024 | 538.1 | 778.9 | 30.9 | 2 | 510.1 | 780.1 | 34.6 | 9 | 503.2 | 760.6 | 33.8 | 9 |
| | 2048 | 538.1 | 778.9 | 30.9 | 2 | 510.3 | 774.0 | 34.1 | 9 | 499.7 | 763.3 | 34.5 | 7 |
| 22 | 400 | 506.8 | 842.9 | 39.9 | 10 | 475.4 | 774.4 | 38.6 | 10 | 463.8 | 791.2 | 41.4 | 11 |
| | 1024 | 506.8 | 787.0 | 35.6 | 11 | 475.4 | 774.0 | 38.6 | 10 | 463.7 | 785.3 | 41.0 | 7 |
| | 2048 | 506.8 | 784.6 | 35.4 | 10 | 475.4 | 774.0 | 38.6 | 9 | 463.7 | 784.6 | 40.9 | 7 |
| 42 | 400 | 513.9 | 783.5 | 34.4 | 2 | 497.5 | 761.1 | 34.6 | 9 | 467.2 | 733.3 | 36.3 | 9 |
| | 1024 | 513.9 | 776.3 | 33.8 | 2 | 497.5 | 755.0 | 34.1 | 9 | 467.2 | 751.3 | 37.8 | 9 |
| | 2048 | 513.9 | 778.7 | 34.0 | 2 | 497.5 | 755.0 | 34.1 | 9 | 467.2 | 751.3 | 37.8 | 9 |
| 59 | 400 | 508.6 | 794.6 | 36.0 | 6 | 486.0 | 747.6 | 35.0 | 10 | 466.8 | 725.2 | 35.6 | 9 |
| | 1024 | 508.8 | 795.6 | 36.1 | 11 | 486.0 | 751.5 | 35.3 | 10 | 466.1 | 724.5 | 35.7 | 7 |
| | 2048 | 508.6 | 781.3 | 34.9 | 6 | 481.3 | 738.2 | 34.8 | 7 | 466.8 | 718.2 | 35.0 | 9 |
| 73 | 400 | 494.7 | 797.3 | 38.0 | 9 | 461.2 | 793.8 | 41.9 | 11 | 447.4 | 743.4 | 39.8 | 7 |
| | 1024 | 493.6 | 790.3 | 37.5 | 7 | 459.4 | 784.9 | 41.5 | 8 | 447.4 | 743.4 | 39.8 | 7 |
| | 2048 | 493.6 | 782.0 | 36.9 | 7 | 459.1 | 768.0 | 40.2 | 7 | 447.4 | 743.4 | 39.8 | 7 |

*search* = width of embedded search, *lb* = lower bound, *ub* = upper bound,
*gap* = optimality gap, *queue* = nodes in the processing queue

Table 6.7 ARP instances with $n = 30$, a relaxed DD-width of 2048, and a 3 day runtime

| Seed | Search | *multi* = 1 | | | | *multi* = 3 | | | | *multi* = 5 | | | |
|---|---|---|---|---|---|---|---|---|---|---|---|---|---|
| | | lb | ub | gap (%) | queue | lb | ub | gap (%) | queue | lb | ub | gap (%) | queue |
| 8 | 400 | 523.5 | 955.5 | 45.2 | 4 | 486.9 | 906.9 | 46.3 | 7 | 471.8 | 904.2 | 47.8 | 7 |
| | 1024 | 523.5 | 935.7 | 44.1 | 4 | 486.9 | 894.8 | 45.6 | 7 | 464.1 | 898.7 | 48.4 | 6 |
| | 2048 | 523.5 | 935.7 | 44.1 | 4 | 486.9 | 892.2 | 45.4 | 7 | 464.1 | 898.7 | 48.4 | 6 |
| 22 | 400 | 608.8 | 901.8 | 32.5 | 5 | 597.5 | 896.2 | 33.3 | 8 | 503.7 | 908.5 | 44.6 | 7 |
| | 1024 | 608.8 | 896.7 | 32.1 | 5 | 593.5 | 889.6 | 33.3 | 7 | 503.7 | 905.6 | 44.4 | 7 |
| | 2048 | 608.8 | 897.9 | 32.2 | 5 | 597.5 | 900.6 | 33.6 | 6 | 503.5 | 892.8 | 43.6 | 5 |
| 42 | 400 | 515.9 | 906.6 | 43.1 | 9 | 486.7 | 880.1 | 44.7 | 7 | 465.7 | 858.6 | 45.8 | 6 |
| | 1024 | 513.7 | 911.8 | 43.7 | 8 | 486.7 | 873.1 | 44.3 | 7 | 465.7 | 854.8 | 45.5 | 6 |
| | 2048 | 512.9 | 861.1 | 40.4 | 7 | 486.7 | 871.3 | 44.1 | 7 | 465.7 | 835.1 | 44.2 | 6 |
| 59 | 400 | 552.0 | 923.7 | 40.2 | 6 | 537.4 | 906.2 | 40.7 | 7 | 449.1 | 872.7 | 48.5 | 3 |
| | 1024 | 552.0 | 910.6 | 39.4 | 6 | 535.7 | 858.1 | 37.6 | 6 | 449.1 | 864.5 | 48.1 | 3 |
| | 2048 | 552.0 | 894.8 | 38.3 | 6 | 534.6 | 868.3 | 38.4 | 2 | 449.1 | 864.1 | 48.0 | 3 |
| 73 | 400 | 504.1 | 896.6 | 43.8 | 5 | 495.1 | 903.9 | 45.2 | 4 | 480.2 | 904.3 | 46.9 | 5 |
| | 1024 | 504.1 | 975.2 | 48.3 | 5 | 495.1 | 932.8 | 46.9 | 3 | 480.2 | 906.3 | 47.0 | 5 |
| | 2048 | 504.1 | 945.1 | 46.7 | 5 | 495.1 | 908.5 | 45.5 | 2 | 478.5 | 882.9 | 45.8 | 2 |

*search* = width of embedded search, *lb* = lower bound, *ub* = upper bound,
*gap* = optimality gap, *queue* = nodes in the processing queue

Table 6.8 Best solutions for $n \in \{25, 30\}$

| n | seed | [75]* | | Peel-and-Bound: Preferred Settings** | | Peel-and-Bound: Best Found*** | |
|---|---|---|---|---|---|---|---|
| | | Average Value | Best Value | Value | Optimality Gap (%) | Value | Optimality Gap (%) |
| 25 | 8 | - | - | 763.3 | 34.5 | **760.6** | 33.8 |
| | 22 | - | - | 784.6 | 40.9 | **774.0** | 38.6 |
| | 42 | 881.5 | 865.7 | 751.3 | 37.8 | **733.3** | 36.3 |
| | 59 | - | - | 718.2 | 35 | 718.2 | 35.0 |
| | 73 | 873.6 | 863.7 | 743.4 | 39.8 | 743.4 | 39.8 |
| 30 | 8 | - | - | 898.7 | 48.4 | **892.2** | 45.4 |
| | 22 | - | - | 892.8 | 43.6 | 892.8 | 43.6 |
| | 42 | 1084.6 | 1065.2 | 835.1 | 44.2 | 835.1 | 44.2 |
| | 59 | - | - | 864.1 | 48.0 | **858.1** | 37.6 |
| | 73 | 967.7 | 952.1 | 882.9 | 45.8 | 882.9 | 45.8 |

* The results from [75] in the *Average Found* column are the average solution cost over several runs of the same stochastic algorithm. *Best Found* reports the best solution found in any run of the algorithm.

** The preferred settings for Peel-and-Bound are: $\omega_s = 2048$, $\omega = 2048$, *multi*= 5.

*** The bold values are the instances where the best found solution by any setting is better than the solution found using the preferred setting.

## 6.8 Opportunities for Parallel Computing

Consider the number of diagrams left in the queues from the results tables. Large values indicate that: (1) a significant amount of work remains to be done before closing those instances, and (2) that work is extremely parallelizable because each DD in the queue represents a sub-problem to be solved that is totally independent from the rest.

We ran all of our experiments on a single thread, but as long as there are unused threads available, each of those DDs could be assigned to a different thread without the need for them to communicate [7, 9, 44]. Thus, an implementation that included parallel processing could handle problems at a much larger scale if many CPUs were available. Additionally, setting $multi > 1$ is parallelizable, as it represents *multi* independent restarts of SQSLP at disjoint areas of the search space.

## 6.9 Conclusions on the Framework for Outer/Inner Optimazation Problems

In this chapter, we study outer-inner optimization problems, where the outer problem is combinatorial and the inner problem is numerical and black-box. We introduce the first optimization framework designed to find exact solutions for such problems under mild assumptions about the inner problem. Global trajectory optimization is one real-world example of such problems, and we use the Asteroid Routing Problem (ARP) as a case study. Although the inner optimizer in the ARP returns a local optimum, we show how to control the likelihood that this local optimum is also global. From the perspective of the outer problem, our proposed method successfully solves instances of up to 15 celestial bodies, and finds high-quality solutions for larger problems. Notably, we find new best-known solutions for several instances, many of them likely to be optimal. Additionally, we have made our implementation, data, and a detailed guide on how to use the solver, available in a public repository.

In the domain of global trajectory optimization, our methods represent a pioneering approach not only for finding optimal solutions but also for discovering high-quality feasible solutions. This work opens the door to future research that could adapt our solver to tackle other complex challenges, such as those involving multiple gravity assists. More broadly, we provide a robust framework for addressing sequencing problems where the cost function is computationally demanding. The proposed approach is highly scalable and future work should explore how to set its parameters according to the number of CPUs available and problem size. The principles underlying our approach are versatile, promising applicability to a diverse range of problems in the future.

## 6.10 Acknowledgements

We received advice about global trajectory optimization from the Advanced Concepts Team at the European Space Agency. We would like to specifically thank Dario Izzo and Emmanuel Blazquez for their input on this project.

# CHAPTER 7 CONCLUSION

When I began the work in this thesis, I had just familiarized myself with DD-based BnB, and I was entranced by the idea. However, it left me wondering: Why do they throw away the DDs at every iteration? That is the question that led to PnB, an algorithm that can trade memory for efficiency. The goal when I started implementing my ideas was to build on the BnB work to prove that a DD-based solver could compete with a traditional cutting edge solver. Around the same time, ddo and Haddock were in pursuit of the same goal. There has since been an enormous increase in the number of researchers using DDs, applying them to a variety of topics, and improving the theory underlying them. However, DD-based solvers are still in their infancy compared to modern MIP and CP solvers which have had decades of refinement. There are so many unanswered questions, and so many simple ideas that have not been explored yet with DD-solvers.

## 7.1 Some Ideas for Future Research

### 7.1.1 Implicit Relaxed DDs Everywhere

The largest single performance boost that I encountered while improving the PnB implementation was the switch to implicit relaxed DDs (Chapter 5). Following that, I gleefully deleted all of the code responsible for managing arc labeling, arc storage, and arc weighting. This is an idea that is easy to test in other applications. It merely requires making the shift from thinking about labeled arcs to thinking about labeled nodes. This combination of being both easy to implement and highly efficient makes it a great target for incorporation with other solvers and applications. There are also unexplored questions about what constraint propagation techniques become available, or worthwhile, when all the nodes in a relaxed DD have an exact label.

### 7.1.2 More Decision Diagrams by Separation

Constructing relaxed DDs by separation has some huge advantages over using top-down compilation. Aside from the advantages laid out in this thesis pertaining to PnB, using separation allows you to mirror your constraint propagators, one working top-down, the other bottom-up. Separation also allows you to start from a state where all equivalent nodes have already been merged, making it easier to generate compact representations. However, there has been significantly less work leveraging separation, apparently due to its perceived

complexity.

Some notable directions for future research:

1. There seems to be a competition among DD researchers to define a modeling language for using DDs, and then get everyone else to use it. However, to the best of my knowledge, all of them account for node merging, and none of them account for node splitting. Work on generic modeling for DDs that incorporates node splitting would be worthwhile.

2. Is there a dynamic method of splitting nodes in a relaxed DD that is more efficient than top-down or bottom-up? I have been unable to find one thus far, but it seems likely that such a method exists. The challenge to overcome is that if you begin with the first layer and proceed top-down, then it is computationally inexpensive to keep all of the state information on the nodes in the layers above and below the splits up to date. However, if instead the nodes are split dynamically, with a new layer being selected for each node split, then many nodes have to be updated to leverage the information gained by the split.

3. Can separation and merging be combined into something better than the sum of its parts? In Section 4.2.3, we explored the idea of a version of PnB that uses top-down compilation at each iteration. This would split at some parts of the algorithm, and merge at others. Whether or not that specific idea is useful, an exploration of techniques that leverage both separation and top down compilation could yield new algorithms that benefit both compilation techniques.

4. Separation provides such a perfect template for rewriting CP constraints as DD-based constraints. There has been work in this area [2, 82, 83], but there is room for substantially more.

### 7.1.3 Exact Solutions to Inner/Outer Optimization Problems

In Chapter 6, we provided a method of finding exact solutions to a problem that was generally thought not to admit them. This is part of a broader class of problems that have an outer combinatorial optimization problem combined with an inner computationally expensive black-box problem. We showed that for the Asteroid Routing Problem, the black-box could be modified to create a version of the black-box capable of generating valid bounds on the weights of arcs in a relaxed DD. This opens up a huge opportunity to apply this concept to other optimization problems with expensive black-box functions.

## 7.2 Final Thoughts

This thesis includes a tutorial to get up to speed with decision diagrams, followed by a thorough discussion of peel-and-bound. In the papers I drew from, we demonstrated that peel-and-bound can achieve cutting edge results even though, like the other DD-based solvers, it is still in its infancy. This thesis serves as a demonstration of how powerful a DD-based solver that leverages separation can be, and calls for more work in this area. It also introduced implicit relaxed DDs, which are not only highly efficient, but will also help make separation easier to implement, which will hopefully broaden their appeal.

The final demonstration in this thesis is the application of peel-and-bound to find exact solutions to global trajectory optimization problems. The framework described has the potential to make an impact not just on trajectory-related research, but also on other areas where the outer combinatorial optimization problem requires solving an expensive inner optimization problem.

This thesis not only advances the understanding and application of decision diagrams through the introduction of innovative methods like peel-and-bound and implicit relaxed DDs, but also sets the stage for future breakthroughs in complex optimization challenges across various fields.

# REFERENCES


[1] D. Bergman, A. Cire, W.-J. van Hoeve, and J. Hooker, *Decision Diagrams for Optimization*. Springer International Publishing, 01 2016.

[2] M. P. Castro, A. A. Cire, and J. C. Beck, "Decision diagrams for discrete optimization: A survey of recent advances," *INFORMS Journal on Computing*, vol. 34, no. 4, pp. 2271–2295, 2022.

[3] J. Bezanson, A. Edelman, S. Karpinski, and V. B. Shah, "Julia: A fresh approach to numerical computing," *SIAM review*, vol. 59, no. 1, pp. 65–98, 2017. [Online]. Available: https://doi.org/10.1137/141000671

[4] X. Gillard, V. Coppé, P. Schaus, and A. A. Cire, "Improving the filtering of branch-and-bound mdd solver," in *Integration of Constraint Programming, Artificial Intelligence, and Operations Research, 18th International Conference, CPAIOR 2021*, ser. Lecture Notes in Computer Science. Springer International Publishing, 2021.

[5] X. Gillard, "Discrete optimization with decision diagrams: design of a generic solver, improved bounding techniques, and discovery of good feasible solutions with large neighborhood search," Ph.D. dissertation, UCL-Université Catholique de Louvain, 2022.

[6] I. Rudich, Q. Cappart, and L.-M. Rousseau, "Peel-and-bound: Generating stronger relaxed bounds with multivalued decision diagrams," in *International Conference on Principles and Practice of Constraint Programming*, 2022.

[7] D. Bergman, A. A. Cire, A. Sabharwal, H. Samulowitz, V. Saraswat, and W.-J. van Hoeve, "Parallel combinatorial optimization with decision diagrams," in *Proceedings of the International Conference on AI and OR Techniques in Constraint Programming for Combinatorial Optimization Problems*, 2014, pp. 351–367.

[8] D. Bergman, A. Cire, W.-J. van Hoeve, and J. Hooker, "Discrete optimization with decision diagrams," *INFORMS Journal on Computing*, vol. 28, pp. 47–66, 02 2016.

[9] I. Rudich, Q. Cappart, and L.-M. Rousseau, "Improved peel-and-bound: Methods for generating dual bounds with multivalued decision diagrams," *Journal of Artificial Intelligence Research*, vol. 77, pp. 1489–1538, 2023.

[10] H. Andersen, T. Hadzic, J. Hooker, and P. Tiedemann, "A constraint store based on multivalued decision diagrams," in *Bessière, C. (eds) Principles and Practice of Constraint Programming – CP 2007*, ser. Lecture Notes in Computer Science, vol. 4741, 09 2007, pp. 118–132.

[11] T. Hadzic, J. Hooker, B. O'Sullivan, and P. Tiedemann, "Approximate compilation of constraints into multivalued decision diagrams," in *Stuckey, P.J. (eds) Principles and Practice of Constraint Programming. CP 2008*, ser. Lecture Notes in Computer Science, 09 2008, pp. 448–462.

[12] S. Hoda, W.-J. van Hoeve, and J. Hooker, "A systematic approach to mdd-based constraint programming," in *Cohen, D. (eds) Principles and Practice of Constraint Programming – CP 2010. CP 2010*, ser. Lecture Notes in Computer Science, vol. 6308, 09 2010, pp. 266–280.

[13] T. Hadzic and J. Hooker, "Discrete global optimization with binary decision diagrams," in *Workshop on Global Optimization: Integrating Convexity, Optimization, Logic Programming, and Computational Algebraic Geometry (GICOLAG). Vienna*, 2006.

[14] T. Hadzic and J. Hooker, "Postoptimality analysis for integer programming using binary decision diagrams," in *GICOLAG Workshop (Global Optimization: Integrating Convexity, Optimization, Logic Programming, and Computational Algebraic Geometry), Vienna. Technical report, Carnegie Mellon University*, 2006.

[15] J. Hooker, "Decision diagrams and dynamic programming," in *Gomes, C., Sellmann, M. (eds) Integration of AI and OR Techniques in Constraint Programming for Combinatorial Optimization Problems. CPAIOR 2013*, ser. Lecture Notes in Computer Science, vol. 7874, 05 2013.

[16] H. M. Salkin and C. A. De Kluyver, "The knapsack problem: a survey," *Naval Research Logistics Quarterly*, vol. 22, no. 1, pp. 127–144, 1975.

[17] L. F. Escudero, "An inexact algorithm for the sequential ordering problem," *European Journal of Operational Research*, vol. 37, no. 2, pp. 236–249, 1988.

[18] Bryant, "Graph-based algorithms for boolean function manipulation," *IEEE Transactions on Computers*, vol. C-35, no. 8, pp. 677–691, 1986.

[19] I. Wegener, *Branching programs and binary decision diagrams: theory and applications*. SIAM, 2000.

[20] D. Bergman, W.-J. van Hoeve, and J. Hooker, "Manipulating mdd relaxations for combinatorial optimization," in *Lecture Notes in Computer Science*, vol. 6697, 05 2011, pp. 20–35.

[21] D. Bergman, A. A. Cire, W.-J. Van Hoeve, and J. N. Hooker, "Variable ordering for the application of bdds to the maximum independent set problem," in *Integration of AI and OR Techniques in Contraint Programming for Combinatorial Optimzation Problems: 9th International Conference, CPAIOR 2012, Nantes, France, May 28–June1, 2012. Proceedings 9*. Springer, 2012, pp. 34–49.

[22] D. Bergman, A. A. Cire, W.-J. van Hoeve, and J. N. Hooker, "Optimization bounds from binary decision diagrams," *INFORMS Journal on Computing*, vol. 26, no. 2, pp. 253–268, 2014.

[23] X. Gillard and P. Schaus, "Large neighborhood search with decision diagrams," in *International Joint Conference on Artificial Intelligence*, 2022.

[24] V. Coppé, X. Gillard, and P. Schaus, "Decision diagram-based branch-and-bound with caching for dominance and suboptimality detection," *INFORMS Journal on Computing*, 2024.

[25] V. Coppé, "Advances in discrete optimization with decision diagrams: Dominance, caching and aggregation-based heuristics," Ph.D. dissertation, Carnegie Mellon University, USA, 2024.

[26] T. Hadzic, J. Hooker, B. O'Sullivan, and P. Tiedemann, "Approximate compilation of constraints into multivalued decision diagrams," in *International Conference on Principles and Practice of Constraint Programming*. Springer, 2008, pp. 448–462.

[27] T. Hadzic, J. N. Hooker, and P. Tiedemann, "Propagating separable equalities in an mdd store," in *International Conference on Integration of Artificial Intelligence (AI) and Operations Research (OR) Techniques in Constraint Programming*. Springer, 2008, pp. 318–322.

[28] A. A. Cire and W.-J. van Hoeve, "Multivalued decision diagrams for sequencing problems," *Operations Research*, vol. 61, no. 6, pp. 1259, 1462, 2013.

[29] J.-C. Régin, "A filtering algorithm for constraints of difference in csps," in *AAAI*, vol. 94, 1994, pp. 362–367.

[30] X. Gillard, P. Schaus, and V. Coppé, "Ddo, a generic and efficient framework for mdd-based optimization," in *Proceedings of the Twenty-Ninth International Conference on International Joint Conferences on Artificial Intelligence*, 2021, pp. 5243–5245.

[31] V. Copp'e, X. Gillard, and P. Schaus, "Branch-and-bound with barrier: Dominance and suboptimality detection for dd-based branch-and-bound," *ArXiv*, vol. abs/2211.13118, 2022.

[32] Z. Tang and W.-J. van Hoeve, "Dual bounds from decision diagram-based route relaxations: An application to truck-drone routing," *Transportation Science*, vol. 58, no. 1, pp. 257–278, 2024.

[33] A. Karahalios and W.-J. van Hoeve, "Column elimination for capacitated vehicle routing problems," in *International Conference on Integration of Constraint Programming, Artificial Intelligence, and Operations Research*. Springer, 2023, pp. 35–51.

[34] W.-J. Hoeve, "Graph coloring with decision diagrams," *Mathematical Programming*, vol. 192, pp. 631–674, 05 2021.

[35] R. Gentzel, L. Michel, and W.-J. v. Hoeve, "Haddock: A language and architecture for decision diagram compilation," in *International Conference on Principles and Practice of Constraint Programming*. Springer, 2020, pp. 531–547.

[36] R. Gentzel, L. Michel, and W.-J. van Hoeve, "Optimization bounds from decision diagrams in haddock," in *International Conference on Integration of Constraint Programming, Artificial Intelligence, and Operations Research*. Springer, 2023, pp. 150–166.

[37] R. Kuroiwa and J. C. Beck, "Domain-independent dynamic programming: Generic state space search for combinatorial optimization," in *Proceedings of the International Conference on Automated Planning and Scheduling*, vol. 33, 2023, pp. 236–244.

[38] F. A. Aloul, I. L. Markov, and K. A. Sakallah, "Force: a fast and easy-to-implement variable-ordering heuristic," in *Proceedings of the 13th ACM Great Lakes symposium on VLSI*, 2003, pp. 116–119.

[39] B. Bollig and I. Wegener, "Improving the variable ordering of obdds is np-complete," *IEEE Transactions on computers*, vol. 45, no. 9, pp. 993–1002, 1996.

[40] M. Rice and S. Kulhari, "A survey of static variable ordering heuristics for efficient bdd/mdd construction," *University of California, Tech. Rep*, p. 130, 2008.

[41] R. Rudell, "Dynamic variable ordering for ordered binary decision diagrams," in *Proceedings of 1993 International Conference on Computer Aided Design (ICCAD)*. IEEE, 1993, pp. 42–47.

[42] A. Parjadis, Q. Cappart, L.-M. Rousseau, and D. Bergman, "Improving branch-and-bound using decision diagrams and reinforcement learning," in *International Conference on Integration of Constraint Programming, Artificial Intelligence, and Operations Research*. Springer, 2021, pp. 446–455.

[43] A. Karahalios and W.-J. Hoeve, "Variable ordering for decision diagrams: A portfolio approach," *Constraints*, vol. 27, no. 1-2, pp. 1–18, 01 2022.

[44] G. Perez and J.-C. Régin, "Parallel algorithms for operations on multi-valued decision diagrams," *Proceedings of the AAAI Conference on Artificial Intelligence*, vol. 32, no. 1, Apr. 2018.

[45] P. Baptiste, C. Le Pape, and W. Nuijten, *Constraint-Based Scheduling: Applying Constraint Programming to Scheduling Problems*, ser. International Series in Operations Research and Management Science, Kluwer. Springer International Publishing, 2001.

[46] G. Reinelt, "Tsplib. a traveling salesman problem library," *INFORMS Journal on Computing*, vol. 3, pp. 376–384, 11 1991.

[47] J. N. Hooker, "Job sequencing bounds from decision diagrams," in *Beck, J. (eds) Principles and Practice of Constraint Programming. CP 2017*, ser. Lecture Notes in Computer Science, 08 2017, pp. 565–578.

[48] J. Hooker, "Improved job sequencing bounds from decision diagrams," in *Schiex, T., de Givry, S. (eds) Principles and Practice of Constraint Programming. CP 2019*, ser. Lecture Notes in Computer Science, vol. 11802, 09 2019, pp. 268–283.

[49] M. López-Ibáñez and C. Blum, "Benchmark instances for the travelling salesman problem with time windows (tsptw)," https://lopez-ibanez.eu/tsptw-instances, Nov 2022, accessed: 2022-01-22. [Online]. Available: https://lopez-ibanez.eu/tsptw-instances

[50] N. Ascheuer, "Hamiltonian path problems in the on-line optimization of flexible manufacturing systems," Ph.D. dissertation, Konrad–Zuse–Zentrum für Informationstechnik Berlin, 1996.

[51] Y. Dumas, J. Desrosiers, E. Gelinas, and M. M. Solomon, "An optimal algorithm for the traveling salesman problem with time windows," *Operations research*, vol. 43, no. 2, pp. 367–371, 1995.

[52] M. Gendreau, A. Hertz, G. Laporte, and M. Stan, "A generalized insertion heuristic for the traveling salesman problem with time windows," *Operations Research*, vol. 46, no. 3, pp. 330–335, 1998.

[53] A. Langevin, M. Desrochers, J. Desrosiers, S. Gélinas, and F. Soumis, "A two-commodity flow formulation for the traveling salesman and the makespan problems with time windows," *Networks*, vol. 23, no. 7, pp. 631–640, 1993.

[54] J. W. Ohlmann and B. W. Thomas, "A compressed-annealing heuristic for the traveling salesman problem with time windows," *INFORMS Journal on Computing*, vol. 19, no. 1, pp. 80–90, 2007.

[55] G. Pesant, M. Gendreau, J.-Y. Potvin, and J.-M. Rousseau, "An exact constraint logic programming algorithm for the traveling salesman problem with time windows," *Transportation Science*, vol. 32, no. 1, pp. 12–29, 1998.

[56] J.-Y. Potvin and S. Bengio, "The vehicle routing problem with time windows part ii: genetic search," *INFORMS journal on Computing*, vol. 8, no. 2, pp. 165–172, 1996.

[57] R. Baldacci, A. Mingozzi, and R. Roberti, "New state-space relaxations for solving the traveling salesman problem with time windows," *INFORMS Journal on Computing*, vol. 24, no. 3, pp. 356–371, 2012.

[58] D. Izzo, I. Getzner, D. Hennes, and L. F. Simões, "Evolving solutions to tsp variants for active space debris removal," in *Proceedings of the 2015 Annual Conference on Genetic and Evolutionary Computation*, 2015, pp. 1207–1214.

[59] J. F. Ehmke, A. M. Campbell, and B. W. Thomas, "Vehicle routing to minimize time-dependent emissions in urban areas," *European Journal of Operational Research*, vol. 251, no. 2, pp. 478–494, 2016.

[60] H. Andersson, K. Fagerholt, and K. Hobbesland, "Integrated maritime fleet deployment and speed optimization: Case study from roro shipping," *Computers & Operations Research*, vol. 55, pp. 233–240, 2015.

[61] A. Shirazi, J. Ceberio, and J. A. Lozano, "Spacecraft trajectory optimization: A review of models, objectives, approaches and solutions," *Progress in Aerospace Sciences*, vol. 102, pp. 76–98, 2018.

[62] D. Izzo, L. F. Simões, M. Märtens, G. C. de Croon, A. Heritier, and C. H. Yam, "Search for a grand tour of the jupiter galilean moons," in *Proceedings of the 15th annual conference on Genetic and evolutionary computation*, 2013, pp. 1301–1308.

[63] O. Abdelkhalik and A. Gad, "Dynamic-size multiple populations genetic algorithm for multigravity-assist trajectory optimization," *Journal of Guidance, Control, and Dynamics*, vol. 35, no. 2, pp. 520–529, 2012.

[64] M. Ceriotti and M. Vasile, "Automated multigravity assist trajectory planning with a modified ant colony algorithm," *Journal of Aerospace Computing, Information, and Communication*, vol. 7, no. 9, pp. 261–293, 2010.

[65] D. Izzo, V. Becerra, D. Myatt, S. Nasuto, and J. Bishop, "Search space pruning and global optimisation of multiple gravity assist spacecraft trajectories," *Journal of Global Optimization*, vol. 38, pp. 283–296, 2007.

[66] M. Vasile and P. De Pascale, "Preliminary design of multiple gravity-assist trajectories," *Journal of Spacecraft and Rockets*, vol. 43, no. 4, pp. 794–805, 2006.

[67] T. Lee, M. Leok, and N. H. McClamroch, "A combinatorial optimal control problem for spacecraft formation reconfiguration," in *2007 46th IEEE Conference on Decision and Control*. IEEE, 2007, pp. 5370–5375.

[68] A. E. Petropoulos, E. P. Bonfiglio, D. J. Grebow, T. Lam, J. S. Parker, J. Arrieta, D. F. Landau, R. L. Anderson, E. D. Gustafson, G. J. Whiffen *et al.*, "Gtoc5: results from the jet propulsion laboratory," *Acta Futura*, vol. 8, no. 1, pp. 21–27, 2014.

[69] D. Hennes and D. Izzo, "Interplanetary trajectory planning with monte carlo tree search," in *Twenty-Fourth International Joint Conference on Artificial Intelligence*, 2015.

[70] L. F. Simões, D. Izzo, E. Haasdijk, and A. Eiben, "Multi-rendezvous spacecraft trajectory optimization with beam p-aco," in *Evolutionary Computation in Combinatorial Optimization: 17th European Conference, EvoCOP 2017, Amsterdam, The Netherlands, April 19-21, 2017, Proceedings 17*. Springer, 2017, pp. 141–156.

[71] M. Zaefferer, J. Stork, M. Friese, A. Fischbach, B. Naujoks, and T. Bartz-Beielstein, "Efficient global optimization for combinatorial problems," in *Proceedings of the 2014 annual conference on genetic and evolutionary computation*, 2014, pp. 871–878.

[72] E. Irurozki and M. López-Ibáñez, "Unbalanced mallows models for optimizing expensive black-box permutation problems," in *Proceedings of the genetic and evolutionary computation conference*, 2021, pp. 225–233.

[73] V. Santucci and M. Baioletti, "A fast randomized local search for low budget optimization in black-box permutation problems," in *2022 IEEE Congress on Evolutionary Computation (CEC)*. IEEE, 2022, pp. 1–8.

[74] F. Chicano, B. Derbel, and S. Verel, "Fourier transform-based surrogates for permutation problems," in *Proceedings of the Genetic and Evolutionary Computation Conference*, 2023, pp. 275–283.

[75] M. López-Ibáñez, F. Chicano, and R. Gil-Merino, "The asteroid routing problem: A benchmark for expensive black-box permutation optimization," in *International Conference on the Applications of Evolutionary Computation (Part of EvoStar)*. Springer, 2022, pp. 124–140.

[76] D. Izzo, "Revisiting Lambert's problem," *Celestial Mechanics and Dynamical Astronomy*, vol. 121, pp. 1–15, 2015.

[77] D. Kraft, "A software package for sequential quadratic programming," *Forschungsbericht- Deutsche Forschungs- und Versuchsanstalt fur Luft- und Raumfahrt*, 1988.

[78] L. F. Simões, D. Izzo, E. Haasdijk, and A. Eiben, "Multi-rendezvous spacecraft trajectory optimization with beam p-aco," in *Evolutionary Computation in Combinatorial Optimization: 17th European Conference, EvoCOP 2017, Amsterdam, The Netherlands, April 19-21, 2017, Proceedings 17*. Springer, 2017, pp. 141–156.

[79] D. Hennes, D. Izzo, and D. Landau, "Fast approximators for optimal low-thrust hops between main belt asteroids," in *2016 IEEE Symposium Series on Computational Intelligence (SSCI)*. IEEE, 2016, pp. 1–7.

[80] J. Nocedal and S. Wright, "Numerical optimization. 2nd edn springer," *New York*, 2006.

[81] N. Hansen and A. Ostermeier, "Completely derandomized self-adaptation in evolution strategies," *Evolutionary computation*, vol. 9, no. 2, pp. 159–195, 2001.

[82] J. Kinable, A. A. Cire, and W.-J. van Hoeve, "Hybrid optimization methods for time-dependent sequencing problems," *European Journal of Operational Research*, vol. 259, no. 3, pp. 887–897, 2017.

[83] L. C. Riascos-Álvarez, M. Bodur, and D. M. Aleman, "A branch-and-price algorithm enhanced by decision diagrams for the kidney exchange problem," *Manufacturing & Service Operations Management*, vol. 26, no. 2, pp. 485–499, 2024.

# APPENDIX A EXPERIMENTAL DATA

| Problem Info | | BnB: width 64 | | | | | PnB: width 64 | | | | | Percent Improvements | | | | |
|---|---|---|---|---|---|---|---|---|---|---|---|---|---|---|---|---|
| Name | n | RB | BS | T | OG | QL | RB | BS | T | OG | QL | RB | BS | T | OG | QL |
| ESC07 | 9 | 2,125 | 2,125 | 0.03 | 0% | - | 2,125 | 2,125 | 0.07 | 0% | - | | | -57% | | |
| ESC11 | 13 | 2,075 | 2,075 | 0.65 | 0% | - | 2,075 | 2,075 | 0.42 | 0% | - | | | 55% | | |
| ESC12 | 14 | 1,675 | 1,675 | 1.99 | 0% | - | 1,675 | 1,675 | 0.64 | 0% | - | | | 211% | | |
| ESC25 | 27 | 1,681 | 1,681 | 956 | 0% | - | 1,681 | 1,681 | 353 | 0% | - | | | 171% | | |
| ESC47 | 49 | 334 | 1,542 | | 78% | 8,842 | 368 | 1,676 | | 78% | 1,295 | 10.2% | -8.0% | | 0.4% | 583% |
| ESC63 | 65 | 8 | 62 | | 87% | 2,756 | 44 | 62 | | 29% | 15 | 450.0% | 0.0% | | 200.0% | 18273% |
| ESC78 | 80 | 2,230 | 19,800 | | 89% | 1,040 | 5,000 | 20,045 | | 75% | 316 | 124.2% | -1.2% | | 18.2% | 229% |
| br17.10 | 18 | 55 | 55 | 260 | 0% | - | 55 | 55 | 5 | 0% | - | | | 4652% | | |
| br17.12 | 18 | 55 | 55 | 138 | 0% | - | 55 | 55 | 21 | 0% | - | | | 546% | | |
| ft53.1 | 54 | 1,785 | 8,478 | | 79% | 8,841 | 3,324 | 8,244 | | 60% | 917 | 86.2% | 2.8% | | 32.3% | 864% |
| ft53.2 | 54 | 1,946 | 8,927 | | 78% | 7,356 | 3,450 | 8,633 | | 60% | 938 | 77.3% | 3.4% | | 30.3% | 684% |
| ft53.3 | 54 | 2,546 | 12,179 | | 79% | 5,594 | 4,234 | 12,327 | | 66% | 1,147 | 66.3% | -1.2% | | 20.5% | 388% |
| ft53.4 | 54 | 3,780 | 14,811 | | 74% | 11,907 | 6,500 | 14,753 | | 56% | 2,372 | 72.0% | 0.4% | | 33.1% | 402% |
| ft70.1 | 71 | 25,444 | 41,926 | | 39% | 4,781 | 31,123 | 41,607 | | 25% | 412 | 22.3% | 0.8% | | 56.0% | 1060% |
| ft70.2 | 71 | 25,239 | 42,805 | | 41% | 3,998 | 31,195 | 42,623 | | 27% | 427 | 23.6% | 0.4% | | 53.1% | 836% |
| ft70.3 | 71 | 25,810 | 48,073 | | 46% | 4,036 | 31,872 | 47,491 | | 33% | 475 | 23.5% | 1.2% | | 40.8% | 750% |
| ft70.4 | 71 | 28,593 | 56,644 | | 50% | 8,642 | 35,974 | 56,552 | | 36% | 1,087 | 25.8% | 0.2% | | 36.1% | 695% |
| kro124p.1 | 101 | 10,773 | 46,158 | | 77% | 2,173 | 17,579 | 46,158 | | 62% | 105 | 63.2% | 0.0% | | 23.8% | 1970% |
| kro124p.2 | 101 | 11,061 | 46,930 | | 76% | 1,898 | 17,633 | 46,930 | | 62% | 109 | 59.4% | 0.0% | | 22.4% | 1641% |
| kro124p.3 | 101 | 12,110 | 55,991 | | 78% | 1,055 | 18,586 | 55,991 | | 67% | 117 | 53.5% | 0.0% | | 17.3% | 802% |
| kro124p.4 | 101 | 13,838 | 85,533 | | 84% | 2,990 | 24,388 | 85,316 | | 71% | 244 | 76.2% | 0.3% | | 17.4% | 1125% |
| p43.1 | 44 | 630 | 29,450 | | 98% | 12,945 | 380 | 29,380 | | 99% | 1,022 | -39.7% | 0.2% | | -0.9% | 1167% |
| p43.2 | 44 | 440 | 29,000 | | 98% | 8,519 | 420 | 29,080 | | 99% | 1,125 | -4.5% | -0.3% | | -0.1% | 657% |
| p43.3 | 44 | 595 | 29,530 | | 98% | 12,802 | 490 | 29,530 | | 98% | 1,122 | -17.6% | 0.0% | | -0.4% | 1041% |
| p43.4 | 44 | 1,370 | 83,855 | | 98% | 21,105 | 1,050 | 83,890 | | 99% | 4,694 | -23.4% | 0.0% | | -0.4% | 350% |
| prob.42 | 42 | 99 | 289 | | 66% | 16,742 | 97 | 286 | | 66% | 2,613 | -2.0% | 1.0% | | -0.5% | 541% |
| prob.100 | 100 | 170 | 1,841 | | 91% | 1,731 | 182 | 1,760 | | 90% | 117 | 7.1% | 4.6% | | 1.2% | 1379% |
| rbg048a | 50 | 76 | 379 | | 80% | 12,938 | 47 | 380 | | 88% | 1,551 | -38.2% | -0.3% | | -8.8% | 734% |
| rbg050c | 52 | 63 | 566 | | 89% | 11,480 | 154 | 512 | | 70% | 1,481 | 144.4% | 10.5% | | 27.1% | 675% |
| rbg109a | 111 | 91 | 1,196 | | 92% | 2,773 | 379 | 1,196 | | 68% | 612 | 316.5% | 0.0% | | 35.3% | 353% |
| rbg150a | 152 | 63 | 1,874 | | 97% | 241 | 565 | 1,865 | | 70% | 222 | 796.8% | 0.5% | | 38.6% | 9% |
| rbg174a | 176 | 119 | 2,157 | | 94% | 809 | 626 | 2,156 | | 71% | 117 | 426.1% | 0.0% | | 33.1% | 591% |
| rbg253a | 255 | 113 | 3,181 | | 96% | 403 | 708 | 3,180 | | 78% | 39 | 526.5% | 0.0% | | 24.1% | 933% |
| rbg323a | 325 | 89 | 3,519 | | 97% | 437 | 289 | 3,529 | | 92% | 17 | 224.7% | -0.3% | | 6.2% | 2471% |
| rbg341a | 343 | 68 | 3,038 | | 98% | 366 | 321 | 3,064 | | 90% | 8 | 372.1% | -0.8% | | 9.2% | 4475% |
| rbg358a | 360 | 69 | 3,359 | | 98% | 289 | 73 | 3,373 | | 98% | 6 | 5.8% | -0.4% | | 0.1% | 4717% |
| rbg378a | 380 | 52 | 3,429 | | 98% | 266 | 50 | 3,429 | | 99% | 5 | -3.8% | 0.0% | | -0.1% | 5220% |
| ry48p.1 | 49 | 5,201 | 17,555 | | 70% | 10,480 | 6,171 | 17,454 | | 65% | 1,395 | 18.7% | 0.6% | | 8.9% | 651% |
| ry48p.2 | 49 | 5,291 | 18,046 | | 71% | 9,286 | 6,577 | 17,840 | | 63% | 1,445 | 24.3% | 1.2% | | 12.0% | 543% |
| ry48p.3 | 49 | 6,207 | 21,161 | | 71% | 9,039 | 6,985 | 20,962 | | 67% | 1,707 | 12.5% | 0.9% | | 6.0% | 430% |
| ry48p.4 | 49 | 13,610 | 34,517 | | 61% | 15,819 | 14,293 | 33,804 | | 58% | 3,217 | 5.0% | 2.1% | | 4.9% | 392% |

Table A.1 Comparison Data for $\omega = 64$ Experiments on SOP

RB = Relaxed Bound, BS = Best Solution, T = Time in Seconds, OG = Optimality Gap, QL = Queue Length. Full time series data is available in the GitHub repository.

| Problem Info | | BnB: width 256 | | | | | PnB: width 256 | | | | | Percent Improvements | | | | |
|---|---|---|---|---|---|---|---|---|---|---|---|---|---|---|---|---|
| Name | n | RB | BS | T | OG | QL | RB | BS | T | OG | QL | RB | BS | T | OG | QL |
| ESC07 | 9 | 2,125 | 2,125 | 0.04 | 0% | - | 2,125 | 2,125 | 0.04 | 0% | - | | | 0% | | |
| ESC11 | 13 | 2,075 | 2,075 | 0.48 | 0% | - | 2,075 | 2,075 | 0.41 | 0% | - | | | 17% | | |
| ESC12 | 14 | 1,675 | 1,675 | 1.66 | 0% | - | 1,675 | 1,675 | 0.34 | 0% | - | | | 388% | | |
| ESC25 | 27 | 1,681 | 1,681 | 2,643 | 0% | - | 1,681 | 1,681 | 303 | 0% | - | | | 771% | | |
| ESC47 | 49 | 312 | 1,590 | | 80% | 720 | 658 | 1,339 | | 51% | 740 | 110.9% | 18.7% | | 58.0% | -3% |
| ESC63 | 65 | 9 | 62 | | 85% | 53 | 44 | 62 | | 29% | 3 | 388.9% | 0.0% | | 194.4% | 1667% |
| ESC78 | 80 | 2,230 | 20,345 | | 89% | 59 | 5,600 | 20,135 | | 72% | 109 | 151.1% | 1.0% | | 23.3% | -46% |
| br17.10 | 18 | 55 | 55 | 275 | 0% | - | 55 | 55 | 3 | 0% | - | | | 9468% | | |
| br17.12 | 18 | 55 | 55 | 105 | 0% | - | 55 | 55 | 5 | 0% | - | | | 2146% | | |
| ft53.1 | 54 | 1,708 | 8,424 | | 80% | 760 | 4,603 | 8,244 | | 44% | 271 | 169.5% | 2.2% | | 80.5% | 180% |
| ft53.2 | 54 | 1,856 | 9,059 | | 80% | 632 | 3,555 | 8,648 | | 59% | 272 | 91.5% | 4.8% | | 35.0% | 132% |
| ft53.3 | 54 | 2,493 | 12,598 | | 80% | 477 | 4,852 | 11,095 | | 56% | 390 | 94.6% | 13.5% | | 42.6% | 22% |
| ft53.4 | 54 | 3,619 | 14,867 | | 76% | 1,240 | 7,560 | 14,611 | | 48% | 797 | 108.9% | 1.8% | | 56.8% | 56% |
| ft70.1 | 71 | 25,507 | 41,686 | | 39% | 373 | 31,122 | 41,235 | | 25% | 108 | 22.0% | 1.1% | | 58.3% | 245% |
| ft70.2 | 71 | 25,261 | 42,901 | | 41% | 297 | 31,630 | 42,182 | | 25% | 123 | 25.2% | 1.7% | | 64.4% | 141% |
| ft70.3 | 71 | 25,891 | 47,806 | | 46% | 377 | 32,539 | 46,488 | | 30% | 151 | 25.7% | 2.8% | | 52.8% | 150% |
| ft70.4 | 71 | 31,186 | 56,366 | | 45% | 958 | 37,984 | 56,366 | | 33% | 356 | 21.8% | 0.0% | | 37.0% | 169% |
| kro124p.1 | 101 | 10,683 | 48,866 | | 78% | 152 | 19,224 | 45,643 | | 58% | 43 | 79.9% | 7.1% | | 35.0% | 253% |
| kro124p.2 | 101 | 10,706 | 52,038 | | 79% | 125 | 19,299 | 48,102 | | 60% | 43 | 80.3% | 8.2% | | 32.6% | 191% |
| kro124p.3 | 101 | 12,078 | 58,562 | | 79% | 64 | 20,145 | 57,358 | | 65% | 45 | 66.8% | 2.1% | | 22.3% | 42% |
| kro124p.4 | 101 | 14,511 | 82,672 | | 82% | 281 | 25,002 | 82,364 | | 70% | 102 | 72.3% | 0.4% | | 18.4% | 175% |
| p43.1 | 44 | 610 | 29,460 | | 98% | 1,033 | 27,255 | 28,635 | | 5% | 146 | 4368% | 2.9% | | 1932% | 608% |
| p43.2 | 44 | 460 | 29,020 | | 98% | 547 | 27,455 | 29,020 | | 5% | 391 | 5868% | 0.0% | | 1725% | 40% |
| p43.3 | 44 | 750 | 29,530 | | 97% | 1,016 | 27,780 | 29,530 | | 6% | 764 | 3604% | 0.0% | | 1545% | 33% |
| p43.4 | 44 | 1,425 | 83,880 | | 98% | 1,365 | 28,195 | 83,435 | | 66% | 1,380 | 1879% | 0.5% | | 48.5% | -1% |
| prob.42 | 42 | 90 | 289 | | 69% | 1,166 | 103 | 275 | | 63% | 617 | 14.4% | 5.1% | | 10.1% | 89% |
| prob.100 | 100 | 157 | 1,886 | | 92% | 113 | 178 | 1,721 | | 90% | 45 | 13.4% | 9.6% | | 2.3% | 151% |
| rbg048a | 50 | 80 | 389 | | 79% | 794 | 80 | 373 | | 79% | 534 | 0.0% | 4.3% | | 1.1% | 49% |
| rbg050c | 52 | 62 | 583 | | 89% | 810 | 175 | 503 | | 65% | 442 | 182.3% | 15.9% | | 37.0% | 83% |
| rbg109a | 111 | 89 | 1,181 | | 92% | 394 | 406 | 1,106 | | 63% | 204 | 356.2% | 6.8% | | 46.1% | 93% |
| rbg150a | 152 | 115 | 1,845 | | 94% | 406 | 571 | 1,845 | | 69% | 100 | 396.5% | 0.0% | | 35.8% | 306% |
| rbg174a | 176 | 362 | 2,172 | | 83% | 337 | 646 | 2,171 | | 70% | 57 | 78.5% | 0.0% | | 18.6% | 491% |
| rbg253a | 255 | 359 | 3,177 | | 89% | 139 | 727 | 3,176 | | 77% | 22 | 102.5% | 0.0% | | 15.0% | 532% |
| rbg323a | 325 | 99 | 3,476 | | 97% | 114 | 346 | 3,480 | | 90% | 14 | 249.5% | -0.1% | | 7.9% | 714% |
| rbg341a | 343 | 84 | 3,016 | | 97% | 120 | 340 | 3,016 | | 89% | 7 | 304.8% | 0.0% | | 9.6% | 1614% |
| rbg358a | 360 | 88 | 3,280 | | 97% | 92 | 88 | 3,382 | | 97% | 5 | 0.0% | -3.0% | | -0.1% | 1740% |
| rbg378a | 380 | 44 | 3,385 | | 99% | 35 | 53 | 3,385 | | 98% | 6 | 20.5% | 0.0% | | 0.3% | 483% |
| ry48p.1 | 49 | 5,470 | 17,464 | | 69% | 897 | 9,432 | 17,071 | | 45% | 377 | 72.4% | 2.3% | | 53.5% | 138% |
| ry48p.2 | 49 | 5,606 | 18,060 | | 69% | 834 | 6,615 | 17,627 | | 62% | 383 | 18.0% | 2.5% | | 10.4% | 118% |
| ry48p.3 | 49 | 6,558 | 21,142 | | 69% | 859 | 8,723 | 20,850 | | 58% | 513 | 33.0% | 1.4% | | 18.6% | 67% |
| ry48p.4 | 49 | 17,359 | 34,074 | | 49% | 1,557 | 17,322 | 33,773 | | 49% | 990 | -0.2% | 0.9% | | 0.7% | 57% |

Table A.2 Comparison Data for $\omega = 256$ Experiments on SOP

RB = Relaxed Bound, BS = Best Solution, T = Time in Seconds, OG = Optimality Gap, QL = Queue Length. Full time series data is available in the GitHub repository.

| Problem Info | | PnB: width 256 | | | PnB: width 2048 | | | Percent Improvements | | |
|---|---|---|---|---|---|---|---|---|---|---|
| Name | n | RB | BS | OG | RB | BS | OG | RB | BS | OG |
| ESC47 | 49 | 658 | 1,339 | 51% | 882 | 1,304 | 32% | 34.0% | 2.7% | 57.2% |
| ESC63 | 65 | 44 | 62 | 29% | 44 | 62 | 29% | 0.0% | 0.0% | 0% |
| ESC78 | 80 | 5,600 | 20,135 | 72% | 6,025 | 20,505 | 71% | 7.6% | -1.8% | 2.2% |
| ft53.1 | 54 | 4,603 | 8,244 | 44% | 5,167 | 8,237 | 37% | 12.3% | 0.1% | 18.5% |
| ft53.2 | 54 | 3,555 | 8,648 | 59% | 4,910 | 8,598 | 43% | 38.1% | 0.6% | 37.3% |
| ft53.3 | 54 | 4,852 | 11,095 | 56% | 7,722 | 11,092 | 30% | 59.2% | 0.0% | 85.2% |
| ft53.4 | 54 | 7,560 | 14,611 | 48% | 7,466 | 14,618 | 49% | -1.2% | 0.0% | -1.4% |
| ft70.1 | 71 | 31,122 | 41,235 | 25% | 33,382 | 41,476 | 20% | 7.3% | -0.6% | 25.7% |
| ft70.2 | 71 | 31,630 | 42,182 | 25% | 32,964 | 41,833 | 21% | 4.2% | 0.8% | 18.0% |
| ft70.3 | 71 | 32,539 | 46,488 | 30% | 34,366 | 46,001 | 25% | 5.6% | 1.1% | 18.6% |
| ft70.4 | 71 | 37,984 | 56,366 | 33% | 40,919 | 56,310 | 27% | 7.7% | 0.1% | 19.3% |
| kro124p.1 | 101 | 19,224 | 45,643 | 58% | 21,954 | 47,425 | 54% | 14.2% | -3.8% | 7.8% |
| kro124p.2 | 101 | 19,299 | 48,102 | 60% | 22,746 | 49,571 | 54% | 17.9% | -3.0% | 10.7% |
| kro124p.3 | 101 | 20,145 | 57,358 | 65% | 25,566 | 54,633 | 53% | 26.9% | 5.0% | 21.9% |
| kro124p.4 | 101 | 25,002 | 82,364 | 70% | 29,377 | 81,050 | 64% | 17.5% | 1.6% | 9.2% |
| p43.1 | 44 | 27,255 | 28,635 | 5% | 27,755 | 28,960 | 4% | 1.8% | -1.1% | 16% |
| p43.2 | 44 | 27,455 | 29,020 | 5% | 27,725 | 29,000 | 4% | 1.0% | 0.1% | 23% |
| p43.3 | 44 | 27,780 | 29,530 | 6% | 27,755 | 29,530 | 6% | -0.1% | 0.0% | -1% |
| p43.4 | 44 | 28,195 | 83,435 | 66% | 28,680 | 83,020 | 65% | 1.7% | 0.5% | 1.2% |
| prob.42 | 42 | 103 | 275 | 63% | 152 | 261 | 42% | 47.6% | 5.4% | 49.8% |
| prob.100 | 100 | 178 | 1,721 | 90% | 220 | 1,735 | 87% | 23.6% | -0.8% | 2.7% |
| rbg048a | 50 | 80 | 373 | 79% | 93 | 367 | 75% | 16.3% | 1.6% | 5.2% |
| rbg050c | 52 | 175 | 503 | 65% | 184 | 501 | 63% | 5.1% | 0.4% | 3.1% |
| rbg109a | 111 | 406 | 1,106 | 63% | 453 | 1,126 | 60% | 11.6% | -1.8% | 5.9% |
| rbg150a | 152 | 571 | 1,845 | 69% | 672 | 1,841 | 63% | 17.7% | 0.2% | 8.7% |
| rbg174a | 176 | 646 | 2,171 | 70% | 1,104 | 2,121 | 48% | 70.9% | 2.4% | 46.5% |
| rbg253a | 255 | 727 | 3,176 | 77% | 1,186 | 3,101 | 62% | 63.1% | 2.4% | 24.9% |
| rbg323a | 325 | 346 | 3,480 | 90% | 421 | 3,449 | 88% | 21.7% | 0.9% | 2.6% |
| rbg341a | 343 | 340 | 3,016 | 89% | 329 | 2,965 | 89% | -3.2% | 1.7% | -0.2% |
| rbg358a | 360 | 88 | 3,382 | 97% | 107 | 3,131 | 97% | 21.6% | 8.0% | 0.8% |
| rbg378a | 380 | 53 | 3,385 | 98% | 74 | 3,338 | 98% | 39.6% | 1.4% | 0.7% |
| ry48p.1 | 49 | 9,432 | 17,071 | 45% | 10,386 | 17,124 | 39% | 10.1% | -0.3% | 13.7% |
| ry48p.2 | 49 | 6,615 | 17,627 | 62% | 7,896 | 17,461 | 55% | 19.4% | 1.0% | 14.0% |
| ry48p.3 | 49 | 8,723 | 20,850 | 58% | 10,558 | 20,686 | 49% | 21.0% | 0.8% | 18.8% |
| ry48p.4 | 49 | 17,322 | 33,773 | 49% | 24,248 | 32,953 | 26% | 40.0% | 2.5% | 84.4% |

Table A.3 Comparison of PnB at $\omega = 2048$ over PnB at $\omega = 256$ on SOP

RB = Relaxed Bound, BS = Best Solution, OG = Optimality Gap.

| Problem Information | | | Baldacci et. al. (2012) | Single Thread: 2048 | | | Seeded Single Thread: 2048 | | |
|---|---|---|---|---|---|---|---|---|---|
| Set | Name | Best Known Solution | LB | LB | UB | OG | LB | UB | OG |
| Dumas | n100w60.001.txt | 655 | NA | 602 | 659 | 8.65 | 602 | 655 | 8.09 |
| Dumas | n100w60.003.txt | 744 | NA | 619 | 749 | 17.36 | 620 | 744 | 16.67 |
| Dumas | n100w60.004.txt | 764 | NA | 657 | - | 100.00 | 656 | 764 | 14.14 |
| Dumas | n150w40.001.txt | 918 | NA | 810 | 919 | 11.86 | 812 | 918 | 11.55 |
| Dumas | n150w40.002.txt | 941 | NA | 804 | 945 | 14.92 | 803 | 941 | 14.67 |
| Dumas | n150w40.003.txt | 727 | NA | 528 | 737 | 28.36 | 525 | 727 | 27.79 |
| Dumas | n150w40.004.txt | 764 | NA | 678 | 782 | 13.30 | 678 | 764 | 11.26 |
| Dumas | n150w40.005.txt | 824 | NA | 585 | - | 100.00 | 566 | 824 | 31.31 |
| Dumas | n150w60.001.txt | 859 | NA | 645 | 906 | 28.81 | 635 | 859 | 26.08 |
| Dumas | n150w60.002.txt | 782 | NA | 530 | 829 | 36.07 | 529 | 782 | 32.35 |
| Dumas | n150w60.003.txt | 793 | NA | 541 | 825 | 34.42 | 540 | 793 | 31.90 |
| Dumas | n150w60.004.txt | 819 | NA | 578 | - | 100.00 | 574 | 819 | 29.91 |
| Dumas | n150w60.005.txt | 840 | NA | 581 | 849 | 31.57 | 570 | 840 | 32.14 |
| Dumas | n200w40.001.txt | 1023 | NA | 643 | 1038 | 38.05 | 638 | 1023 | 37.63 |
| Dumas | n200w40.002.txt | 948 | NA | 605 | 983 | 38.45 | 605 | 948 | 36.18 |
| Dumas | n200w40.003.txt | 933 | NA | 645 | - | 100.00 | 568 | 933 | 39.12 |
| Dumas | n200w40.004.txt | 980 | NA | 731 | 1030 | 29.03 | 714 | 980 | 27.14 |
| Dumas | n200w40.005.txt | 1037 | NA | 659 | 1056 | 37.59 | 607 | 1037 | 41.47 |
| Dumas | n60w100.005.txt | 451 | NA | 390 | 460 | 15.22 | 391 | 451 | 13.3 |
| Dumas | n80w80.002.txt | 592 | NA | 508 | 605 | 16.03 | 506 | 592 | 14.53 |
| Dumas | n80w80.003.txt | 589 | NA | 500 | 598 | 16.39 | 500 | 589 | 15.11 |
| Dumas | n80w80.004.txt | 594 | NA | 506 | 620 | 18.39 | 505 | 594 | 14.98 |
| OhlmannThomas | n150w120.001.txt | 734 | 725.50 | 324 | 809 | 59.95 | 324 | 734 | 55.86 |
| OhlmannThomas | n150w120.002.txt | 677 | 668.40 | 209 | 717 | 70.85 | 209 | 677 | 69.13 |
| OhlmannThomas | n150w120.003.txt | 747 | 746.40 | 416 | 807 | 48.45 | 416 | 747 | 44.31 |
| OhlmannThomas | n150w120.004.txt | 763 | 761.60 | 381 | 835 | 54.37 | 381 | 763 | 50.07 |
| OhlmannThomas | n150w120.005.txt | 689 | 684.70 | 266 | 754 | 64.72 | 274 | 689 | 60.23 |
| OhlmannThomas | n150w140.001.txt | 762 | 754.00 | 394 | 893 | 55.88 | 394 | 762 | 48.29 |
| OhlmannThomas | n150w140.002.txt | 755 | 752.00 | 407 | 855 | 52.40 | 416 | 755 | 44.90 |
| OhlmannThomas | n150w140.003.txt | 613 | 608.50 | 215 | 738 | 70.87 | 215 | 613 | 64.93 |
| OhlmannThomas | n150w140.005.txt | 663 | 662.00 | 197 | 750 | 73.73 | 197 | 663 | 70.29 |
| OhlmannThomas | n150w160.001.txt | 706 | 701.40 | 293 | 777 | 62.29 | 293 | 706 | 58.50 |
| OhlmannThomas | n150w160.002.txt | 711 | 709.70 | 286 | 826 | 65.38 | 286 | 711 | 59.77 |
| OhlmannThomas | n150w160.003.txt | 608 | 603.20 | 170 | 772 | 77.98 | 170 | 608 | 72.04 |
| OhlmannThomas | n150w160.004.txt | 672 | 672.00 | 336 | 749 | 55.14 | 344 | 672 | 48.81 |
| OhlmannThomas | n150w160.005.txt | 658 | 655.00 | 320 | 736 | 56.52 | 320 | 658 | 51.37 |
| OhlmannThomas | n200w120.001.txt | 799 | 793.30 | 312 | 910 | 65.71 | 312 | 799 | 60.95 |
| OhlmannThomas | n200w120.002.txt | 721 | 713.90 | 184 | 822 | 77.62 | 184 | 721 | 74.48 |
| OhlmannThomas | n200w120.003.txt | 880 | 868.60 | 336 | 983 | 65.82 | 336 | 880 | 61.82 |
| OhlmannThomas | n200w120.004.txt | 777 | 775.80 | 291 | 887 | 67.19 | 291 | 777 | 62.55 |
| OhlmannThomas | n200w120.005.txt | 841 | 833.20 | 258 | 960 | 73.12 | 371 | 841 | 55.89 |
| OhlmannThomas | n200w140.001.txt | 834 | 826.20 | 177 | 1053 | 83.19 | 177 | 834 | 78.78 |
| OhlmannThomas | n200w140.002.txt | 760 | 756.20 | 180 | 895 | 79.89 | 180 | 760 | 76.32 |
| OhlmannThomas | n200w140.003.txt | 758 | 756.00 | 241 | 897 | 73.13 | 252 | 758 | 66.75 |
| OhlmannThomas | n200w140.004.txt | 816 | 807.10 | 284 | 932 | 69.53 | 284 | 816 | 65.20 |
| OhlmannThomas | n200w140.005.txt | 822 | 819.60 | 148 | 927 | 84.03 | 148 | 822 | 82.00 |
| SolomonPesant | rc203.0 | 727.45 | 726.22 | 608.28 | 734.00 | 17.13 | 608.24 | 727.45 | 16.39 |
| SolomonPesant | rc204.2 | 778.40 | 774.77 | 667.18 | 905.93 | 26.35 | 685.22 | 778.40 | 11.97 |

Table A.4 **(Part 1 of 2)** TSP-TW Results of PnB at $\omega = 2048$ on Open Problems: Seeded and Unseeded

LB = Lower Bound, UB = Upper Bound, OG = Optimality Gap.

| Problem Information | | | Baldacci et. al. (2012) | Single Thread: 2048 | | | Seeded Single Thread: 2048 | | |
|---|---|---|---|---|---|---|---|---|---|
| Set | Name | Best Known Solution | LB | LB | UB | OG | LB | UB | OG |
| AFG | rbg049a.tw | 10018 | 10006.10 | 9877 | 10034 | 1.56 | 9877 | 10018 | 1.41 |
| AFG | rbg050b.tw | 9863 | 9855.80 | 9711 | 9876 | 1.67 | 9713 | 9863 | 1.52 |
| AFG | rbg050c.tw | 10024 | 10020.40 | 9745 | 10074 | 3.27 | 9746 | 10024 | 2.77 |
| AFG | rbg132.2.tw | 8192 | 8188.20 | 6701 | 8316 | 19.42 | 6695 | 8192 | 18.27 |
| AFG | rbg152.3.tw | 9788 | 9785.20 | 7240 | 9982 | 27.47 | 7240 | 9788 | 26.03 |
| AFG | rbg193.2.tw | 12142 | 12136.30 | 9755 | 12441 | 21.59 | 9755 | 12142 | 19.66 |
| GendreauDumas | n100w100.004.txt | 684 | 680.58 | 484 | 738 | 34.42 | 485 | 684 | 29.09 |
| GendreauDumas | n100w120.002.txt | 540 | 535.68 | 279 | 581 | 51.98 | 279 | 540 | 48.33 |
| GendreauDumas | n100w120.004.txt | 663 | 660.01 | 383 | 713 | 46.28 | 383 | 663 | 42.23 |
| GendreauDumas | n100w140.005.txt | 509 | 504.42 | 346 | 571 | 39.40 | 346 | 509 | 32.02 |
| GendreauDumas | n100w160.002.txt | 532 | 528.94 | 287 | 601 | 52.25 | 286 | 532 | 46.24 |
| GendreauDumas | n100w160.005.txt | 586 | 585.41 | 327 | 642 | 49.07 | 327 | 586 | 44.20 |
| GendreauDumas | n100w80.002.txt | 668 | 666.00 | 542 | 681 | 20.41 | 549 | 668 | 17.81 |
| GendreauDumas | n40w180.004.txt | 354 | 352.58 | 280 | 359 | 22.01 | 283 | 354 | 20.06 |
| GendreauDumas | n40w200.003.txt | 339 | 322.05 | 305 | 340 | 10.29 | 305 | 339 | 10.03 |
| GendreauDumas | n40w200.004.txt | 301 | 300.10 | 232 | 301 | 22.92 | 229 | 301 | 23.92 |
| GendreauDumas | n60w140.001.txt | 423 | 421.31 | 331 | 425 | 22.12 | 332 | 423 | 21.51 |
| GendreauDumas | n60w140.002.txt | 462 | 461.08 | 394 | 469 | 15.99 | 400 | 462 | 13.42 |
| GendreauDumas | n60w140.005.txt | 460 | 455.40 | 334 | 462 | 27.71 | 335 | 460 | 27.17 |
| GendreauDumas | n60w160.001.txt | 560 | 556.08 | 457 | 572 | 20.10 | 457 | 560 | 18.39 |
| GendreauDumas | n60w160.003.txt | 434 | 432.70 | 212 | 464 | 54.31 | 212 | 434 | 51.15 |
| GendreauDumas | n60w180.001.txt | 411 | 407.30 | 234 | 460 | 49.13 | 234 | 411 | 43.07 |
| GendreauDumas | n60w180.003.txt | 445 | 440.00 | 314 | 458 | 31.44 | 314 | 445 | 29.44 |
| GendreauDumas | n60w180.004.txt | 456 | 455.54 | 272 | 490 | 44.49 | 272 | 456 | 40.35 |
| GendreauDumas | n60w180.005.txt | 395 | 388.68 | 274 | 409 | 33.01 | 274 | 395 | 30.63 |
| GendreauDumas | n60w200.003.txt | 455 | 444.08 | 319 | 471 | 32.27 | 321 | 455 | 29.45 |
| GendreauDumas | n60w200.004.txt | 431 | 429.71 | 343 | 441 | 22.22 | 347 | 431 | 19.49 |
| GendreauDumas | n60w200.005.txt | 427 | 425.29 | 292 | 449 | 34.97 | 292 | 427 | 31.62 |
| GendreauDumas | n80w120.001.txt | 498 | 497.50 | 362 | 514 | 29.57 | 362 | 498 | 27.31 |
| GendreauDumas | n80w120.002.txt | 577 | 576.42 | 415 | 587 | 29.30 | 416 | 577 | 27.90 |
| GendreauDumas | n80w120.004.txt | 501 | 491.48 | 301 | 509 | 40.86 | 301 | 501 | 39.92 |
| GendreauDumas | n80w120.005.txt | 591 | 586.86 | 415 | 594 | 30.13 | 415 | 591 | 29.78 |
| GendreauDumas | n80w140.002.txt | 470 | 469.06 | 346 | 528 | 34.47 | 347 | 470 | 26.17 |
| GendreauDumas | n80w140.003.txt | 580 | 574.78 | 297 | 636 | 53.30 | 295 | 580 | 49.14 |
| GendreauDumas | n80w140.004.txt | 423 | 420.31 | 262 | 449 | 41.65 | 262 | 423 | 38.06 |
| GendreauDumas | n80w160.002.txt | 549 | 547.45 | 197 | 638 | 69.12 | 197 | 549 | 64.12 |
| GendreauDumas | n80w180.001.txt | 551 | 550.45 | 373 | 560 | 33.39 | 373 | 551 | 32.30 |
| GendreauDumas | n80w200.001.txt | 490 | 486.57 | 150 | 555 | 72.97 | 150 | 490 | 69.39 |
| GendreauDumas | n80w200.002.txt | 488 | 487.51 | 270 | 572 | 52.80 | 271 | 488 | 44.47 |
| GendreauDumas | n80w200.003.txt | 464 | 462.14 | 194 | 495 | 60.81 | 194 | 464 | 58.19 |
| GendreauDumas | n80w200.004.txt | 526 | 521.27 | 291 | 565 | 48.50 | 292 | 526 | 44.49 |
| GendreauDumas | n80w200.005.txt | 439 | 438.12 | 235 | 484 | 51.45 | 235 | 439 | 46.47 |
| SolomonPotvinBengio | rc_203.2.txt | 784.16 | 781.64 | 659.63 | 784.16 | 15.88 | 658.22 | 784.16 | 16.06 |
| SolomonPotvinBengio | rc_203.3.txt | 817.53 | 810.46 | 735.91 | 823.44 | 10.63 | 756.34 | 817.53 | 7.48 |
| SolomonPotvinBengio | rc_204.1.txt | 878.64 | 872.62 | 791.45 | 889.53 | 11.03 | 794.15 | 878.64 | 9.62 |
| SolomonPotvinBengio | rc_204.2.txt | 662.16 | 650.94 | 525.69 | 664.52 | 20.89 | 526.72 | 662.16 | 20.45 |
| SolomonPotvinBengio | rc_208.3.txt | 634.44 | 622.48 | 549.17 | 670.56 | 18.10 | 550.15 | 634.44 | 13.29 |

Table A.5 **(Part 2 of 2)** TSP-TW Results of PnB at $\omega = 2048$ on Open Problems: Seeded and Unseeded

LB = Lower Bound, UB = Upper Bound, OG = Optimality Gap.

| Problem Information | | | Baldacci et. al. (2012) | Single Thread: 2048 | | | | Seeded Single Thread: 2048 | | | |
|---|---|---|---|---|---|---|---|---|---|---|---|
| Set | Name | Best Known Solution | LB | LB | UB | OG | Time | LB | UB | OG | Time |
| AFG | rbg010a.tw | 671 | O | 671 | 671 | 0 | 0.08 | 671 | 671 | 0 | 0.26 |
| AFG | rbg016a.tw | 938 | O | 938 | 938 | 0 | 0.22 | 938 | 938 | 0 | 0.28 |
| AFG | rbg016b.tw | 1304 | O | 1304 | 1304 | 0 | 5.62 | 1304 | 1304 | 0 | 4.43 |
| AFG | rbg017.2.tw | 852 | O | 852 | 852 | 0 | 9.08 | 852 | 852 | 0 | 4.71 |
| AFG | rbg017.tw | 893 | O | 893 | 893 | 0 | 3.92 | 893 | 893 | 0 | 2.96 |
| AFG | rbg017a.tw | 4296 | O | 4296 | 4296 | 0 | 0.28 | 4296 | 4296 | 0 | 0.22 |
| AFG | rbg019a.tw | 1262 | O | 1262 | 1262 | 0 | 0.21 | 1262 | 1262 | 0 | 0.19 |
| AFG | rbg019b.tw | 1866 | O | 1866 | 1866 | 0 | 12.96 | 1866 | 1866 | 0 | 5.67 |
| AFG | rbg019c.tw | 4536 | O | 4536 | 4536 | 0 | 2.91 | 4536 | 4536 | 0 | 3.64 |
| AFG | rbg019d.tw | 1356 | O | 1356 | 1356 | 0 | 3.66 | 1356 | 1356 | 0 | 0.37 |
| AFG | rbg020a.tw | 4689 | O | 4689 | 4689 | 0 | 0.22 | 4689 | 4689 | 0 | 0.23 |
| AFG | rbg021.2.tw | 4528 | O | 4528 | 4528 | 0 | 10.08 | 4528 | 4528 | 0 | 5.45 |
| AFG | rbg021.3.tw | 4528 | O | 4528 | 4528 | 0 | 15.74 | 4528 | 4528 | 0 | 7.80 |
| AFG | rbg021.4.tw | 4525 | O | 4525 | 4525 | 0 | 25.67 | 4525 | 4525 | 0 | 9.71 |
| AFG | rbg021.5.tw | 4515 | O | 4515 | 4515 | 0 | 25.13 | 4515 | 4515 | 0 | 12.88 |
| AFG | rbg021.6.tw | 4480 | O | 4480 | 4480 | 0 | 2458.01 | 4480 | 4480 | 0 | 2501.88 |
| AFG | rbg021.7.tw | 4479 | O | 1050 | 4480 | 76.56 | - | 1050 | 4479 | 76.56 | - |
| AFG | rbg021.8.tw | 4478 | O | 1042 | 4480 | 76.74 | - | 1041 | 4478 | 76.75 | - |
| AFG | rbg021.9.tw | 4478 | O | 1037 | 4480 | 76.85 | - | 1039 | 4478 | 76.8 | - |
| AFG | rbg021.tw | 4536 | O | 4536 | 4536 | 0 | 3.11 | 4536 | 4536 | 0 | 2.81 |
| AFG | rbg027a.tw | 5091 | O | 5091 | 5091 | 0 | 10.69 | 5091 | 5091 | 0 | 8.34 |
| AFG | rbg031a.tw | 1863 | O | 1863 | 1863 | 0 | 28.16 | 1863 | 1863 | 0 | 13.51 |
| AFG | rbg033a.tw | 2069 | O | 2069 | 2069 | 0 | 33.44 | 2069 | 2069 | 0 | 18.26 |
| AFG | rbg034a.tw | 2222 | O | 2222 | 2222 | 0 | 83.72 | 2222 | 2222 | 0 | 34.02 |
| AFG | rbg035a.2.tw | 2056 | O | 1837 | 2088 | 12.02 | - | 1838 | 2056 | 10.6 | - |
| AFG | rbg035a.tw | 2144 | O | 2144 | 2144 | 0 | 44.80 | 2144 | 2144 | 0 | 28.45 |
| AFG | rbg038a.tw | 2480 | O | 2480 | 2480 | 0 | 75.79 | 2480 | 2480 | 0 | 17.41 |
| AFG | rbg040a.tw | 2378 | 2376.9 | 2378 | 2378 | 0 | 57.1 | 2378 | 2378 | 0 | 36.71 |
| AFG | rbg041a.tw | 2598 | O | 2598 | 2598 | 0 | 109.23 | 2598 | 2598 | 0 | 81.37 |
| AFG | rbg042a.tw | 2772 | O | 2772 | 2772 | 0 | 154.46 | 2772 | 2772 | 0 | 88.88 |
| AFG | rbg048a.tw | 9383 | O | 9011 | 9419 | 4.33 | - | 9013 | 9383 | 3.94 | - |
| AFG | rbg050a.tw | 2953 | O | 2361 | 2990 | 21.04 | - | 2362 | 2953 | 20.01 | - |
| AFG | rbg055a.tw | 3761 | O | 3761 | 3761 | 0 | 405.98 | 3761 | 3761 | 0 | 121.22 |
| AFG | rbg067a.tw | 4625 | O | 4625 | 4625 | 0 | 634.69 | 4625 | 4625 | 0 | 158.26 |
| AFG | rbg125a.tw | 7936 | O | 7918 | 8051 | 1.65 | - | 7936 | 7936 | 0 | 2479.97 |
| AFG | rbg132.tw | 8468 | O | 8449 | 8530 | 0.95 | - | 8468 | 8468 | 0 | 549.16 |
| AFG | rbg152.tw | 10032 | O | 10024 | 10086 | 0.61 | - | 10032 | 10032 | 0 | 1011.24 |
| AFG | rbg172a.tw | 10950 | O | 10082 | 11172 | 9.76 | - | 10082 | 10950 | 7.93 | - |
| AFG | rbg193.tw | 12535 | O | 11994 | 12781 | 6.16 | - | 11958 | 12535 | 4.6 | - |
| AFG | rbg201a.tw | 12948 | O | 11528 | 13240 | 12.93 | - | 11753 | 12948 | 9.23 | - |
| AFG | rbg233.2.tw | 14495 | O | 11634 | 14827 | 21.54 | - | 11634 | 14495 | 19.74 | - |
| AFG | rbg233.tw | 14992 | O | 13355 | 15330 | 12.88 | - | 12988 | 14992 | 13.37 | - |
| Dumas | n100w20.001.txt | 738 | NA | 738 | 738 | 0 | 32.87 | 738 | 738 | 0 | 5.06 |
| Dumas | n100w20.002.txt | 715 | NA | 715 | 715 | 0 | 64.56 | 715 | 715 | 0 | 30.67 |
| Dumas | n100w20.003.txt | 762 | NA | 762 | 762 | 0 | 49.73 | 762 | 762 | 0 | 42.79 |
| Dumas | n100w20.004.txt | 799 | NA | 799 | 799 | 0 | 51.93 | 799 | 799 | 0 | 28.00 |
| Dumas | n100w20.005.txt | 774 | NA | 774 | 774 | 0 | 45.66 | 774 | 774 | 0 | 35.66 |
| Dumas | n100w40.001.txt | 770 | NA | 770 | 770 | 0 | 178.71 | 770 | 770 | 0 | 129.09 |
| Dumas | n100w40.002.txt | 653 | NA | 653 | 653 | 0 | 573.14 | 653 | 653 | 0 | 455.42 |
| Dumas | n100w40.003.txt | 736 | NA | 736 | 736 | 0 | 390.53 | 736 | 736 | 0 | 341.37 |
| Dumas | n100w40.004.txt | 651 | NA | 651 | 651 | 0 | 500.63 | 651 | 651 | 0 | 406.68 |
| Dumas | n100w40.005.txt | 699 | NA | 699 | 699 | 0 | 518.71 | 699 | 699 | 0 | 455.31 |
| Dumas | n100w60.002.txt | 659 | NA | 659 | 659 | 0 | 1348.85 | 659 | 659 | 0 | 1503.28 |
| Dumas | n100w60.005.txt | 661 | NA | 661 | 661 | 0 | 1027.05 | 661 | 661 | 0 | 1054.34 |
| Dumas | n150w20.001.txt | 925 | NA | 925 | 925 | 0 | 380.14 | 925 | 925 | 0 | 248.27 |
| Dumas | n150w20.002.txt | 864 | NA | 864 | 864 | 0 | 234.78 | 864 | 864 | 0 | 126.45 |
| Dumas | n150w20.003.txt | 834 | NA | 834 | 834 | 0 | 410.38 | 834 | 834 | 0 | 305.72 |
| Dumas | n150w20.004.txt | 873 | NA | 873 | 873 | 0 | 343.26 | 873 | 873 | 0 | 304.33 |
| Dumas | n150w20.005.txt | 846 | NA | 846 | 846 | 0 | 423.04 | 846 | 846 | 0 | 452.06 |
| Dumas | n200w20.001.txt | 1019 | NA | 1019 | 1019 | 0 | 2739.07 | 1019 | 1019 | 0 | 2898.58 |
| Dumas | n200w20.002.txt | 972 | NA | 971 | 1000 | 2.9 | - | 972 | 972 | 0 | 614.20 |
| Dumas | n200w20.003.txt | 1050 | NA | 1050 | 1050 | 0 | 1330.33 | 1050 | 1050 | 0 | 1523.48 |
| Dumas | n200w20.004.txt | 984 | NA | 984 | 984 | 0 | 2360.97 | 984 | 984 | 0 | 3345.67 |
| Dumas | n200w20.005.txt | 1020 | NA | 1020 | 1020 | 0 | 445.04 | 1020 | 1020 | 0 | 1059.73 |
| Dumas | n20w100.001.txt | 237 | NA | 237 | 237 | 0 | 7.62 | 237 | 237 | 0 | 4.32 |
| Dumas | n20w100.002.txt | 222 | NA | 222 | 222 | 0 | 10.21 | 222 | 222 | 0 | 4.97 |
| Dumas | n20w100.003.txt | 310 | NA | 310 | 310 | 0 | 8.85 | 310 | 310 | 0 | 4.35 |
| Dumas | n20w100.004.txt | 349 | NA | 349 | 349 | 0 | 2.56 | 349 | 349 | 0 | 0.70 |
| Dumas | n20w100.005.txt | 258 | NA | 258 | 258 | 0 | 10.40 | 258 | 258 | 0 | 6.06 |

Table A.6 **(Part 1 of 6)** TSP-TW Results of PnB at $\omega = 2048$ on Closed Problems: Seeded and Unseeded

LB = Lower Bound, UB = Upper Bound, OG = Optimality Gap, O = Optimality Proved.

| Problem Information | | | Baldacci et. al. (2012) | Single Thread: 2048 | | | | Seeded Single Thread: 2048 | | | |
|---|---|---|---|---|---|---|---|---|---|---|---|
| Set | Name | Best Known Solution | LB | LB | UB | OG | Time | LB | UB | OG | Time |
| Dumas | n20w20.001.txt | 378 | NA | 378 | 378 | 0 | 0.06 | 378 | 378 | 0 | 0.18 |
| Dumas | n20w20.002.txt | 286 | NA | 286 | 286 | 0 | 0.08 | 286 | 286 | 0 | 0.18 |
| Dumas | n20w20.003.txt | 394 | NA | 394 | 394 | 0 | 0.07 | 394 | 394 | 0 | 0.18 |
| Dumas | n20w20.004.txt | 396 | NA | 396 | 396 | 0 | 0.06 | 396 | 396 | 0 | 0.18 |
| Dumas | n20w20.005.txt | 352 | NA | 352 | 352 | 0 | 0.07 | 352 | 352 | 0 | 0.26 |
| Dumas | n20w40.001.txt | 254 | NA | 254 | 254 | 0 | 0.12 | 254 | 254 | 0 | 0.31 |
| Dumas | n20w40.002.txt | 333 | NA | 333 | 333 | 0 | 0.07 | 333 | 333 | 0 | 0.24 |
| Dumas | n20w40.003.txt | 317 | NA | 317 | 317 | 0 | 0.07 | 317 | 317 | 0 | 0.19 |
| Dumas | n20w40.004.txt | 388 | NA | 388 | 388 | 0 | 0.07 | 388 | 388 | 0 | 0.20 |
| Dumas | n20w40.005.txt | 288 | NA | 288 | 288 | 0 | 0.08 | 288 | 288 | 0 | 0.20 |
| Dumas | n20w60.001.txt | 335 | NA | 335 | 335 | 0 | 2.22 | 335 | 335 | 0 | 1.48 |
| Dumas | n20w60.002.txt | 244 | NA | 244 | 244 | 0 | 0.56 | 244 | 244 | 0 | 0.21 |
| Dumas | n20w60.003.txt | 352 | NA | 352 | 352 | 0 | 0.10 | 352 | 352 | 0 | 0.22 |
| Dumas | n20w60.004.txt | 280 | NA | 280 | 280 | 0 | 7.50 | 280 | 280 | 0 | 3.67 |
| Dumas | n20w60.005.txt | 338 | NA | 338 | 338 | 0 | 0.62 | 338 | 338 | 0 | 0.22 |
| Dumas | n20w80.001.txt | 329 | NA | 329 | 329 | 0 | 2.00 | 329 | 329 | 0 | 1.37 |
| Dumas | n20w80.002.txt | 338 | NA | 338 | 338 | 0 | 1.27 | 338 | 338 | 0 | 1.34 |
| Dumas | n20w80.003.txt | 320 | NA | 320 | 320 | 0 | 0.74 | 320 | 320 | 0 | 0.41 |
| Dumas | n20w80.004.txt | 304 | NA | 304 | 304 | 0 | 1.99 | 304 | 304 | 0 | 0.90 |
| Dumas | n20w80.005.txt | 264 | NA | 264 | 264 | 0 | 8.19 | 264 | 264 | 0 | 4.24 |
| Dumas | n40w100.001.txt | 429 | NA | 429 | 429 | 0 | 67.70 | 429 | 429 | 0 | 68.84 |
| Dumas | n40w100.002.txt | 358 | NA | 358 | 358 | 0 | 84.97 | 358 | 358 | 0 | 73.49 |
| Dumas | n40w100.003.txt | 364 | NA | 364 | 364 | 0 | 71.79 | 364 | 364 | 0 | 50.69 |
| Dumas | n40w100.004.txt | 357 | NA | 357 | 357 | 0 | 66.54 | 357 | 357 | 0 | 58.87 |
| Dumas | n40w100.005.txt | 377 | NA | 377 | 377 | 0 | 82.67 | 377 | 377 | 0 | 52.66 |
| Dumas | n40w20.001.txt | 500 | NA | 500 | 500 | 0 | 0.51 | 500 | 500 | 0 | 0.41 |
| Dumas | n40w20.002.txt | 552 | NA | 552 | 552 | 0 | 2.08 | 552 | 552 | 0 | 0.54 |
| Dumas | n40w20.003.txt | 478 | NA | 478 | 478 | 0 | 1.11 | 478 | 478 | 0 | 0.34 |
| Dumas | n40w20.004.txt | 404 | NA | 404 | 404 | 0 | 1.19 | 404 | 404 | 0 | 0.34 |
| Dumas | n40w20.005.txt | 499 | NA | 499 | 499 | 0 | 0.09 | 499 | 499 | 0 | 0.29 |
| Dumas | n40w40.001.txt | 465 | NA | 465 | 465 | 0 | 2.41 | 465 | 465 | 0 | 0.61 |
| Dumas | n40w40.002.txt | 461 | NA | 461 | 461 | 0 | 18.31 | 461 | 461 | 0 | 10.02 |
| Dumas | n40w40.003.txt | 474 | NA | 474 | 474 | 0 | 4.11 | 474 | 474 | 0 | 1.86 |
| Dumas | n40w40.004.txt | 452 | NA | 452 | 452 | 0 | 13.72 | 452 | 452 | 0 | 9.67 |
| Dumas | n40w40.005.txt | 453 | NA | 453 | 453 | 0 | 20.16 | 453 | 453 | 0 | 8.88 |
| Dumas | n40w60.001.txt | 494 | NA | 494 | 494 | 0 | 15.85 | 494 | 494 | 0 | 16.40 |
| Dumas | n40w60.002.txt | 470 | NA | 470 | 470 | 0 | 24.24 | 470 | 470 | 0 | 15.00 |
| Dumas | n40w60.003.txt | 408 | NA | 408 | 408 | 0 | 21.72 | 408 | 408 | 0 | 13.27 |
| Dumas | n40w60.004.txt | 382 | NA | 382 | 382 | 0 | 64.78 | 382 | 382 | 0 | 51.30 |
| Dumas | n40w60.005.txt | 328 | NA | 328 | 328 | 0 | 32.39 | 328 | 328 | 0 | 11.37 |
| Dumas | n40w80.001.txt | 395 | NA | 395 | 395 | 0 | 31.40 | 395 | 395 | 0 | 21.92 |
| Dumas | n40w80.002.txt | 431 | NA | 431 | 431 | 0 | 59.08 | 431 | 431 | 0 | 52.11 |
| Dumas | n40w80.003.txt | 412 | NA | 412 | 412 | 0 | 28.76 | 412 | 412 | 0 | 20.84 |
| Dumas | n40w80.004.txt | 417 | NA | 417 | 417 | 0 | 33.35 | 417 | 417 | 0 | 28.22 |
| Dumas | n40w80.005.txt | 344 | NA | 344 | 344 | 0 | 58.02 | 344 | 344 | 0 | 47.72 |
| Dumas | n60w100.001.txt | 515 | NA | 515 | 515 | 0 | 1063.65 | 515 | 515 | 0 | 970.51 |
| Dumas | n60w100.002.txt | 538 | NA | 538 | 538 | 0 | 456.89 | 538 | 538 | 0 | 453.45 |
| Dumas | n60w100.003.txt | 560 | NA | 560 | 560 | 0 | 361.90 | 560 | 560 | 0 | 397.47 |
| Dumas | n60w100.004.txt | 510 | NA | 510 | 510 | 0 | 264.85 | 510 | 510 | 0 | 313.67 |
| Dumas | n60w20.001.txt | 551 | NA | 551 | 551 | 0 | 6.33 | 551 | 551 | 0 | 2.46 |
| Dumas | n60w20.002.txt | 605 | NA | 605 | 605 | 0 | 4.83 | 605 | 605 | 0 | 1.78 |
| Dumas | n60w20.003.txt | 533 | NA | 533 | 533 | 0 | 6.45 | 533 | 533 | 0 | 1.23 |
| Dumas | n60w20.004.txt | 616 | NA | 616 | 616 | 0 | 7.34 | 616 | 616 | 0 | 1.77 |
| Dumas | n60w20.005.txt | 603 | NA | 603 | 603 | 0 | 4.11 | 603 | 603 | 0 | 0.64 |
| Dumas | n60w40.001.txt | 591 | NA | 591 | 591 | 0 | 45.45 | 591 | 591 | 0 | 35.15 |
| Dumas | n60w40.002.txt | 621 | NA | 621 | 621 | 0 | 72.70 | 621 | 621 | 0 | 63.07 |
| Dumas | n60w40.003.txt | 603 | NA | 603 | 603 | 0 | 51.21 | 603 | 603 | 0 | 41.32 |
| Dumas | n60w40.004.txt | 597 | NA | 597 | 597 | 0 | 22.87 | 597 | 597 | 0 | 11.06 |
| Dumas | n60w40.005.txt | 539 | NA | 539 | 539 | 0 | 28.22 | 539 | 539 | 0 | 15.14 |
| Dumas | n60w60.001.txt | 609 | NA | 609 | 609 | 0 | 77.16 | 609 | 609 | 0 | 71.60 |
| Dumas | n60w60.002.txt | 566 | NA | 566 | 566 | 0 | 96.04 | 566 | 566 | 0 | 91.61 |
| Dumas | n60w60.003.txt | 485 | NA | 485 | 485 | 0 | 130.48 | 485 | 485 | 0 | 124.08 |
| Dumas | n60w60.004.txt | 571 | NA | 571 | 571 | 0 | 106.17 | 571 | 571 | 0 | 84.95 |
| Dumas | n60w60.005.txt | 569 | NA | 569 | 569 | 0 | 76.37 | 569 | 569 | 0 | 71.14 |
| Dumas | n60w80.001.txt | 458 | NA | 458 | 458 | 0 | 546.14 | 458 | 458 | 0 | 444.94 |
| Dumas | n60w80.002.txt | 498 | NA | 498 | 498 | 0 | 147.40 | 498 | 498 | 0 | 146.75 |
| Dumas | n60w80.003.txt | 550 | NA | 550 | 550 | 0 | 133.79 | 550 | 550 | 0 | 129.27 |
| Dumas | n60w80.004.txt | 566 | NA | 566 | 566 | 0 | 207.43 | 566 | 566 | 0 | 178.19 |

Table A.7 **(Part 2 of 6)** TSP-TW Results of PnB at $\omega = 2048$ on Closed Problems: Seeded and Unseeded

LB = Lower Bound, UB = Upper Bound, OG = Optimality Gap, O = Optimality Proved.

| Problem Information | | | Baldacci et. al. (2012) | Single Thread: 2048 | | | | Seeded Single Thread: 2048 | | | |
|---|---|---|---|---|---|---|---|---|---|---|---|
| Set | Name | Best Known Solution | LB | LB | UB | OG | Time | LB | UB | OG | Time |
| Dumas | n60w80.005.txt | 468 | NA | 468 | 468 | 0 | 363.20 | 468 | 468 | 0 | 363.03 |
| Dumas | n80w20.001.txt | 616 | NA | 616 | 616 | 0 | 58.66 | 616 | 616 | 0 | 31.87 |
| Dumas | n80w20.002.txt | 737 | NA | 737 | 737 | 0 | 30.47 | 737 | 737 | 0 | 20.49 |
| Dumas | n80w20.003.txt | 667 | NA | 667 | 667 | 0 | 14.48 | 667 | 667 | 0 | 5.52 |
| Dumas | n80w20.004.txt | 615 | NA | 615 | 615 | 0 | 41.62 | 615 | 615 | 0 | 32.25 |
| Dumas | n80w20.005.txt | 748 | NA | 748 | 748 | 0 | 23.05 | 748 | 748 | 0 | 10.52 |
| Dumas | n80w40.001.txt | 606 | NA | 606 | 606 | 0 | 313.45 | 606 | 606 | 0 | 245.90 |
| Dumas | n80w40.002.txt | 618 | NA | 618 | 618 | 0 | 135.46 | 618 | 618 | 0 | 132.07 |
| Dumas | n80w40.003.txt | 674 | NA | 674 | 674 | 0 | 109.76 | 674 | 674 | 0 | 131.28 |
| Dumas | n80w40.004.txt | 557 | NA | 557 | 557 | 0 | 115.15 | 557 | 557 | 0 | 112.15 |
| Dumas | n80w40.005.txt | 695 | NA | 695 | 695 | 0 | 130.12 | 695 | 695 | 0 | 126.17 |
| Dumas | n80w60.001.txt | 554 | NA | 554 | 554 | 0 | 237.93 | 554 | 554 | 0 | 239.36 |
| Dumas | n80w60.002.txt | 633 | NA | 633 | 633 | 0 | 488.91 | 633 | 633 | 0 | 562.44 |
| Dumas | n80w60.003.txt | 651 | NA | 651 | 651 | 0 | 421.10 | 651 | 651 | 0 | 404.65 |
| Dumas | n80w60.004.txt | 619 | NA | 619 | 619 | 0 | 319.16 | 619 | 619 | 0 | 220.47 |
| Dumas | n80w60.005.txt | 575 | NA | 575 | 575 | 0 | 765.78 | 575 | 575 | 0 | 918.69 |
| Dumas | n80w80.001.txt | 624 | NA | 624 | 624 | 0 | 995.03 | 624 | 624 | 0 | 919.20 |
| Dumas | n80w80.005.txt | 570 | NA | 570 | 570 | 0 | 285.37 | 570 | 570 | 0 | 348.52 |
| GendreauDumas | n100w100.001.txt | 643 | O | 467 | 670 | 30.3 | - | 467 | 643 | 27.37 | - |
| GendreauDumas | n100w100.002.txt | 619 | O | 480 | 629 | 23.69 | - | 477 | 619 | 22.94 | - |
| GendreauDumas | n100w100.003.txt | 685 | O | 474 | 703 | 32.57 | - | 474 | 685 | 30.8 | - |
| GendreauDumas | n100w100.005.txt | 572 | O | 365 | 617 | 40.84 | - | 367 | 572 | 35.84 | - |
| GendreauDumas | n100w120.001.txt | 629 | O | 405 | 639 | 36.62 | - | 405 | 629 | 35.61 | - |
| GendreauDumas | n100w120.003.txt | 617 | O | 451 | 634 | 28.86 | - | 451 | 617 | 26.9 | - |
| GendreauDumas | n100w120.005.txt | 537 | O | 306 | 592 | 48.31 | - | 306 | 537 | 43.02 | - |
| GendreauDumas | n100w140.001.txt | 604 | O | 393 | 704 | 44.18 | - | 393 | 604 | 34.93 | - |
| GendreauDumas | n100w140.002.txt | 615 | O | 403 | 650 | 38 | - | 403 | 615 | 34.47 | - |
| GendreauDumas | n100w140.003.txt | 481 | O | 229 | 494 | 53.64 | - | 229 | 481 | 52.39 | - |
| GendreauDumas | n100w140.004.txt | 533 | O | 342 | 570 | 40 | - | 343 | 533 | 35.65 | - |
| GendreauDumas | n100w160.001.txt | 582 | O | 415 | 614 | 32.41 | - | 416 | 582 | 28.52 | - |
| GendreauDumas | n100w160.003.txt | 495 | O | 301 | 551 | 45.37 | - | 302 | 495 | 38.99 | - |
| GendreauDumas | n100w160.004.txt | 580 | O | 391 | 627 | 37.64 | - | 392 | 580 | 32.41 | - |
| GendreauDumas | n100w80.001.txt | 670 | O | 591 | 683 | 13.47 | - | 591 | 670 | 11.79 | - |
| GendreauDumas | n100w80.003.txt | 691 | O | 480 | 691 | 30.54 | - | 480 | 691 | 30.54 | - |
| GendreauDumas | n100w80.004.txt | 700 | O | 574 | - | 100 | - | 573 | 700 | 18.14 | - |
| GendreauDumas | n100w80.005.txt | 603 | O | 416 | 648 | 35.8 | - | 427 | 603 | 29.19 | - |
| GendreauDumas | n20w120.001.txt | 267 | O | 267 | 267 | 0 | 14.18 | 267 | 267 | 0 | 7.09 |
| GendreauDumas | n20w120.002.txt | 218 | O | 218 | 218 | 0 | 13.27 | 218 | 218 | 0 | 8.66 |
| GendreauDumas | n20w120.003.txt | 303 | O | 303 | 303 | 0 | 11.09 | 303 | 303 | 0 | 5.49 |
| GendreauDumas | n20w120.004.txt | 300 | O | 300 | 300 | 0 | 9.41 | 300 | 300 | 0 | 5.67 |
| GendreauDumas | n20w120.005.txt | 240 | O | 240 | 240 | 0 | 12.67 | 240 | 240 | 0 | 8.52 |
| GendreauDumas | n20w140.001.txt | 176 | O | 176 | 176 | 0 | 11.91 | 176 | 176 | 0 | 6.26 |
| GendreauDumas | n20w140.002.txt | 272 | O | 272 | 272 | 0 | 11.35 | 272 | 272 | 0 | 7.76 |
| GendreauDumas | n20w140.003.txt | 236 | O | 236 | 236 | 0 | 13.22 | 236 | 236 | 0 | 6.43 |
| GendreauDumas | n20w140.004.txt | 255 | O | 255 | 255 | 0 | 12.99 | 255 | 255 | 0 | 6.01 |
| GendreauDumas | n20w140.005.txt | 225 | O | 225 | 225 | 0 | 10.73 | 225 | 225 | 0 | 6.15 |
| GendreauDumas | n20w160.001.txt | 241 | O | 241 | 241 | 0 | 14.81 | 241 | 241 | 0 | 5.58 |
| GendreauDumas | n20w160.002.txt | 201 | O | 201 | 201 | 0 | 11.25 | 201 | 201 | 0 | 7.81 |
| GendreauDumas | n20w160.003.txt | 201 | O | 201 | 201 | 0 | 10.86 | 201 | 201 | 0 | 5.00 |
| GendreauDumas | n20w160.004.txt | 203 | O | 203 | 203 | 0 | 19.55 | 203 | 203 | 0 | 8.33 |
| GendreauDumas | n20w160.005.txt | 245 | O | 245 | 245 | 0 | 13.27 | 245 | 245 | 0 | 8.35 |
| GendreauDumas | n20w180.001.txt | 253 | O | 253 | 253 | 0 | 11.97 | 253 | 253 | 0 | 5.78 |
| GendreauDumas | n20w180.002.txt | 265 | O | 265 | 265 | 0 | 16.99 | 265 | 265 | 0 | 7.46 |
| GendreauDumas | n20w180.003.txt | 271 | O | 271 | 271 | 0 | 18.30 | 271 | 271 | 0 | 9.70 |
| GendreauDumas | n20w180.004.txt | 201 | O | 201 | 201 | 0 | 17.58 | 201 | 201 | 0 | 7.11 |
| GendreauDumas | n20w180.005.txt | 193 | O | 193 | 193 | 0 | 32.53 | 193 | 193 | 0 | 8.59 |
| GendreauDumas | n20w200.001.txt | 233 | O | 233 | 233 | 0 | 20.03 | 233 | 233 | 0 | 10.08 |
| GendreauDumas | n20w200.002.txt | 203 | O | 203 | 203 | 0 | 25.27 | 203 | 203 | 0 | 9.63 |
| GendreauDumas | n20w200.003.txt | 249 | O | 249 | 249 | 0 | 21.51 | 249 | 249 | 0 | 9.40 |
| GendreauDumas | n20w200.005.txt | 227 | O | 227 | 227 | 0 | 21.91 | 227 | 227 | 0 | 7.87 |
| GendreauDumas | n40w120.001.txt | 434 | O | 434 | 434 | 0 | 91.00 | 434 | 434 | 0 | 83.12 |
| GendreauDumas | n40w120.002.txt | 445 | O | 445 | 445 | 0 | 141.74 | 445 | 445 | 0 | 97.37 |
| GendreauDumas | n40w120.003.txt | 357 | O | 357 | 357 | 0 | 881.45 | 357 | 357 | 0 | 1338.21 |
| GendreauDumas | n40w120.004.txt | 303 | O | 303 | 303 | 0 | 105.54 | 303 | 303 | 0 | 96.98 |
| GendreauDumas | n40w120.005.txt | 350 | O | 350 | 350 | 0 | 80.86 | 350 | 350 | 0 | 62.93 |
| GendreauDumas | n40w140.001.txt | 328 | O | 328 | 328 | 0 | 196.16 | 328 | 328 | 0 | 148.20 |
| GendreauDumas | n40w140.002.txt | 383 | O | 383 | 383 | 0 | 2768.09 | 383 | 383 | 0 | 2677.04 |
| GendreauDumas | n40w140.003.txt | 398 | O | 398 | 398 | 0 | 125.13 | 398 | 398 | 0 | 72.96 |

Table A.8 **(Part 3 of 6)** TSP-TW Results of PnB at $\omega = 2048$ on Closed Problems: Seeded and Unseeded

LB = Lower Bound, UB = Upper Bound, OG = Optimality Gap, O = Optimality Proved.

| Problem Information | | | Baldacci et. al. (2012) | Single Thread: 2048 | | | | Seeded Single Thread: 2048 | | | |
|---|---|---|---|---|---|---|---|---|---|---|---|
| Set | Name | Best Known Solution | LB | LB | UB | OG | Time | LB | UB | OG | Time |
| GendreauDumas | n40w140.004.txt | 342 | O | 246 | 342 | 28.07 | - | 246 | 342 | 28.07 | - |
| GendreauDumas | n40w140.005.txt | 371 | O | 371 | 371 | 0 | 471.26 | 371 | 371 | 0 | 289.28 |
| GendreauDumas | n40w160.001.txt | 348 | O | 348 | 348 | 0 | 179.81 | 348 | 348 | 0 | 159.90 |
| GendreauDumas | n40w160.002.txt | 337 | O | 337 | 337 | 0 | 127.84 | 337 | 337 | 0 | 115.75 |
| GendreauDumas | n40w160.003.txt | 346 | O | 346 | 346 | 0 | 301.12 | 346 | 346 | 0 | 156.85 |
| GendreauDumas | n40w160.004.txt | 288 | O | 288 | 288 | 0 | 313.23 | 288 | 288 | 0 | 292.72 |
| GendreauDumas | n40w160.005.txt | 315 | O | 315 | 315 | 0 | 1389.91 | 315 | 315 | 0 | 704.93 |
| GendreauDumas | n40w180.001.txt | 337 | O | 274 | 352 | 22.16 | - | 337 | 337 | 0 | 2852.42 |
| GendreauDumas | n40w180.002.txt | 347 | O | 347 | 347 | 0 | 689.55 | 347 | 347 | 0 | 652.55 |
| GendreauDumas | n40w180.003.txt | 279 | O | 196 | 279 | 29.75 | - | 192 | 279 | 31.18 | - |
| GendreauDumas | n40w180.005.txt | 335 | O | 237 | 340 | 30.29 | - | 238 | 335 | 28.96 | - |
| GendreauDumas | n40w200.001.txt | 330 | O | 208 | 343 | 39.36 | - | 208 | 330 | 36.97 | - |
| GendreauDumas | n40w200.005.txt | 296 | O | 239 | 302 | 20.86 | - | 251 | 296 | 15.2 | - |
| GendreauDumas | n60w120.001.txt | 384 | O | 274 | 396 | 30.81 | - | 274 | 384 | 28.65 | - |
| GendreauDumas | n60w120.002.txt | 427 | O | 371 | 435 | 14.71 | - | 370 | 427 | 13.35 | - |
| GendreauDumas | n60w120.003.txt | 407 | O | 304 | 438 | 30.59 | - | 306 | 407 | 24.82 | - |
| GendreauDumas | n60w120.004.txt | 490 | O | 425 | 490 | 13.27 | - | 425 | 490 | 13.27 | - |
| GendreauDumas | n60w120.005.txt | 547 | O | 498 | 549 | 9.29 | - | 501 | 547 | 8.41 | - |
| GendreauDumas | n60w140.003.txt | 427 | O | 364 | 448 | 18.75 | - | 369 | 427 | 13.58 | - |
| GendreauDumas | n60w140.004.txt | 488 | O | 394 | 498 | 20.88 | - | 394 | 488 | 19.26 | - |
| GendreauDumas | n60w160.002.txt | 423 | O | 325 | 431 | 24.59 | - | 326 | 423 | 22.93 | - |
| GendreauDumas | n60w160.004.txt | 401 | O | 288 | 409 | 29.58 | - | 289 | 401 | 27.93 | - |
| GendreauDumas | n60w160.005.txt | 502 | O | 368 | 512 | 28.12 | - | 368 | 502 | 26.69 | - |
| GendreauDumas | n60w180.002.txt | 399 | O | 305 | 412 | 25.97 | - | 305 | 399 | 23.56 | - |
| GendreauDumas | n60w200.001.txt | 410 | O | 297 | 437 | 32.04 | - | 298 | 410 | 27.32 | - |
| GendreauDumas | n60w200.002.txt | 414 | O | 251 | 431 | 41.76 | - | 253 | 414 | 38.89 | - |
| GendreauDumas | n80w100.001.txt | 565 | O | 433 | 580 | 25.34 | - | 432 | 565 | 23.54 | - |
| GendreauDumas | n80w100.002.txt | 567 | O | 439 | - | 100 | - | 436 | 567 | 23.1 | - |
| GendreauDumas | n80w100.003.txt | 580 | O | 422 | 605 | 30.25 | - | 423 | 580 | 27.07 | - |
| GendreauDumas | n80w100.005.txt | 532 | O | 396 | 560 | 29.29 | - | 396 | 532 | 25.56 | - |
| GendreauDumas | n80w120.003.txt | 540 | O | 361 | 558 | 35.3 | - | 368 | 540 | 31.85 | - |
| GendreauDumas | n80w140.001.txt | 512 | O | 346 | 560 | 38.21 | - | 347 | 512 | 32.23 | - |
| GendreauDumas | n80w140.005.txt | 545 | O | 332 | 555 | 40.18 | - | 332 | 545 | 39.08 | - |
| GendreauDumas | n80w160.001.txt | 506 | O | 340 | 530 | 35.85 | - | 340 | 506 | 32.81 | - |
| GendreauDumas | n80w160.003.txt | 521 | O | 305 | 574 | 46.86 | - | 307 | 521 | 41.07 | - |
| GendreauDumas | n80w160.004.txt | 509 | O | 252 | 575 | 56.17 | - | 252 | 509 | 50.49 | - |
| GendreauDumas | n80w160.005.txt | 439 | O | 246 | 519 | 52.6 | - | 246 | 439 | 43.96 | - |
| GendreauDumas | n80w180.002.txt | 479 | O | 239 | 532 | 55.08 | - | 239 | 479 | 50.1 | - |
| GendreauDumas | n80w180.003.txt | 524 | O | 368 | 575 | 36 | - | 368 | 524 | 29.77 | - |
| GendreauDumas | n80w180.004.txt | 479 | O | 277 | 504 | 45.04 | - | 277 | 479 | 42.17 | - |
| GendreauDumas | n80w180.005.txt | 470 | O | 263 | 486 | 45.88 | - | 264 | 470 | 43.83 | - |
| Langevin | N20ft301.dat | 661.6 | O | 661.6 | 661.6 | 0 | 0.06 | 661.6 | 661.6 | 0 | 0.18 |
| Langevin | N20ft302.dat | 684.2 | O | 684.2 | 684.2 | 0 | 0.06 | 684.2 | 684.2 | 0 | 0.18 |
| Langevin | N20ft303.dat | 746.4 | O | 746.4 | 746.4 | 0 | 0.06 | 746.4 | 746.4 | 0 | 0.18 |
| Langevin | N20ft304.dat | 817 | O | 817 | 817 | 0 | 0.06 | 817 | 817 | 0 | 0.18 |
| Langevin | N20ft305.dat | 716.5 | O | 716.5 | 716.5 | 0 | 0.06 | 716.5 | 716.5 | 0 | 0.20 |
| Langevin | N20ft306.dat | 727.8 | O | 727.8 | 727.8 | 0 | 0.06 | 727.8 | 727.8 | 0 | 0.18 |
| Langevin | N20ft307.dat | 691.8 | O | 691.8 | 691.8 | 0 | 0.08 | 691.8 | 691.8 | 0 | 0.20 |
| Langevin | N20ft308.dat | 788.2 | O | 788.2 | 788.2 | 0 | 0.06 | 788.2 | 788.2 | 0 | 0.20 |
| Langevin | N20ft309.dat | 730.7 | O | 730.7 | 730.7 | 0 | 0.06 | 730.7 | 730.7 | 0 | 0.18 |
| Langevin | N20ft310.dat | 683 | O | 683 | 683 | 0 | 0.06 | 683 | 683 | 0 | 0.18 |
| Langevin | N20ft401.dat | 660.8 | O | 660.8 | 660.8 | 0 | 0.06 | 660.8 | 660.8 | 0 | 0.20 |
| Langevin | N20ft402.dat | 684.2 | O | 684.2 | 684.2 | 0 | 0.07 | 684.2 | 684.2 | 0 | 0.20 |
| Langevin | N20ft403.dat | 746.4 | O | 746.4 | 746.4 | 0 | 0.07 | 746.4 | 746.4 | 0 | 0.18 |
| Langevin | N20ft404.dat | 817 | O | 817 | 817 | 0 | 0.07 | 817 | 817 | 0 | 0.18 |
| Langevin | N20ft405.dat | 716.5 | O | 716.5 | 716.5 | 0 | 0.07 | 716.5 | 716.5 | 0 | 0.20 |
| Langevin | N20ft406.dat | 727.8 | O | 727.8 | 727.8 | 0 | 0.06 | 727.8 | 727.8 | 0 | 0.19 |
| Langevin | N20ft407.dat | 691.8 | O | 691.8 | 691.8 | 0 | 0.08 | 691.8 | 691.8 | 0 | 0.19 |
| Langevin | N20ft408.dat | 757.3 | O | 757.3 | 757.3 | 0 | 0.09 | 757.3 | 757.3 | 0 | 0.19 |
| Langevin | N20ft409.dat | 730.7 | O | 730.7 | 730.7 | 0 | 0.07 | 730.7 | 730.7 | 0 | 0.18 |
| Langevin | N20ft410.dat | 683 | O | 683 | 683 | 0 | 0.07 | 683 | 683 | 0 | 0.19 |
| Langevin | N40ft201.dat | 1100.6 | O | 1100.6 | 1100.6 | 0 | 0.07 | 1100.6 | 1100.6 | 0 | 0.31 |
| Langevin | N40ft202.dat | 1010.4 | O | 1010.4 | 1010.4 | 0 | 0.08 | 1010.4 | 1010.4 | 0 | 0.24 |
| Langevin | N40ft203.dat | 876.8 | O | 876.8 | 876.8 | 0 | 0.07 | 876.8 | 876.8 | 0 | 0.24 |
| Langevin | N40ft204.dat | 885.8 | O | 885.8 | 885.8 | 0 | 0.07 | 885.8 | 885.8 | 0 | 0.27 |
| Langevin | N40ft205.dat | 940.9 | O | 940.9 | 940.9 | 0 | 0.08 | 940.9 | 940.9 | 0 | 0.28 |
| Langevin | N40ft206.dat | 1054.2 | O | 1054.2 | 1054.2 | 0 | 0.07 | 1054.2 | 1054.2 | 0 | 0.27 |
| Langevin | N40ft207.dat | 867.5 | O | 867.5 | 867.5 | 0 | 0.09 | 867.5 | 867.5 | 0 | 0.27 |

Table A.9 **(Part 4 of 6)** TSP-TW Results of PnB at $\omega = 2048$ on Closed Problems: Seeded and Unseeded

LB = Lower Bound, UB = Upper Bound, OG = Optimality Gap, O = Optimality Proved.

| Problem Information | | | Baldacci et. al. (2012) | Single Thread: 2048 | | | | Seeded Single Thread: 2048 | | | |
|---|---|---|---|---|---|---|---|---|---|---|---|
| Set | Name | Best Known Solution | LB | LB | UB | OG | Time | LB | UB | OG | Time |
| Langevin | N40ft208.dat | 1050.7 | O | 1050.7 | 1050.7 | 0 | 0.08 | 1050.7 | 1050.7 | 0 | 0.24 |
| Langevin | N40ft209.dat | 1013.9 | O | 1013.9 | 1013.9 | 0 | 0.07 | 1013.9 | 1013.9 | 0 | 0.29 |
| Langevin | N40ft210.dat | 1026.3 | O | 1026.3 | 1026.3 | 0 | 0.08 | 1026.3 | 1026.3 | 0 | 0.28 |
| Langevin | N40ft401.dat | 1085 | O | 1085 | 1085 | 0 | 0.11 | 1085 | 1085 | 0 | 0.79 |
| Langevin | N40ft402.dat | 995.6 | O | 995.6 | 995.6 | 0 | 0.07 | 995.6 | 995.6 | 0 | 0.34 |
| Langevin | N40ft403.dat | 845.8 | O | 845.8 | 845.8 | 0 | 2.03 | 845.8 | 845.8 | 0 | 0.41 |
| Langevin | N40ft404.dat | 868 | O | 868 | 868 | 0 | 0.22 | 868 | 868 | 0 | 0.32 |
| Langevin | N40ft405.dat | 936.5 | O | 936.5 | 936.5 | 0 | 1.50 | 936.5 | 936.5 | 0 | 0.38 |
| Langevin | N40ft406.dat | 969.1 | O | 969.1 | 969.1 | 0 | 0.86 | 969.1 | 969.1 | 0 | 0.32 |
| Langevin | N40ft407.dat | 831.2 | O | 831.2 | 831.2 | 0 | 0.54 | 831.2 | 831.2 | 0 | 1.57 |
| Langevin | N40ft408.dat | 1002.7 | O | 1002.7 | 1002.7 | 0 | 0.32 | 1002.7 | 1002.7 | 0 | 0.36 |
| Langevin | N40ft409.dat | 1000.5 | O | 1000.5 | 1000.5 | 0 | 0.10 | 1000.5 | 1000.5 | 0 | 0.32 |
| Langevin | N40ft410.dat | 983.8 | O | 983.8 | 983.8 | 0 | 0.08 | 983.8 | 983.8 | 0 | 0.29 |
| Langevin | N60ft201.dat | 1353.5 | O | 1353.5 | 1353.5 | 0 | 0.11 | 1353.5 | 1353.5 | 0 | 0.48 |
| Langevin | N60ft202.dat | 1161.6 | O | 1161.6 | 1161.6 | 0 | 0.08 | 1161.6 | 1161.6 | 0 | 1.13 |
| Langevin | N60ft203.dat | 1182.9 | O | 1182.9 | 1182.9 | 0 | 0.10 | 1182.9 | 1182.9 | 0 | 0.49 |
| Langevin | N60ft204.dat | 1257.5 | O | 1257.5 | 1257.5 | 0 | 0.08 | 1257.5 | 1257.5 | 0 | 0.52 |
| Langevin | N60ft205.dat | 1184.1 | O | 1184.1 | 1184.1 | 0 | 0.07 | 1184.1 | 1184.1 | 0 | 0.50 |
| Langevin | N60ft206.dat | 1199.6 | O | 1199.6 | 1199.6 | 0 | 0.34 | 1199.6 | 1199.6 | 0 | 0.54 |
| Langevin | N60ft207.dat | 1299 | O | 1299 | 1299 | 0 | 0.07 | 1299 | 1299 | 0 | 0.43 |
| Langevin | N60ft208.dat | 1113 | O | 1113 | 1113 | 0 | 1.19 | 1113 | 1113 | 0 | 0.54 |
| Langevin | N60ft209.dat | 1171.3 | O | 1171.3 | 1171.3 | 0 | 0.18 | 1171.3 | 1171.3 | 0 | 0.56 |
| Langevin | N60ft210.dat | 1234.3 | O | 1234.3 | 1234.3 | 0 | 2.35 | 1234.3 | 1234.3 | 0 | 0.62 |
| Langevin | N60ft301.dat | 1337 | O | 1337 | 1337 | 0 | 0.67 | 1337 | 1337 | 0 | 1.46 |
| Langevin | N60ft302.dat | 1089.5 | O | 1089.5 | 1089.5 | 0 | 4.40 | 1089.5 | 1089.5 | 0 | 1.03 |
| Langevin | N60ft303.dat | 1179 | O | 1179 | 1179 | 0 | 0.20 | 1179 | 1179 | 0 | 0.59 |
| Langevin | N60ft304.dat | 1230 | O | 1230 | 1230 | 0 | 6.64 | 1230 | 1230 | 0 | 3.07 |
| Langevin | N60ft305.dat | 1151.6 | O | 1151.6 | 1151.6 | 0 | 2.32 | 1151.6 | 1151.6 | 0 | 0.73 |
| Langevin | N60ft306.dat | 1167.9 | O | 1167.9 | 1167.9 | 0 | 4.87 | 1167.9 | 1167.9 | 0 | 0.76 |
| Langevin | N60ft307.dat | 1220.1 | O | 1220.1 | 1220.1 | 0 | 0.28 | 1220.1 | 1220.1 | 0 | 1.24 |
| Langevin | N60ft308.dat | 1097.6 | O | 1097.6 | 1097.6 | 0 | 4.88 | 1097.6 | 1097.6 | 0 | 0.72 |
| Langevin | N60ft309.dat | 1140.6 | O | 1140.6 | 1140.6 | 0 | 3.22 | 1140.6 | 1140.6 | 0 | 0.74 |
| Langevin | N60ft310.dat | 1219.2 | O | 1219.2 | 1219.2 | 0 | 12.93 | 1219.2 | 1219.2 | 0 | 5.55 |
| Langevin | N60ft401.dat | 1335 | O | 1335 | 1335 | 0 | 10.41 | 1335 | 1335 | 0 | 3.18 |
| Langevin | N60ft402.dat | 1088.1 | O | 1088.1 | 1088.1 | 0 | 9.70 | 1088.1 | 1088.1 | 0 | 3.29 |
| Langevin | N60ft403.dat | 1173.7 | O | 1173.7 | 1173.7 | 0 | 4.23 | 1173.7 | 1173.7 | 0 | 1.71 |
| Langevin | N60ft404.dat | 1184.7 | O | 1184.7 | 1184.7 | 0 | 4.59 | 1184.7 | 1184.7 | 0 | 0.80 |
| Langevin | N60ft405.dat | 1146.2 | O | 1146.2 | 1146.2 | 0 | 3.30 | 1146.2 | 1146.2 | 0 | 0.90 |
| Langevin | N60ft406.dat | 1140.2 | O | 1140.2 | 1140.2 | 0 | 17.09 | 1140.2 | 1140.2 | 0 | 7.23 |
| Langevin | N60ft407.dat | 1198.9 | O | 1198.9 | 1198.9 | 0 | 9.75 | 1198.9 | 1198.9 | 0 | 3.11 |
| Langevin | N60ft408.dat | 1029.4 | O | 1029.4 | 1029.4 | 0 | 7.47 | 1029.4 | 1029.4 | 0 | 1.23 |
| Langevin | N60ft409.dat | 1121.4 | O | 1121.4 | 1121.4 | 0 | 8.25 | 1121.4 | 1121.4 | 0 | 1.07 |
| Langevin | N60ft410.dat | 1189.6 | O | 1189.6 | 1189.6 | 0 | 19.56 | 1189.6 | 1189.6 | 0 | 7.72 |
| OhlmannThomas | n150w120.001.txt | 734 | 725.5 | 324 | 809 | 59.95 | - | 324 | 734 | 55.86 | - |
| OhlmannThomas | n150w120.002.txt | 677 | 668.4 | 209 | 717 | 70.85 | - | 209 | 677 | 69.13 | - |
| OhlmannThomas | n150w120.003.txt | 747 | 746.4 | 416 | 807 | 48.45 | - | 416 | 747 | 44.31 | - |
| OhlmannThomas | n150w120.004.txt | 763 | 761.6 | 381 | 835 | 54.37 | - | 381 | 763 | 50.07 | - |
| OhlmannThomas | n150w120.005.txt | 689 | 684.7 | 266 | 754 | 64.72 | - | 274 | 689 | 60.23 | - |
| OhlmannThomas | n150w140.001.txt | 762 | 754 | 394 | 893 | 55.88 | - | 394 | 762 | 48.29 | - |
| OhlmannThomas | n150w140.002.txt | 755 | 752 | 407 | 855 | 52.4 | - | 416 | 755 | 44.9 | - |
| OhlmannThomas | n150w140.003.txt | 613 | 608.5 | 215 | 738 | 70.87 | - | 215 | 613 | 64.93 | - |
| OhlmannThomas | n150w140.004.txt | 676 | O | 391 | 834 | 53.12 | - | 391 | 676 | 42.16 | - |
| OhlmannThomas | n150w140.005.txt | 663 | 662 | 197 | 750 | 73.73 | - | 197 | 663 | 70.29 | - |
| OhlmannThomas | n150w160.001.txt | 706 | 701.4 | 293 | 777 | 62.29 | - | 293 | 706 | 58.5 | - |
| OhlmannThomas | n150w160.002.txt | 711 | 709.7 | 286 | 826 | 65.38 | - | 286 | 711 | 59.77 | - |
| OhlmannThomas | n150w160.003.txt | 608 | 603.2 | 170 | 772 | 77.98 | - | 170 | 608 | 72.04 | - |
| OhlmannThomas | n150w160.004.txt | 672 | 672 | 336 | 749 | 55.14 | - | 344 | 672 | 48.81 | - |
| OhlmannThomas | n150w160.005.txt | 658 | 655 | 320 | 736 | 56.52 | - | 320 | 658 | 51.37 | - |
| OhlmannThomas | n200w120.001.txt | 799 | 793.3 | 312 | 910 | 65.71 | - | 312 | 799 | 60.95 | - |
| OhlmannThomas | n200w120.002.txt | 721 | 713.9 | 184 | 822 | 77.62 | - | 184 | 721 | 74.48 | - |
| OhlmannThomas | n200w120.003.txt | 880 | 868.6 | 336 | 983 | 65.82 | - | 336 | 880 | 61.82 | - |
| OhlmannThomas | n200w120.004.txt | 777 | 775.8 | 291 | 887 | 67.19 | - | 291 | 777 | 62.55 | - |
| OhlmannThomas | n200w120.005.txt | 841 | 833.2 | 258 | 960 | 73.12 | - | 371 | 841 | 55.89 | - |
| OhlmannThomas | n200w140.001.txt | 834 | 826.2 | 177 | 1053 | 83.19 | - | 177 | 834 | 78.78 | - |
| OhlmannThomas | n200w140.002.txt | 760 | 756.2 | 180 | 895 | 79.89 | - | 180 | 760 | 76.32 | - |
| OhlmannThomas | n200w140.003.txt | 758 | 756 | 241 | 897 | 73.13 | - | 252 | 758 | 66.75 | - |
| OhlmannThomas | n200w140.004.txt | 816 | 807.1 | 284 | 932 | 69.53 | - | 284 | 816 | 65.2 | - |
| OhlmannThomas | n200w140.005.txt | 822 | 819.6 | 148 | 927 | 84.03 | - | 148 | 822 | 82 | - |

Table A.10 **(Part 5 of 6)** TSP-TW Results of PnB at $\omega = 2048$ on Closed Problems: Seeded and Unseeded

LB = Lower Bound, UB = Upper Bound, OG = Optimality Gap, O = Optimality Proved.

| Problem Information | | | Baldacci et. al. (2012) | Single Thread: 2048 | | | | Seeded Single Thread: 2048 | | | |
|---|---|---|---|---|---|---|---|---|---|---|---|
| Set | Name | Best Known Solution | LB | LB | UB | OG | Time | LB | UB | OG | Time |
| SolomonPesant | rc201.0 | 628.62 | O | 628.62 | 628.62 | 0 | 3.36 | 628.62 | 628.62 | 0 | 2.13 |
| SolomonPesant | rc201.1 | 654.7 | O | 654.70 | 654.70 | 0 | 3.97 | 654.70 | 654.70 | 0 | 2.56 |
| SolomonPesant | rc201.2 | 707.65 | O | 707.65 | 707.65 | 0 | 3.34 | 707.65 | 707.65 | 0 | 1.63 |
| SolomonPesant | rc201.3 | 422.54 | O | 422.54 | 422.54 | 0 | 0.52 | 422.54 | 422.54 | 0 | 0.73 |
| SolomonPesant | rc202.0 | 496.22 | O | 496.22 | 496.22 | 0 | 19.91 | 496.22 | 496.22 | 0 | 12.48 |
| SolomonPesant | rc202.1 | 426.53 | O | 426.53 | 426.53 | 0 | 14.76 | 426.53 | 426.53 | 0 | 10.34 |
| SolomonPesant | rc202.2 | 611.77 | O | 611.77 | 611.77 | 0 | 19.53 | 611.77 | 611.77 | 0 | 9.32 |
| SolomonPesant | rc202.3 | 627.85 | O | 627.85 | 627.85 | 0 | 27.07 | 627.85 | 627.85 | 0 | 13.18 |
| SolomonPesant | rc203.2 | 617.46 | O | 617.46 | 617.46 | 0 | 42.21 | 617.46 | 617.46 | 0 | 20.88 |
| SolomonPesant | rc204.0 | 541.45 | O | 495.85 | 551.56 | 10.1 | - | 541.45 | 541.45 | 0 | 1560.34 |
| SolomonPesant | rc204.1 | 485.37 | O | 485.37 | 485.37 | 0 | 184.27 | 485.37 | 485.37 | 0 | 101.42 |
| SolomonPesant | rc205.0 | 511.65 | O | 511.65 | 511.65 | 0 | 17.52 | 511.65 | 511.65 | 0 | 9.86 |
| SolomonPesant | rc205.1 | 491.22 | O | 491.22 | 491.22 | 0 | 13.18 | 491.22 | 491.22 | 0 | 9.71 |
| SolomonPesant | rc205.2 | 714.69 | O | 714.69 | 714.69 | 0 | 17.80 | 714.69 | 714.69 | 0 | 11.57 |
| SolomonPesant | rc205.3 | 601.24 | O | 601.24 | 601.24 | 0 | 10.30 | 601.24 | 601.24 | 0 | 10.06 |
| SolomonPesant | rc206.0 | 835.23 | O | 835.23 | 835.23 | 0 | 49.27 | 835.23 | 835.23 | 0 | 30.81 |
| SolomonPesant | rc206.1 | 664.73 | O | 664.73 | 664.73 | 0 | 54.26 | 664.73 | 664.73 | 0 | 25.98 |
| SolomonPesant | rc206.2 | 655.37 | O | 655.37 | 655.37 | 0 | 89.91 | 655.37 | 655.37 | 0 | 29.53 |
| SolomonPesant | rc207.0 | 806.69 | O | 806.69 | 806.69 | 0 | 116.56 | 806.69 | 806.69 | 0 | 62.17 |
| SolomonPesant | rc207.1 | 726.36 | O | 726.36 | 726.36 | 0 | 93.50 | 726.36 | 726.36 | 0 | 61.84 |
| SolomonPesant | rc207.2 | 546.41 | O | 546.41 | 546.41 | 0 | 159.83 | 546.41 | 546.41 | 0 | 33.82 |
| SolomonPesant | rc208.0 | 820.56 | O | 728.35 | 837.66 | 13.05 | - | 757.44 | 820.56 | 7.69 | - |
| SolomonPesant | rc208.1 | 509.04 | O | 509.04 | 509.04 | 0 | 309.35 | 509.04 | 509.04 | 0 | 50.02 |
| SolomonPesant | rc208.2 | 503.92 | O | 503.92 | 503.92 | 0 | 280.49 | 503.92 | 503.92 | 0 | 19.23 |
| SolomonPotvinBengio | rc_201.1.txt | 444.54 | O | 444.54 | 444.54 | 0 | 0.74 | 444.54 | 444.54 | 0 | 1.31 |
| SolomonPotvinBengio | rc_201.2.txt | 711.54 | O | 711.54 | 711.54 | 0 | 0.63 | 711.54 | 711.54 | 0 | 1.07 |
| SolomonPotvinBengio | rc_201.3.txt | 790.61 | O | 790.61 | 790.61 | 0 | 7.28 | 790.61 | 790.61 | 0 | 3.12 |
| SolomonPotvinBengio | rc_201.4.txt | 793.64 | O | 793.64 | 793.64 | 0 | 0.27 | 793.64 | 793.64 | 0 | 0.27 |
| SolomonPotvinBengio | rc_202.1.txt | 771.78 | O | 771.78 | 771.78 | 0 | 577.89 | 771.78 | 771.78 | 0 | 556.81 |
| SolomonPotvinBengio | rc_202.2.txt | 304.14 | O | 304.14 | 304.14 | 0 | 1.57 | 304.14 | 304.14 | 0 | 0.61 |
| SolomonPotvinBengio | rc_203.1.txt | 453.48 | O | 453.48 | 453.48 | 0 | 10.84 | 453.48 | 453.48 | 0 | 6.52 |
| SolomonPotvinBengio | rc_203.4.txt | 314.29 | O | 314.29 | 314.29 | 0 | 9.24 | 314.29 | 314.29 | 0 | 1.69 |
| SolomonPotvinBengio | rc_204.3.txt | 455.03 | O | 455.03 | 455.03 | 0 | 682.03 | 455.03 | 455.03 | 0 | 139.37 |
| SolomonPotvinBengio | rc_205.1.txt | 343.21 | O | 343.21 | 343.21 | 0 | 0.35 | 343.21 | 343.21 | 0 | 0.32 |
| SolomonPotvinBengio | rc_205.2.txt | 755.93 | O | 755.93 | 755.93 | 0 | 9.24 | 755.93 | 755.93 | 0 | 8.16 |
| SolomonPotvinBengio | rc_205.3.txt | 825.06 | O | 825.06 | 825.06 | 0 | 59.00 | 825.06 | 825.06 | 0 | 36.06 |
| SolomonPotvinBengio | rc_206.1.txt | 117.85 | O | 117.85 | 117.85 | 0 | 0.06 | 117.85 | 117.85 | 0 | 0.20 |
| SolomonPotvinBengio | rc_206.3.txt | 574.42 | O | 574.42 | 574.42 | 0 | 21.92 | 574.42 | 574.42 | 0 | 12.96 |
| SolomonPotvinBengio | rc_207.4.txt | 119.64 | O | 119.64 | 119.64 | 0 | 0.06 | 119.64 | 119.64 | 0 | 0.20 |
| SolomonPotvinBengio | rc_208.2.txt | 533.78 | O | 533.78 | 533.78 | 0 | 835.29 | 533.78 | 533.78 | 0 | 37.47 |

Table A.11 **(Part 6 of 6)** TSP-TW Results of PnB at $\omega = 2048$ on Closed Problems: Seeded and Unseeded

LB = Lower Bound, UB = Upper Bound, OG = Optimality Gap, O = Optimality Proved.

| Problem Information | | | Single Thread: 2048 | | | Seeded Single Thread: 2048 | | |
|---|---|---|---|---|---|---|---|---|
| Set | Name | Best Known Solution | LB | UB | Time | LB | UB | Time |
| AFG | rbg010a.tw | 3840 | 3840 | 3840 | 0.10 | 3840 | 3840 | 0.27 |
| AFG | rbg016a.tw | 2596 | 2596 | 2596 | 0.59 | 2596 | 2596 | 0.23 |
| AFG | rbg016b.tw | 2094 | 2094 | 2094 | 1.79 | 2094 | 2094 | 0.74 |
| AFG | rbg017.2.tw | 2351 | 2351 | 2351 | 4.68 | 2351 | 2351 | 2.93 |
| AFG | rbg017.tw | 2351 | 2351 | 2351 | 1.55 | 2351 | 2351 | 0.97 |
| AFG | rbg017a.tw | 4296 | 4296 | 4296 | 0.29 | 4296 | 4296 | 0.25 |
| AFG | rbg019a.tw | 2694 | 2694 | 2694 | 0.55 | 2694 | 2694 | 0.20 |
| AFG | rbg019b.tw | 3840 | 3840 | 3840 | 5.79 | 3840 | 3840 | 4.11 |
| AFG | rbg019c.tw | 4536 | 4536 | 4536 | 2.56 | 4536 | 4536 | 2.72 |
| AFG | rbg019d.tw | 3479 | 3479 | 3479 | 1.71 | 3479 | 3479 | 0.25 |
| AFG | rbg020a.tw | 4689 | 4689 | 4689 | 0.28 | 4689 | 4689 | 0.24 |
| AFG | rbg021.2.tw | 4528 | 4528 | 4528 | 9.20 | 4528 | 4528 | 4.82 |
| AFG | rbg021.3.tw | 4528 | 4528 | 4528 | 14.33 | 4528 | 4528 | 6.57 |
| AFG | rbg021.4.tw | 4525 | 4525 | 4525 | 19.95 | 4525 | 4525 | 6.64 |
| AFG | rbg021.5.tw | 4516 | 4516 | 4516 | 18.36 | 4516 | 4516 | 6.19 |
| AFG | rbg021.6.tw | 4492 | 4492 | 4492 | 116.12 | 4492 | 4492 | 15.35 |
| AFG | rbg021.7.tw | 4481 | 4481 | 4481 | 330.28 | 4481 | 4481 | 89.87 |
| AFG | rbg021.8.tw | 4481 | 4481 | 4481 | 397.88 | 4481 | 4481 | 136.81 |
| AFG | rbg021.9.tw | 4481 | 4481 | 4481 | 387.29 | 4481 | 4481 | 104.94 |
| AFG | rbg021.tw | 4536 | 4536 | 4536 | 2.56 | 4536 | 4536 | 2.91 |
| AFG | rbg027a.tw | 5093 | 5093 | 5093 | 9.35 | 5093 | 5093 | 8.87 |
| AFG | rbg031a.tw | 3498 | 3498 | 3498 | 12.87 | 3498 | 3498 | 5.94 |
| AFG | rbg033a.tw | 3757 | 3757 | 3757 | 26.84 | 3757 | 3757 | 11.43 |
| AFG | rbg034a.tw | 3314 | 3314 | 3314 | 18.78 | 3314 | 3314 | 10.52 |
| AFG | rbg035a.2.tw | 3325 | 3325 | 3325 | 31.96 | 3325 | 3325 | 18.98 |
| AFG | rbg035a.tw | 3388 | 3388 | 3388 | 17.85 | 3388 | 3388 | 9.03 |
| AFG | rbg038a.tw | 5699 | 5699 | 5699 | 22.98 | 5699 | 5699 | 9.84 |
| AFG | rbg040a.tw | 5679 | 5679 | 5679 | 20.86 | 5679 | 5679 | 10.07 |
| AFG | rbg041a.tw | 3793 | 3793 | 3793 | 23.72 | 3793 | 3793 | 11.82 |
| AFG | rbg042a.tw | 3260 | 3260 | 3260 | 133.16 | 3260 | 3260 | 55.62 |
| AFG | rbg048a.tw | 9799 | 9799 | 9799 | 47.50 | 9799 | 9799 | 32.45 |
| AFG | rbg049a.tw | 13257 | 13257 | 13257 | 43.08 | 13257 | 13257 | 24.53 |
| AFG | rbg050a.tw | 12050 | 12050 | 12050 | 76.87 | 12050 | 12050 | 42.58 |
| AFG | rbg050c.tw | 10985 | 10985 | 10985 | 608.13 | 10985 | 10985 | 41.37 |
| AFG | rbg055a.tw | 6929 | 6929 | 6929 | 37.86 | 6929 | 6929 | 19.52 |
| AFG | rbg067a.tw | 10331 | 10331 | 10331 | 50.47 | 10331 | 10331 | 26.74 |
| AFG | rbg086a.tw | 16899 | 16899 | 16899 | 55.93 | 16899 | 16899 | 23.52 |
| AFG | rbg092a.tw | 12501 | 12501 | 12501 | 105.84 | 12501 | 12501 | 57.06 |
| AFG | rbg125a.tw | 14214 | 14214 | 14214 | 240.51 | 14214 | 14214 | 159.05 |
| AFG | rbg132.2.tw | 18524 | 18524 | 18524 | 383.13 | 18524 | 18524 | 256.79 |
| AFG | rbg132.tw | 18524 | 18524 | 18524 | 166.49 | 18524 | 18524 | 109.79 |
| AFG | rbg152.3.tw | 17455 | 17455 | 17455 | 708.13 | 17455 | 17455 | 449.59 |
| AFG | rbg152.tw | 17455 | 17455 | 17455 | 293.16 | 17455 | 17455 | 214.97 |
| AFG | rbg193.2.tw | 21401 | 21401 | 21401 | 1072.79 | 21401 | 21401 | 890.64 |
| AFG | rbg193.tw | 21401 | 21401 | 21401 | 408.75 | 21401 | 21401 | 397.71 |
| AFG | rbg201a.tw | 21380 | 21380 | 21380 | 690.22 | 21380 | 21380 | 516.17 |
| AFG | rbg233.2.tw | 26143 | 26143 | 26143 | 1386.83 | 26143 | 26143 | 880.14 |
| AFG | rbg233.tw | 26143 | 26143 | 26143 | 310.61 | 26143 | 26143 | 543.33 |
| Dumas | n100w20.001.txt | 827 | 827 | 827 | 22.60 | 827 | 827 | 4.66 |
| Dumas | n100w20.002.txt | 801 | 801 | 801 | 27.68 | 801 | 801 | 20.23 |
| Dumas | n100w20.003.txt | 834 | 834 | 834 | 29.63 | 834 | 834 | 29.75 |
| Dumas | n100w20.004.txt | 828 | 828 | 828 | 40.49 | 828 | 828 | 19.34 |
| Dumas | n100w20.005.txt | 825 | 825 | 825 | 43.67 | 825 | 825 | 29.66 |
| Dumas | n100w40.001.txt | 841 | 841 | 841 | 81.21 | 841 | 841 | 49.35 |
| Dumas | n100w40.002.txt | 786 | 786 | 786 | 233.56 | 786 | 786 | 179.21 |
| Dumas | n100w40.003.txt | 835 | 835 | 835 | 164.55 | 835 | 835 | 162.40 |
| Dumas | n100w40.004.txt | 809 | 809 | 809 | 110.67 | 809 | 809 | 48.29 |
| Dumas | n100w40.005.txt | 834 | 834 | 834 | 242.46 | 834 | 834 | 117.29 |
| Dumas | n100w60.001.txt | 824 | 824 | 824 | 128.02 | 824 | 824 | 162.88 |
| Dumas | n100w60.002.txt | 782 | 782 | 782 | 148.01 | 782 | 782 | 104.97 |
| Dumas | n100w60.003.txt | 856 | 856 | 856 | 393.23 | 856 | 856 | 124.66 |
| Dumas | n100w60.004.txt | 834 | 834 | 834 | 86.16 | 834 | 834 | 95.44 |
| Dumas | n100w60.005.txt | 790 | 790 | 790 | 330.56 | 790 | 790 | 87.49 |
| Dumas | n150w20.001.txt | 1034 | 1034 | 1034 | 95.90 | 1034 | 1034 | 82.38 |
| Dumas | n150w20.002.txt | 967 | 967 | 967 | 95.51 | 967 | 967 | 58.82 |
| Dumas | n150w20.003.txt | 959 | 959 | 959 | 184.01 | 959 | 959 | 101.22 |
| Dumas | n150w20.004.txt | 975 | 975 | 975 | 113.70 | 975 | 975 | 83.60 |
| Dumas | n150w20.005.txt | 957 | 957 | 957 | 172.32 | 957 | 957 | 174.31 |

Table A.12 **(Part 1 of 7)** Makespan Results of PnB at $\omega = 2048$ on Closed Problems: Seeded and Unseeded

LB = Lower Bound, UB = Upper Bound.

| Problem Information | | | Single Thread: 2048 | | | Seeded Single Thread: 2048 | | |
|---|---|---|---|---|---|---|---|---|
| Set | Name | Best Known Solution | LB | UB | Time | LB | UB | Time |
| Dumas | n150w40.001.txt | 1058 | 1058 | 1058 | 1189.38 | 1058 | 1058 | 183.42 |
| Dumas | n150w40.002.txt | 1072 | 1072 | 1072 | 302.80 | 1072 | 1072 | 227.35 |
| Dumas | n150w40.003.txt | 894 | 894 | 894 | 202.91 | 894 | 894 | 495.32 |
| Dumas | n150w40.004.txt | 948 | 948 | 948 | 261.44 | 948 | 948 | 162.54 |
| Dumas | n150w40.005.txt | 980 | 980 | 980 | 3533.27 | 980 | 980 | 194.03 |
| Dumas | n150w60.001.txt | 1024 | 1024 | 1024 | 1306.06 | 1024 | 1024 | 1361.14 |
| Dumas | n150w60.003.txt | 984 | 984 | 984 | 1541.55 | 984 | 984 | 493.46 |
| Dumas | n150w60.004.txt | 998 | 998 | 998 | 604.28 | 998 | 998 | 316.13 |
| Dumas | n150w60.005.txt | 997 | 997 | 997 | 537.80 | 997 | 997 | 506.47 |
| Dumas | n200w20.001.txt | 1139 | 1139 | 1139 | 236.02 | 1139 | 1139 | 591.72 |
| Dumas | n200w20.002.txt | 1124 | 1124 | 1124 | 477.22 | 1124 | 1124 | 178.85 |
| Dumas | n200w20.003.txt | 1178 | 1178 | 1178 | 382.11 | 1178 | 1178 | 252.84 |
| Dumas | n200w20.004.txt | 1125 | 1125 | 1125 | 889.15 | 1125 | 1125 | 815.18 |
| Dumas | n200w20.005.txt | 1123 | 1123 | 1123 | 569.79 | 1123 | 1123 | 403.14 |
| Dumas | n200w40.001.txt | 1188 | 1188 | 1188 | 272.29 | 1188 | 1188 | 561.61 |
| Dumas | n200w40.003.txt | 1134 | 1134 | 1134 | 383.87 | 1134 | 1134 | 1001.46 |
| Dumas | n200w40.004.txt | 1150 | 1150 | 1150 | 1004.33 | 1150 | 1150 | 854.40 |
| Dumas | n200w40.005.txt | 1171 | 1171 | 1171 | 494.15 | 1171 | 1171 | 675.02 |
| Dumas | n20w100.001.txt | 309 | 309 | 309 | 4.80 | 309 | 309 | 2.83 |
| Dumas | n20w100.002.txt | 285 | 285 | 285 | 7.64 | 285 | 285 | 3.10 |
| Dumas | n20w100.003.txt | 358 | 358 | 358 | 9.12 | 358 | 358 | 4.41 |
| Dumas | n20w100.004.txt | 379 | 379 | 379 | 2.14 | 379 | 379 | 1.05 |
| Dumas | n20w100.005.txt | 327 | 327 | 327 | 5.79 | 327 | 327 | 2.96 |
| Dumas | n20w20.001.txt | 387 | 387 | 387 | 0.08 | 387 | 387 | 0.19 |
| Dumas | n20w20.002.txt | 296 | 296 | 296 | 0.09 | 296 | 296 | 0.19 |
| Dumas | n20w20.003.txt | 403 | 403 | 403 | 0.11 | 403 | 403 | 0.19 |
| Dumas | n20w20.004.txt | 401 | 401 | 401 | 0.07 | 401 | 401 | 0.19 |
| Dumas | n20w20.005.txt | 365 | 365 | 365 | 0.07 | 365 | 365 | 0.19 |
| Dumas | n20w40.001.txt | 280 | 280 | 280 | 0.12 | 280 | 280 | 0.24 |
| Dumas | n20w40.002.txt | 357 | 357 | 357 | 0.07 | 357 | 357 | 0.19 |
| Dumas | n20w40.003.txt | 355 | 355 | 355 | 0.08 | 355 | 355 | 0.21 |
| Dumas | n20w40.004.txt | 397 | 397 | 397 | 0.10 | 397 | 397 | 0.21 |
| Dumas | n20w40.005.txt | 325 | 325 | 325 | 0.09 | 325 | 325 | 0.24 |
| Dumas | n20w60.001.txt | 400 | 400 | 400 | 2.10 | 400 | 400 | 1.03 |
| Dumas | n20w60.002.txt | 300 | 300 | 300 | 0.68 | 300 | 300 | 0.22 |
| Dumas | n20w60.003.txt | 381 | 381 | 381 | 0.08 | 381 | 381 | 0.23 |
| Dumas | n20w60.004.txt | 337 | 337 | 337 | 3.11 | 337 | 337 | 2.13 |
| Dumas | n20w60.005.txt | 392 | 392 | 392 | 0.59 | 392 | 392 | 0.24 |
| Dumas | n20w80.001.txt | 403 | 403 | 403 | 2.12 | 403 | 403 | 1.70 |
| Dumas | n20w80.002.txt | 397 | 397 | 397 | 1.24 | 397 | 397 | 0.88 |
| Dumas | n20w80.003.txt | 365 | 365 | 365 | 0.75 | 365 | 365 | 0.31 |
| Dumas | n20w80.004.txt | 345 | 345 | 345 | 1.84 | 345 | 345 | 1.00 |
| Dumas | n20w80.005.txt | 307 | 307 | 307 | 5.82 | 307 | 307 | 2.75 |
| Dumas | n40w100.001.txt | 471 | 471 | 471 | 78.64 | 471 | 471 | 65.33 |
| Dumas | n40w100.002.txt | 452 | 452 | 452 | 55.80 | 452 | 452 | 25.75 |
| Dumas | n40w100.003.txt | 458 | 458 | 458 | 44.81 | 458 | 458 | 29.04 |
| Dumas | n40w100.004.txt | 476 | 476 | 476 | 25.18 | 476 | 476 | 16.11 |
| Dumas | n40w100.005.txt | 458 | 458 | 458 | 26.47 | 458 | 458 | 13.81 |
| Dumas | n40w20.001.txt | 523 | 523 | 523 | 0.54 | 523 | 523 | 0.36 |
| Dumas | n40w20.002.txt | 607 | 607 | 607 | 2.21 | 607 | 607 | 0.56 |
| Dumas | n40w20.003.txt | 514 | 514 | 514 | 1.37 | 514 | 514 | 0.35 |
| Dumas | n40w20.004.txt | 442 | 442 | 442 | 1.04 | 442 | 442 | 0.30 |
| Dumas | n40w20.005.txt | 520 | 520 | 520 | 0.11 | 520 | 520 | 0.31 |
| Dumas | n40w40.001.txt | 510 | 510 | 510 | 2.45 | 510 | 510 | 0.52 |
| Dumas | n40w40.002.txt | 519 | 519 | 519 | 16.34 | 519 | 519 | 9.47 |
| Dumas | n40w40.003.txt | 536 | 536 | 536 | 4.86 | 536 | 536 | 1.98 |
| Dumas | n40w40.004.txt | 508 | 508 | 508 | 9.24 | 508 | 508 | 5.51 |
| Dumas | n40w40.005.txt | 488 | 488 | 488 | 17.23 | 488 | 488 | 6.18 |
| Dumas | n40w60.001.txt | 535 | 535 | 535 | 13.88 | 535 | 535 | 11.12 |
| Dumas | n40w60.002.txt | 509 | 509 | 509 | 13.42 | 509 | 509 | 10.98 |
| Dumas | n40w60.003.txt | 465 | 465 | 465 | 23.80 | 465 | 465 | 14.94 |
| Dumas | n40w60.004.txt | 475 | 475 | 475 | 20.68 | 475 | 475 | 12.92 |
| Dumas | n40w60.005.txt | 423 | 423 | 423 | 25.15 | 423 | 423 | 8.20 |
| Dumas | n40w80.001.txt | 497 | 497 | 497 | 31.58 | 497 | 497 | 20.59 |
| Dumas | n40w80.002.txt | 498 | 498 | 498 | 37.16 | 498 | 498 | 19.14 |
| Dumas | n40w80.003.txt | 488 | 488 | 488 | 24.64 | 488 | 488 | 8.43 |
| Dumas | n40w80.004.txt | 462 | 462 | 462 | 31.94 | 462 | 462 | 21.09 |
| Dumas | n40w80.005.txt | 488 | 488 | 488 | 50.14 | 488 | 488 | 25.29 |

Table A.13 **(Part 2 of 7)** Makespan Results of PnB at $\omega = 2048$ on Closed Problems: Seeded and Unseeded

LB = Lower Bound, UB = Upper Bound.

| Problem Information | | | Single Thread: 2048 | | | Seeded Single Thread: 2048 | | |
|---|---|---|---|---|---|---|---|---|
| Set | Name | Best Known Solution | LB | UB | Time | LB | UB | Time |
| Dumas | n60w100.001.txt | 576 | 576 | 576 | 47.90 | 576 | 576 | 41.17 |
| Dumas | n60w100.002.txt | 622 | 622 | 622 | 49.11 | 622 | 622 | 31.61 |
| Dumas | n60w100.003.txt | 610 | 610 | 610 | 51.91 | 610 | 610 | 28.48 |
| Dumas | n60w100.004.txt | 625 | 625 | 625 | 56.84 | 625 | 625 | 55.01 |
| Dumas | n60w100.005.txt | 668 | 668 | 668 | 85.20 | 668 | 668 | 42.20 |
| Dumas | n60w20.001.txt | 586 | 586 | 586 | 6.05 | 586 | 586 | 2.00 |
| Dumas | n60w20.002.txt | 656 | 656 | 656 | 4.56 | 656 | 656 | 1.72 |
| Dumas | n60w20.003.txt | 593 | 593 | 593 | 6.96 | 593 | 593 | 1.26 |
| Dumas | n60w20.004.txt | 670 | 670 | 670 | 7.91 | 670 | 670 | 1.76 |
| Dumas | n60w20.005.txt | 629 | 629 | 629 | 4.24 | 629 | 629 | 0.60 |
| Dumas | n60w40.001.txt | 664 | 664 | 664 | 22.66 | 664 | 664 | 14.66 |
| Dumas | n60w40.002.txt | 697 | 697 | 697 | 32.01 | 697 | 697 | 26.93 |
| Dumas | n60w40.003.txt | 675 | 675 | 675 | 29.48 | 675 | 675 | 19.28 |
| Dumas | n60w40.004.txt | 628 | 628 | 628 | 15.52 | 628 | 628 | 7.76 |
| Dumas | n60w40.005.txt | 608 | 608 | 608 | 27.57 | 608 | 608 | 12.15 |
| Dumas | n60w60.001.txt | 722 | 722 | 722 | 24.45 | 722 | 722 | 30.56 |
| Dumas | n60w60.002.txt | 715 | 715 | 715 | 36.76 | 715 | 715 | 23.87 |
| Dumas | n60w60.003.txt | 619 | 619 | 619 | 123.67 | 619 | 619 | 49.79 |
| Dumas | n60w60.004.txt | 639 | 639 | 639 | 101.05 | 639 | 639 | 97.53 |
| Dumas | n60w60.005.txt | 669 | 669 | 669 | 39.90 | 669 | 669 | 20.10 |
| Dumas | n60w80.001.txt | 606 | 606 | 606 | 70.71 | 606 | 606 | 48.23 |
| Dumas | n60w80.002.txt | 611 | 611 | 611 | 45.52 | 611 | 611 | 34.00 |
| Dumas | n60w80.003.txt | 656 | 656 | 656 | 116.60 | 656 | 656 | 33.02 |
| Dumas | n60w80.004.txt | 679 | 679 | 679 | 59.47 | 679 | 679 | 42.62 |
| Dumas | n60w80.005.txt | 589 | 589 | 589 | 86.38 | 589 | 589 | 44.11 |
| Dumas | n80w20.001.txt | 729 | 729 | 729 | 40.45 | 729 | 729 | 29.10 |
| Dumas | n80w20.002.txt | 798 | 798 | 798 | 23.83 | 798 | 798 | 13.71 |
| Dumas | n80w20.003.txt | 727 | 727 | 727 | 16.35 | 727 | 727 | 5.47 |
| Dumas | n80w20.004.txt | 694 | 694 | 694 | 29.54 | 694 | 694 | 13.28 |
| Dumas | n80w20.005.txt | 793 | 793 | 793 | 16.04 | 793 | 793 | 7.97 |
| Dumas | n80w40.001.txt | 743 | 743 | 743 | 76.57 | 743 | 743 | 64.60 |
| Dumas | n80w40.002.txt | 701 | 701 | 701 | 34.24 | 701 | 701 | 32.70 |
| Dumas | n80w40.003.txt | 731 | 731 | 731 | 49.56 | 731 | 731 | 59.81 |
| Dumas | n80w40.004.txt | 662 | 662 | 662 | 38.17 | 662 | 662 | 47.81 |
| Dumas | n80w40.005.txt | 791 | 791 | 791 | 69.94 | 791 | 791 | 28.40 |
| Dumas | n80w60.001.txt | 674 | 674 | 674 | 123.69 | 674 | 674 | 46.05 |
| Dumas | n80w60.002.txt | 733 | 733 | 733 | 141.75 | 733 | 733 | 88.40 |
| Dumas | n80w60.003.txt | 743 | 743 | 743 | 127.93 | 743 | 743 | 165.29 |
| Dumas | n80w60.004.txt | 718 | 718 | 718 | 98.69 | 718 | 718 | 64.72 |
| Dumas | n80w60.005.txt | 695 | 695 | 695 | 71.97 | 695 | 695 | 48.39 |
| Dumas | n80w80.001.txt | 728 | 728 | 728 | 85.54 | 728 | 728 | 61.20 |
| Dumas | n80w80.002.txt | 690 | 690 | 690 | 314.50 | 690 | 690 | 290.70 |
| Dumas | n80w80.003.txt | 730 | 730 | 730 | 110.76 | 730 | 730 | 68.74 |
| Dumas | n80w80.004.txt | 743 | 743 | 743 | 206.81 | 743 | 743 | 108.65 |
| Dumas | n80w80.005.txt | 682 | 682 | 682 | 166.66 | 682 | 682 | 127.21 |
| GendreauDumas | n100w100.001.txt | 787 | 787 | 787 | 182.66 | 787 | 787 | 211.74 |
| GendreauDumas | n100w100.002.txt | 780 | 780 | 780 | 123.94 | 780 | 780 | 80.68 |
| GendreauDumas | n100w100.004.txt | 844 | 844 | 844 | 159.35 | 844 | 844 | 138.09 |
| GendreauDumas | n100w100.005.txt | 749 | 749 | 749 | 429.20 | 749 | 749 | 235.80 |
| GendreauDumas | n100w120.001.txt | 882 | 882 | 882 | 304.59 | 882 | 882 | 251.81 |
| GendreauDumas | n100w120.002.txt | 893 | 893 | 893 | 214.04 | 893 | 893 | 133.62 |
| GendreauDumas | n100w120.003.txt | 909 | 909 | 909 | 193.51 | 909 | 909 | 115.35 |
| GendreauDumas | n100w120.004.txt | 923 | 923 | 923 | 262.32 | 923 | 923 | 189.78 |
| GendreauDumas | n100w120.005.txt | 870 | 870 | 870 | 342.28 | 870 | 870 | 294.69 |
| GendreauDumas | n100w140.001.txt | 1008 | 1008 | 1008 | 275.39 | 1008 | 1008 | 200.57 |
| GendreauDumas | n100w140.002.txt | 1021 | 1021 | 1021 | 249.58 | 1021 | 1021 | 158.90 |
| GendreauDumas | n100w140.003.txt | 844 | 844 | 844 | 245.12 | 844 | 844 | 177.10 |
| GendreauDumas | n100w140.004.txt | 854 | 854 | 854 | 264.06 | 854 | 854 | 157.21 |
| GendreauDumas | n100w140.005.txt | 805 | 805 | 805 | 477.20 | 805 | 805 | 177.25 |
| GendreauDumas | n100w160.001.txt | 868 | 868 | 868 | 1258.25 | 868 | 868 | 887.56 |
| GendreauDumas | n100w160.002.txt | 791 | 791 | 791 | 861.44 | 791 | 791 | 513.75 |
| GendreauDumas | n100w160.003.txt | 935 | 935 | 935 | 232.75 | 935 | 935 | 129.39 |
| GendreauDumas | n100w160.004.txt | 814 | 814 | 814 | 569.60 | 814 | 814 | 307.28 |
| GendreauDumas | n100w160.005.txt | 917 | 917 | 917 | 622.96 | 917 | 917 | 331.31 |
| GendreauDumas | n100w80.001.txt | 797 | 797 | 797 | 2557.77 | 797 | 797 | 167.87 |
| GendreauDumas | n100w80.002.txt | 790 | 790 | 790 | 83.34 | 790 | 790 | 74.09 |
| GendreauDumas | n100w80.004.txt | 854 | 854 | 854 | 119.96 | 854 | 854 | 131.93 |
| GendreauDumas | n100w80.005.txt | 759 | 759 | 759 | 262.46 | 759 | 759 | 252.80 |

Table A.14 **(Part 3 of 7)** Makespan Results of PnB at $\omega = 2048$ on Closed Problems: Seeded and Unseeded

LB = Lower Bound, UB = Upper Bound.

| Problem Information | | | Single Thread: 2048 | | | Seeded Single Thread: 2048 | | |
|---|---|---|---|---|---|---|---|---|
| Set | Name | Best Known Solution | LB | UB | Time | LB | UB | Time |
| GendreauDumas | n20w120.001.txt | 337 | 337 | 337 | 5.13 | 337 | 337 | 4.10 |
| GendreauDumas | n20w120.002.txt | 246 | 246 | 246 | 6.13 | 246 | 246 | 5.79 |
| GendreauDumas | n20w120.003.txt | 347 | 347 | 347 | 8.12 | 347 | 347 | 3.19 |
| GendreauDumas | n20w120.004.txt | 353 | 353 | 353 | 9.36 | 353 | 353 | 5.69 |
| GendreauDumas | n20w120.005.txt | 315 | 315 | 315 | 11.88 | 315 | 315 | 7.86 |
| GendreauDumas | n20w140.001.txt | 230 | 230 | 230 | 7.33 | 230 | 230 | 5.63 |
| GendreauDumas | n20w140.002.txt | 307 | 307 | 307 | 5.99 | 307 | 307 | 3.57 |
| GendreauDumas | n20w140.003.txt | 301 | 301 | 301 | 12.81 | 301 | 301 | 7.32 |
| GendreauDumas | n20w140.004.txt | 318 | 318 | 318 | 6.35 | 318 | 318 | 5.07 |
| GendreauDumas | n20w140.005.txt | 275 | 275 | 275 | 8.33 | 275 | 275 | 3.07 |
| GendreauDumas | n20w160.001.txt | 347 | 347 | 347 | 16.31 | 347 | 347 | 9.73 |
| GendreauDumas | n20w160.002.txt | 250 | 250 | 250 | 12.65 | 250 | 250 | 9.72 |
| GendreauDumas | n20w160.003.txt | 331 | 331 | 331 | 5.24 | 331 | 331 | 3.20 |
| GendreauDumas | n20w160.004.txt | 287 | 287 | 287 | 7.85 | 287 | 287 | 4.51 |
| GendreauDumas | n20w160.005.txt | 342 | 342 | 342 | 14.35 | 342 | 342 | 8.68 |
| GendreauDumas | n20w180.001.txt | 353 | 353 | 353 | 6.90 | 353 | 353 | 5.81 |
| GendreauDumas | n20w180.002.txt | 347 | 347 | 347 | 7.44 | 347 | 347 | 5.66 |
| GendreauDumas | n20w180.003.txt | 315 | 315 | 315 | 17.43 | 315 | 315 | 4.43 |
| GendreauDumas | n20w180.004.txt | 284 | 284 | 284 | 30.96 | 284 | 284 | 16.48 |
| GendreauDumas | n20w180.005.txt | 257 | 257 | 257 | 9.46 | 257 | 257 | 7.35 |
| GendreauDumas | n20w200.001.txt | 259 | 259 | 259 | 9.02 | 259 | 259 | 8.05 |
| GendreauDumas | n20w200.002.txt | 242 | 242 | 242 | 32.44 | 242 | 242 | 10.46 |
| GendreauDumas | n20w200.003.txt | 305 | 305 | 305 | 8.32 | 305 | 305 | 4.56 |
| GendreauDumas | n20w200.004.txt | 326 | 326 | 326 | 26.12 | 326 | 326 | 14.22 |
| GendreauDumas | n20w200.005.txt | 277 | 277 | 277 | 9.29 | 277 | 277 | 6.64 |
| GendreauDumas | n40w120.001.txt | 470 | 470 | 470 | 42.95 | 470 | 470 | 24.57 |
| GendreauDumas | n40w120.002.txt | 557 | 557 | 557 | 26.93 | 557 | 557 | 16.01 |
| GendreauDumas | n40w120.003.txt | 464 | 464 | 464 | 37.06 | 464 | 464 | 13.26 |
| GendreauDumas | n40w120.004.txt | 392 | 392 | 392 | 59.60 | 392 | 392 | 30.90 |
| GendreauDumas | n40w120.005.txt | 470 | 470 | 470 | 24.70 | 470 | 470 | 16.39 |
| GendreauDumas | n40w140.001.txt | 460 | 460 | 460 | 77.30 | 460 | 460 | 53.39 |
| GendreauDumas | n40w140.002.txt | 459 | 459 | 459 | 30.01 | 459 | 459 | 20.75 |
| GendreauDumas | n40w140.003.txt | 476 | 476 | 476 | 23.65 | 476 | 476 | 11.08 |
| GendreauDumas | n40w140.004.txt | 458 | 458 | 458 | 103.45 | 458 | 458 | 41.30 |
| GendreauDumas | n40w140.005.txt | 438 | 438 | 438 | 79.34 | 438 | 438 | 35.90 |
| GendreauDumas | n40w160.001.txt | 470 | 470 | 470 | 93.24 | 470 | 470 | 61.27 |
| GendreauDumas | n40w160.002.txt | 451 | 451 | 451 | 131.65 | 451 | 451 | 50.20 |
| GendreauDumas | n40w160.003.txt | 415 | 415 | 415 | 73.22 | 415 | 415 | 36.75 |
| GendreauDumas | n40w160.004.txt | 425 | 425 | 425 | 34.02 | 425 | 425 | 19.69 |
| GendreauDumas | n40w160.005.txt | 373 | 373 | 373 | 77.57 | 373 | 373 | 36.81 |
| GendreauDumas | n40w180.001.txt | 444 | 444 | 444 | 134.27 | 444 | 444 | 99.12 |
| GendreauDumas | n40w180.002.txt | 448 | 448 | 448 | 137.02 | 448 | 448 | 83.30 |
| GendreauDumas | n40w180.003.txt | 398 | 398 | 398 | 69.47 | 398 | 398 | 26.74 |
| GendreauDumas | n40w180.004.txt | 409 | 409 | 409 | 59.34 | 409 | 409 | 22.53 |
| GendreauDumas | n40w180.005.txt | 438 | 438 | 438 | 168.31 | 438 | 438 | 89.39 |
| GendreauDumas | n40w200.001.txt | 416 | 416 | 416 | 44.65 | 416 | 416 | 32.94 |
| GendreauDumas | n40w200.002.txt | 402 | 402 | 402 | 90.46 | 402 | 402 | 51.80 |
| GendreauDumas | n40w200.003.txt | 408 | 408 | 408 | 107.36 | 408 | 408 | 48.11 |
| GendreauDumas | n40w200.004.txt | 426 | 426 | 426 | 37.55 | 426 | 426 | 24.35 |
| GendreauDumas | n40w200.005.txt | 408 | 408 | 408 | 182.99 | 408 | 408 | 50.26 |
| GendreauDumas | n60w120.001.txt | 536 | 536 | 536 | 101.97 | 536 | 536 | 68.94 |
| GendreauDumas | n60w120.002.txt | 606 | 606 | 606 | 160.15 | 606 | 606 | 96.68 |
| GendreauDumas | n60w120.003.txt | 541 | 541 | 541 | 215.21 | 541 | 541 | 40.41 |
| GendreauDumas | n60w120.004.txt | 607 | 607 | 607 | 72.17 | 607 | 607 | 29.59 |
| GendreauDumas | n60w120.005.txt | 579 | 579 | 579 | 167.99 | 579 | 579 | 70.92 |
| GendreauDumas | n60w140.001.txt | 596 | 596 | 596 | 136.02 | 596 | 596 | 54.80 |
| GendreauDumas | n60w140.002.txt | 647 | 647 | 647 | 69.59 | 647 | 647 | 40.44 |
| GendreauDumas | n60w140.003.txt | 625 | 625 | 625 | 89.37 | 625 | 625 | 63.29 |
| GendreauDumas | n60w140.004.txt | 578 | 578 | 578 | 72.23 | 578 | 578 | 48.45 |
| GendreauDumas | n60w140.005.txt | 554 | 554 | 554 | 96.83 | 554 | 554 | 39.83 |
| GendreauDumas | n60w160.001.txt | 672 | 672 | 672 | 148.81 | 672 | 672 | 57.99 |
| GendreauDumas | n60w160.002.txt | 665 | 665 | 665 | 65.43 | 665 | 665 | 36.21 |
| GendreauDumas | n60w160.003.txt | 569 | 569 | 569 | 115.57 | 569 | 569 | 78.76 |
| GendreauDumas | n60w160.004.txt | 573 | 573 | 573 | 280.64 | 573 | 573 | 214.91 |
| GendreauDumas | n60w160.005.txt | 619 | 619 | 619 | 162.69 | 619 | 619 | 72.59 |
| GendreauDumas | n60w180.001.txt | 556 | 556 | 556 | 120.08 | 556 | 556 | 85.01 |
| GendreauDumas | n60w180.002.txt | 561 | 561 | 561 | 206.83 | 561 | 561 | 59.32 |
| GendreauDumas | n60w180.003.txt | 606 | 606 | 606 | 100.03 | 606 | 606 | 64.04 |

Table A.15 **(Part 4 of 7)** Makespan Results of PnB at $\omega = 2048$ on Closed Problems: Seeded and Unseeded

LB = Lower Bound, UB = Upper Bound.

| Problem Information | | | Single Thread: 2048 | | | Seeded Single Thread: 2048 | | |
|---|---|---|---|---|---|---|---|---|
| Set | Name | Best Known Solution | LB | UB | Time | LB | UB | Time |
| GendreauDumas | n60w180.004.txt | 629 | 629 | 629 | 264.17 | 629 | 629 | 110.83 |
| GendreauDumas | n60w180.005.txt | 528 | 528 | 528 | 219.24 | 528 | 528 | 102.20 |
| GendreauDumas | n60w200.001.txt | 526 | 526 | 526 | 846.26 | 526 | 526 | 645.07 |
| GendreauDumas | n60w200.002.txt | 572 | 572 | 572 | 235.71 | 572 | 572 | 68.66 |
| GendreauDumas | n60w200.004.txt | 575 | 575 | 575 | 286.27 | 575 | 575 | 53.71 |
| GendreauDumas | n60w200.005.txt | 618 | 618 | 618 | 292.92 | 618 | 618 | 159.49 |
| GendreauDumas | n80w100.001.txt | 676 | 676 | 676 | 966.52 | 676 | 676 | 43.50 |
| GendreauDumas | n80w100.002.txt | 721 | 721 | 721 | 1071.28 | 721 | 721 | 232.78 |
| GendreauDumas | n80w100.003.txt | 729 | 729 | 729 | 99.03 | 729 | 729 | 110.61 |
| GendreauDumas | n80w100.004.txt | 759 | 759 | 759 | 435.13 | 759 | 759 | 351.61 |
| GendreauDumas | n80w100.005.txt | 671 | 671 | 671 | 423.50 | 671 | 671 | 244.70 |
| GendreauDumas | n80w120.001.txt | 675 | 675 | 675 | 260.17 | 675 | 675 | 136.39 |
| GendreauDumas | n80w120.002.txt | 748 | 748 | 748 | 102.10 | 748 | 748 | 50.59 |
| GendreauDumas | n80w120.003.txt | 677 | 677 | 677 | 681.72 | 677 | 677 | 280.42 |
| GendreauDumas | n80w120.004.txt | 644 | 644 | 644 | 247.44 | 644 | 644 | 108.18 |
| GendreauDumas | n80w120.005.txt | 743 | 743 | 743 | 315.00 | 743 | 743 | 140.92 |
| GendreauDumas | n80w140.001.txt | 689 | 689 | 689 | 185.95 | 689 | 689 | 123.68 |
| GendreauDumas | n80w140.002.txt | 651 | 651 | 651 | 155.80 | 651 | 651 | 101.24 |
| GendreauDumas | n80w140.003.txt | 673 | 673 | 673 | 1408.64 | 673 | 673 | 303.24 |
| GendreauDumas | n80w140.004.txt | 612 | 612 | 612 | 326.50 | 612 | 612 | 122.16 |
| GendreauDumas | n80w160.001.txt | 624 | 624 | 624 | 217.47 | 624 | 624 | 91.49 |
| GendreauDumas | n80w160.003.txt | 690 | 690 | 690 | 2930.56 | 690 | 690 | 1014.22 |
| GendreauDumas | n80w160.004.txt | 655 | 655 | 655 | 944.97 | 655 | 655 | 389.99 |
| GendreauDumas | n80w160.005.txt | 645 | 645 | 645 | 488.20 | 645 | 645 | 325.87 |
| GendreauDumas | n80w180.001.txt | 678 | 678 | 678 | 349.91 | 678 | 678 | 98.66 |
| GendreauDumas | n80w180.003.txt | 680 | 680 | 680 | 148.69 | 680 | 680 | 98.86 |
| GendreauDumas | n80w180.004.txt | 659 | 659 | 659 | 689.71 | 659 | 659 | 554.48 |
| GendreauDumas | n80w200.001.txt | 626 | 626 | 626 | 271.52 | 626 | 626 | 79.82 |
| GendreauDumas | n80w200.002.txt | 638 | 638 | 638 | 916.82 | 638 | 638 | 637.81 |
| GendreauDumas | n80w200.003.txt | 679 | 679 | 679 | 548.18 | 679 | 679 | 164.24 |
| GendreauDumas | n80w200.005.txt | 621 | 621 | 621 | 2143.38 | 621 | 621 | 1627.26 |
| Langevin | N20ft301.dat | 661.6 | 661.6 | 661.6 | 0.06 | 661.6 | 661.6 | 0.19 |
| Langevin | N20ft302.dat | 703 | 703 | 703 | 0.06 | 703 | 703 | 0.19 |
| Langevin | N20ft303.dat | 746.4 | 746.4 | 746.4 | 0.06 | 746.4 | 746.4 | 0.19 |
| Langevin | N20ft304.dat | 817 | 817 | 817 | 0.06 | 817 | 817 | 0.19 |
| Langevin | N20ft305.dat | 724.7 | 724.7 | 724.7 | 0.06 | 724.7 | 724.7 | 0.19 |
| Langevin | N20ft306.dat | 729.5 | 729.5 | 729.5 | 0.06 | 729.5 | 729.5 | 0.19 |
| Langevin | N20ft307.dat | 691.8 | 691.8 | 691.8 | 0.06 | 691.8 | 691.8 | 0.20 |
| Langevin | N20ft308.dat | 788.2 | 788.2 | 788.2 | 0.06 | 788.2 | 788.2 | 0.24 |
| Langevin | N20ft309.dat | 751.8 | 751.8 | 751.8 | 0.06 | 751.8 | 751.8 | 0.19 |
| Langevin | N20ft310.dat | 693.8 | 693.8 | 693.8 | 0.06 | 693.8 | 693.8 | 0.21 |
| Langevin | N20ft401.dat | 660.9 | 660.9 | 660.9 | 0.07 | 660.9 | 660.9 | 0.20 |
| Langevin | N20ft402.dat | 701 | 701 | 701 | 0.07 | 701 | 701 | 0.23 |
| Langevin | N20ft403.dat | 746.4 | 746.4 | 746.4 | 0.08 | 746.4 | 746.4 | 0.19 |
| Langevin | N20ft404.dat | 817 | 817 | 817 | 0.08 | 817 | 817 | 0.21 |
| Langevin | N20ft405.dat | 724.7 | 724.7 | 724.7 | 0.08 | 724.7 | 724.7 | 0.20 |
| Langevin | N20ft406.dat | 728.5 | 728.5 | 728.5 | 0.06 | 728.5 | 728.5 | 0.22 |
| Langevin | N20ft407.dat | 691.8 | 691.8 | 691.8 | 0.06 | 691.8 | 691.8 | 0.20 |
| Langevin | N20ft408.dat | 786.1 | 786.1 | 786.1 | 0.06 | 786.1 | 786.1 | 0.19 |
| Langevin | N20ft409.dat | 749.8 | 749.8 | 749.8 | 0.06 | 749.8 | 749.8 | 0.21 |
| Langevin | N20ft410.dat | 693.8 | 693.8 | 693.8 | 0.06 | 693.8 | 693.8 | 0.21 |
| Langevin | N40ft201.dat | 1109.3 | 1109.3 | 1109.3 | 0.06 | 1109.3 | 1109.3 | 0.26 |
| Langevin | N40ft202.dat | 1017.4 | 1017.4 | 1017.4 | 0.06 | 1017.4 | 1017.4 | 0.25 |
| Langevin | N40ft203.dat | 903.1 | 903.1 | 903.1 | 0.09 | 903.1 | 903.1 | 0.25 |
| Langevin | N40ft204.dat | 897.4 | 897.4 | 897.4 | 0.06 | 897.4 | 897.4 | 0.27 |
| Langevin | N40ft205.dat | 983.6 | 983.6 | 983.6 | 0.07 | 983.6 | 983.6 | 0.27 |
| Langevin | N40ft206.dat | 1081.9 | 1081.9 | 1081.9 | 0.06 | 1081.9 | 1081.9 | 0.26 |
| Langevin | N40ft207.dat | 884.9 | 884.9 | 884.9 | 0.07 | 884.9 | 884.9 | 0.27 |
| Langevin | N40ft208.dat | 1051.6 | 1051.6 | 1051.6 | 0.08 | 1051.6 | 1051.6 | 0.24 |
| Langevin | N40ft209.dat | 1027.5 | 1027.5 | 1027.5 | 0.06 | 1027.5 | 1027.5 | 0.29 |
| Langevin | N40ft210.dat | 1035.3 | 1035.3 | 1035.3 | 0.06 | 1035.3 | 1035.3 | 0.27 |
| Langevin | N40ft401.dat | 1105.2 | 1105.2 | 1105.2 | 0.11 | 1105.2 | 1105.2 | 0.29 |
| Langevin | N40ft402.dat | 1016.4 | 1016.4 | 1016.4 | 0.06 | 1016.4 | 1016.4 | 0.29 |
| Langevin | N40ft403.dat | 903.1 | 903.1 | 903.1 | 2.57 | 903.1 | 903.1 | 0.41 |
| Langevin | N40ft404.dat | 897.4 | 897.4 | 897.4 | 0.16 | 897.4 | 897.4 | 0.34 |
| Langevin | N40ft405.dat | 982.6 | 982.6 | 982.6 | 1.10 | 982.6 | 982.6 | 0.37 |
| Langevin | N40ft406.dat | 1081.9 | 1081.9 | 1081.9 | 0.88 | 1081.9 | 1081.9 | 0.30 |
| Langevin | N40ft407.dat | 872.2 | 872.2 | 872.2 | 0.60 | 872.2 | 872.2 | 0.34 |

Table A.16 **(Part 5 of 7)** Makespan Results of PnB at $\omega = 2048$ on Closed Problems: Seeded and Unseeded

LB = Lower Bound, UB = Upper Bound.

| Problem Information | | | Single Thread: 2048 | | | Seeded Single Thread: 2048 | | |
|---|---|---|---|---|---|---|---|---|
| Set | Name | Best Known Solution | LB | UB | Time | LB | UB | Time |
| Langevin | N40ft408.dat | 1043.5 | 1043.5 | 1043.5 | 0.25 | 1043.5 | 1043.5 | 0.33 |
| Langevin | N40ft409.dat | 1025.5 | 1025.5 | 1025.5 | 0.12 | 1025.5 | 1025.5 | 0.35 |
| Langevin | N40ft410.dat | 1034.3 | 1034.3 | 1034.3 | 0.07 | 1034.3 | 1034.3 | 0.30 |
| Langevin | N60ft201.dat | 1375.4 | 1375.4 | 1375.4 | 0.13 | 1375.4 | 1375.4 | 0.46 |
| Langevin | N60ft202.dat | 1186.4 | 1186.4 | 1186.4 | 0.09 | 1186.4 | 1186.4 | 0.44 |
| Langevin | N60ft203.dat | 1194.2 | 1194.2 | 1194.2 | 0.08 | 1194.2 | 1194.2 | 0.45 |
| Langevin | N60ft204.dat | 1283.6 | 1283.6 | 1283.6 | 0.09 | 1283.6 | 1283.6 | 0.53 |
| Langevin | N60ft205.dat | 1215.5 | 1215.5 | 1215.5 | 0.07 | 1215.5 | 1215.5 | 0.47 |
| Langevin | N60ft206.dat | 1238.8 | 1238.8 | 1238.8 | 0.34 | 1238.8 | 1238.8 | 0.57 |
| Langevin | N60ft207.dat | 1305.3 | 1305.3 | 1305.3 | 0.07 | 1305.3 | 1305.3 | 0.42 |
| Langevin | N60ft208.dat | 1172.6 | 1172.6 | 1172.6 | 1.17 | 1172.6 | 1172.6 | 0.47 |
| Langevin | N60ft209.dat | 1243.8 | 1243.8 | 1243.8 | 0.23 | 1243.8 | 1243.8 | 0.60 |
| Langevin | N60ft210.dat | 1273.2 | 1273.2 | 1273.2 | 2.22 | 1273.2 | 1273.2 | 0.51 |
| Langevin | N60ft301.dat | 1375.4 | 1375.4 | 1375.4 | 0.72 | 1375.4 | 1375.4 | 0.53 |
| Langevin | N60ft302.dat | 1184.4 | 1184.4 | 1184.4 | 2.10 | 1184.4 | 1184.4 | 0.57 |
| Langevin | N60ft303.dat | 1194.2 | 1194.2 | 1194.2 | 0.23 | 1194.2 | 1194.2 | 0.53 |
| Langevin | N60ft304.dat | 1283.6 | 1283.6 | 1283.6 | 3.33 | 1283.6 | 1283.6 | 0.63 |
| Langevin | N60ft305.dat | 1214.5 | 1214.5 | 1214.5 | 2.24 | 1214.5 | 1214.5 | 0.59 |
| Langevin | N60ft306.dat | 1237.8 | 1237.8 | 1237.8 | 4.87 | 1237.8 | 1237.8 | 0.65 |
| Langevin | N60ft307.dat | 1298.4 | 1298.4 | 1298.4 | 0.30 | 1298.4 | 1298.4 | 0.55 |
| Langevin | N60ft308.dat | 1168.8 | 1168.8 | 1168.8 | 3.93 | 1168.8 | 1168.8 | 0.56 |
| Langevin | N60ft309.dat | 1242.8 | 1242.8 | 1242.8 | 3.51 | 1242.8 | 1242.8 | 0.68 |
| Langevin | N60ft310.dat | 1273.2 | 1273.2 | 1273.2 | 2.91 | 1273.2 | 1273.2 | 1.98 |
| Langevin | N60ft401.dat | 1375.4 | 1375.4 | 1375.4 | 6.22 | 1375.4 | 1375.4 | 0.74 |
| Langevin | N60ft402.dat | 1183.4 | 1183.4 | 1183.4 | 4.65 | 1183.4 | 1183.4 | 1.46 |
| Langevin | N60ft403.dat | 1194.2 | 1194.2 | 1194.2 | 3.74 | 1194.2 | 1194.2 | 1.81 |
| Langevin | N60ft404.dat | 1283.6 | 1283.6 | 1283.6 | 5.46 | 1283.6 | 1283.6 | 0.77 |
| Langevin | N60ft405.dat | 1212.5 | 1212.5 | 1212.5 | 4.10 | 1212.5 | 1212.5 | 0.85 |
| Langevin | N60ft406.dat | 1236.8 | 1236.8 | 1236.8 | 10.36 | 1236.8 | 1236.8 | 4.25 |
| Langevin | N60ft407.dat | 1296.4 | 1296.4 | 1296.4 | 4.46 | 1296.4 | 1296.4 | 0.66 |
| Langevin | N60ft408.dat | 1150 | 1150 | 1150 | 5.79 | 1150 | 1150 | 1.41 |
| Langevin | N60ft409.dat | 1241.8 | 1241.8 | 1241.8 | 6.75 | 1241.8 | 1241.8 | 1.18 |
| Langevin | N60ft410.dat | 1273.2 | 1273.2 | 1273.2 | 10.13 | 1273.2 | 1273.2 | 3.92 |
| OhlmannThomas | n150w120.001.txt | 972 | 972 | 972 | 1164.11 | 972 | 972 | 825.73 |
| OhlmannThomas | n150w120.002.txt | 917 | 917 | 917 | 654.04 | 917 | 917 | 561.33 |
| OhlmannThomas | n150w120.003.txt | 909 | 909 | 909 | 1189.99 | 909 | 909 | 1001.17 |
| OhlmannThomas | n150w120.005.txt | 907 | 907 | 907 | 1591.25 | 907 | 907 | 876.81 |
| OhlmannThomas | n150w140.001.txt | 1008 | 1008 | 1008 | 462.98 | 1008 | 1008 | 342.39 |
| OhlmannThomas | n150w140.003.txt | 844 | 844 | 844 | 3630.57 | 844 | 844 | 519.89 |
| OhlmannThomas | n150w160.001.txt | 959 | 959 | 959 | 1907.07 | 959 | 959 | 553.85 |
| OhlmannThomas | n150w160.003.txt | 934 | 934 | 934 | 2623.29 | 934 | 934 | 581.80 |
| OhlmannThomas | n150w160.005.txt | 920 | 920 | 920 | 2762.04 | 920 | 920 | 1329.53 |
| OhlmannThomas | n200w120.003.txt | 1128 | 1128 | 1128 | 1855.39 | 1128 | 1128 | 696.30 |
| OhlmannThomas | n200w120.004.txt | 1072 | 1072 | 1072 | 1564.66 | 1072 | 1072 | 1445.56 |
| OhlmannThomas | n200w120.005.txt | 1073 | 1073 | 1073 | 1665.78 | 1073 | 1073 | 599.20 |
| OhlmannThomas | n200w140.002.txt | 1087 | 1087 | 1087 | 3097.33 | 1087 | 1087 | 1927.46 |
| OhlmannThomas | n200w140.004.txt | 1100 | 1100 | 1100 | 2265.02 | 1100 | 1100 | 791.76 |
| SolomonPesant | rc201.0 | 853.71 | 853.71 | 853.71 | 3.17 | 853.71 | 853.71 | 1.84 |
| SolomonPesant | rc201.1 | 850.48 | 850.48 | 850.48 | 5.02 | 850.48 | 850.48 | 2.08 |
| SolomonPesant | rc201.2 | 883.97 | 883.97 | 883.97 | 4.70 | 883.97 | 883.97 | 1.31 |
| SolomonPesant | rc201.3 | 722.43 | 722.43 | 722.43 | 1.62 | 722.43 | 722.43 | 0.31 |
| SolomonPesant | rc202.0 | 850.48 | 850.48 | 850.48 | 10.65 | 850.48 | 850.48 | 7.31 |
| SolomonPesant | rc202.1 | 702.28 | 702.28 | 702.28 | 19.59 | 702.28 | 702.28 | 7.96 |
| SolomonPesant | rc202.2 | 853.71 | 853.71 | 853.71 | 11.40 | 853.71 | 853.71 | 7.55 |
| SolomonPesant | rc202.3 | 883.97 | 883.97 | 883.97 | 42.31 | 883.97 | 883.97 | 27.06 |
| SolomonPesant | rc203.0 | 870.52 | 870.52 | 870.52 | 247.92 | 870.52 | 870.52 | 48.78 |
| SolomonPesant | rc203.1 | 850.48 | 850.48 | 850.48 | 41.22 | 850.48 | 850.48 | 24.01 |
| SolomonPesant | rc203.2 | 853.71 | 853.71 | 853.71 | 53.03 | 853.71 | 853.71 | 9.52 |
| SolomonPesant | rc204.0 | 839.24 | 839.24 | 839.24 | 36.25 | 839.24 | 839.24 | 24.46 |
| SolomonPesant | rc204.1 | 492.60 | 492.60 | 492.60 | 254.83 | 492.60 | 492.60 | 62.26 |
| SolomonPesant | rc205.0 | 834.62 | 834.62 | 834.62 | 11.58 | 834.62 | 834.62 | 9.49 |
| SolomonPesant | rc205.1 | 899.24 | 899.24 | 899.24 | 6.65 | 899.24 | 899.24 | 6.72 |
| SolomonPesant | rc205.2 | 908.79 | 908.79 | 908.79 | 12.72 | 908.79 | 908.79 | 10.47 |
| SolomonPesant | rc205.3 | 684.21 | 684.21 | 684.21 | 10.51 | 684.21 | 684.21 | 8.72 |
| SolomonPesant | rc206.0 | 893.21 | 893.21 | 893.21 | 40.68 | 893.21 | 893.21 | 22.23 |
| SolomonPesant | rc206.1 | 756.45 | 756.45 | 756.45 | 61.77 | 756.45 | 756.45 | 19.49 |
| SolomonPesant | rc206.2 | 776.19 | 776.19 | 776.19 | 115.81 | 776.19 | 776.19 | 32.61 |
| SolomonPesant | rc207.0 | 847.63 | 847.63 | 847.63 | 224.89 | 847.63 | 847.63 | 102.04 |

Table A.17 **(Part 6 of 7)** Makespan Results of PnB at $\omega = 2048$ on Closed Problems: Seeded and Unseeded

LB = Lower Bound, UB = Upper Bound.

| Problem Information | | | Single Thread: 2048 | | | Seeded Single Thread: 2048 | | |
|---|---|---|---|---|---|---|---|---|
| Set | Name | Best Known Solution | LB | UB | Time | LB | UB | Time |
| SolomonPesant | rc207.1 | 785.37 | 785.37 | 785.37 | 132.40 | 785.37 | 785.37 | 39.23 |
| SolomonPesant | rc207.2 | 650.8 | 650.80 | 650.80 | 252.09 | 650.80 | 650.80 | 35.39 |
| SolomonPesant | rc208.0 | 836.04 | 836.04 | 836.04 | 2256.13 | 836.04 | 836.04 | 1484.62 |
| SolomonPesant | rc208.1 | 615.51 | 615.51 | 615.51 | 417.09 | 615.51 | 615.51 | 160.41 |
| SolomonPesant | rc208.2 | 596.21 | 596.21 | 596.21 | 276.60 | 596.21 | 596.21 | 46.52 |
| SolomonPotvinBengio | rc_201.1.txt | 592.06 | 592.06 | 592.06 | 1.75 | 592.06 | 592.06 | 0.53 |
| SolomonPotvinBengio | rc_201.2.txt | 860.17 | 860.17 | 860.17 | 1.06 | 860.17 | 860.17 | 0.49 |
| SolomonPotvinBengio | rc_201.3.txt | 853.71 | 853.71 | 853.71 | 4.57 | 853.71 | 853.71 | 1.32 |
| SolomonPotvinBengio | rc_201.4.txt | 889.18 | 889.18 | 889.18 | 0.32 | 889.18 | 889.18 | 0.28 |
| SolomonPotvinBengio | rc_202.1.txt | 850.48 | 850.48 | 850.48 | 29.56 | 850.48 | 850.48 | 18.33 |
| SolomonPotvinBengio | rc_202.2.txt | 338.52 | 338.52 | 338.52 | 1.54 | 338.52 | 338.52 | 0.56 |
| SolomonPotvinBengio | rc_202.3.txt | 894.1 | 894.10 | 894.10 | 9.24 | 894.10 | 894.10 | 6.64 |
| SolomonPotvinBengio | rc_202.4.txt | 853.71 | 853.71 | 853.71 | 11.17 | 853.71 | 853.71 | 10.08 |
| SolomonPotvinBengio | rc_203.1.txt | 488.42 | 488.42 | 488.42 | 5.00 | 488.42 | 488.42 | 3.19 |
| SolomonPotvinBengio | rc_203.2.txt | 853.71 | 853.71 | 853.71 | 24.89 | 853.71 | 853.71 | 19.70 |
| SolomonPotvinBengio | rc_203.3.txt | 921.44 | 921.44 | 921.44 | 229.75 | 921.44 | 921.44 | 144.62 |
| SolomonPotvinBengio | rc_203.4.txt | 338.52 | 338.52 | 338.52 | 2.70 | 338.52 | 338.52 | 1.18 |
| SolomonPotvinBengio | rc_204.2.txt | 690.06 | 690.06 | 690.06 | 445.91 | 690.06 | 690.06 | 21.80 |
| SolomonPotvinBengio | rc_204.3.txt | 455.03 | 455.03 | 455.03 | 571.24 | 455.03 | 455.03 | 20.02 |
| SolomonPotvinBengio | rc_205.1.txt | 417.81 | 417.81 | 417.81 | 0.26 | 417.81 | 417.81 | 0.24 |
| SolomonPotvinBengio | rc_205.2.txt | 820.19 | 820.19 | 820.19 | 11.47 | 820.19 | 820.19 | 9.12 |
| SolomonPotvinBengio | rc_205.3.txt | 950.05 | 950.05 | 950.05 | 20.15 | 950.05 | 950.05 | 12.70 |
| SolomonPotvinBengio | rc_205.4.txt | 837.71 | 837.71 | 837.71 | 13.12 | 837.71 | 837.71 | 7.29 |
| SolomonPotvinBengio | rc_206.1.txt | 117.85 | 117.85 | 117.85 | 0.06 | 117.85 | 117.85 | 0.20 |
| SolomonPotvinBengio | rc_206.2.txt | 870.49 | 870.49 | 870.49 | 95.97 | 870.49 | 870.49 | 74.81 |
| SolomonPotvinBengio | rc_206.3.txt | 650.59 | 650.59 | 650.59 | 22.40 | 650.59 | 650.59 | 12.57 |
| SolomonPotvinBengio | rc_206.4.txt | 911.98 | 911.98 | 911.98 | 249.85 | 911.98 | 911.98 | 107.78 |
| SolomonPotvinBengio | rc_207.1.txt | 804.67 | 804.67 | 804.67 | 289.99 | 804.67 | 804.67 | 171.01 |
| SolomonPotvinBengio | rc_207.2.txt | 713.9 | 713.90 | 713.90 | 110.75 | 713.90 | 713.90 | 43.02 |
| SolomonPotvinBengio | rc_207.3.txt | 745.77 | 745.77 | 745.77 | 664.62 | 745.77 | 745.77 | 499.02 |
| SolomonPotvinBengio | rc_207.4.txt | 133.14 | 133.14 | 133.14 | 0.09 | 133.14 | 133.14 | 0.22 |
| SolomonPotvinBengio | rc_208.1.txt | 810.7 | 810.70 | 810.70 | 1870.15 | 810.70 | 810.70 | 560.76 |
| SolomonPotvinBengio | rc_208.2.txt | 579.51 | 579.51 | 579.51 | 496.96 | 579.51 | 579.51 | 91.32 |

Table A.18 **(Part 7 of 7)** Makespan Results of PnB at $\omega = 2048$ on Closed Problems: Seeded and Unseeded

LB = Lower Bound, UB = Upper Bound.